

Investigating the SUMOylation and transcriptional regulation of Nurr1 and the splice variant Nurr-1a

Submitted by

Jade Edey

Supervised by

Dr. Andrew Bennett

Dr. Gareth Hathway

This thesis is submitted to the University of Nottingham for the degree of Doctor of Philosophy

Table of Contents

.....i

Abstract v

Posters and Presentations viii

Acknowledgements ix

List of Abbreviations x

List of Figures xiv

List of Tables xvii

Declaration xviii

Chapter 1 ..... *1*

Introduction *1*

1.2 Nuclear receptors 2

1.2.1 Structure of Nuclear receptors 5

1.2.2 Receptor subtype 7

1.2.3 Nuclear receptor transcriptional regulation 8

1.2.4 Nuclear receptor regulation through PTMs 12

1.3 SUMOylation 14

1.3.1 SUMO isoforms 14

1.3.2 SUMOylation cycle 15

1.3.3 E3 Ligases 17

1.3.4 SENPs 19

1.3.5 SUMO consensus motifs 20

1.3.6 SUMO interaction motifs 21

1.3.7 SUMOylation in disease 22

1.4 Nurr1 26

1.4.1 Structure and ligand binding 26

1.4.2 Isoforms 28

1.4.3 Dimerisation and response element binding 31

1.4.4 Nurr1 expression: Neuronal 32

1.4.5 Nurr1 expression: Microglia and Macrophages 35

1.4.6 Nurr1 in Parkinson's Disease 39

1.5 Project aims and objectives 45

Chapter 2 ..... *46*

Materials and Methods *46*

2.1 Chemicals and reagents 47

2.2 Cell culture 52

2.2.1 Frozen cells 52

2.2.2 Cell maintenance 53

2.2.3 Cryopreservation 53

2.3.4 Cell counting 53

2.3 Cloning and mutagenesis 55

2.3.1 RNA isolation 55

2.3.2 cDNA synthesis 55

2.3.3 Cloning 55
2.3.4 Restriction endonuclease digestion 58
2.3.5 Agarose gel electrophoresis 58
2.3.6 Gel extraction and Ligation 59
2.3.7 Bacterial transformation 60
2.3.8 Colony PCR 61
2.3.9 Plasmid Purification 61
2.3.10 Site Directed Mutagenesis 61
2.3.11 DNA sequencing 62

2.4 Gene expression assays 63
2.4.1 Transfection and luciferase reporter assay 63
2.4.2 RT-qPCR 63

2.5 In-vitro SUMOylation assay 66
2.5.1 Ni-NTA pull-down 66
2.5.2 Protein concentration assay 68
2.5.3 Western Blot 69
2.5.4 Proximity Ligase Assay (PLA) 70

2.6 Immunocytochemistry (ICC) 72

2.7 Lentivirus production 73
2.7.1 Designing attB PCR primers 73
2.7.2 Production and purification of attB PCR products 74
2.7.3 BP reaction (PCR fragment + donor vector = entry clone) 74
2.7.4 LR reaction (entry clone + destination vector = expression clone) 74
2.7.5 Production and purification of lentiviral vectors 75
2.7.6 Lentiviral infection 77

2.8 Primary monocyte isolation 79
2.8.1 Monocyte isolation 79
2.8.2 Induction into microglia like cells (iMGL) and macrophages 79
2.8.3 Macrophage and iMGL ICC 80
2.8.4 Phagocytosis assay 80
2.8.5 RT-qPCR 81
2.8.6 SYBR green qPCR 81

2.9 iPSC culture and differentiation 83
2.9.1 Maintenance and subculture 83
2.9.2 Assessment of pluripotency 85
2.9.3 Differentiation into haematopoietic (HP) cells 86
2.9.3 Differentiation into microglia 87
2.9.4 Differentiation into dopaminergic neurons 87

Chapter 3 ..... ***90***

SUMOylation of Nurr1 and Nurr-1a ***90***

3.1 Introduction 91

3.2 Results 95
3.2.1 Cloning wild type Nurr1 and Nurr-1a 95
3.2.2 SUMO isoforms of Nurr1 and Nurr-1a 95
3.2.3 PIASg both SUMOylates Nurr-1a and stabilises its protein expression independent of its E3 ligase activity 98
3.2.4 K91 is the principal site of SUMOylation in both Nurr1 and Nurr-1a 100
3.2.5 Investigating the Nurr-1a SUMO Interaction Motif (SIM) 108
3.2.6 Effect of ligands on Nurr1 and Nurr-1a 111
3.2.7 Evaluating the Nurr1/1a-SUMO interaction 115

3.2.8 Nurr1/1a transactivation of the TH promoter 120
3.2.9 SUMO enhanced transcriptional activation is cell specific 129
3.2.10 The effect of ligands on transactivation 131

3.2 Discussion 133

Chapter 4 146

The development of human based inflammatory and neuronal models to investigate the role of Nurr1 and Nurr-1a 146

4.1 Introduction: induced pluripotent stem cells 147

4.2 Results: iPSCs 150
4.2.1 Optimisation of iPSC culture 150
4.2.2 Assessment of pluripotency 153
4.2.3 iPSC derived dopaminergic neurons 158
4.2.4 iPSC derived microglia 165

4.2 Discussion: iPSCs 171

4.3 Introduction: monocyte derived macrophages and microglial-like cells 176

4.4 Results: monocyte derived macrophages and microglial-like cells 181
4.4.1 Isolation and differentiation of peripheral blood derived monocytes into macrophages and microglial-like cells 181
4.4.2 Markers expressed by macrophage and iMGL cells 184
4.4.3 Phagocytosis assay in monocyte derived macrophages and iMGL cells 187
4.4.4 Macrophages and iMGL can function as inflammatory models 189
4.4.5 The role of Nurr1 in immune tolerance 193
4.4.6 Cloning human Nurr-1a from total brain RNA 199
4.4.7 Lentiviral cloning and expression of Nurr1 and Nurr-1a 202
4.4.8 Investigating the effect Nurr1/1a has on inflammation 206

4.5 Discussion: monocyte derived macrophages and microglial-like cells 212

Chapter 5 218

Significant findings, general discussion, and future work 218

5.1 Summary of Significant findings 219

5.2 General discussion 219

6.3 Limitations and future work 227

Appendices 230

Abstract

Nuclear receptor-related 1 protein (also known as Nurr1 or NR4A2) is an orphan nuclear receptor with multiple roles in many different tissues and pathological settings. It is most commonly known for its vital role in the development, maintenance and survival of dopaminergic (DA) neurons throughout the midbrain, particularly in the *substantia nigra* (Jankovic et al., 2005). Nurr1 also has a reported role in inflammatory cells such as microglia and macrophages, where it is suggested to dampen down the inflammatory response to prevent excessive inflammation (Lallier et al., 2016, Smith et al., 2015). This reduction in inflammation, thought to be preceded by Nurr1 LBD SUMOylation, is believed to protect surrounding cells such as DA neurons from potentially damaging inflammatory mediators (Saijo et al., 2009). Nurr1 has many reported splice variants found in the human brain. However one of particular interest, termed Nurr-1a, is reported to have truncated LBD whilst retaining an intact AF-1; previously described as the key region for transcriptional regulation in NR42 nuclear receptors (Michelhaugh et al., 2005, Ichinose et al., 1999, Maxwell and Muscat, 2006). Albeit the function of Nurr-1a remains to be investigated. Fully understanding the mechanisms in which Nurr1 regulates the expression of key neuronal and inflammatory genes, and any role Nurr-1a may or may not have in these processes, will help to clarify, or reveal targets for therapeutic manipulation in diseases with a neuroinflammatory component such as Parkinson's Disease. Therefore, this work aimed to clarify the mechanisms surrounding Nurr1 and Nurr-1a SUMOylation, and the effect this may have on gene transcription. Whilst also focusing on the development of human based neuronal and inflammatory models which can better recapitulate diseases with a neuroinflammatory factor.

To investigate the SUMOylation of Nurr1 and Nurr-1a initial experiments employed a SUMO-pulldown assay to enrich conjugates overexpressed in HeLa cells followed by western blotting. In combination with site directed mutagenesis of a predicted SUMO site, this data revealed Nurr-1a is SUMOylated significantly more than Nurr1, occurring in both receptors at a site dissimilar from the LBD which had been previously described. In addition, the E3 ligase PIASg, previously reported as a key interaction partner of Nurr1, was also found to be the E3 ligase responsible for Nurr-1a SUMOylation and exhibited important activity as a stabilising factor independent of its E3 ligase role. The transcriptional activity of Nurr1 and Nurr-1a was investigated in the neuronal cell line SH-SY5Y using a TH promoter driven luciferase reporter. In accordance with previous reports, Nurr-1a was found to be less transcriptionally active than Nurr1. However, the transcriptional activity of both receptors was significantly enhanced by the presence of SUMO. This was further validated through the use of SUMO site mutants. Furthermore, ligands were unable to majorly affect the SUMOylation of either receptor and had little effect on the transcriptional activity. Highlighting transcriptional activity is largely dependent on cell type (HEK293 vs SH-SY5Y) and whether a natural TH or synthetic 3XNBRE promoter driven reporter was used.

Human based models were developed so that Nurr1 and Nurr-1a transcriptional regulation of key genes could be investigated in setting more representative of human physiology than cell lines and overexpressed rodent genes. Human iPSC's were differentiated into DA neurons using a polycistronic vector which overexpressed Nurr1 ,in addition to two other key transcriptional factors, and validated through ICC. Blood derived monocytes were differentiated into macrophages and microglial-like cells which were characterised though RT-qPCR, ICC and functional assays. Macrophages were

subsequently used to investigate the role of Nurr1 in immune tolerance; the reduced responsiveness of immune response after repeated TLR activation. Identifying Nurr1 is superinduced during tolerance and may therefore have an important function dampening down the production of inflammatory mediators during this state.

Overall, these data reveal Nurr-1a partakes in many of the same mechanisms reported for Nurr1. Albeit a lesser ability to transcriptionally activate genes, it appears Nurr-1a is capable of a greater and more versatile level of SUMOylation. Which may suggest a more prolific role in the inflammatory transrepression mechanism previously reported. Although the SUMOylation in this mechanism was previously reported to occur within the LBD, this study demonstrates SUMOylation occurs within the AF-1 domain of both Nurr1 and Nurr-1a. Highlighting AF-1 as a key region of transcriptional regulation, aligning with other members of the NR4A family. SUMOylation may contribute to the fine tuning of transcriptional regulation by Nurr1 and Nurr-1a, exemplified by its ability to enhance transcriptional activation in neuronal cells whilst being reported to feature in the transrepression of inflammatory genes in microglia and macrophages. The successful generation of DA neurons through the transduction of iPSC's with Nurr1 amongst two other TF's again highlights the importance of Nurr1 in DA neuronal development and provides a framework model to identify the role of Nurr-1a, if any, in this process. Lastly the exploration of Nurr1 and inflammatory gene expression during immune tolerance may suggest a novel function for Nurr1 in regulating this protective process. Immune tolerance may have a role in PD and could be abrogated due to increases in IFNy which has been reported in PD patients. Therefore, fully understanding what happens to Nurr1 in this process is important if it is to be considered a therapeutic target.

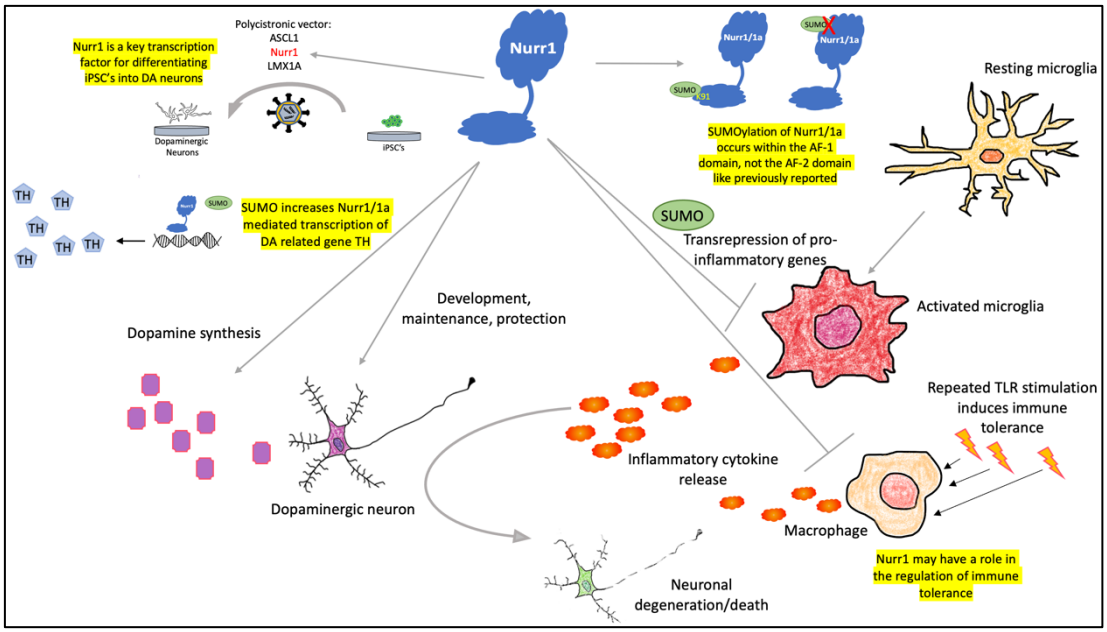


Figure 1 Nurr1 and Nur1a – what is currently known, and new results are outlined in this thesis.

Schematic of Nurr1 and Nurr-1a involvement in microglia, dopaminergic neurons, and macrophages. Findings outlined in this thesis are highlighted in yellow.

Posters and Presentations

1. European Neuroscience Conference by doctoral Students 2021: Investigating the molecular mechanisms of Nurr1 and its splice variant Nurr-1a.
2. International Conference on Molecular Neurobiology 2022: SUMOylation enhances Nurr1/1a mediated transactivation in a neuronal cell type.
3. University of Nottingham Life Science Symposium 2022: The effect of immune tolerance on Nurr1 in macrophages and how it relates to Parkinson's Disease.

Acknowledgements

I would like to thank my supervisors: Associate Professor Andrew Bennett and Associate Professor Gareth Hathway for all of the guidance and support they have given me throughout my PhD. From troubleshooting a failed experiment to instilling confidence in my ability to present at conferences I have felt encouraged in every aspect and for that I will be forever grateful.

I extend my thanks to both the Neuroscience Support Group at the Queen's Medical Centre and the FRAME Lab at the University of Nottingham for Financial support throughout my studies. For whom without this work would have not been possible.

I am also thankful for Nicola De vivo and Monika Owen for their guidance and wisdom for working in a laboratory environment. In addition to constant kindness and support from lab colleagues.

Lastly, I extend my deepest gratitude to Razan Al-Momani, a fantastic mentor who taught me so much of what I know today. Who guided me to believe in myself and was always there to help and offer advice.

List of Abbreviations

6-mp	6-mercaptopurine
A	Amps
AF-1	Activation function 1
AF-2	Activation function 2
Akt	Protein kinase B
AP-1	Activator protein 1
AQ	Amodiaquine
Ascl1	Achaete-Scute family BHLH transcription factor 1
ATP	Adenosine triphosphate
BBB	Blood brain barrier
BCA	Bicinchoninic acid
BCP	1-bromo-3-chloropropane
BMDM	Bone marrow derived macrophages
bp	Base pair
BSA	Bovine serum albumin
C-DIM12	1,1-bis(3'-indolyl)-1-(*p*-chlorophenyl) methane
cAMP	Cyclic adenosine monophosphate
cDNA	Complementary DNA
cDNA	Complementary DNA
CNS	Central nervous system
CoREST	Rest corepressor
CREB	cAMP response element binding protein
CSF	Cerebral spinal fluid
D3	Dopamine receptor 3
DA	Dopaminergic
DAMP	Damage associated molecular pattern
DAPI	4',6-diamidino-2-phenylindole
DAT	Dopamine transporter
DBD	DNA binding domain
DCC	Netrin receptor DCC
DeSI	DeSUMOylating iso-peptidase
DHA	Docosahexaenoic acid
DHI	Dopamine metabolite 5,6-dihydroxyindole
DMEM	Dulbecco's modified eagle medium
DMSO	Dimethyl sulfoxide
DNA	Deoxyribonucleotide
dNTP	Deoxyribonucleotide triphosphate
DR5	Direct repeat 5
DTT	Dithiothreitol
EDTA	Ethylenediaminetetraacetic acid
ERK	Extracellular signal regulated kinases
FBS	Fetal bovine serum
FFA	Free fatty acid
FITC	Fluorescein isothiocyanate
GAPDH	Glyceraldehyde-3-phosphate dehydrogenase
GFP	Green fluorescent protein
gm	gram

GM-CSF	Granulocyte macrophage colony stimulating factor
GSK3β	Glycogen synthase kinase 3 beta
HDACs	Histone deacetylases
HEK	Human embryonic kidney
HPLC	High performance liquid chromatography
Hr	Hour
HRE	Hormone response element
ICC	Immunocytochemistry
IFNy	Interferon gamma
IκB	Inhibitory kappa B
IKK	Inhibitory kappa B kinase
IL	Interleukin
iMGL	Induced microglial-like cells
iPSC	Induced pluripotent stem cells
JNK	c-Jun N-terminal kinase
K	Lysine
kb	Kilobases
kDa	Kilodalton
L	litre
LBD	Ligand binding domain
LBP	Ligand binding pocket
LMX1 A/B	LIM homeobox transcription factor alpha/beta
LPS	Lipopolysaccharide
LRH-1	Liver receptor homolog 1
LXR	Liver X receptor
M	Molar
M-CSF	Macrophage colony stimulating factor
MAPK	Mitogen-activated protein kinase
mg	Milligram
Min	Minute
miRNAs	MicroRNAs
ml	Millilitre
mM	Millimolar
mRNA	Messenger RNA
mTOR	Mammalian target of rapamycin
NBRE	NGFI-B responsive element
NCoR	Nuclear receptor corepressor
NDSM	Negatively charged amino acid dependent SUMOylation motif
NFκB	Nuclear factor kappa B
ng	Nanogram
ng/ml	Nanogram per millilitre
NHR	Nuclear hormone receptor
NLK	Nemo like kinase
NLS	Nuclear localisation signal
nm	Nanometre
NMR	Nuclear magnetic resonance
NOR-1	Neuron derived orphan receptor 1 (NR4A3)
NR	Nuclear receptor
Nur77	NGFI-B (NR4A1)

Nurr-1a	Nuclear related receptor 1a
Nurr1	Nuclear related receptor 1 (NR4A2)
NurRE	Nur response element
PAMP	Pathogen associated molecular pattern
PBMC	Peripheral blood derived mononuclear cells
PBS	Phosphate buffered saline
PCR	Polymerase chain reaction
PD	Parkinson's disease
PDSM	Phosphorylation dependent SUMOylation motifs
PGA1	Prostaglandin A1
PGE1	Prostaglandin E1
PI3K	Phosphoinositide 3-kinase
PIAS	Protein inhibitor of activated STAT
PIASg	Protein inhibitor of activated STAT gamma
PLA	Proximity ligase assay
PML	Promyelocytic leukaemia protein
PPAR	Peroxisome proliferator activated receptor
PRR	Pattern recognition receptor
PTM	Post translational modification
R	Arginine
RanBP2	RAN binding protein 2
RanGAP1	Ran GTPase activating protein 1
RAR	Retinoic acid receptor
RIPA	Radioimmunoprecipitation assay
RPMI	Roswell Park Memorial Institute
RT	Room temperature
RT-qPCR	Real time quantitative PCR
RXR	Retinoid X receptor
Sae	SUMO activating enzyme subunit
SDS-PAGE	Sodium dodecyl sulphate-Polyacrylamide gel electrophoresis
SEM	Standard error of mean
SENPs	SUMO-Specific proteases/iso-peptidases
SIM	SUMO-interacting motif
STAT	Signal transducer and activator of transcription
SUMO	Small ubiquitin like modifier
TAE	Tris-acetate-ethylene-diamine-tetra acetic acid
TBST	Tris buffered saline in Tween 20
TDG	Thymine DNA glycosylase
TEMED	Tetramethyl ethylenediamine
TH	TH
TINUR	Transcriptionally inducible nuclear receptor
TLR	Toll-like receptor
TNFα	Tumour necrosis factor alpha
TR	Thyroid receptor
TRITC	Tetramethyl rhodamine-isothiocyanate
USPL1	Ubiquitin specific protease like 1
UTR	Untranslated region
V	Volt
v/v	Volume/volume

VMAT	Vesicular monoamine transporter
w/v	Weight/volume
µg	Microgram
µl	Microlitre
µM	Micromole

List of Figures

.....viii
Figure 1 Nurr1 and Nur1a – what is currently known, and new results are outlined in this thesis. viii
Figure 1.2-1 Nuclear Hormone Receptor structure 7
Figure 1.2-2 Classes of Nuclear hormone receptor 8
Figure 1.2-3 PPARγ transrepression 10
Figure 1.2-4 Nurr1 transrepression 11
Figure 1.3-1 The SUMOylation cycle 17
Figure 1.3-2 SUMO-SIM diversity 22
..... 30
Figure 1.4-1 Schematic of Nurr1, Nurr-1a and TINUR 30
Figure 1.4-2 Nur1 response element binding 32
..... 36
Figure 1.4-3 Common inflammatory signalling pathways in microglia and macrophages 36
Figure 2.3-1 Primer design and schematic overview of the TH cloning process. 56
Figure 2.5-1 Schematic of the *in vitro* SUMO pulldown assay described in Springer Protocols (Pourcet et al., 2013) 66
Figure 2.7-1 Morphology of HEK293FT cells during lentiviral production 77
Figure 3.1-1 Nurr1 SUMOylation sites as reported in the literature 93
Figure 3.2-1 SUMO3 isoform SUMOylates Nurr1 and Nurr-1a the greatest 95
Figure 3.2-2 Nurr-1a is SUMOylated to a greater level than Nurr1 97
Figure 3.2-3 PIASg is required for stable Nurr-1a expression 99
Figure 3.2-4 C342A PIASg protein expression is lower than the wildtype 100
Figure 3.2-5 Predicted SUMO sites of Nurr1 and Nurr-1a 101
Figure 3.2-6 Alignment of Human and Rat Nurr1 and Nurr-1a sequences 102
Figure 3.2-7 Reported Nuclear Localisation Signal sites of Nurr1 104
Figure 3.2-8 Subcellular localisation of Nurr1 and Nurr-1a K91 mutants 105
Figure 3.2-9 Subcellular localisation of Nurr1 and Nurr-1a K91 mutants with PIASg 106
Figure 3.2-10 K91 is the major SUMOylation site of Nurr-1a 108
Figure 3.2-11 Mutating the Nurr-1a SIM site 109
Figure 3.2-12 Nurr-1a SIM mutation sequence 109
Figure 3.2-13 Nurr-1a SIM mutation reduces protein stability 110
Figure 3.2-14 Ligands affect the expression of Nurr-1a 113
Figure 3.2-15 Concentration dependent effect of ligands upon Nurr-1a protein levels 115
Figure 3.2-16 Schematic diagram of the Proximity Ligase assay 116
Figure 3.2-17 Controls used in the PLA 117
Figure 3.2-18 Proximity Ligase Assay investigating Nurr-SUMO interactions 118
Figure 3.2-19 Co-transfection of Nurr1/1a and SUMO2 in HeLa cells 119
Figure 3.2-20 Schematic diagram of the cloned TH promoter 121
Figure 3.2-21 Morphology of SH-SY5Y cells 121
Figure 3.2-22 Protein expression in SH-SY5Y cells 122
Figure 3.2-23 Plasmid expression in SH-SY5Y cells 123
Figure 3.2-24 Nurr1 plasmid concentration alters luciferase activity 124
Figure 3.2-25 Nurr1 and Nurr-1a's transactivation of the TH promoter is repressed by PIASg 125

Figure 3.2-26 Nurr-1a is stabilized by endogenous PIASg in SH-SY5Y cells..... 126
Figure 3.2-27 K91 mutants activate the TH promoter less than wildtype, and are similarly repressed by PIASg..... 127
Figure 3.2-28 SUMO enhances Nurr1 and Nurr-1a mediated..... 128
Figure 3.2-29 SUMO enhances Nurr1 and Nurr-1a mediated transactivation of the TH promoter..... 130
Figure 3.2-30 Nurr1 expression is greater than Nurr-1a in transfected HEK293 cells 131
Figure 3.2-31 The effect of ligands on Nurr mediated transcriptional activation.... 132
Figure 3.2-32. NGFI-B response element-like sequences which bind Nurr1 140
Figure 4.1-1 iPSC differentiation into Microglia and DA neurons..... 149
Figure 4.2-1 Assessment of typical iPSC morphology 150
Figure 4.2-2 Example of differentiated cells within an iPSC culture 151
Figure 4.2-3 ReLeSR does not dislodge differentiated cell aggregates 152
Figure 4.2-4 Passing with and without ROCKi 153
Figure 4.2-5 Schematic diagram of iPSC trilineage differentiation..... 154
Figure 4.2-6 iPSCs differentiate into all three germ types..... 155
Figure 4.2-7 iPSCs express pluripotency markers 156
Figure 4.2-8 Analysis of 8 common chromosomal mutations in iPSCs generates varied results 157
..... 159
Figure 4.2-9 rtTA is required for transcription of ALN genes..... 159
Figure 4.2-10 Ultracentrifuged virus transduce iPSCs efficiently 160
Figure 4.2-11 Doxycycline induces the expression of ALN..... 161
Figure 4.2-12 iPSC dopaminergic neuron differentiation timeline..... 162
Figure 4.2-13 iPSC dopaminergic neurons express key markers 163
Figure 4.2-14 iPSC derived microglial differentiation timeline 165
Figure 4.2-15 iPSCs were differentiated using the STEMdiff Hematopoietic Kit .. 166
Figure 4.2-16 Hematopoietic cells express key markers 167
Figure 4.2-17 iPSCs were unable to differentiate into hematopoietic cells using a cytokine cocktail method 168
Figure 4.2-18 The differentiation of hematopoietic cells using STEMdiff microglia differentiation kits did not morphologically resemble microglia..... 169
Figure 4.2-19 iPSC derived microglia express Iba1 and TMEM119..... 170
Figure 4.2-10 Protocol to differentiate iPSC into Dopaminergic neurons. 173
Figure 4.3-1 Schematic representation Nurr1's repressive role during inflammation 177
Figure 4.4-1 Schematic representation of human monocyte isolation and differentiation into macrophage and iMGL cells 181
Figure 4.4-2 Isolated untreated monocytes 182
Figure 4.4-3 Morphology of monocyte derived macrophages..... 183
Figure 4.4-4 Morphology of monocyte derived iMGL cells..... 184
Figure 4.4-5 Macrophage and iMGL cells express typical cell surface markers..... 185
Figure 4.4-6 Macrophage and iMGL cells express key markers 187
Figure 4.4-7 Macrophage and iMGL cells phagocytose GFP latex beads..... 188
Figure 4.4-8 Macrophage and iMGL cells phagocytose GFP latex beads..... 189
Figure 4.4-9 iMGL cells express inflammatory mediators 190
Figure 4.4-10 Macrophages express inflammatory mediators..... 192
Figure 4.4-11 Macrophage temporal expression of inflammatory mediators..... 194
Figure 4.4-12 IFNy enhances and supresses different LPS induced genes..... 195

Figure 4.4-13 Tolerisation superinduces Nurr1 whilst repressing inflammatory cytokines 196
Figure 4.4-14 IFNy treatment of tolerized cells promotes a pro-inflammatory phenotype 198
Figure 4.4-15 Schematic diagram of a Nurr1 frameshift mutation which generates Nurr-1a 199
Figure 4.4-16 Nurr1 and Nurr-1a are present in human total brain RNA 200
Figure 4.4-17 Cloning human Nurr-1a from total brain RNA 201
Figure 4.4-18 Human Nurr1 and Nurr-1a inserts were present in pINDUCER20 viral vector after cloning 202
Figure 4.4-19 Human Nurr1 and Nurr-1a lentiviruses transduce HeLa cells 203
Figure 4.4-20 Human PBMC differentiated macrophages are minimally transduced by GFP 204
Figure 4.4-21 Human PBMC differentiated macrophages are minimally transduced by Nurr1 and Nurr-1a viruses 205
Figure 4.4-22 Doxycycline significantly increases IL-10 expression in macrophages 206
Figure 4.4-23 Human PBMC differentiated macrophages show Nurr1 and Nurr-1a gene expression after lentiviral transduction 207
Figure 4.4-24 Viral transduction has no clear effect on inflammatory gene expression 209
Figure 4.4-25 Site Directed Mutagenesis of K91 in lentiviral vectors 210
Figure 4.5-1 Immune tolerized cells vs pre-treatment with IFNy 215
Figure 5.2-1 Previous and current suggested models of Nurr1 and Nurr-1a SUMOyaltion. 221
Figure 5.2-2 Nurr1 inflammatory feedback mechanism in healthy and diseased states 225

List of Tables

Table 1.4-1 Natural and synthetic Nurr1 ligands 28
Table 2.1-1 Chemicals and reagents used 47
Table 2.1-2 Plasmids 49
Table 2.1-3 Antibodies 51
Table 2.2-1 Cells used 52
Table 2.3-1 Reverse Transcription reaction 55
Table 2.3-2 Primers used for cloning 57
Table 2.3-3 PCR reaction 57
Table 2.3-4 Reaction conditions 58
Table 2.3-5 Restriction digest reaction 58
Table 2.3-6 Ligation Reaction 59
Table 2.3-7 Blunt end ligation Reactions 60
Table 2.3-8 Primers for Site-Directed Mutagenesis 62
Table 2.4-1 Manual Primer and probe Design Parameters 64
Table 2.4-2 RT-PCR reaction mix 64
Table 2.4-3 RT-qPCR reaction profile 64
Table 2.5-1 Transfection conditions 67
Table 2.5-2 Pull-down reagent recipes 68
Table 2.5-3 Western blot reagents 70
Table 2.5-4 PLA recipes 71
Table 2.6-1 ICC Reagents 72
Table 2.7-1 attB PCR primers 73
Table 2.7-2 BP reaction reagents 74
Table 2.7-3 LR reaction reagents 75
Table 2.7-4 Viral cloning colony PCR primers 75
Table 2.8-1 Macrophage and iMGL cell ICC 80
Table 2.8-2 SYBR green reaction mix 81
Table 2.8-3 RT-qPCR reaction profile 81
Table 2.8-4 RT-qPCR human primers and probes 82
Table 2.9-1 ICC reagents 85
Table 2.9-3 ICC antibodies 86
Table 2.9-4 Media composition 87
Table 2.9-5 Neuronal induction reagents 88
Table 2.9.6 ICC reagents 89
Table 3.2-1 Concentration of ligands 111

Declaration

I declare the research presented in this thesis is original work carried out by the author Jade Edey, PhD student at the University of Nottingham between August 2020 and July 2022. All work was performed by the author under the supervision of Associate Professor Andrew Bennett and Associate Professor Gareth Hathway.

Chapter 1
Introduction

1.2 Nuclear receptors

Nuclear receptors (NRs) are a family of transcription factors regulated by steroids and other lipid soluble signals. There are forty-eight known NRs encoded in the human genome many of which have identified ligands (de Vera, 2018, Germain et al., 2006). There are several NRs which do not have identified natural ligands, these are termed "orphan receptors" (Burris et al., 2012). Additionally, there is another category of NRs known as "adopted" which were initially thought to be orphan-type but now have reported ligands; however whether or not the function of these receptors is ligand regulated remains unclear (de Vera, 2018). Six evolutionary groups of nuclear receptors were classified by their sequence alignment and phylogenetic tree construction (Germain et al., 2006). These are listed in Table 1.2-1. Of particular interest throughout this thesis is the NR4 family, specifically Nurr1 and its splice variant Nurr-1a (see section 1.4), which were initially considered to be orphan nuclear receptors but are now mostly thought of as adopted. They are targets with increasing research into their therapeutic manipulation in multiple diseases including those with a neurodegenerative aetiology (de Vera, 2018, Maxwell and Muscat, 2006).

Group	Receptors	Status	Association with disease
NR1	TRα/β (NR1A1-2)	Endocrine	Hyper/hypothyroidism, mutations can lead to susceptibility to autoimmunity (Davies et al., 2005).
	RARα/β/γ (NR1B1-3)	Endocrine	Targets for treatments of disorders such as Type 2 diabetes, high cholesterol, immune disorders and cancer.
	PPARα/β/γ (NR1C1-3)	Adopted	Metabolic disorders – targets for pharmacological treatment of diabetes/dyslipidaemia (Wagner and Wagner, 2020).
	Rev-erbα/β (NR1D1-2)	Adopted	Involved in the regulation of circadian rhythms/metabolism (Uriz-Huarte et al., 2020).
	RORα/β/γ (NR1F1-3)	Adopted	Inactive in breast/prostate cancer; target for autoimmune disorders. Implicated in development of colorectal cancers.
	LXRα/β (NR1H2-3)	Adopted	Cholesterol metabolism, inflammation, autoimmunity and cancer (Bilotta et al., 2020).
	FXRα/β (NR1H4-5)	Adopted	Gastrointestinal diseases (Ding et al., 2015).
	VDR (NR1I1)	Endocrine	Mutations associated with rickets, important in intestinal homeostasis (Sun and Zhang, 2022).
	PXR (NR1I2)	Adopted	Chronic liver disease (Sayaf et al., 2021).
	CAR (NR1I3)	Adopted	Governs detoxifying mechanisms, important in the response to stress (Oliviero et al., 2020).
NR2	HNF4α/β (NR2A1-2)	Adopted	Monogenic diabetes (Azizi et al., 2019).
	RXRα/β/γ (NR2B1-3	Adopted	Target for manipulation in AD, PD and MS (Sharma et al., 2022).
	TR2/TR4 (NR2C1-2)	Adopted	Cancer, metabolic syndrome, cardiovascular diseases, fertility, and brain development (Lin et al., 2014)
	TLX (NR2E1)	Orphan	Neurological disorders and brain tumours (Sun et al., 2017).
	PNR (NR2E3)	Endocrine	High expression correlates with good breast cancer outcome.
	COUP-TFI/II (NR2F1-2)	Orphan	Expressed in prostate tumours.
	EAR2 (NR2F6)	Orphan	Expressed highly in lymphoma/colorectal tumours.
NR3	ERα/β (NR3A1-2)	Endocrine	Implicated in breast/ovarian cancer.
	ERRα/β/γ (NR3B1-3)	Adopted	Increased expression in breast cancers, inhibits growth of prostate cancer cells.
	GR (NR3C1)	Endocrine	Target for Cushing's syndrome and inflammatory disease (Caratti et al., 2015).
	MR (NR3C2)	Endocrine	Stress, cognitive and behavioural functions (Paul et al., 2022).
	PR (NR3C3)	Endocrine	Breast cancer (Azeez et al., 2021).
	AR (NR3C4)	Endocrine	Androgen insensitive syndrome, prostate cancer, and spinal bulbar muscular atrophy (Matsumoto et al., 2013)
NR4	NGFI-B/Nur77 (NR4A1)	Adopted	Activated in pancreas, colon and liver cancers. Potential target for treatment of neurodegenerative disease.
	NURR1 (NR4A2)	Adopted	Activated in bladder and lung cancers. Potential target for treatment of neurodegenerative disease and schizophrenia.

	NOR-1 (NR4A3)	Orphan	Inactivated in nasopharyngeal carcinoma, aberrant expression in metabolic disorders.
NR5	SF1 (NR5A1)	Adopted	Mutations have been associated with disorders of gonadal and adrenal function (El-Khairi and Achermann, 2012).
	LRH1 (NR5A2)	Adopted	Activated in pancreatic/breast cancers. Target for treating diabetes and metabolic disease.
NR6	GCNF (NR6A1)	Orphan	Expression lower in breast cancer, indicates susceptibility to anticancer drug trabectedin.
NR0	DAX-1 (NR0B1)	Orphan	Promotes cervical cancer growth, associated with adrenal hypoplasia congenita and hypogonadotropic hypogonadism.
	SHP (NR0B2)	Orphan	Increased expression in hepatocellular carcinomas.

Table 1.2-1: Classification of Nuclear receptors.

Nuclear receptors classified by nomenclature and ligand status with examples of their reported involvement in various pathologies. Biology and disease associations described by De Vera et al (2018) or Germain et al (2006) unless referenced otherwise.

Typically, activation of NRs induces a conformational change which recruits coactivators. Ultimately leading to the regulation of genes involved in a variety of biological processes including growth, metabolism, differentiation and inflammation. Transcriptional modulation by NRs occurs through several distinct mechanisms including both activation and repression; which can be ligand dependent, independent, and can involve transrepressive mechanisms (Germain et al., 2006). Primarily NRs function as transcription factors in the nucleus however some are also found to regulate cellular activity within the cytoplasm. Such as non-nuclear activation of the oestrogen receptor which underlies the migration and growth responses of endothelial cells to oestrogen (Wu et al., 2011). Due to the essential roles played by NRs in a plethora of vital cellular processes, they provide interesting targets for therapeutic manipulation during disease.

1.2.1 Structure of Nuclear receptors

NRs are comprised of a common modular structure consisting of five distinct regions (A/B-F). The F region is not present in all NRs, it comprises the C-terminus and its function is poorly understood. The amino N-terminal region (A/B) is highly variable and contains the activation function 1 domain (AF-1) which, in contrast to the activation function 2 domain (AF-2) located in the ligand binding domain (LBD), can mediate its effects through a ligand-independent manner (Germain et al., 2006). The AF-1 domain is also reported to be the target site of post-translational modifications (PTMs), including phosphorylation and SUMOylation (Germain et al., 2006, Walther et al., 2005, Poukka et al., 2000, Ohshima et al., 2004). Additionally, this region can interact with co-regulators, and has also been shown to synergise or communicate with the C-terminus to mediate its activity (Benecke et al., 2000).

The AF-1 region is followed by a highly conserved DNA binding domain (DBD), referred to as the C region, and a subsequent hinge region (D). It is through this domain that NRs recognise and bind to specific sequences known as hormone response elements (HRE) (Kumar et al., 1986, Sever and Glass, 2013). Crystallographic and nuclear magnetic resonance (NMR) studies of the glucocorticoid and oestrogen receptors revealed the DBD consists of sixty-six residues, a highly conserved core comprised of two zinc finger motifs and a COOH extension containing T and A boxes; important in monomeric DNA binding (Luisi et al., 1991, Schwabe et al., 1993). Each zinc finger has an alpha helix and at the base there are sequence elements known as P and D boxes; which are reported to contribute to response element specificity and half site spacing (Umesono and Evans, 1989).

The hinge region connects the DBD with the LBD and serves to allow their rotation. It is poorly conserved and may allow the DBD and LBD to adopt different conformations in order to synergise or avoid steric hinderance (Zwart et al., 2010). In some NRs this region is reported to contain nuclear localisation signals (NLS) and thus can regulate NR subcellular distribution (Tanner et al., 2010, Burns et al., 2011).

The LBD of NRs is functionally complex and is comprise of four surfaces: a dimerisation surface, ligand binding pocket, coregulator binding site and the AF-2 which mediates ligand-dependent transactivation (Germain et al., 2006). The ligand binding pocket is mostly lined with hydrophobic residues, and its specificity is partly determined by the shape and size of the pocket (Germain et al., 2004). In orphan receptors, this pocket can be occupied by bulky hydrophobic side chains or completely enclosed (Wang et al., 2003, Sablin et al., 2003). The AF-2 region is allosterically controlled by ligand binding, where it undergoes a conformational change exposing an interaction surface for coactivators to bind to (Boitier et al., 2003).

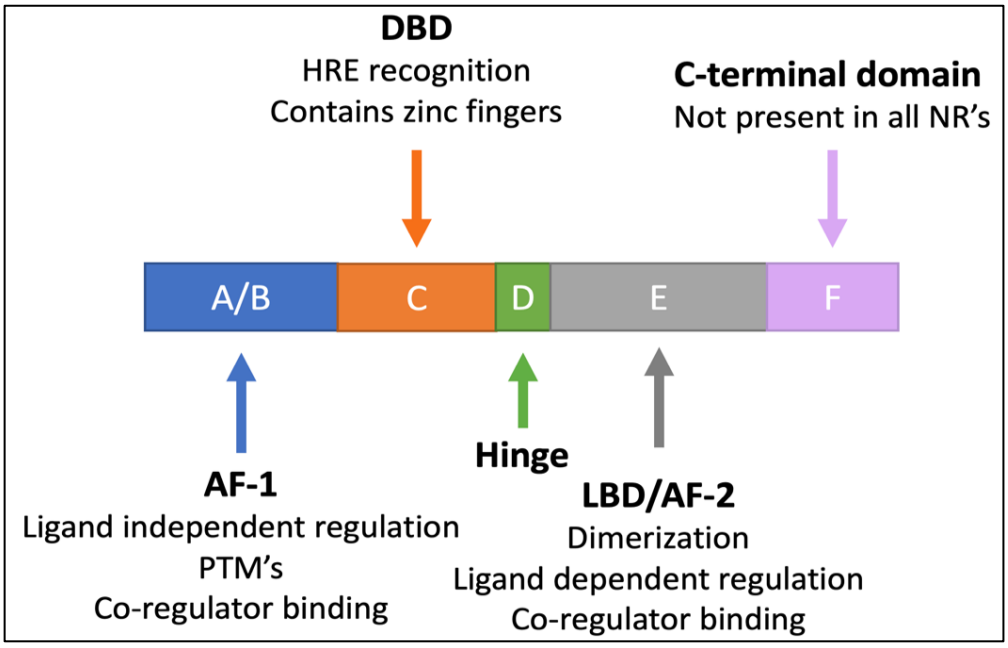


Figure 1.2-1 Nuclear Hormone Receptor structure

Schematic representation of nuclear receptor domains with their key functions listed. N-terminal region (A/B) contains the activation function 1 (AF-1) domain, followed by the DNA binding domain (DBD) which is linked to the ligand binding domain (LBD) and AF-2 through a flexible hinge region. The F region is located within the C-terminus. *Abbreviations: NRs, nuclear receptors; HRE, hormone response element; PTMs, post-translational modifications.*

1.2.2 Receptor subtype

NRs exist as monomers, homodimers, or heterodimers which recognise specific HREs (Sever and Glass, 2013). Receptors can be divided into four classes depending on their mode of action. Type I NRs, are steroid receptors which are ligand activated and undergo homodimerisation allowing them to bind to inverted HRE repeats (Sever and Glass, 2013) (Khorasanizadeh and Rastinejad, 2001). Type II are Retinoic X receptor (RXR) heterodimers such as Liver X Receptors (LXRs) or Peroxisome Proliferator Activator Receptor (PPAR) which require dimerisation with RXR for activation. In the absence of ligand binding RXR can still bind DNA and recruit co-repressors to repress gene expression (Chen and Evans, 1995)

(Watson et al., 2012, Sever and Glass, 2013). Type III NRs are homodimeric receptors, some of which can be orphan, they bind to direct HRE repeats and have highly constitutive gene regulatory functions (Mangelsdorf and Evans, 1995). Lastly, type IV NRs can function as both monomers and dimers. They can also be orphan receptors and only bind to a single half-site HRE (Mangelsdorf et al., 1995, Sever and Glass, 2013).

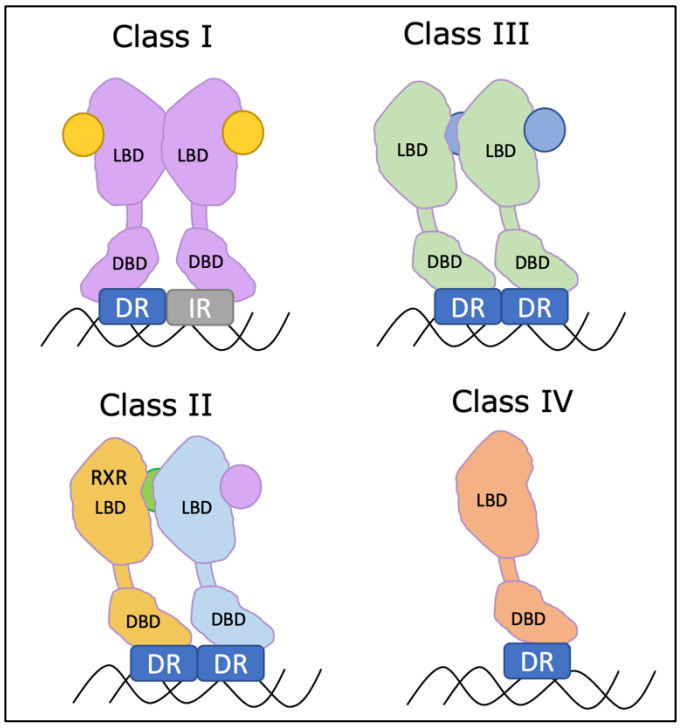


Figure 1.2-2 Classes of Nuclear hormone receptor

Schematic representation of nuclear receptor classes Type I–IV defined by their mode of action. Class I, steroid receptors; Class II, RXR heterodimers; Class III, homodimers; and Class IV, monomeric receptors (frequently orphan receptors). *Abbreviations: LBD, ligand binding domain; DBD, DNA binding domain; DR, direct repeat; IR, inverted repeat.*

1.2.3 Nuclear receptor transcriptional regulation

NRs are highly regulated and can control transcription through several distinct mechanisms including activation and repression. After recognition of specific HREs, NRs can recruit coactivators or

corepressors to mediate gene regulation. Transcriptional activation generally involves a ligand-dependent conformational change within the LBD of the NR (Bourguet et al., 2000). Resulting in the dissociation of a co-repressor complex and recruitment of a coactivator to modify chromatin structure and encourage the assembly of transcription initiation complexes at promoters. Additionally, transcriptional activation can occur in the absence of ligands, such as for the constitutive androstane receptor (CAR) or orphan/adopted NRs such as Nurr1 and NOR-1 (Greschik et al., 2002).

Transcriptional repression can occur through different individual mechanisms. Repression through unliganded receptors can involve corepressor complexes binding to NRs already bound to DNA which influences the structure of chromatin subsequently leading to compact transcriptionally inactive chromatin structures (Weston et al., 2003). Additionally, corepressors bound to NRs can also prevent them from binding to DNA (Ishizuka and Lazar, 2003). Direct repression by liganded receptors involves ligand bound NRs negatively regulating gene expression by binding to negative response elements such as the GC receptor (White et al., 2004, Chatterjee et al., 1989).

Lastly transrepression, where the activation of a gene is repressed by a nuclear receptor interacting with another protein. Transrepression can involve a variety of mechanisms which are promoter specific but do not involve sequence-specific DNA binding and so is often referred to as tethered. Transrepressive pathways can include the upregulation of the inhibitor of Nuclear Factor Kappa B (IκB), direct interaction with NFκB or Activator Protein-1 (AP-1), coactivator competition or inhibition, and inhibition of corepressor

clearance (Auphan et al., 1995, Saijo et al., 2009, Ghisletti et al., 2007, Pascual and Glass, 2006).

The process of transrepression is reported to modulate inflammation in the central nervous system (CNS) and the immune system in addition to the liver (Glass and Saijo, 2010, Huang and Glass, 2010). This has been reported for numerous nuclear receptors including Peroxisome Proliferator Activator Receptor's (PPARs) and Nurr1. In macrophages, PPARγ has been shown to prevent the transcription of proinflammatory cytokines, when exposed to an inflammatory stimulus, through transrepression of NFκB target genes. Ligand dependent PPARγ SUMOylation, facilitated by the E3 ligase PIAS1, promotes interaction with the NCoR/HDAC3 corepressor complex, preventing its clearance and therefore transrepressing NFκB mediated proinflammatory gene expression (Pascual et al., 2005).

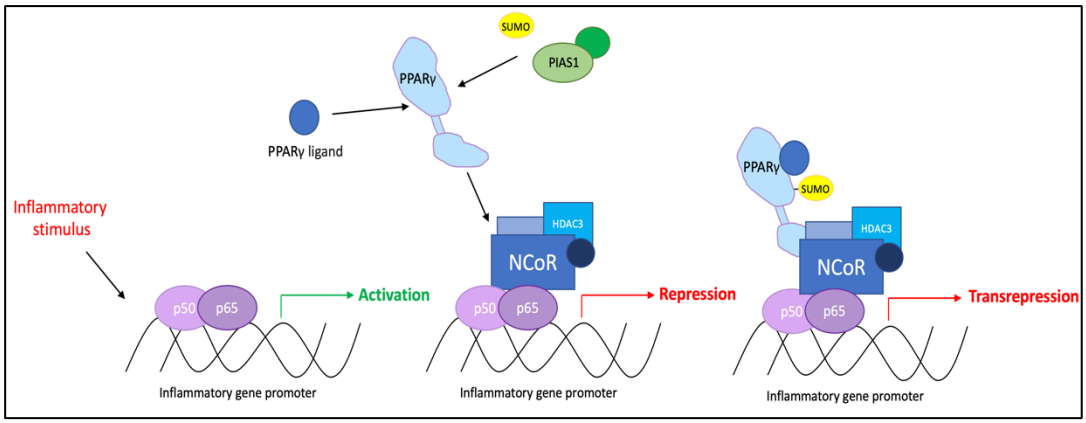


Figure 1.2-3 PPARγ transrepression

Schematic of PPARγ SUMO based transrepression. Ligand induced SUMOylation of PPARγ induces its recruitment to the NCoR repressor complex bound to inflammatory gene promoters, preventing NCoR clearance. *Abbreviations: NCoR, Nuclear Receptor Corepressor; PPARγ, Peroxisome Proliferator Activator Receptor; PIAS1, protein inhibitor of activated STAT 1; histone deacetylase 3, HDAC3.*

Nurr1 has been reported to regulate inflammation through a different transrepressive mechanism in microglia and astrocytes

(Saijo et al., 2009). The mechanism proposed suggests SUMOylated Nurr1 directly interacts with the p65 subunit of the NFκB transcription factor on pro-inflammatory gene promoters. This direct interaction is preceded by PIASg dependent SUMOylation of Nurr1, and glycogen synthase kinase-3 beta (GSK3β) phosphorylation of the p65 subunit. Nurr1 bound to NFκB then recruits the CoREST repressor complex in a Nemo-like kinase (NLK) phosphorylation dependent manner, which then actively clears the p65 from the target promoter. This was demonstrated in BV2 and RAW264.7 cells using an iNOS promoter target (Saijo et al., 2009). Additionally, HDAC1 is reported in the corepressor complex and is known to regulate acylation of the NFκB p65 subunit which governs transcription; therefore, it may promote p65 clearance from the promoter, contributing to the anti-inflammatory effects (Ashburner et al., 2001).

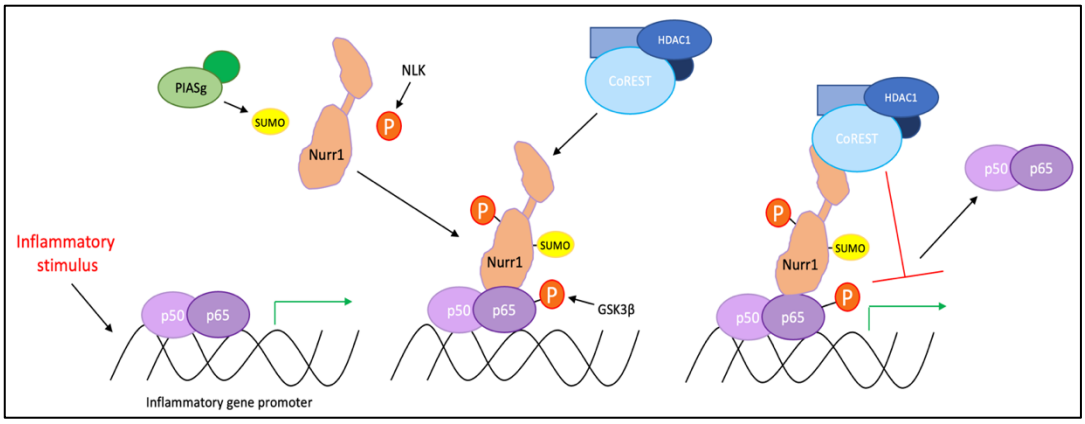


Figure 1.2-4 Nurr1 transrepression

Schematic of Nurr1 SUMO based transrepression. Inflammation induced SUMOylation of Nurr1 by PIASg precedes Nurr1 binding to p65 subunit. SUMOylated Nurr1 recruits CoREST corepressor complex which actively clears p65 from the target promoter. *Abbreviations: Nurr1, Nuclear Receptor Related protein 1; PIASg, protein inhibitor of activated STAT gamma; NLK, nemo-like kinase; GSK3β, glycogen synthase kinase-3 beta; CoREST, Corepressor for element-1-silencing transcription factor.*

1.2.4 Nuclear receptor regulation through PTMs

PTM is the modification of proteins following transcription and translation. They are mostly enzyme catalysed involving phosphatases, ligases, kinases and transferases which work to add or remove proteins, lipids and sugars to/from a target. Common modifications of NRs and coregulatory proteins include phosphorylation, acylation ubiquitination and SUMOylation. It is thought crosstalk between these PTMs are largely responsible for the diverse regulation of NRs (Wu and Chiang, 2009). These mechanisms are important for the precise, responsive and cell specific regulation of NRs, and are thought to be the primary mode of action for orphan NRs (Berrabah et al., 2011).

Phosphorylation is known to activate some NRs irrespective of ligand binding, in particular orphan NRs (Berrabah et al., 2011). However, it can act in a ligand-dependent fashion to activate NRs, induce DNA dissociation or decrease ligand affinity (Bastien and Rochette-Egly, 2004). This has been observed for the Steroidogenic factor 1 (SF-1) where phosphorylation of a serine residue within its AF-1 domain is reported to be crucial for cofactor recruitment and the activity of the receptor (Hammer et al., 1999). Phosphorylation sites are frequently located in the A/B region but can also be found in both the DBD and LBD (Delmotte et al., 1999, Germain et al., 2006, Bastien and Rochette-Egly, 2004). Ubiquitination has a vital role in the tagging of proteins such as NRs for proteasomal degradation (Alarid, 2006), and therefore can result in the inhibition of ligand dependent hormonal signalling (Lee and Lee, 2012).

Nuclear receptor SUMOylation is largely considered a repressive function and can mediate its repression through a variety of mechanisms (Glass and Saijo, 2010) (Gill, 2005). One of which

inhibits NR activation through the prevention of receptor dimerisation. This was demonstrated by Venteclef et al, who revealed RXRs were not recruited to SUMO (small ubiquitin like modifier) modified LXRs, therefore dimerisation and subsequent activation was inhibited (Venteclef et al., 2010, Treuter and Venteclef, 2011). SUMOylation can also change the intranuclear localisation of nuclear receptors, moving the receptors away from their target genes in order to dampen transcriptional activation. This was demonstrated for the liver receptor homologue-1 (LRH-1) and steroidogenic factor 1 where SUMOylation relocates the NRs to specific subnuclear domains such as promyelocytic leukaemia protein (PML) bodies where they are unable to access chromatin (Chalkiadaki and Talianidis, 2005, Lee et al., 2005).

Additionally, cross talk between SUMOylation and other PTMs can result in inhibitory mechanisms, such as the antagonistic relationship of ubiquitin and SUMO (Hunter and Sun, 2008). Ubiquitin targets the transcriptional inhibitor known as inhibitor of kappa B (IκB) for degradation, however SUMOylation can block this degradation which keeps NFκB sequestered in an inactive state in the cytoplasm (Desterro et al., 1998). SUMOylation is also reported to cause coactivator dissociation and corepressor recruitment (Treuter and Venteclef, 2011). Lastly, as suggested in the aforementioned transrepression mechanisms of PPARγ and Nurr1, SUMOylation can generate a new interaction surface on NRs which promotes the recruitment of corepressor complexes (Ouyang et al., 2009, Ouyang and Gill, 2009, Pascual et al., 2005, Saijo et al., 2009).

1.3 SUMOylation

SUMOylation is a PTM where a small ubiquitin-related modifier (SUMO) becomes covalently attached to a target protein via an iso-peptide link with a lysine residue (Josa-Prado et al., 2019, Rytinki et al., 2009). The SUMO family of proteins are highly conserved in eukaryotes and share both a likeness in conjugation and structural similarities with ubiquitin (Capili and Lima, 2007). However, unlike ubiquitination which targets proteins for proteasomal degradation, SUMOylation shares no overlapping functions. Instead, evidence suggests SUMO modification may even act antagonistically towards ubiquitin degradation; blocking modification of the same lysine (Melchior, 2000, Sentis et al., 2005, Desterro et al., 1998). The functional role of SUMOylation is extremely diverse, it is involved in transcription, subcellular localisation and DNA repair (Hardeland et al., 2002, Mahajan et al., 1997). Its reversible nature allows SUMOylation cycles to be carried out indefinitely throughout the cell (Dohmen, 2004).

1.3.1 SUMO isoforms

There are four mammalian SUMO isoforms highly conserved in all eukaryotes. SUMO2 and SUMO3 share 97% similarity, differing only by three N-terminal residues (Tatham et al., 2001). Additionally, antibodies cannot distinguish between the two and so they are frequently referred to as SUMO2/3 (Josa-Prado et al., 2019). SUMO2/3 share 46% similarity with SUMO1 (Gareau and Lima, 2010). Unlike SUMO1, SUMO2/3 possess a conserved lysine residue (K11) which readily enables them to form poly-SUMO chains (Tatham et al., 2001). Despite the absence of this internal lysine, proteomic analyses have revealed SUMO1 may contain additional motifs which can promote chain formation (Hendriks et al., 2014,

Hendriks and Vertegaal, 2016). These three isoforms all require COOH terminal processing to yield mature SUMO capable of protein conjugation. SUMO4 shares an 87% similarity with SUMO2/3, and also requires processing. However, the SUMO4 precursor protein includes a proline residue (P90) which has been reported to limit its processing (Owerbach et al., 2005). Under normal physiological conditions SUMO4 is rapidly degraded, however in serum deprived cells it has been shown to conjugate proteins involved in the stress response (Wei et al., 2008).

SUMOs 1-3 are expressed throughout eukaryotic cells whilst SUMO-4 has only been discovered in renal, pancreatic and immune cells, in addition to the placenta during development (Baczyk et al., 2017). Subcellularly, SUMO2/3 are similarly distributed throughout the nucleoplasm unlike SUMO1 which is uniquely distributed to the nuclear envelope and nucleolus (Ayaydin and Dasso, 2004). At rest there is a large repertoire of unconjugated SUMO2/3 but little SUMO1 and it is thought that SUMO2/3 conjugation may be involved in the cellular response to environmental stress (Ayaydin and Dasso, 2004, Saitoh and Hinchey, 2000).

1.3.2 SUMOylation cycle

The enzymes that catalyse the SUMOylation cycle are conserved in humans. All cycles involve the same activating (E1) and conjugating (E2) enzymes, but a different SUMO ligase (E3). Initially, SUMO precursors are cleaved by SUMO-specific proteases (SENPs) into mature SUMO (Yeh et al., 2000). This involves the removal of 4, 11 and 2 C-terminal amino acids from SUMO1, SUMO2 and SUMO3 respectively which exposes a di-glycine motif facilitative of SUMO conjugation (Mukhopadhyay and Dasso, 2007).

Conjugation to specific lysine residues begins with E1 and a mature SUMO isoform. E1 is a heterodimer comprised of SUMO activating enzyme subunit 1 (SAE1, also known as Aos1p) and 2 (SAE2, also known as Uba2p), which uses ATP to catalyse the formation of a thioester bond. In a two-step reaction 1) the C-terminal glycine of mature SUMO interacts with ATP forming SUMO-AMP, 2) followed by an interaction with a catalytic cysteine in the active site of SAE2, resulting in a thioester bond between SUMO and the E1 heterodimer (Lois and Lima, 2005, Johnson et al., 1997).

The activated SUMO is then transferred to E2 (Ubc9), forming a second thioester linkage. Executed by Ubc9 binding to E1 via a ubiquitin fold domain in SAE2 and forming its own thioester bond with SUMO (Truong et al., 2012, Wang et al., 2007). The catalytic cleft of Ubc9 can directly interact with target proteins through sequence and structural motifs. It is therefore involved in target specificity and, in few cases, is adequate for direct ligation to the substrate provided that the lysine falls within a SUMO-conjugation motif (Pereira et al., 2011, Yunus and Lima, 2006, Bernier-Villamor et al., 2002). However, in the majority of cases E3 ligases are required to enhance the transfer of SUMO from E2 to the substrate by accelerating catalysis or improving substrate specificity. This is accomplished by correct positioning of the E2 enzyme for optimal transfer or by stabilising interactions between the substrate and SUMO-E2 (Yeh et al., 2000). Catalysing the conjugation of SUMO to the substrate protein via an iso-peptide bond to a specific lysine residue.

SUMOylation is a reversible process such that deconjugated SUMO can be returned to the free pool and partake in the cycle indefinitely. Similar to SUMO maturation, deconjugation is carried out by SENPS

which cleave the amide bond between SUMO and the target lysine (Gong et al., 2000, Xu and Au, 2005).

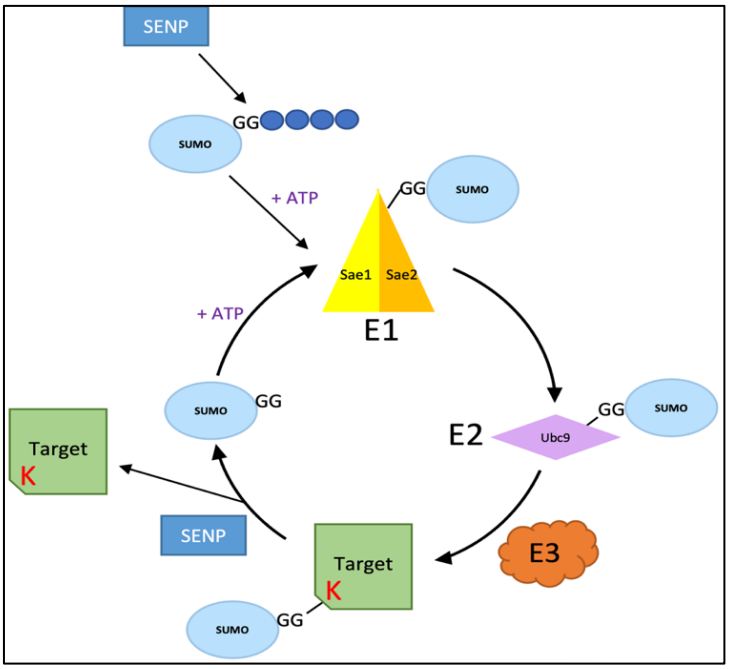


Figure 1.3-1 The SUMOylation cycle

Simplified schematic of the SUMO pathway. Mature SUMO is first generated by SENP proteins, then activated by E1 (SAE1/SAE2). SUMO is passed from E1 to E2 (Ubc9) before finally SUMO is conjugated to the substrate protein with the help of E3. SENPs can cleave SUMO from substrates to generate free mature SUMO. Diagram adapted from (Andreou and Tavernarakis, 2009). *Abbreviations: SAE1/SAE2, SUMO activating enzyme subunit 1 and 2; SENP, SUMO-specific proteases; ATP, adenosine triphosphate.*

1.3.3 E3 Ligases

The direct interaction between Ubc9 and the consensus motif of a substrate is relatively weak and therefore E3 ligases are required in many cases (Henley et al., 2014). Siz proteins were the first E3 ligases identified. They facilitated SUMOylation in *S. cerevisiae* (Johnson and Gupta, 2001). The equivalent in mammals is known as the protein inhibitor of activated STAT (signal transducer and activator of transcription) family of proteins (PIAS). In humans there are four genes encoding seven members, the genes are as follows:

PIAS1, PIAS2 (also known as PIASx), PIAS3 and PIAS4 (also known as PIASg).

The PIAS family all share a high level of sequence similarity within their N-terminal amino acids but vary in overall size. Each member is comprised of 4 structural motifs: N-terminal scaffold attachment factor-A/B/acinus/PIAS motif (SAP), PINIT motif, RING motif, and a SUMO interaction motif (SIM) (Duval et al., 2003, Hochstrasser, 2001, Tan et al., 2002, Rytinki et al., 2009). The RING domain forms a zinc finger of 30-40 residues. In combination with the C-terminus, the RING domain is responsible for facilitating the enzymatic activity of this family. It is accomplished through the RING domain binding to Ubc9 and its C-terminal to SUMO. This then positions Ubc9 in a conformation facilitative of SUMO transfer (Yunus and Lima, 2009).

Conversely, there are proteins identified as E3 ligase-like factors which do not contain a RING domain. One of which is the nuclear pore protein RanBP2, which directly interacts with Ubc9 forming a complex with SUMO enhancing transfer to the substrate (Pichler et al., 2002, Pichler et al., 2004, Flotho and Werner, 2012). Additionally human Topors have been shown enhance SUMOylation (SUMO1) of p53 in HeLa cells in a manner independent of its RING motif (Weger et al., 2005). Evidence suggests histone deacetylases (HDAC) may play a role to promote SUMOylation independent of deacetylation. HDAC4, HDAC7 and HDAC2 are reported to demonstrate E3 ligase-like ability. However, whether they are fully accepted as E3 ligases remains to be determined as they comprise a different structure and are thought to act by promoting SUMOylation rather than direct E3 ligase activity (Xu et al., 2010, Ghisletti et al., 2007).

The regulation and specificity of SUMOylation can be credited to the diversity of E3 ligases as to date E1 and E2 are singular complexes.

Therefore, distribution, specificity, and differential regulation of these E3 ligases are of great interest when researching SUMOylation.

1.3.4 SENPs

SENPs are responsible for maturing and deconjugating SUMO proteins in mammals. SENPs are C48 cystine proteases and share a conserved ~200 amino acid sequence in the C-terminal catalytic domain (Mukhopadhyay and Dasso, 2007). In humans, there are six different SENPs: SENP1-3 and SENP5-7. SENP4's sequence was found to correspond to SENP3 and therefore it was removed (Gong et al., 2000). SENPs can be regulated through environmental influences, transcriptional control, localisation, SENP-substrate binding and SENP activity (Li et al., 2008, Cheng et al., 2006, Yang et al., 2007). SENPs have varying specificities and subcellular localisations, for example SENP1-2 have broad specificities for SUMO1-3 and partake in both maturation and deconjugation predominantly in the nuclear envelope. Whereas SENP3 and SENP5 preferentially favour SUMO2/3 over SUMO1 and only function to deconjugate SUMO proteins from substrates mainly in the nucleolus but also in the nucleoplasm. SENP6-7 are mostly involved in poly-sumo chain editing in the nucleoplasm (Hickey et al., 2012).

It is noteworthy to add there are other specific proteases in mammals such as DeSUMOylating iso-peptidase 1 and 2 (DeSI-1/2) which localise to the cytoplasm (Shin et al., 2012). Or ubiquitin specific protease like 1 (USPL1) found in the nucleus, specifically in Cajal bodies (Schulz et al., 2012).

1.3.5 SUMO consensus motifs

SUMOylation occurs at lysine residues on target substrates, often these reside in the same minimal consensus motif ΨKxD/E. Where Ψ is an aliphatic residue; ideally I, L or V, and x is any residue (Johnson, 2004, Bernier-Villamor et al., 2002). This consensus sequence has been demonstrated to mediate direct interactions with SUMO conjugation enzyme Ubc9 and in few cases is sufficient for some substrate targeting (Sampson et al., 2001, Bernier-Villamor et al., 2002). The target protein with the specific SUMO consensus motif must adopt an extended conformation during the formation of complexes with Ubc9 which is favourable of SUMOylation, otherwise SUMO modification does not occur. Therefore, not all substrates which contain this motif are SUMOylated. The hydrophobic groove on Ubc9 facilitates the insertion of the acceptor lysine and permits recognition of the consensus motif through electrostatic and hydrogen bonding interactions between substrate residues flanking the acceptor lysine and Ubc9 (Bernier-Villamor et al., 2002). It is noteworthy to add that only approximately half of SUMOylated sites conform to this motif, therefore SUMO modification can occur at alternative sites (Hendriks et al., 2014, Rodriguez et al., 2001, Sampson et al., 2001).

Additional motifs include negatively charged amino acid dependent SUMO motifs (NDSMs) and phosphorylation-dependent SUMO motifs (PDSMs). PDSM's have a serine residue within the motif and are often referred to as the phospho-SUMOyl switch because they sequentially couple phosphorylation and SUMOylation. The conjugation is enhanced by phosphorylation as a basic patch on Ubc9 interacts with the phosphorylated serine side chain (Yang and Gregoire, 2006). It is thought NDSM's function in a similar mechanism where negatively charged residues downstream of the

consensus site interact with the same basic patch, promoting SUMOylation (Bernier-Villamor et al., 2002). This motif is observed in peroxisome proliferator-activated receptor gamma (PPARγ), where the consecutive phosphorylation and SUMOylation contributes to the negative regulation of PPARγs transactivation function (Yamashita et al., 2004).

1.3.6 SUMO interaction motifs

In addition to covalent modifications at lysine residues, a number of non-covalent low-affinity interactions are also be made. These occur via SUMO interaction motifs (SIM's) which are found in SUMO enzymes and substrate proteins (Namanja et al., 2012, Henley et al., 2014). There are many SIM variants often differing in charge cluster, orientation and SUMO preference. However, interactions are principally mediated by an interaction motif comprised of a hydrophobic core of 3-4 aliphatic residues flanked by negatively charged acidic amino acids (Kerscher, 2007, Song et al., 2004). The hydrophobic core of SIM's bind to a patch on the surface of the SUMO protein, specifically between the α-helix and β-sheet. The flanking negatively charged residues dictate SUMO isoform preference and influence the binding affinities. SIM's can bind SUMO in different orientations as they extend the β-sheet by one β-strand in either orientation (Jardin et al., 2015, Kerscher, 2007).

SIM's contribute to the diversity of SUMOylation through multiple functions. They can be accountable for recognising SUMOylated substrates, demonstrated by the interaction of RanBP2 and SUMOylated RanGAP1 (Song et al., 2004). In some substrates such as TDG (thymine DNA glycosylase), SIM's are found to promote SUMO modification by first interacting non-covalently followed by covalent conjugation (Meulmeester et al., 2008, Kerscher, 2007,

Takahashi et al., 2005). In other substrates SIM's drive complex assembly and/or recruitment, as seen in some DNA repair machinery for double stranded breaks (Psakhye and Jentsch, 2012).

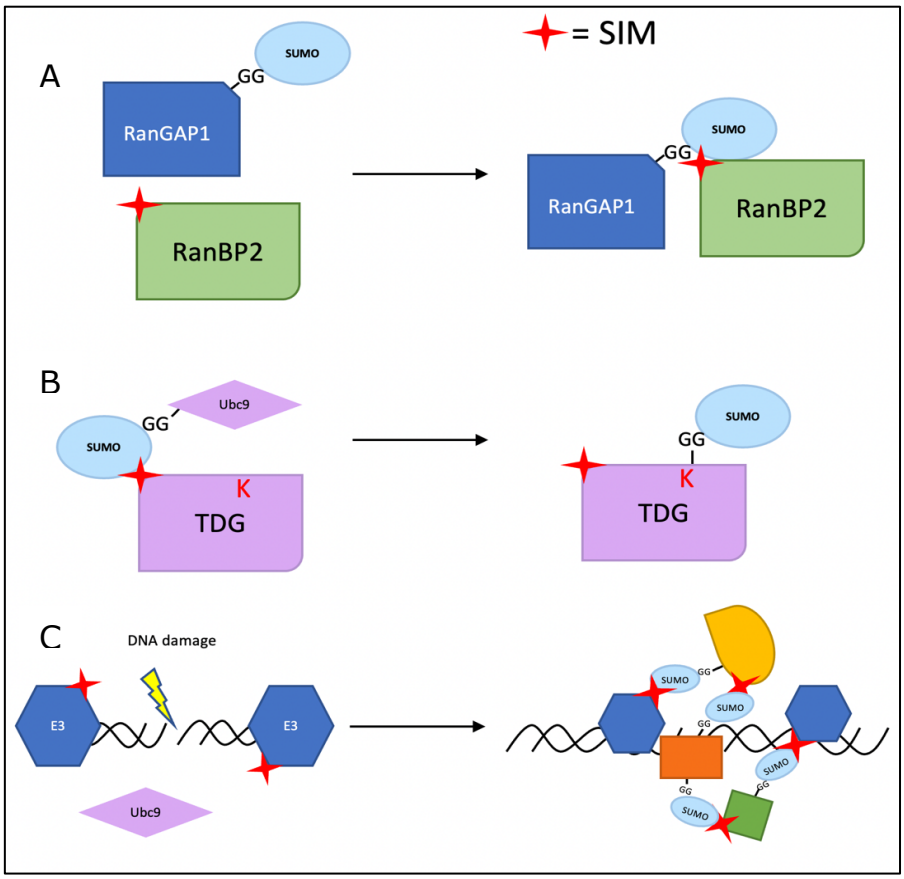


Figure 1.3-2 SUMO-SIM diversity

(A) SIM's can be used to recognise SUMOylated targets. (B) SIM's can mediate the SUMOylation of a substrate by first promoting a non-covalent interaction followed by covalent SUMO conjugation. (C) SIM's can drive the assembly of complexes and recruitment of proteins, as demonstrated after DNA damage. *Abbreviations: SIM, SUMO interacting motif; RanGAP1, Ran GTPase-activating protein 1; RANBP2, RAN binding protein 2; TDG, thymine DNA glycosylase.*

1.3.7 SUMOylation in disease

SUMOylation is critical for numerous cellular processes, including normal synaptic and neuronal functioning. Therefore, it is unsurprising that the dysregulation of this PTM has been associated with proteins implicated in human diseases such as cancer,

Amyotrophic Lateral Sclerosis (ALS), Parkinson's and Alzheimer's disease (AD). However, as with many diseases, it is unknown if dysregulated SUMOylation is causative or symptomatic.

In multiple human cancers increased Ubc9 levels are observed, and overexpression can be found to increase cancer cell growth (Mo et al., 2005). Additionally, SUMOylation can regulate the action of some tumour suppressor proteins such as P53, therefore any alterations can cause dysregulation and influence cancer states (Seeler et al., 2007).

Mutations in the superoxide dismutase 1 (SOD1) gene have been associated with at least twenty percent of familial ALS cases and it is believed that the aggregation of this mutant SOD1 is a primary factor in disease pathogenesis (Boillée et al., 2006, Gonzalez de Aguilar et al., 2007, Shaw and Valentine, 2007). Proteomic studies have identified a single SUMOylation site for human SOD1, lysine 75. This PTM is observed in both wild type and ALS associated mutant SOD1 (Fei et al., 2006). Substituting lysine 75 for a non-SUMOylatable residue coincides with increased SOD1 aggregation, thus the lack of SUMOylation due to mutations in SOD1 may contribute to ALS pathogenesis (Fei et al., 2006).

There are three known characteristics of PD which have been associated with SUMOylation, the first is the generation of Lewy bodies in the cytosol of dopaminergic neurons. These inclusions are comprised of a natively unfolded protein α-synuclein which is a known SUMO substrate (Dorval and Fraser, 2006). Whilst Lewy bodies themselves are considered non-toxic; oligomerisation can result in toxic fibril structures that insert themselves into neuronal plasma membranes. This can ultimately result in the toxic α-synuclein leaking into the brain parenchyma where it functions as

damage-associated molecular patterns (DAMP's) to activate myeloid phagocytes and subsequent inflammation (Fusco et al., 2017). Studies concerning the impact of SUMO modification on α-synuclein aggregation are controversial, some rat models of PD have suggested that SUMOylation reduced aggregation and toxicity, whilst others suggest it increases aggregation (Oh et al., 2011, Dorval and Fraser, 2006).

Mutations in the transcriptional regulator DJ-1 are reported to be responsible for 1-2% of early onset PD cases, and one of its major roles is cellular response to oxidative stress (Eckermann, 2013, Taira et al., 2004). A relatively rare DJ-1 mutation, L166P, leads to the aberrant SUMOylation of DJ-1 and protein solubility thus contributing to protein aggregation and reduced oxidative stress response (Shinbo et al., 2006, Moore et al., 2003). Finally, mutations in the PARK2 gene which encodes the ubiquitin E3 ligase PARKIN are associated with the most common autosomal recessive form of PD. PARKIN is found in Lewy bodies and interacts noncovalently with SUMO-1 which increases its E3 ligase activity and nuclear transport. Therefore this interaction with SUMO-1 plays a regulatory role however it is unknown if or how this interaction is related to PD (Um and Chung, 2006).

AD is the most common age related neurogenerative disease and it is thought to be credited to the formation of amyloid plaques and neurofibrillary tangles. Plaques are generated by the incorrect cleavage of the Amyloid Precursor Protein (APP) which results in insoluble amyloid-β (Aβ), and neurofibrillary tangles are caused by hyperphosphorylated Tau (LaFerla et al., 2007). Studies regarding the role of SUMOylation in the formation of Aβ often have opposing views, with some suggesting that overexpression of SUMO can lead

to an increase in Aβ (Dorval et al., 2007, Yun et al., 2013), whilst others report that SUMOylation can cause a decrease in Aβ aggregates (Zhang and Sarge, 2008, Hoppe et al., 2013). In heterologous cells Tau is SUMOylated predominantly at a Lysine-340 site. Furthermore Lysine-340 is also a site of ubiquitination and, as briefly stated earlier, these PTM's may act antagonistically towards each other (Dorval and Fraser, 2006). Thus, any dysregulation in the SUMOylation of Tau at this site could lead to an increase in ubiquitination. Tau SUMOylation can be increased by phosphatase inhibition thus phosphorylation is a regulation mechanism. In the TG2576 APP mouse model of AD phosphor-tau aggregates stain positive for SUMO-1, linking tau-SUMOylation to the pathogenesis of AD (Takahashi et al., 2008). However, this has not been recapitulated in post mortem human brains (Pountney et al., 2003). Due to conflicting results from these studies it is difficult to conclude the effects of aging on SUMOylation and the subsequent impact this may have on target proteins.

1.4 Nurr1

Nuclear Receptor Related protein-1 (Nurr1, also known as NR4A2) was first identified by Law et al., from a mouse brain cDNA library as a protein with an amino acid sequence closely related to that of Nur77 (Law et al., 1992). Nurr1 part of the nuclear receptor superfamily subgroup denoted NR4A, which includes Nur77 (NR4A1) and NOR-1 (NR4A3) (Maxwell and Muscat, 2006). The receptors are immediate early genes rapidly induced by multiple stimuli such as cAMP, inflammatory signals, growth factors and calcium (Maxwell and Muscat, 2006). Initially these receptors were considered to be orphan, as they had no identified endogenous ligands. However now Nurr1 and Nu77 are referred to as adopted, due to the recent identification of unsaturated fatty acids as potential ligands (de Vera et al., 2016, de Vera, 2018).

1.4.1 Structure and ligand binding

Nurr1 is considered to have an "adopted" nuclear receptor structure, absent of the canonical ligand binding pocket which is characteristic of many nuclear hormone receptors (de Vera, 2018). X-ray crystallography studies revealed the LBD of Nurr1 adopts a fold resembling that of an agonist bound receptor with two key features. Firstly, due to the tight packing of bulky hydrophobic residues, Nurr1 has no cavity for ligands to bind (Moras and Gronemeyer, 1998). Secondly, the classical hydrophobic coactivator binding cleft seen in other NRs is replaced with a charged surface. Suggesting Nurr1 is unable to recruit and interact with coregulators in the same way as other NRs (Wang et al., 2003).

However, despite this lack of space, a plethora of synthetic small molecule ligands have been developed which are reported to

modulate the activity of Nurr1. Using NMR chemical shift foot printing to map ligand binding, Kim et al., demonstrated a class of compounds including amodiaquine and chloroquine were able to bind to an epitope within the LBD of Nurr1 (Kim et al., 2015). Ordentlich et al., identified a ligand that could bind to the AF-1 domain of Nurr1 and enhance its transcriptional activity. The author also suggested 6-mercaptpurine (6-MP) might influence Nurr1 activity through the regulation of PTMs (Ordentlich et al., 2003). Additionally, Pramipexole is a Nurr1 modulator reported to upregulate its expression. Pan et al., demonstrated Pramipexole had a inductive effect on the expression of Nurr1 at the level of both transcription and translation through modulating the dopamine 3 (D3) receptor (Pan et al., 2005). There are a variety of other synthetic ligands reported for Nurr1, some of which are listed in Table 1.

Responsible for its switch from orphan to adopted status, is the more recent development which demonstrates the ability of Nurr1 to bind to fatty acids. De Vera et al., showed through solution NMR and mass spectrometry, that the ligand binding pocket of Nurr1 alternates between two or more conformations; allowing the pocket to open up and become accessible to docosahexaenoic acid (DHA) (de Vera et al., 2016). Interestingly the authors found the interaction epitope was similar to that of the synthetic ligand amodiaquine, suggesting that both natural and synthetic ligands bind to the same region and may activate the receptor in similar ways (Kim et al., 2015, de Vera et al., 2019). In addition, Rajan et al., reported prostaglandin E1 (PGE1) and its metabolite prostaglandin A1 (PGA1) to be natural ligands of Nurr1. The author shows PGE1/PGA1 can bind to the LBD of Nurr1 in the nanomolar range and activate the transcriptional function of Nurr1 in primary rodent cells (Rajan et al., 2020).

Ligand	Binding region	Mode of action	Model	Reference
Natural ligands				
PGE1/PGA1	LBD	Increases Nurr1 transcriptional activity	SK-NBE2(C) Primary rat coculture Rodent *in vivo*	(Rajan et al., 2020)
DHA	LBD	Decreases Nurr1 transcriptional activity	HEK293T MN9D	(de Vera et al., 2016, de Vera et al., 2019)
DHI	LBD	Increases Nurr1 transcriptional activity	JEG-3 Zebrafish *in vivo*	(Bruning et al., 2019)
Synthetic ligands				
AQ/CQ	LBD	Increases Nurr1 transcriptional activity	Primary rat microglia BV-2	(Kim et al., 2015)
6-MP	AF-1	Increases Nurr1 transcriptional activity	CV-1	Ordentlich et al., 2003)
C-DIM12	Coactivator binding site (LBD)	Increases Nurr1 transcriptional activity	PC12 MPTP mice N2A N27 BV-2	(Hammond et al., 2018, Hammond et al., 2015, De Miranda et al., 2015)
Pramipexole	D3 receptor	Increases Nurr1 expression	SH-SY5Y	(Smits et al., 2003, Pan et al., 2005)
BRF110	Nurr1:RXR (binds to RXR)	Increase Nurr1 transcriptional activity	Mice *in vivo*	(Spathis et al., 2017)

Table 1.4-1 Natural and synthetic Nurr1 ligands

1.4.2 Isoforms

The human Nurr1 gene is approximately 8.3Kb long and composed of 598 amino acids. Comprising eight exons and seven introns it has a molecular mass of 66kDa (Torii et al., 1999). There are several splice variants of Nurr1 which have been reported, credited to alternative splicing by cyclic adenosine monophosphate (cAMP)

responsive element-binding protein (CREB) regulated transcription co-activators (Amelio et al., 2009). Ichinose et al., through screening of human fetal brain DNA using a Nurr1 mouse cDNA probe, identified seven positive clones of Nurr1 (Ichinose et al., 1999). One of which denoted Transcriptionally-inducible nuclear receptor (TINUR) had been previously described, and was reported to be a result of alternative splicing in exon 3 generating a 63 amino acid truncation in the AF-1 domain (Okabe et al., 1995). In addition, the author reported the presence of Nurr-1a which, from this point on, will be the splicing variant of focus in this thesis.

Nuclear receptor related protein variant a (Nurr-1a) was first identified by Castillo et al., when characterising the organisation of the Nurr1 gene using a mouse genomic phage library (Castillo et al., 1997). Nurr-1a has the same exons 1-6 as Nurr1, however alternative splicing in exon 7 generates a frameshift resulting in an early stop codon and a 143 amino acid truncation from its C-terminus. Specifically, the LBD/AF-2 domain, resulting in a 455 amino acid coding sequence (Castillo et al., 1997, Michelhaugh et al., 2005). Castillo et al., show the presence of Nurr-1a in postnatal mouse brains through reverse transcription-PCR of total brain RNA. The authors reveal mRNA expression of both Nurr-1a and its full-length variant were highest at postnatal day 1, which decreased thereafter until the last sample reviewed at 4 weeks (Castillo et al., 1998b). Human Nurr-1a was first identified by Ichinose., who used mouse Nurr1 cDNA as a probe to screen a human fetal cDNA library (Ichinose et al., 1999). Nurr-1a was later identified in human adult ventral midbrain, in addition to rat midbrain again using reverse transcription-PCR (Michelhaugh et al., 2005).

Following the identification of Nurr-1a, there were few further studies which investigated its function or cellular expression. Castillo

et al., reported the transcriptional activity of Nurr-1a to be less than 50% than that of Nurr1 in NIH3TC cells using a monomeric Nurr1/Nur77 response element denoted B1A (5'-AAAGGTCA-3') in a thymidine kinase-chloramphenicol acetyltransferase reporter assay (Castillo et al., 1998b). Michelhaugh et al., then used the neuronal SK-N-AS cell line to demonstrate Nurr-1a activated the 3xNBRE (5'-AAAGGTCA-3') response element ~60-fold less than the full length Nurr1 (Michelhaugh et al., 2005). The most recent report regarding Nurr-1a similarly revealed that it activates the naturally occurring TH (TH) promoter, as well as the 3xNBRE reporter, significantly less than Nurr1 in SH-SY5Y cells. However, in HB1.F3 cells using the same two reporter constructs the authors revealed the luciferase activity produced by transfection of the reporters alone was repressed by the overexpression of Nurr1 and repressed even greater by Nurr-1a (Kim et al., 2013).

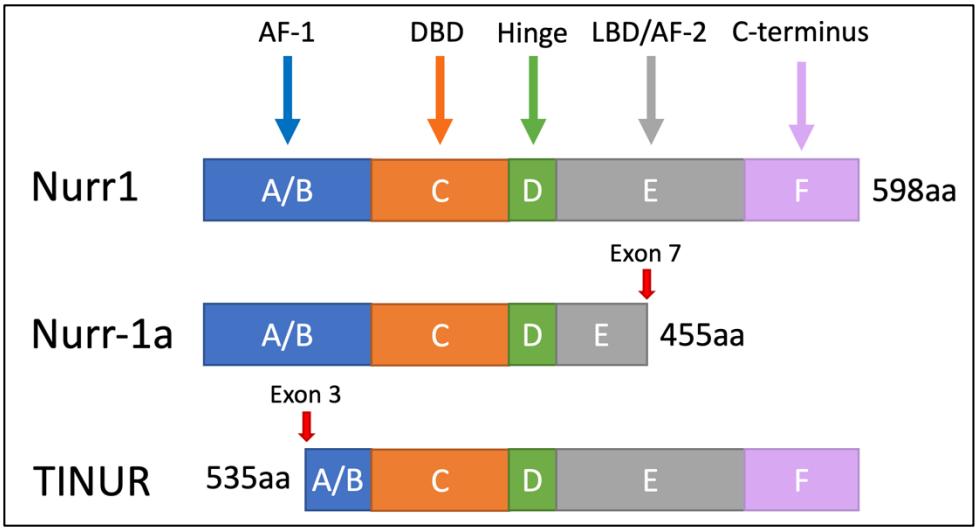


Figure 1.4-1 Schematic of Nurr1, Nurr-1a and TINUR

Simplified diagram of Nurr1, Nurr-1a and TINUR demonstrating truncated regions. *Abbreviations: AF-1, activation function 1; DBD, DNA binding domain; LBD, ligand binding domain; AF-2, activation function*

1.4.3 Dimerisation and response element binding

Nurr1 is a type IV NR meaning it can mediate its activity as both a monomer or dimer through binding to HREs on target genes and influencing transcription (Mangelsdorf et al., 1995, Sever and Glass, 2013). Nurr1 functions as a monomer by recognising and binding the classic NBRE motif (5'-AAAGGTCA-3'). It has been suggested that the monomeric activity of Nurr1 enables its constitutive transcriptional activation, however this is dependent on cell type (Castro et al., 1999).

Nurr1 can bind RXR and mediate its activity as a heterodimer, recognising a direct repeat element from the RAR-β gene promoter separated by 5 nucleotides (5'-GGTTCAccgaaAGTTCA-3') referred to as DR5. The 5 nucleotide spacer between the two hexametric half sites dictates (Perlmann and Jansson, 1995). Hetero dimerisation was shown to rely on the LBD, specifically an intact I box region; an interface previously verified as critical for dimerisation of NR both as homodimers and RXR heterodimers (Aarnisalo et al., 2002). In the absence of RXR ligands, heterodimerisation with RXR is reported to supress the constitutive activity of Nurr1 bound to the NBRE through the induction of a non-permissive conformation for co-activator interactors or due to steric hindrance (Perlmann and Jansson, 1995). In complexes with other NRs including retinoic acid receptor (RAR) and thyroid hormone receptor (TR), ligands cannot efficiently activate RXR. However, when in a heterodimer with Nurr1, RXR is efficiently activated by its cognate ligands and binds DR5 (Perlmann and Jansson, 1995, Forman et al., 1995) (Aarnisalo et al., 2002).

Lastly, Nurr1 can function as a homodimer by binding to the Nur response element (NurRE), consisting of everted repeats of the canonical NBRE motif separated by 6 nucleotides (5'-TGACCTTT-N6-AAAGGTCA-3') (Maira et al., 1999). There is some evidence to

suggest that members of the NR4 family can dimerise and act on NurRE as heterodimers however this relies on interactions between the receptors ligand binding domains (Maira et al., 1999). Whether Nurr1-a would be capable of heterodimerising with other family members or perhaps even Nurr1 remains to be investigated.

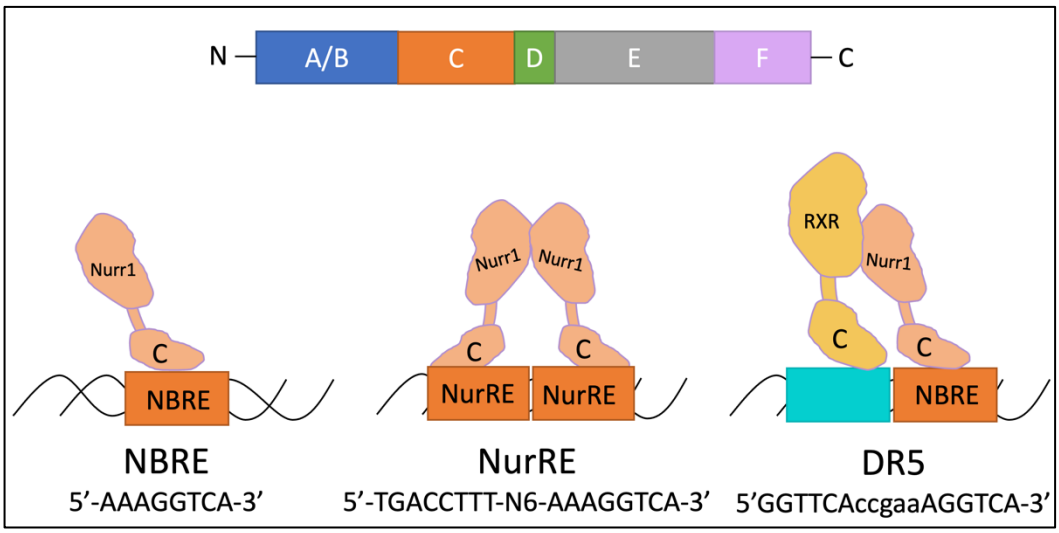


Figure 1.4-2 Nur1 response element binding

Schematic of Nurr1 response element binding as a monomer to NBRE motif, Nurr1 homodimer binding to NurRE and Nurr1 heterodimerising with RXR subsequently binding to the DR5 response element. *Abbreviations: RXR, retinoic acid receptor; NBRE, NGFI-B response element; NurRE, Nur response element; DR5, direct repeat 5.*

1.4.4 Nurr1 expression: Neuronal

Nurr1 was first identified through the screening of a mouse brain cDNA library. After analysing the distribution of Nurr1 in a variety of mouse tissues its expression was considered to be predominantly in the brain, which suggested a role in brain development and function (Law et al., 1992). This was supported by later studies which demonstrated the expression of Nurr1 largely in midbrain DA neurons in both rodent and human samples (Michelhaugh et al., 2005, Zetterström et al., 1996, Bäckman et al., 1999). Within the

DA neurons, Nurr1 was shown to be almost exclusively localised to the neuronal nuclei in human brain samples (Chu et al., 2002).

The importance of Nurr1 in brain development and function was exemplified by Nurr1 knock out studies in mice. Homozygous Nurr1 knock out mice failed to generate midbrain dopamine neurons, displayed obvious motor defects and died soon after birth (Zetterström et al., 1997). Additionally, heterozygous mice showed no clear motor defects, however they displayed reduced Nurr1 protein levels and dopamine secretion, suggesting nigrostriatal DA levels are influenced by Nurr1 mRNA dosage (Zetterström et al., 1996, Zetterström et al., 1997). Moreover Le et al., suggested DA neurons of Nurr1 heterozygous mice displayed a higher susceptibility to neurotoxins compared to wild type, implying Nurr1 is important in maintaining and protecting mature DA neuronal function (Le et al., 1999).

Nurr1 is also paramount in cognitive processing. Colon-Cesario et al., demonstrated Nurr1 heterozygous mice had impaired hippocampal dependent memory (Colón-Cesario et al., 2006). Furthermore Kim et al., revealed treatment of adult mice with Nurr1 agonist amodiaquine was able to increase hippocampal neurogenesis and enhance both short and long term memory (Kim et al., 2016).

The importance of Nurr1 in DA neurons is likely due to its transcriptional regulation of key genes, such as those involved in dopamine synthesis: TH (TH), dopa decarboxylase (DDC), vesicular mono amine transporter 2 (VMAT2) and dopamine transporter (DAT) (Hermanson et al., 2003). Backman et al., demonstrated the majority of TH immunoreactive neurons (96%) in the substantia nigra of mice also expressed Nurr1, suggesting a strong colocalization of Nurr1 and TH (Bäckman et al., 1999). Additionally,

Nurr1 expression precedes that of TH during development, supporting its regulatory role (Zetterström et al., 1996, Solberg et al., 1993). Nurr1 is reported to bind NBRE sites within the TH promoter and activate transcription specifically in the midbrain (Sakurada et al., 1999). Interestingly the TH promoter contains multiple NBRE like motifs, differing only by one residue, which are reported to bind specifically to Nurr1 (Kim et al., 2003a, Kim et al., 2013, Iwawaki et al., 2000, Maira et al., 1999).

Nurr1 expression is highest during embryogenesis and decreases with age, however it still remains in DA neurons (Castillo et al., 1998b, Bäckman et al., 1999, Zetterström et al., 1996, Ahn et al., 2018). Post-mortem human studies have revealed decreases of Nurr1 expression, corresponding with decreases in TH and DAT expression, during the normal course of aging (Bannon and Whitty, 1997). However, the reduction in these markers does not necessarily suggest neuronal degeneration. Exemplified by Chu et al., who demonstrated levels of melanin containing neurons in the human adult substantia nigra remained consistent despite a reduction in Nurr1 and TH (Chu et al., 2002). This is not to say in degenerative diseases such as PD, changes in Nurr1 and TH expression are not correlative of disease pathogenesis.

More recently, in the development of human based neuronal models with the aim of investigating degeneration, Nurr1 has been implicated as a key transcription factor in the differentiation of induced pluripotent stem cells (iPSCs) into DA neurons (Powell et al., 2021, Theka et al., 2013). Multiple *in vitro* experiments differentiating embryonic stem cells into DA neurons have involved the overexpression Nurr1 whilst transitioning the cells through mimicked developmental stages (Andersson et al., 2007, Lee et al., 2010, Park et al., 2008) However, more recent studies demonstrate

Nurr1 alongside two others key transcription factors (LIM homeobox transcription factor 1 alpha/beta (LMX1A/B) and Achaete-scute family BHLH transcription factor 1 (ASCL1)) are sufficient for a one step differentiation of iPSCs to DA neurons (Powell et al., 2021, Theka et al., 2013). Creating human-based models such as this allow more accurate disease modelling than animal models used previously, providing a beneficial tool for therapeutic targeting.

1.4.5 Nurr1 expression: Microglia and Macrophages

In addition to its expression in neurons, Nurr1 has been identified in microglia and macrophages (Saijo et al., 2009). The expression of Nurr1 in these cells has been linked to inflammation, suggesting that Nurr1 has a key regulatory role in dampening down the expression of proinflammatory cytokines. Nurr1 is reported to be constitutively active in neurons, however as an immediate early gene, its expression can be rapidly induced in microglia and macrophages by a variety of stimuli including cytokines and TLR ligands (Maxwell and Muscat, 2006, Bonta et al., 2006, McEvoy et al., 2002).

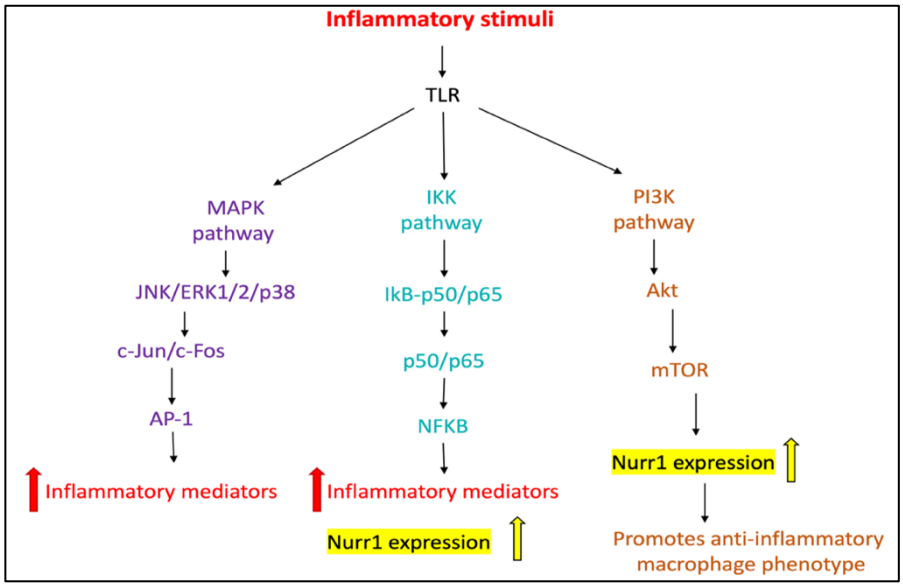


Figure 1.4-3 Common inflammatory signalling pathways in microglia and macrophages

Inflammatory pathways described in microglia and macrophages which increase inflammatory mediator production and/or Nurr1 expression. *Abbreviations: TLR, toll-like receptor; MAPK, mitogen activated protein kinase; JNK, Jun N-terminal kinase; ERK, extracellular signal-related kinase; AP-1, activator protein 1; IκK, IκB kinase; IκB, inhibitor of kappa B; NFκB, Nuclear factor kappa-light-chain-enhancer of activated B cells; PI3K, phosphoinositide 3-kinases; Akt, Akt serine/threonine kinase family; mTOR, mammalian target of rapamycin.*

Microglia

Microglia are the primary resident immune cells of the CNS which develop from yolk-sac fetal macrophages, dissimilar from other macrophages (Lenz and Nelson, 2018). The formation of microglial precursors initially depends on a variety of transcription factors and colony stimulating factor 1-receptor (CSF1-R) signalling, for which IL-34 and CSF-1 are the likely ligands (Greter et al., 2012). Under normal physiological conditions the number and function of microglia is tightly regulated by interactions with surrounding cells and the microenvironment. However, in response to certain stimuli, microglia can shift into different functional states with altered morphology, migration, release of inflammatory mediators and phagocytic activity (Cuadros and Navascues, 1998, Sierra et al.,

2013, Le et al., 2001). Microglia can be stimulated through pathogen associated molecular patterns (PAMPs) and damage associated molecular patterns (DAMPs) which can act on pattern recognition receptors (PRR's) such as toll-like receptors (TLRs) (Bachiller et al., 2018). Stimulation of microglial TLRs, with stimuli such as LPS or α-synuclein, results in a sequence of events which lead to the activation of MAPK and/or translocation of NFκB into the nucleus followed by the production of inflammatory mediators (Kawai and Akira, 2007, Symons et al., 2006, Roodveldt et al., 2013, Dzamko et al., 2017). Inflammatory mediators produced can be 1) pro-inflammatory cytokines to enhance the inflammatory response, 2) chemokines to recruit other inflammatory cells, 3) anti-inflammatory cytokines which help to relieve inflammation, 4) other factors such as the expression of Nurr1 to dampen down inflammation (Saijo et al., 2009, Wyss-Coray and Mucke, 2002).

Saijo et al., reported in microglia and astrocytes that the expression of Nurr1 was rapidly induced by LPS and lead to the subsequent transrepression of pro-inflammatory mediators. This transrepression mechanism (as described in section 1.2.3) is suggested to be based upon the SUMOylation of Nurr1, which facilitates the recruitment of the CoREST corepressor complex to the pro-inflammatory promoters of NFκB target genes (Saijo et al., 2009). Nurr1 expression itself is reported to be regulated through the NFκB pathway, highlighting the role of Nurr1 in an inflammatory negative feedback loop (Lilley et al., 2022, Saijo et al., 2009). Fan et al., also suggested Nurr1 induction via LPS is mediated through the PI3K-Akt pathway (Fan et al., 2009).

As SUMOylation of Nurr1 was suggested to underpin this repressive mechanism, research into the enzymes and the specific SUMO site involved was carried out. Through a yeast two hybrid screen PIASg

was identified as the E3 ligase responsible for Nurr1 SUMOylation. The authors report Nurr1 transcriptional activation of both 3xNBRE and TH driven reporters were repressed by PIASg mediated SUMOylation of Nurr1 (Galleguillos et al., 2004). Similarly Arredondo et al., demonstrates PIASg affects the activity of Nurr1 in HEK293 cells though both SUMO dependent and independent mechanisms (Arredondo et al., 2013). There are contradicting reports as to the specific site at which Nurr1 SUMOylation occurs. Arredondo et al., suggests modification occurs solely at K91 within the AF-1 domain. However, Saijo et al., reports K558 and K576 to be the predominant sites. Whilst Galleguillos et al., in part agrees with K91 however additionally suggests K577 (Galleguillos et al., 2004).

An additional method of Nurr1 inflammatory regulation was also described by Oh et al., who demonstrated in BV-2 cells that Nurr1 modulated LPS-induced inflammation by binding to the RasGRP1 gene and negatively regulating its expression. Repressing RasGRP1 then resulted in a decrease of proinflammatory cytokines through the Ras-Raf-MEK-ERK signalling cascade. However, the author states this is not the sole mechanism of inflammatory repression, and it is likely Nurr1 partakes in additional pathways such as the NFκB pathway (Oh et al., 2020, Saijo et al., 2009).

Macrophages

Macrophages are effector cells of the innate immune system, important in the inflammatory repose and homeostatic maintenance. They originate from monocytes circulating in the blood (Hirayama et al., 2017). In response to inflammation, monocytes can differentiate into macrophages which can phagocytose dead or damaged cells, tumour cells and bacteria. In addition, they can secrete inflammatory mediators. Like microglia, they exist in a state of flux, which can shift into different functional states, enhancing or

resolving inflammation, dependent on the activating stimulus (Nahrendorf and Swirski, 2016). *In vitro*, primary macrophages are induced into either end of the spectrum by the addition of GM-CSF/IFNy or M-CSF/IL-4 respectively (Nielsen et al., 2020). Macrophages can also respond to stimuli through TLRs, and mediate their effect through numerous pathways including NFκB, PI3K and MAPK (Fang et al., 2017).

In macrophages Pei et al., demonstrated Nurr1 expression was rapidly induced by LPS. The authors also suggest this expression is credited to the NFκB pathway (Pei et al., 2005). Similarly, Bonta et al., show Nurr1 expression is induced in response to LPS and TNFα in both primary and THP-1 derived macrophages. The increase in Nurr1 expression results in decreased proinflammatory cytokine and foam cell production in atherosclerosis (Bonta et al., 2006). Conversely, Mahajan et al., suggest Nurr1 induction in bone marrow derived macrophages (BMDM) is a result of LPS induction of the PI3K-Akt-mTOR pathway. It is implied that the induction of Nurr1 helps to polarise the macrophages towards a more anti-inflammatory phenotype. Most interestingly the authors show mice transduced with Nurr1 had greater survival when challenged with a lethal dose of LPS, which lead to uncontrolled systemic inflammation in non-transduced mice. This also correlated with lower serum concentration of pro-inflammatory cytokines (Mahajan et al., 2015).

1.4.6 Nurr1 in Parkinson's Disease

PD is a progressive neurodegenerative disease whose incidence increases with age. It results in symptoms such as bradykinesia, tremor, rigidity and a variety of cognitive defects. Pathologically it is characterised by deterioration of DA neurons within the SN, the

presence of α-synuclein containing Lewy bodies and neuroinflammation (Jankovic et al., 2005, Deleidi and Gasser, 2013). More recently, research has highlighted the involvement of the peripheral immune system in PD (Houser and Tansey, 2017, Romano et al., 2021). Considering the involvement of Nurr1 in inflammatory regulation in addition to its regulatory role in DA neurones, Nurr1 presents as an interesting target to investigate in PD pathophysiology.

CNS inflammation

The first evidence for inflammation in PD was reported by McGeer et al., who revealed the presence of reactive microglia in the substantia nigra of post-mortem PD patients (McGeer et al., 1988). Following studies then highlighted the increase incidence of proinflammatory mediators in PD patients. For example Sawada et al., demonstrated elevated levels of proinflammatory mediators such as TNFα, IL-1β, and IL-6 in the brains and cerebral spinal fluid (CSF) of PD patients (Sawada et al., 2006). This was further supported in a meta-analysis of 71 studies analysing the CSF of PD patients (Chen et al., 2018). Increased cytokine levels in the CNS are indicative of microglial activation. Microglial activation and excessive production of pro-inflammatory cytokines has been associated with the damage and subsequent death of surrounding DA cells (Olanow et al., 2019, Saijo et al., 2009). Positron emission topography has also shown pronounced microglial activation in the brains of PD patients (Gerhard et al., 2006, Gerhard, 2016). It is reported in microglia that Nurr1 reduces the production of proinflammatory cytokines (Lallier et al., 2016, Saijo et al., 2009). However in post mortem brain of PD patients, Nurr1 was found to be significantly reduced (Chu et al., 2006, Saijo et al., 2009, Lallier et al., 2016)

One debated question is to whether microglial activation is a symptom of PD or causative factor. Initially it was decided that misfolded proteins or debris from damaged neurons was responsible for microglial activation (Heneka et al., 2014, Mosley et al., 2012). However more recent studies suggest activation precedes neuronal damage and death (Olanow et al., 2019, Lee et al., 2002). Olanow et al demonstrated, through the grafting of embryonic DA neurons into PD brains, that the invasion of activated microglia was present years before α-synuclein accumulated in the DA neurons (Olanow et al., 2019). However this is not to say that α-synuclein does not continue microglial activation throughout PD pathogenesis as there is also evidence in support of this (Su et al., 2008).

Peripheral inflammation

To what extent the peripheral immune system is involved in PD remains questioned. Initial research disregarded peripheral inflammation as a contributing factor to PD due to the presence of the blood brain barrier (BBB) which limits the entrance of peripheral immune cells into the CNS. However, there is data to suggest that BBB dysfunction increases its permeability and in turn the infiltration of inflammatory cells and mediators which can activate microglia and damage neurons (Kortekaas et al., 2005, Rite et al., 2007). Yan et al., used mouse models of PD to demonstrate that a reduction of activated macrophages in the peripheral immune system reduced the level of inflammatory cytokines produced and thus ameliorated microglial activation in the substantia nigra (Yan et al., 2018).

Additionally, elevated cytokine levels in the peripheral blood mononuclear cells (PBMCs) of PD patients compared to heathy controls has been reported. Moreover the same study found a correlation between increased cytokines and reduced Nurr1 expression (Li et al., 2018). Interestingly, stimulation of the

peripheral immune system has been reported to be neuroprotective in some scenarios. Yao et al., demonstrated that pre-treating mice with peripheral injections of LPS induced endotoxin tolerance, which inhibited the activation of microglia induced by following LPS treatments (Yao et al., 2022). Endotoxin tolerance (also referred to as immune tolerance) is the reduced responsiveness of the immune response when exposed to PAMPs and DAMPs through TLR stimulation (Butcher et al., 2018). Like the role of Nurr1, endotoxin tolerance results in decreased pro-inflammatory cytokines and therefore may be protective against chronic or dysregulated inflammation.

α-*synuclein*

α-synuclein is expressed throughout the brain. However in PD patients misfolded α-synuclein is deposits are a major component of Lewy bodies (Constantino and Honig, 2001). The relationship between Nurr1 and α-synuclein has been investigated. Chu et al., demonstrated neurons containing α-synuclein had reduced Nurr1 expression in PD brains (Chu et al., 2006). α-synuclein has also been reported to supress the expression of Nurr1 and therefore reducing the expression of Nurr1 target genes (Kadkhodaei et al., 2009, Baptista et al., 2003). Jia et al (2020) reported that α-synuclein partly mediates its effect on Nurr1 via NFkB. The authors demonstrated α-synuclein overexpression reduced NFKB protein levels in the nucleus and therefore reduced binding to Nurr1's promoter (Jia et al., 2020). Other evidence suggests α-synuclein overexpression can promote the proteosome associated degradation of Nurr1 (Lin et al., 2012). The result of reduced Nurr1 mRNA synthesis may reduce the inflammatory suppressive effects provided by Nurr1 mediated transrepression.

Genetic basis

A series of PD related genes has previously been identified, and research has highlighted abnormalities in the Nurr1 gene that may be risk factors for both familial and PD disease. Xu et al., highlighted a homozygous polymorphism (7048G7049) in intron 6 of Nurr1 was significantly higher in familial (9.5%) and sporadic (4.2%) PD compared to health age-matched controls (0.9%) (Xu et al., 2002). Le et al., revealed two mutations in the first exon Nurr1, within the 5' untranslated region, which affects one allele in 10 of 107 familial PD patients, with no mutations found in sporadic cases or the healthy controls. The first mutation was a T deletion (-291T) affecting 8/10 patients, the second being a T>G substitution (-245T) affecting 2/10 patients. These mutations were found to express reduced Nurr1 mRNA (87-95% less) when introduced into HEK293 and SH-SY5Y cell lines, in addition to reduced transcription of the TH gene (Le et al., 2003). The first mutation identified to be within a translated region of Nurr1 was described by Grimes et al., who found a single missense mutation in exon 3 which was thought to affect phosphorylation. However out of 202 PD patients, only one presented with this mutation (Grimes et al., 2006). Overall, it appears that mutations within the Nurr1 gene associated with PD have a low prevalence.

The role of Nurr1 in PD treatment

A decline in Nurr1 caused by aging or dysregulation may reduce its compensatory protective ability and increase the susceptibility to develop PD. Whether through the absence of neuronal gene regulation or unrestricted inflammation. Fully understanding the pathways Nurr1 is involved in may provide insight into therapeutic methods to restore its function and mitigate PD pathophysiology. Increasing Nurr1's expression or transcriptional activity through modulators and ligands is one avenue already in investigation (Pan

et al., 2005, Kim et al., 2015). An additional direction of therapeutic treatment involves the overexpression of Nurr1 in transfected or transplanted cells. Chung et al., reported transfecting embryonic mouse stem cells with Nurr1 yielded an enriched population of midbrain stem cells with demonstrated electrophysical and behavioural properties of DA neurons (Chung et al., 2002). More recently Qian et al., transplanted neural stem cells and microglia with forced Nurr1 expressing into the striatum of a rat PD model. The authors report the transplantation increased TH positive cells in the striatum, and the differentiated DA neurons from the graft were still detected after 5 months (Qian et al., 2020).

1.5 Project aims and objectives

As aforementioned Nurr1 is reported to be an important transcriptional regulator of neuronal and inflammatory genes. The mechanism by which Nurr1 mediates the repression of pro-inflammatory genes is said to be based upon SUMOylation. Research into Nurr1 SUMOylation is limited and studies report contradicting results in terms of SUMO isoform preference and the specific site of modification. Additionally, there is a reported splice variant of Nurr1, termed Nurr-1a, which has been identified in neuronal cells but neglected in terms of its function. Nurr1 has been linked to PD because of its involvement with DA neurons and suggested protective role during neuroinflammation. However, many previous studies use cell lines or animal models which are not representative of human disease.

Therefore, the main aims of this study were to:

1. Investigate the SUMOylation of Nurr1 and Nurr-1a.
2. Determine how SUMOylation affects Nurr1 and Nurr-1a mediated inflammatory and neuronal gene regulation.
3. Develop human based inflammatory and neuronal models in which to decipher the potential role of the receptors in PD disease pathophysiology and how SUMOyaltion may or may not affect these pathways.

Chapter 2
Materials and Methods

2.1 Chemicals and reagents

Table 2.1-1 Chemicals and reagents used

Reagents and chemicals	Supplier
Cell culture	
DMEM/F12	Thermo Fisher Scientific #D9785
Trypsin	Sigma #T3924
Non-Essential Amino Acids	Sigma #M7145
Sodium Pyruvate	Gibco #11360-039
Fetal Bovine Serum	Sigma #F7524
L-glutamine	Sigma #G7513
Penicillin Streptomycin	Sigma #P0781
Transfection and ligand treatment	
X-tremeGene HP DNA transfection reagent	Roche #06366236001
Amodiaquine dihydrochloride dihydrate	APExBIO #B6134
Pramipexole dihydrochloride	APExBIO #A3733
C-DIM12	Sigma #SML1508
6-Mercaptopurine	Tocris #4103
Docosahexaenoic acid	Tocris #3687
LPS	Sigma #L2630
ATP	Sigma #A26209
SUMO assay and western blotting	
Complete EDTA-free Protease Inhibitor Cocktail	Roche #05056489001
Ni-NTA agarose beads	QIAGEN #R901-01
Nitrocellulose membrane; 0.45 µm pore size	Thermo Fisher Scientific #LC2001
PierceTM BCA Protein Assay Kit	Thermo Fisher Scientific #23227
PageRuler Plus Preset ladder	Thermo Fisher Scientific #26620
Duolink in situ PLA kit	Sigma #DUO92101
PCR	
Primers and probes	Eurofins
qPCRBIO probe mix	PCR Bio systems #PB013622-030-5
5X Phusion HF Buffer	NEB #M0530
dNTP’s	NEB #N0440-3S
Phusion DNA polymerase	NEB #M0530
Random primers	Invitrogen #58875
RNAseOUT	Invitrogen #100000840
AffinityScript Multi-Temp Reverse Transcriptase	Agilent #600107
Glycogen	Thermo scientific #R0551§

SYBR green qPCR Master Mix	Agilent #600892-51
Cloning, transformation, and DNA-prep	
NEB 10-beta Competent E coli (High Efficiency)	NEB #C3019
Ethidium bromide	Thermo Fisher Scientific #17898
DNA ladder and Loading dye	NEB #N3232
Molecular biology enzymes	NEB
Gateway BP Clonase II Enzyme	Invitrogen #11791-020
QIAprep Spin Miniprep Kit	QIAGEN #27104
QIAquick Gel Extraction Kit	QIAGEN #28704
QIAquick PCR purification kit	QIAGEN #28104
GeneJET genomic DNA purification kit	Genejet #K0721
HPLC water	Thermo Fisher Scientific
Site Directed Mutagenesis	
QuikChange XL site-directed mutagenesis	Agilent #200516
FPLC purified primers	Eurofins
XL-Gold Ultracompetent cells	Agilent #200314
Luciferase assay	
Luciferase Assay System	Promega #E1500
Passive lysis buffer 5x	Promega #E1941
Lentivirus	
Opti-MEM	Thermo Fisher Scientific #11058021
iPSC culture and maintenance	
ReLeSR	Stemcell Technologies #05872
TeSR-E8 media	Stemcell Technologies #05991
Human Stem cell qualified Matrigel Membrane Matrix (RGF)	Corning #07181
Stem Cell Qualified (RGF) Cultrex	R&D #3434-005-02
hPSC Genetic Analysis Kit	Stemcell Technologies #07550
Stemdiff Trilineage Differentiation kit	Stemcell Technologies #05230
CryoStor	Stemcell Technologies #07959
iPSC microglia differentiation	
STEMdiff Haematopoietic kit	Stemcell Technologies # 05310
STEMdiff Microglia Differentiation Kit	Stemcell Technologies #1000019
STEMdiff Microglia Maturation Kit	Stemcell Technologies #1000020
Stemline serum free Hematopoietic expansion media II	Sigma #S0192
Insulin-Transferrin-Selenium	Thermo Fisher Scientific #51500-056
BMP4	R&D Systems #314BP
Vascular endothelial growth factor	R&D Systems #298VS
Stem cell factor	R&D Systems #255SC
Recombinant Human thrombopoietin	R&D Systems #288TP
IL3	R&D Systems #203IL

G-CSF	R&D Systems #214CS
FLT-3	R&D Systems #308FK
IL-34	R&D #5265IL
N2	Thermo Fisher Scientific #17502048
GlutaMax	Thermo Fisher Scientific #35050061
1-Thioglycerol	Merk #M6145
Recombinant Human IL-34	Peprotech #20034
Recombinant Human TGF- β1	Peprotech #10021
Recombinant Human Fractalkine	Peprotech #30031
CD200	R&D #100032
M-CSF	Peprotech #30025
GM-CSF	Peprotech #3003
iPSC Dopaminergic neuron differentiation	
Accutase	Sigma #A6964
Sodium Selenite	Sigma #S9133
Insulin solution human	Sigma #I9278
Apo-Transferrin Bovine	Sigma #T1428
Progesterone	Sigma #P8783
Putrescine	Sigma #P5780
50X B27	Thermo Fisher Scientific #17504044
Doxycycline Hyclate	Sigma #D9891
Ara-C	Sigma #C1768
PBMC culture and differentiation	
RPMI-1640	Sigma #R0883
Histopaque	Sigma #10771
Fluorescent latex beads (1μM diameter)	Sigma #L1030
GlutaMAX	Gibco #35050-061
GM-CSF	Peprotech #300-03
IL-34	R&D #5265-CF
RNA isolation and RT-qPCR	
TRI Reagent	Sigma #T9424
Chloroform	Sigma #650498
BCP	Sigma #B62404
Phenol:Chlroform:Isoamyl:Alcohol	Thermo Fisher Scientifc #15593031
Total human brain RNA	Thermo Fisher Scientific #AM7962

Table 2.1-2 Plasmids

Plasmid	Vector	Source
pcDNA3.1(+) zeo	Empty vector	Invitrogen
TH-Luc Reporter	PGL4.1 (luc2)	Developed in this work

iNOS-Luc Reporter	PGL4.1 (luc2)	Kindly provided by Dr. Dawson (University of Nottingham)
Rat FLAG-Nurr1 wild type	p3xFLAG pcDNA3.1(+) zeo N-Terminal tag	Developed in the FRAME lab (University of Nottingham)
Rat FLAG-Nurr-1a wild type	p3xFLAG pcDNA3.1(+) zeo N-Terminal tag	Developed in the FRAME lab (University of Nottingham)
Rat FLAG-Nurr1 K91	p3xFLAG pcDNA3.1(+) zeo N-Terminal tag	Developed in the FRAME lab (University of Nottingham)
Rat FLAG-Nurr-1a K91	p3xFLAG pcDNA3.1(+) zeo N-Terminal tag	Developed in the FRAME lab (University of Nottingham)
Rat FLAG-Nurr-1a SIM mutant	pcDNA3.1(+) zeo	Developed in this work
HA-Ubc-9	pcDNA3.1(+) zeo	Developed in the FRAME lab (University of Nottingham)
6xHis-SUMO1	pSG5	6598-HisSUMO1GG was a gift from Anne Dejean
6xHis-SUMO2	pSG5	Developed in the FRAME lab (University of Nottingham)
6xHis-SUMO3	pSG5	Developed in the FRAME lab (University of Nottingham)
PIASγ wild type	pcDNA3.1(+) zeo	Developed in the FRAME lab (University of Nottingham)
C342A PIASγ	pcDNA3.1(+) zeo	Developed in the FRAME lab (University of Nottingham)
Human Nurr1	pReciever-Lv158	GeneCopoeia
Human PIASγ	pReciever-Lv105	GeneCopoeia
Human Nurr-1a	pcDNA3.1(+) zeo	Developed in this work
Human Nurr-1a	pINDUCER20	Developed in this work
Human Nurr1 K91	pReciever-Lv158	Developed in this work
Human Nurr-1a k91	pINDUCER20	Developed in this work
GFP	pINDUCER20	Developed in the FRAME lab (University of Nottingham)
Doner vector	pDONR221	Invitrogen 12536017
Envelope plasmid	PMD2.G	pMD2.G was a gift from Didier Trono
Packaging plasmid	psPAX2	psPAX2 was a gift from Didier Trono
Tet-O-ALN	FU-tetO-Gateway	TetO-ALN was a gift from John Gearhart #43918
FUW-M2rtTA	FUW	FUW-M2rtTA was a gift from Rudolf Jaenisch #20342

Table 2.1-3 Antibodies

Antibody	Application	Source	Host
Primary			
FLAG-M2 Monoclonal IgG	WB, ICC	Sigma F3165	Mouse mAB
β-Actin Monoclonal IgG	WB	Sigma A5441	Mouse mAB
PIAS4	WB	Cell Signalling #4392S	Rabbit mAB
PIAS4	WB	Insight Biotechnology #SC166706	Mouse mAB
Nurr1	WB	PP-N1404-00	Mouse mAB
Otx2	ICC	R&D 1979	Goat pAB
Brachyury	ICC	R&D AF2085	Goat pAB
SOX17		R&D AF1924	Goat pAB
6xHis	WB	Clontech 631212	Mouse mAB
TMEM119		Proteintech #275851AP	Rabbit pAB
Iba	ICC	Thermo Fisher Scientific #15784267	Mouse mAB
TH	ICC	Sigma #AB152	Rabbit pAB
P2RY12	ICC	Proteintech #HPA014518	Rabbit pAB
MAP2	ICC	Sigma #M9942	Mouse mAB
GFAP	ICC	Sigma #SAB4501162	Rabbit pAB
NeuN	ICC	Merk Life Sciences #MAB377	Mouse mAB
Secondary			
IRDye 800cw IgG	WB	LI-COR #925/32212	Donkey anti-mouse
IRDye 680LT	WB	LI-COR #926/69023	Donkey anti-rabbit
Alexa Fluor 594	ICC	Invitrogen #A11058	Donkey anti-goat
Alexa Fluor 488	ICC	Invitrogen #A21202	Donkey anti-mouse
Alexa Fluor 488	ICC	Invitrogen #A21206	Donkey anti-rabbit
Alexa Fluor 568	ICC	Life technologies #A110004	Goat anti-mouse
Duolink in-situ PLA Probe MINUS	PLA	Sigma #DUO92005	Donkey anti-rabbit
Duolink in-situ PLA Probe PLUS	PLA	Sigma #DUO92001	Donkey anti-mouse

2.2 Cell culture

Table 2.2-1 Cells used

Cell line	Organism/tissue	Medium	Purpose
HeLa	Human cervical cancer	EMEM (#M4526)	SUMO pulldown
HEK293	Human embryonic kidney	EMEM (#M4526)	Transactivation assay
HEK293FT	Human embryonic kidney	DMEM high glucose (#5671)	Lentiviral generation
SH-SY5Y	Human neuroblastoma	DMEM/F12 (#6421)	Transactivation assay
iPSCs	Human Fibroblast	TeSR-E8 (#05991)	DA neurons and microglia
Monocyte	Human blood	RPMI-1640 (#R0883)	Monocytes and iMGL cells

The majority of cells were originally sourced from American Type Culture Collection (ATCC) and cultured according to ATCC guidelines with DMEM, EMEM or DMEM/F-12 dependent upon cell type. Media was supplemented with 10% fetal bovine serum (FBS), 2mM L-glutamine and (dependent on cell type) 1x non-essential amino acids/ 1 x sodium pyruvate. Primary human monocytes and human iPSCs were the exception to these methods, their detailed protocol can be found in depth later in this chapter.

2.2.1 Frozen cells

Cells stored in liquid nitrogen were removed and thawed quickly in a 37°C water bath, ensuring the vial was not submerged in the water and was fully decontaminated using 70% ethanol. Following this, everything was carried out under aseptic conditions in a biological safety cabinet. Cells were transferred into 5ml of media and centrifuged at 300xg for 5 min. The pellet was resuspended in 5ml

of media and transferred to a T-75cm^2 flask containing 10ml of fresh media. Cells were incubated in a humidified atmosphere of 5% CO_2 at 37 °C.

2.2.2 Cell maintenance

Subculturing of cells was carried out every 2-5 days in a 1:10 ratio when cells were 70-80% confluent, up to passage 20. Cell media was aspirated, and cells were washed with 1xPBS. Cells were detached using 0.05% trypsin/EDTA by adding 2-3ml to the flask and incubating at 37°C for 5min. Trypsin was deactivated by the addition of 3x complete media. The appropriate volume of cell suspension was added to a fresh T75 or T175 flask containing 15ml or 30ml respectively. Cells were incubated in a humidified atmosphere of 5% CO_2 at 37 °C.

2.2.3 Cryopreservation

Cells with high viability were harvested, centrifuged at 300xg for 5min and resuspended in cryopreservation media to a concentration of approximately 2×10^6 cells/ml. Cryopreservation media was composed of 90% FBS and 10% DMSO (dimethyl sulphoxide). The suspension was aliquoted into 1ml cryovials and placed in a Mr Frosty overnight at -80°C before transfer to liquid nitrogen for long term storage.

2.3.4 Cell counting

Cell counting was performed using a haemocytometer. A 1:2 volume of cells to Trypan blue was used to create 30µl sample, of which 10µl was loaded onto the haemocytometer and covered using a coverslip.

Under a light microscope the four outer corner squares were counted. The cell concentration was calculated using this formula:

$$\text{Total cells / ml} = \frac{(\text{Total cell count X Dilution factor})}{4} \text{ X } 10^4$$

Additionally, cells were counted using an automated Cedex XS cell counting system, using the same Trypan blue dilution.

2.3 Cloning and mutagenesis

2.3.1 RNA isolation

RNA isolation (mRNA) was carried out using TRI-reagent as per the manufacturer's instructions. Pellets were resuspended in 20-50µl DEPC-treated water, the concentration was measured using FLUOstar omega with a LVis plate.

2.3.2 cDNA synthesis

Reverse transcription of RNA was carried out in the reaction below:

Table 2.3-1 Reverse Transcription reaction

Component	Volume
Total RNA	250-2000ng
Random Primers (0.1µg/µl) OR Gene specific primers (10µM)	3ul OR 1ul
DEPC-treated water	Up to 13.7ul
Reaction was heated at 65°C for 5min, followed by a 10min incubation at RT. The following reagents were added to a total volume of 20µl:	
10x AffinityScript RT Buffer	2µl
Dithiothreitol (DTT) 100mM	2µl
dNTP mix (25mM each dNTP)	0.8µl
RNase Block Ribonuclease Inhibitor (40U/µl)	0.5µl
AffinityScript Multiple Temperature Reverse Transcriptase	1µl
The reaction was gently mixed then subjected to the following incubation in an automated heating block:	
25°C	10 min
55°C	1h
70°C	15 min

The cDNA was then used in PCR-cloning and TaqMan qRT-PCR.

2.3.3 Cloning

To assess the transcriptional activity mediated by Nurr1 and Nurr-1a, a TH promoter driven luciferase reporter was developed. To

clone the TH promoter sequence into a reporter construct primers were designed according to the sequence obtained from Addgene (#80336). 1022bp of the rat TH promoter region including the NL1, NL2 and NL3 (Kim et al., 2003a) was cloned into the PGL4.1 Luciferase reporter from PCR amplified homogenised rat brain tissue. Forward (Fw) and reverse (Rev) primers were designed using APE software by choosing primers with a Tm near 60°C and a GC content between 40-60%. Secondary structure analysis and primer dimer formation were checked using OligoAnalyser 3.1 IDT. Finally, the annealing temperature of primers was checked using NEB Tm calculator.

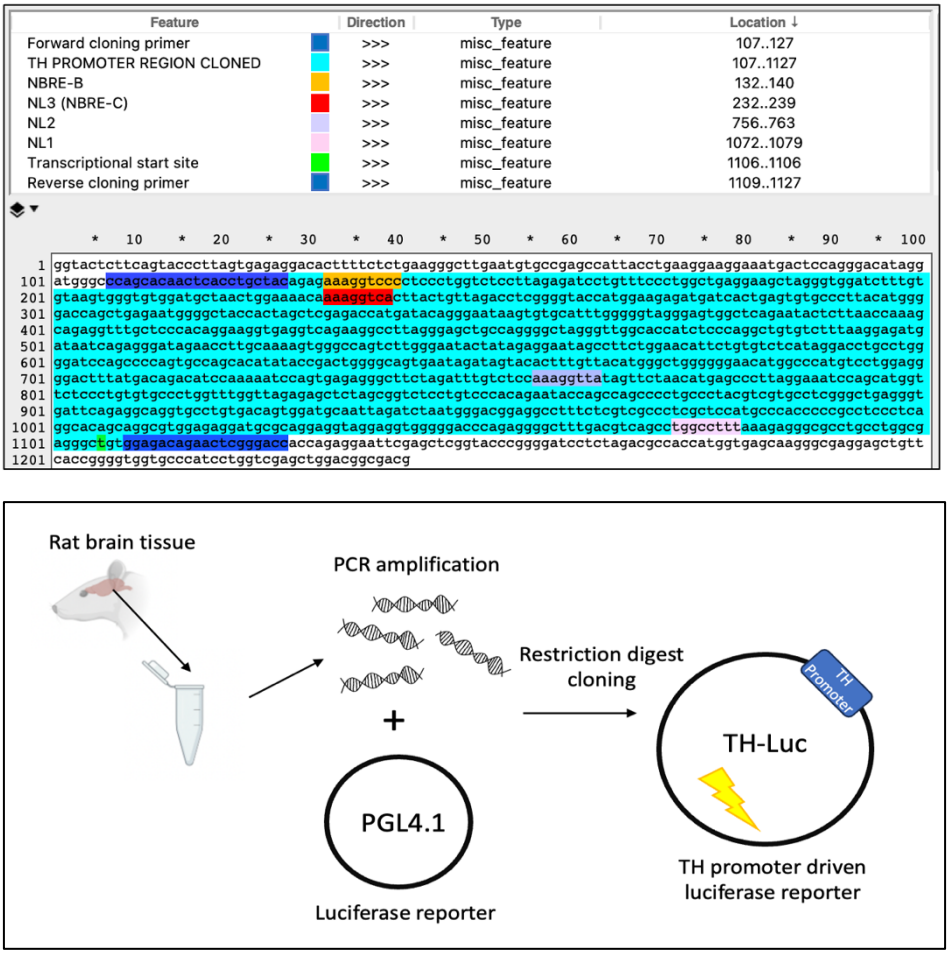


Figure 2.3-1 Primer design and schematic overview of the TH cloning process.

Primers designed using APE software.

To clone the Human Nurr-1a plasmid; gene specific primers for reverse transcription were designed (as above) which spanned the N and C terminal of the Human Nurr-1a coding sequence. Total human brain RNA was subjected to RT with only the reverse gene specific primer, before PCR amplification with both forward and reverse. See appendix for Rat Nurr1 and Nurr-1a sequence alignment.

Table 2.3-2 Primers used for cloning

Gene	Primers	Restriction Enzyme	Vector	DNA template used
Human Nurr-1a (56°C)	ATGCCTTGTGTTCAGG TCATATTCTGTATGCTAATCG	**EcoRV**	PcDNA3.1 (+) zeo	Human Total Brain RNA
Rat TH (66°C)	GATCGATATCCCAGCACAACTCACCTGCTAC GATCAAGCTTTGGTCCCGAGTTCTGTCTCC	**EcoRV** (F) **HindIII** (R)	PGL4.1 (luc2)	Rat brain tissue

Primers were resuspended to a concentration of 100µM in RNase free water as per the manufacturer's instructions. For the PCR the primers were diluted further 1:10 to a final concentration of 10µM. The reaction was as follows:

Table 2.3-3 PCR reaction

Reagent	Volume
5X Phusion HF Buffer	10µl
10mM dNTP's	1µl
10pmol/µl FW Primer	2.5µl
10pmol/µl REV Primer	2.5µl
Template DNA (100ng-1µg)	2µl
Phusion DNA Polymerase	0.5µl
HPLC grade H_2O	Final volume up to 50µl

PCR reaction was preformed using a thermal cycler (gen Amp PCR system 9700, Perkin Elmer, USA). The reaction conditions were as follows:

Table 2.3-4 Reaction conditions

Cycle step	Temperature	Time
Initial Denaturation	98°C	30s
Denaturation	98°C	10s
Annealing (35 cycles)	Dependent upon primer annealing Tm	30s per 1 Kb
Final extension	72°C	7 min
Hold	4°C	Indefinitely

3µl of the PCR product was run on a 1% w/v agarose gel with Ethidium Bromide and visualised using ultraviolet light (Syngene bio imaging system). Once correct size was confirmed the product was purified using QIAquick PCR Purification kit as per the manufacturer's instructions.

2.3.4 Restriction endonuclease digestion

Purified PCR products and the chosen empty vector were digested with the appropriate restriction enzymes for sticky or blunt end cloning. The reaction was prepared according to the table below, mixed by gentle pipetting and incubated at 37°C for 2 hours.

Table 2.3-5 Restriction digest reaction

Reagent	Volume
PCR product OR DNA plasmid	1µg plasmid
10X Cut Smart buffer	5µl
FW restriction enzyme	1µl
REV restriction enzyme	1µl
HPLC grade H2O	Final volume up to 50µl

2.3.5 Agarose gel electrophoresis

The digested DNA was run on a 1% w/v agarose gel, made by dissolving 1g of agarose in 100ml 1X Tris-Acetate-EDTA (TAE)

(40mM Tris, 20mM acetic acid, and 1 mM EDTA, pH8.3) and heating in a microwave until completely dissolved. The gel was poured into a cassette and left at RT for ~ 45 min until the gel had set. The gel was run in 1X TAE buffer.

The sample was prepared by adding 45µl digested DNA with 5µl SYBR Green dye followed by a 10 min RT incubation and the addition of 1X loading dye. A 1kb DNA ladder was used to determine size and the gel was run for 1h at 100V.

2.3.6 Gel extraction and Ligation

QIAquick Gel extraction Kit was used to extract the required DNA fragments from the gel as per the manufacturer's instructions. Ligation of the DNA insert to the appropriate plasmid was carried out in a 4:1 ratio (insert: vector). The reaction was incubated at 16°C overnight.

Table 2.3-6 Ligation Reaction

Reagent	Volume
10X T4 ligase buffer	2µl
Insert DNA	75ng
Vector DNA	25ng
T4 DNA ligase	2µl
HPLC grade H_2O	Final volume up to 20µl

Alternatively, for blunt ended ligation the insert was treated with T4 Polynucleotide kinase for 30 min at 37°C, followed by a 65°C 20 min heat inactivation. The vector was treated with Alkaline Phosphatase for 30 min at 37°C, followed by DNA purification using the QIAquick PCR purification kit. The reactions were as follows:

Table 2.3-7 Blunt end ligation Reactions

Reagent	Volume
Dephosphorylate vector	
DNA	0.5µg
CutSmart Buffer 10X	2µl
Calf Intestinal Phosphatase	1 unit
HPLC grade H2O	Final volume up to 20µl
Phosphorylate insert	
DNA	20µl
T4 PNK Reaction Buffer 10X	5µl
T4 PNK enzyme	1µl
HPLC grade H2O	Final volume up to 50µl

Ligation of processed blunt ended products followed as shown in Table 2.3-6 using 5µl of the vector and 10µl insert.

2.3.7 Bacterial transformation

Transformation was carried out using E. coli competent cells (XL-10 gold, Stbl3 or Top-10). 2-5µl of DNA was added to 50µl of thawed cells and incubated on ice for 30 min. Cells were then heat shocked for 45s at 42°C followed by a 2 min incubation on ice. 250µl of pre warmed SOC media was added to the cells which then underwent a 1h incubation at 37°C with 225RPMshaking. 20-200ul of bacterial culture was then spread in agar plates (LB medium + 1.5% w/v agar) with the appropriate selection markers and incubated overnight at 37°C. The following day Colony PCR was carried out as in 2.3.8. The remainder of each colony chosen for PCR was transferred into 5ml mini culture of LB media containing + antibiotics and incubated for 5-8 hours with shaking at 37°C. 400µl of bacterial mini culture was added to 200ml of LB media + antibiotic and subjected to overnight incubation in a shaking incubator at 37°C. Plasmid DNA was isolated the following day using the QIAGEN midi-prep kit.

2.3.8 Colony PCR

The edges of each colony selected for PCR were gently touched by a 10µl sterile pipette tip and resuspended in the 50µl reaction containing Phusion High Fidelity DNA Polymerase as shown in Table 2.3-3. The reaction conditions were as shown in 2.3-4. 20µl of each PCR was mixed with 1x loading dye and run alongside a 1kb DNA ladder on a 1% w/v agarose gel containing Ethidium Bromide. The gel was visualised using ultraviolet light (Syngene bio imaging system).

2.3.9 Plasmid Purification

Once the correct band size for the product was confirmed by Colony PCR the corresponding midi culture underwent purification using the QIAGEN plasmid Midi-prep kit as per the manufacturer's instructions. DNA concentration was determined using an LVis plate on a FLUOstar Omega.

2.3.10 Site Directed Mutagenesis

To mutate the K91 sites in Nurr1/1a in addition to the SIM site in Nurr-1a, the Agilent QuikChange Multi site-directed mutagenesis kit was used according to the manufacturer's instructions. Primers were designed online using QuikChange Primer Design.

Table 2.3-8 Primers for Site-Directed Mutagenesis

Gene	Forward Primer 5′ > 3′	Reverse Primer 5′ > 3′	Mutation
Rt Nurr1 K91 (Not made in this work)	GAATGTCTTCTACCC TAATGGAGGACTGC TGTCC	GGACAGCAGTCCTCC ATTAGGGTAGAAGAC ATTC	A272G
Rt Nurr-1a K91 (Not made in this work)	GAATGTCTTCTACCC TAATGGAGGACTGC TGTCC	GGACAGCAGTCCTCC ATTAGGGTAGAAGAC ATTC	A272G
Rt Nurr-1a SIM	TTCATATTCTGTATG CTAAGCGTGCAGCA AATAATTCTAAGAAA GCTGATTCAAAAAG CAGG	CCTGCTTTTTGAATCA GCTTTCTTAGAATTAT TTGCTGCACGCTTAG CATACAGAATATGAA	V448A, L449A
Hu Nurr1 K91	GAATGTCTTCTACCC TAATGGAGGACTGC TGTCC	GGACAGCAGTCCTCC ATTAGGGTAGAAGAC ATTC	A272G
Hu Nurr1 K91	GAATGTCTTCTACCC TAATGGAGGACTGC TGTCC	GGACAGCAGTCCTCC ATTAGGGTAGAAGAC ATTC	A272G

2.3.11 DNA sequencing

DNA plasmids were sequenced by Source BioScience and analysed using A plasmid Editor (ApE) software. DNA concentrations were measured with a FLUOstar Omega using an LVis plate.

2.4 Gene expression assays

2.4.1 Transfection and luciferase reporter assay

Cells were seeded 24h prior to transfection with the desired plasmids using X-tremeGENE HP transfection reagent. The ratio of reagent to DNA for HeLa, HEK293 and SH-SY5Y cells was 2:1. Cells were all transfected in 0.5% low lipid serum for either 24h or 48h. Cells harvested or assayed at 48h had a fresh media change after 24h. Any ligand treatments were carried out for 24h.

A luciferase assay was used to measure the luciferase activity within cells transfected with an TH-Luc reporter plasmid. 24h or 48h post transfection, cell media was aspirated, and wells washed with PBS. Cells were then lysed on an orbital shaker in 20-100µl 1x passive lysis buffer depending on culture ware (96 well and 48 well plates respectively) for 10-15 min. 100µl of Luciferase Assay Reagent (LAR) was added to each well of a 96 well plate, or 20µl of lysate was mixed with 100µl of LAR in luminometer tubes. The activity was then measured using FLUOstar Omega or a Luminometer (TD20/20, Turner designs) respectively.

2.4.2 RT-qPCR

To quantify gene expression, TaqMan quantitative real-time PCR was carried out using an AriaMax Real-time PCR System (Agilent). Primers and probes were designed manually on ApE software using sequences obtained from NCBI and the parameters below. Primers were analysed using OligoAnalyzer 3.1 IDT and Tm checked via NEB Tm calculator.

Table 2.4-1 Manual Primer and probe Design Parameters

Criteria	Rule
Location	Within the CDS, probe crossing exon
Length	18-25 base pairs
GC content	30-60%
Tm primers	54-60°C, no more than 2°C difference between FW and REV primer.
Tm probe	8-10°C more than that of primers
Repeats	No more than 3 of the same residues in a row
Last 5 bases of each primer	No more than 3 G's or C's
OligoAnalyzer analysis	
Hairpin	At least 10°C lower than the primer Tm
Self-dimer	More positive than -9
Heterodimer	More positive than -9

Primers were ordered from Sigma or Eurofins are reconstituted with DEPC-H_2O to a stock concentration of 100µM. Primers were aliquoted and further diluted to 10µM working concentration. A list of RT-qPCR primers and probes used can be found in Table 2.8-4.

After isolating RNA from cells and reverse transcribing it into cDNA, RT-qPCR was preformed to measure gene expression. The reaction components were as follows:

Table 2.4-2 RT-PCR reaction mix

Reagent	Volume
qPCRBIO master mix	6.5µl
Fw primer	0.4µl
Rev primer	0.4µl
Probe	0.25µl
Nuclease free water	2.45µl
cDNA	3µl

Table 2.4-3 RT-qPCR reaction profile

Step	Temperature	Time	Cycle(s)
Hot start	95°C	2 min	1
Denaturation	95°C	5 sec	40
Data collection	60°C	25 sec	

A no enzyme control, a negative template control and a relative standard curve was included in every PCR run. An equal aliquot of each cDNA sample was added to a super neat pool and a series of dilutions were carried out to produce a five-point standard curve (1:2, 1:4, 1:8, 1:16, 1:32 or 1:4, 1:8, 1:16, 1:32, 1:64). Measurements were carried out in triplicates and relative quantities were assessed from the standard curve using the relative standard curve method (Schmittgen and Livak, 2008). The reaction was acceptable if there was less than 0.5 Ct (Cycle threshold) between triplicate values and the standard curve slope fell between -3.2 to -3.6. Reactions with an r^2 value between 0.95-0.99 and a slope of -3.32 was considered 100% efficient amplification. Results were normalised to the appropriate reference gene expression.

2.5 In-vitro SUMOylation assay

In order to investigate the SUMOylation of Nurr1 and Nurr-1a an *in vitro* SUMOylation assay was performed according to a protocol published in Springer protocols (Pourcet et al., 2013).

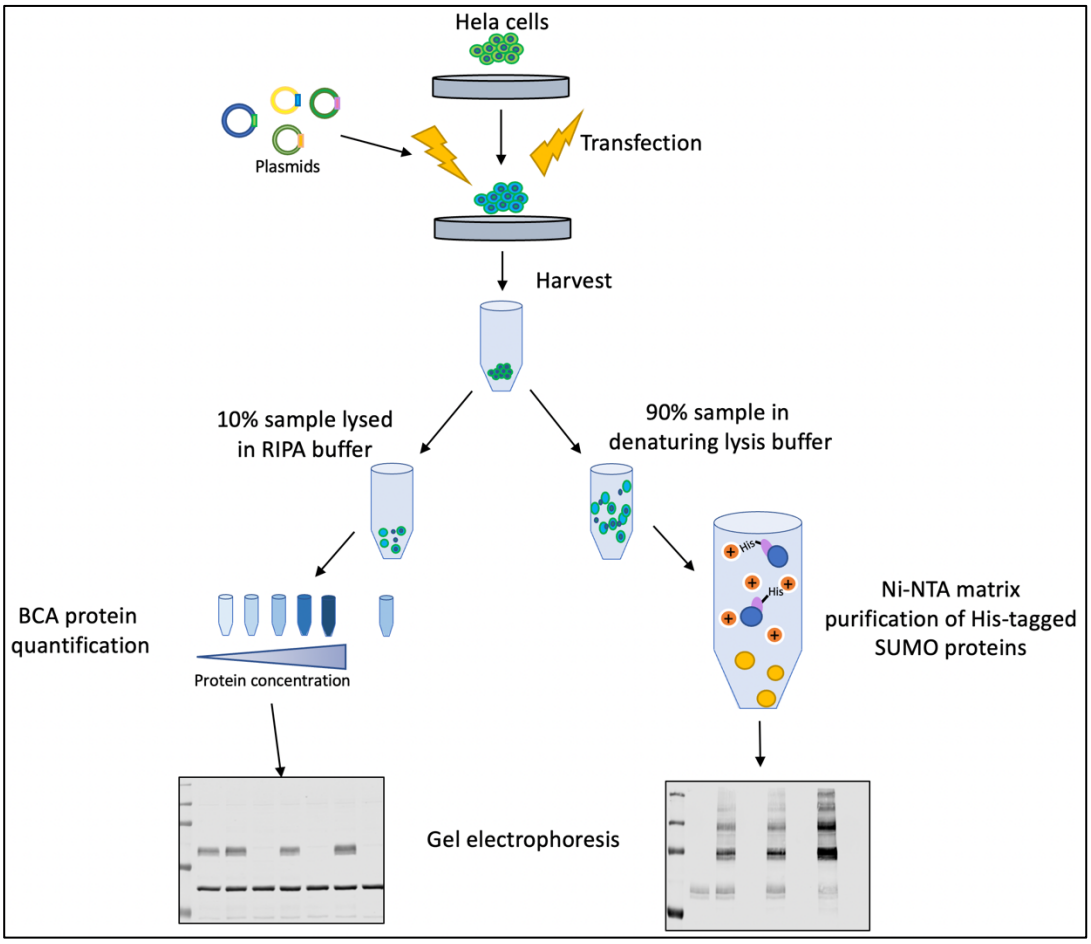


Figure 2.5-1 Schematic of the *in vitro* SUMO pulldown assay described in Springer Protocols (Pourcet et al., 2013)

2.5.1 Ni-NTA pull-down

$3x10^6$ HeLa cells were seeded in $10cm^2$ Petri dishes 24h prior to transfection with appropriate plasmids. Transfection was carried out for 48h with a media change halfway through. A total of 9µg of DNA was transfected per plate, the ratio of plasmid DNA was previously optimised in our lab and was as follows:

Table 2.5-1 Transfection conditions

Gene	Amount
6xHis-SUMO3GG (or SUMO2 or SUMO1)	2.5µg
FLAG-Nurr1 (Or Nurr-1a, or K91 mutants)	2.5µg
HA-Ubc-9	2µg
PIASγ (Or C342A mutant)	2µg
PcDNA3.1 Zeo +	Up to 9µg total DNA
Transfection reaction:	
Serum free media	900µl
X-tremeGENE	18µl
Mixed and added to each tube containing 9µg of plasmid DNA. This was then mixed well and incubated at RT for 30 min. After incubation 900µl was added to each cell culture dish.	

As stated previously, the cells were harvested 48h post transfection. Cells were washed twice with 1xPBS then harvested in 1xPBS using a cell scraper. The suspension was centrifuged at 800xg for 5 min at 4°C. The pellet was resuspended in 1ml 1xPBS before 100µl was removed and processed as an input sample in RIPA buffer. The remaining 900µl was used for protein isolation using nickel beads; initially samples were lysed in denaturing lysis buffer followed by sonication. Both input and isolation lysates were incubated for 30 min at 4°C on a roller followed by a 15 min 4°C centrifugation at 20,000xg. The input sample was then stored at -20°C for protein quantification and further analysis using Pierce BCA Protein Assay Kit.

The protein isolation sample was incubated overnight with a 70µl slurry of 50% v/v Ni-NTA matrix, on a roller at 4°C. The matrix was prepared by washing the beads twice in denaturing lysis buffer before resuspension in the same volume of buffer to create a 50% slurry. After the overnight incubation beads were washed by the addition of 1ml washing buffer followed by vortexing and centrifugation at 5000xg for 2 min at 4°C. Washes were repeated

thrice in Wash buffer I, thrice in Wash Buffer II, and twice in ice cold 1xPBS. Finally, His-tagged proteins were eluted from the beads via the addition of 60µl of 500mM imidazole and a 30s vortex. Following a 10 min RT incubation, 30µl of 3x Laemmli buffer was added, the sample vortexed and finally centrifuged at 20,000g for 1 min at 4°C, before storage at -20°C for further analysis. Both protein isolation and input samples were resolved via SDS-PAGE and immunoblotted using the appropriate antibodies.

Table 2.5-2 Pull-down reagent recipes

Buffer	Recipe
RIPA buffer	10 mM Tris-HCl, 150 mM NaCl, 0.5% Na Deoxycholate, 1 mM EDTA, 1% Triton X-100, 0.1% SDS and 1x EDTA- free protease inhibitor
Lysis buffer	6 M guanidine-HCl, 10 mM Tris-HCl (pH 8.0), 100 mM NaH2PO4, 10 mM imidazole and 1x EDTA-free protease inhibitor adjusted to pH 8
Wash buffer I	6 M Guanidine-HCl; 1 mM Tris-HCl, pH 8.0; 100 mM NaH2PO4; 10 mM imidazole; 300 mM NaCl; 0.5% Triton X-100; 1x protease inhibitor complete EDTA-free
Wash buffer II	8 M urea, 10 mM Tris-HCl, pH 8.0; 100 mM NaH2PO4; 20 mM imidazole; 300 mM NaCl; 0.5% Triton X-100; 1x protease inhibitor complete EDTA-free

2.5.2 Protein concentration assay

To determine protein concentration, a Pierce BCA Protein Assay Kit was used. A standard curve using BSA was prepared according to the manufacturer's standard protocol. In a 96 well plate 10µl of each standard curve mix as well as samples of interest were added to wells in triplicates. 200µl of BCA reagent A was mixed with 10ml of BCA reagent B, and 200µl was added to each well before the plate was covered in foil and incubated at 37°C for 30 min. The absorbance was measured at 562nm on a FLUOstar Omega plate reader.

2.5.3 Western Blot

Western blotting was used throughout this work to visualise protein expression for reasons such as: checking the expression of transfected plasmids in cells, analysing the protein isolation samples from the Ni-NTA matrix, in addition to checking lentiviral infection and protein expression was successful.

Cells were typically harvested 48 hours post transfection or infection in 1xPBS as mentioned previously. Pellets were centrifuged at 800xg for 5 min at 4°C, lysed in RIPA buffer and incubated on a rolled for 30 min at 4°C. Samples were centrifuged at 20,000xg for 15 min at 4°C and protein concentration was determined using the Pierce BCA Protein Assay Kit.

Equal amounts of protein (usually 30 µg) were loaded into previously prepared 10% acrylamide SDS-PAGE gels. Except for the Ni-NTA samples, where 40µl of each sample was added. The gels were run in running buffer at 100V for 15 min followed by 200V for 45 min. The proteins were then transferred onto a 0.45µm nitrocellulose membrane (Amersham Protran #10600003) by sandwiching the gel together with the membrane between filter papers and running the transfer in ice cold transfer buffer for 90 min at 300mA. The membranes were then trimmed down and blocked using 5% milk in TBST for 1h at RT before they were incubated with the appropriate primary antibody overnight on a roller at 4°C. the following day the blot was washed for 10 min thrice with TBST before it was incubated with the corresponding IRDye secondary antibody for 1h at RT. Finally, the blot was washed again for 5 min 3 times with TBST and bands were visualised with a Li-Cor Odyssey imaging system.

Table 2.5-3 Western blot reagents

Buffer	Recipe
RIPA buffer	25 mM Tris-HCl, 150 mM NaCl, 1% Na Deoxycholate, 1 mM EDTA, 1% Triton X-100, 0.1% SDS and 1x EDTA- free protease inhibitor
Running buffer	0.1% SDS, 25 mM Tris, 190 mM glycine
Transfer buffer	25 mM Tris, 190 mM glycine and 20% methanol
TBST	20 mM Tris, 150 mM NaCl, 0.1% Tween 20

2.5.4 Proximity Ligase Assay (PLA)

The PLA was carried out using Duolink in situ PLA kit. $1.8x10^4$ HeLa cells were seeded per well of an 8 well chamber slide. The following day cells were transfected with 50ng of both SUMO2 and either Nurr1/K91 or Nurr-1a/K91, in addition to non-transfected controls for 24h. Cells were fixed with 4%PFA for 15 min at RT followed by two washes with 1xPBS. Permeabilization solution was added for 10 min before two washes with 1xPBS. A drop of Duolink blocking buffer was added to each chamber for 1h at 37°C, from this point on everything must be warmed to and carried out at 37°C unless stated otherwise. Primary antibodies were diluted in Duolink antibody dilutant: Rabbit monoclonal anti-SUMO (1:500) and mouse monoclonal anti-Nurr1 (1:100). 40µl of the appropriate antibody solution was added to each well and incubated overnight at 4°C in a humidified chamber. The following day, slides were washed in RT buffer A. PLA plus and minus probes (1:1) were diluted 1:5 in dilutant. 40µl was added to each well in a humidity chamber at 37°C for 1h. Slides were washed twice in wash buffer A, ligation stock was diluted in HPLC H_2O (1:5) and ligase was added (1:40) directly before use. 40µl of ligation-ligase solution was added to each well which was incubated as before for 30 min. Slides were washed as before in buffer A. Amplification stock was diluted 1:5 in HPLC H_2O, polymerase was added directly before use (1:80), 40µl was added

to each well which was protected from light and incubated as before for 100 min. Slides were washed in 1x wash buffer B twice for 10 min. Followed by a single wash in 0.01x wash buffer B for 1 min. slides were incubated with DAPI (1:500) for 2 min before a wash with 1xPBS and coverslip mounting. Slides were imaged using a Zeiss Exciter Wide field microscope.

Table 2.5-4 PLA recipes

Buffer	Recipe
1x Wash buffer A	0.01M Tris, 0.15M NaCl, 0.05% Tween 20 (Filter solution through 0.22µm filter and store at 4°C)
1x Wash buffer B	0.2M Tris, 0.1M NaCl (Filter solution through 0.22µm filter and store at 4°C)
Permeabilization solution	0.2% w/v triton-X-100 in 1xPBS

2.6 Immunocytochemistry (ICC)

Cells to be visualised using ICC were washed with 1xPBS followed by fixation with 4% (v/v) paraformaldehyde (PFA) for 15 min at RT, and 3 more washes for 5 min in ice cold 1xPBS. Samples were then incubated with permeabilization buffer for 10 min at RT on a shaker followed by 3 washes with 1xPBS for 5 min. Cells were then incubated with a blocking buffer for 30 min at RT before incubation with the appropriate primary antibody overnight with shaking at 4°C. Again, the cells were washed for 5 min 3 times in 1xPBS before they were incubated with the corresponding secondary antibody diluted in dilution buffer (1:1000) for 1h in the dark. Cells were then washed in 1xPBS twice for 5 min. After which, DAPI was used to stain the nuclei 1:500 in 1xPBS at RT for 2 min. Cells were finally washed twice in 1xPBS for 5 min. Cells were either mounted with a coverslip or left in 1xPBS for imaging using a Zeiss 200M fluorescent microscope.

Table 2.6-1 ICC Reagents

Buffer	Recipe
Permeabilization buffer	0.2% w/v triton X-100 in 1xPBS
Blocking buffer	10% Goat serum, 1% BSA, 0.1% Triton X-100 in 1xPBS
Dilution buffer	1% BSA, 0.1% Triton X-100 in 1xPBS

2.7 Lentivirus production

To generate lentiviruses, genes of interest first needed to be cloned from their original plasmid (eg. PcDNA 3.1+Zeo) into destination vectors (pINDUCER20) to create expression clones. These clones in conjunction with a viral packaging (PMD2.G) and envelope plasmid (psPAX2), are then able to produce lentiviruses capable of cell transduction. Cloning into a destination vector followed a "One-Tube" protocol using the Gateway Clonase II system; where a BP recombination reaction is carried out immediately followed by an LR recombination reaction with no intermediate steps.

2.7.1 Designing attB PCR primers

To commence the first BP reaction of Gateway cloning, PCR products flanked with attB sites were generated to allow recombination into a donor vector. To do so, primers were designed to contain four guanine (G) residues at the 5' end, followed by a **25 bp attB1 or 2** site and 18–25 bp of gene-specific sequences. A Kozak sequence was added before the gene specific bp in the Fw primer as recommended by the Gateway cloning protocol. Additional bp's were added when needed to keep the read in frame. Primers used are listed below:

Table 2.7-1 attB PCR primers

Gene	Sequence 5' > 3'
Human Nurr-1a	Fw: GGGG**acaagtttgtacaaaaaagcaggct**tc gccaccATGCCTTGTGTTCAGGCG Rev: GGGG**accactttgtacaagaaagctgggt** tTCATATTCTGTATGCTAATCGA
Human Nurr1	Fw: GGGG**acaagtttgtacaaaaaagcaggct**tc gccaccATGCCTTGTGTTCAGGCG Rev: GGGG**accactttgtacaagaaagctgggt** tTTAGAAAGGTAAAGTGTCCAGG

2.7.2 Production and purification of attB PCR products

The PCR reaction was carried out with Phusion HF polymerase as shown in Table 2.3-3. The reaction conditions were the same as those found in Table 2.3-4 with the annealing temperature being 64°C for 30s.

5µl of the PCR product was first run on a 1% w/v agarose gel and visualised with UV light to check the success of the reaction. This was then followed by gel purification using the remaining 45µl of the reaction mixed with 10µl dye and 5µl Sybr green. The gel was run according to the methods in section 2.3-5. Gel extraction and purification was then carried out using QIAquick Gel Extraction Kit as per the manufacturer's instructions.

2.7.3 BP reaction (PCR fragment + donor vector = entry clone)

The reagents were added as seen in the table below and incubated on a heat block at 25°C for 24h.

Table 2.7-2 BP reaction reagents

Reagent	Amount
attB PCR product	100ng
attP DNA (pDONER221)	1.3µl (150ng/µl)
Gateway BP Clonase II enzyme	3µl
TE buffer	Final volume of 15µl (pH 8.0 (10 mM Tris-HCl, pH 8.0, 1 mM EDTA)

2.7.4 LR reaction (entry clone + destination vector = expression clone)

Remove 5µl of the overnight reaction and add 2µl of proteinase K, incubate at 37°C for 10 min; this can be stored in -20°C and used later to transform bacteria and trouble shoot if the final

transformation does not work. The LR reaction continued with the remaining 10µl as shown below:

Table 2.7-3 LR reaction reagents

Reagent	Amount
LR reaction	10µl
Destination vector (pINDUCER20)	2µl (150ng/µl)
Gateway LR Clonase II enzyme	3µl

The LR reaction was mixed and incubated at 25°C overnight. The following day 2µl of proteinase K was added and incubated for 10 min at 37°C before 2µl of the reaction was used to transform Stbl3 bacteria as seen in section 2.3.7. Colony PCR was then carried out alongside a bacterial media prep and positive colony preps were sent for sequencing for confirmation (Methods 2.3.7, 2.3.8, 2.3.9, 2.3.11).

Table 2.7-4 Viral cloning colony PCR primers

Primer	Sequence 5’ > 3’
LNCX Fw	AGCTCGTTTAGTGAACCGTCAGATC
PIND20 Rev	GGTTACTCCAGACTGCCTTGG

2.7.5 Production and purification of lentiviral vectors

All steps involved with lentivirus were carried out in a biological safety cabinet class 2. Equipment was decontaminated with 2% Distel for 24h prior to disposal.

Day 1: HEK293FT cell seeding
$1.3x10^6$ HEK293FT cells were plated on 10cm culture dishes in 10ml of EMEM media supplemented with 10% FBS and incubated at 37°C for 24 hours to produce 70-80% confluency.

Day 2: Transfection of HEK293FT cells

In a 2ml tube 2µg of each expression vector (eg. pINDUCER20-Nurr1, pINDUCER20-GFP) was added to 600µl of Opti-MEM media (11058021, Gibco), alongside 2µg of packaging plasmid (PMD2.G) and 2µg of envelope plasmid (psPAX2). 18µl of X-tremeGENE HP DNA Transfection Reagent was added to the 2ml tube (1:3 ratio of transfection reagent to plasmid) and mixed gently by pipetting before a 30 min RT incubation. The cell media was carefully removed and replaced with 7ml of Opti-MEM before the transfection complex was added in a dropwise manner and the plate swirled gently to mix. This was incubated for 6 hours at 37°C, after which the media was aspirated and replaced with 12ml of fresh EMEM 10% FBS media, followed by a further 37°C incubation for 48h.

Day 4: Harvest lentivirus

The media was harvested in a 15ml syringe and filtered through 0.45µm syringe filter into a 15ml tube. This was stored at 4°C for up to 2 weeks.

Day 5: Concentrating the virus via ultracentrifugation

10ml thin wall centrifuge tubes were rinsed with sterile water then absolute ethanol and left standing to dry. 1ml of 10% sucrose was then added to the bottom of the ultracentrifugation tube to create a density gradient. Carefully the filtered lentivirus was added on top of the sucrose with a Pasteur pipette, ensuring the two layers do not mix. The virus was centrifuged at 100,000xg (28,000rpm) at 4°C for 2 hours in a SW41 To rotor. The supernatant was discarded without disturbing the pellet, and the pellet was resuspended in 200-300µl PBS (dependent upon pellet size). This was stored at 4°C overnight. Following this 200-300µl of 50% glycerol was added, mixed and

samples were aliquoted into 50µl sterile screw cap tubes to be stored at -80°C.

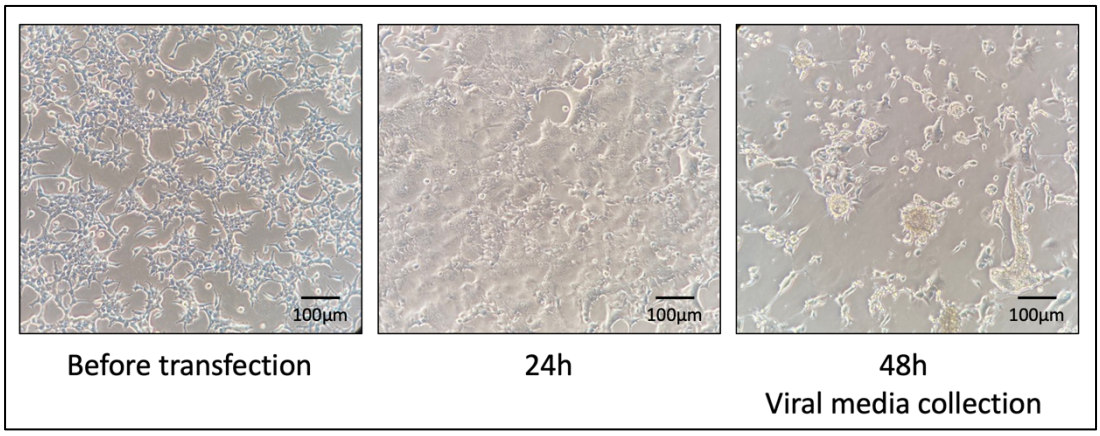


Figure 2.7-1 Morphology of HEK293FT cells during lentiviral production

Images show normal cell morphology before transfection. 24h post infection cells begin to show the effects of viral infection such as the fusing of neighbouring cells. By the time of virus harvest (48h) cell death is apparent displaying aggregates and floating cells.

2.7.6 Lentiviral infection

The amount of lentivirus to use was optimised to each new lentiviral production by observing the proportion of cells infected with different concentrations of GFP under a Zeiss 200M fluorescent microscope. This was initially carried out in HEK293 or HeLa cells, which are known to be easily transduced, before repeating in the cells of interest (eg. iPSCs, iMGL, DA neurons). Once an appropriate volume of lentivirus to produce a suitable level of GFP infection was chosen, cells were transduced with the lentivirus containing the protein of interest. Western blotting was then carried out with antibodies against the protein of interest to check expression was adequate.

Cells were seeded in their respective complete media and incubated at 37°C overnight to achieve 70% confluency the following day. Cell media was aspirated, and fresh media was added containing

10µg/ml polybrene (requires optimisation for different cell types), the appropriate volume of freshly ice-thawed lentivirus was added dropwise and swirled in the well. The plate was then incubated at 37°C for 4h, before the media was refreshed and 10µg/ml doxycycline was added. Cells were incubated for 48h before they were harvested or visualised using a Zeiss 200M fluorescent microscope.

2.8 Primary monocyte isolation

Human blood samples were purchased from the NHS Blood and Transplant service. Buffy coats were used less than 24h after human extraction to ensure maximum viability. All experiments were carried out in accordance with The Human Tissue Act (2004).

2.8.1 Monocyte isolation

The blood sample was aliquoted into 15ml tubes, each containing 5ml histopaque-1077 followed by 5ml of blood carefully layered on top. The sample was centrifuged at 400xg for 30 min at RT (break and acceleration off). The upper layer was aspirated, the middle opaque buffy coat layer was collected and added to a fresh tube. 10ml 1xPBS was gently mixed with the sample, centrifuged at 300xg for 10min (breaks and acceleration on) and the supernatant discarded. This wash was repeated a total of 3 times. A final wash with 1xPBS was repeated and centrifuged for 10 min on 200xg to remove platelets. Finally, the pellet was resuspended in 2ml of complete media RPMI-1640 with 10% FBS. Cells were counted and $1.8x10^6$ cells/ml were seeded onto Cultrexs coated culture ware for iMGL induction, or uncoated culture ware for macrophage induction. The plate was incubated for 2 at 37°C before non-adherent cells were washed away with warm RPMI-1640. Cells were then cultured in the appropriate induction media.

2.8.2 Induction into microglia like cells (iMGL) and macrophages

The protocol used for generating iMGL cells was based on methods described by (Banerjee et al., 2021). To the adherent cells which

remained after washing, iMGL media was added (RPMI-1640, 1xGlutamax, GM-CSF 10ng/ml, IL-34 100ng/ml. Cells were cultured for 14 days with iMGL media changes every 3-4 days.

For macrophage induction, a cocktail of RPMI-1640, 10% FBS and 10ng/µl GM-CSF was added to cells. Fresh media changes occurred after 3 days. Macrophages were ready for assay between days 6-10.

2.8.3 Macrophage and iMGL ICC

Immunocytochemistry was carried out using microglial specific antibodies TMEM119 and P2RY12 alongside a common myeloid marker Iba1. Cells were first fixed with 4% PFA for 20 min at RT followed by 3 x 5 min washes with 1xPBS. Cells were then permeabilised with permeabilization buffer for 30 min, blocked for 1h at RT and incubated with the primary antibody in blocking buffer overnight at 4°C. This was followed by incubation with the corresponding secondary antibody (1:1000) diluted in blocking buffer for 1h at RT in the dark. Finally, cells were washed thrice with 1xPBS, incubated with DAPI (1:500) diluted in 1xPBS for 2min followed by three final 1xPBS washes. Cells were imaged using a Zeiss Exciter Wide field microscope.

Table 2.8-1 Macrophage and iMGL cell ICC

Buffer	Recipe
Permeabilization buffer	0.1% Triton-X-100 in 1xPBS
Blocking buffer	1% BSA in 1xPBS

2.8.4 Phagocytosis assay

Latex GFP beads are first opsonised with FBS (1 beads: 5 FBS) for 1h at 37°C protected from light. During this time cells can be

stimulated with LPS/ATP/IFNy if required. Refresh the cell media and add the required volume of beads to reach the final concentration of 0.05% (v/v), cells are then incubated for 24h. Wash cells 3 times with 1xPBS, followed by a 10min incubation with 4%PFA at 37°C. Cells were washed with 1xPBS thrice before a 2 min incubation with DAPI (1:500) and two additional 1xPBS washes. Cells were visualised using a Zeiss Exciter Wide field microscope.

2.8.5 RT-qPCR

RT-qPCR was carried out as described in section 2.4.2. Human primers and probes used in this thesis are listed below in Table 2.8-2.

2.8.6 SYBR green qPCR

As a successful primer and probe set could not be developed for Nurr-1a RT-qPCR. SYBR qPCR was carried out using just primers, following the same methods described for RT-qPCR except for the reaction mix and profile:

Table 2.8-2 SYBR green reaction mix

Reagent	Volume
Brilliant III Ultra-Fast SYBR green low ROX qPCR master mix	5µl
Fw primer	0.4µl
Rev primer	0.4µl
Nuclease free water	1.2µl
cDNA	3µl

Table 2.8-3 RT-qPCR reaction profile

Step	Temperature	Time	Cycle(s)
Hot start	95°C	3 min	1
Amplification	95°C	5 sec	40
	60°C	10 sec	
Melt	95°C	15 sec	1
	60°C	1 min	
	95°C	15 sec	

Table 2.8-4 RT-qPCR human primers and probes

Human Gene	5’ > 3’
Nurr1	Fw: ACATCGACATTTCTGCCTTCT Rev: TGCAGTTCTTCCACTCTCTTG Probe: TATGGTCACAGAGAGACACGGGCT
GAPDH (Glyceraldehyde 3-phosphate dehydrogenase)	Fw: CAA CAG CCT CAA GAT CAT CAG C Rev: TGG CAT GGA CTG TGG TCA TGA G Probe: CCT GGC CAA GGT CAT CCA TGA CAA C
TNFα (Tumour Necrosis Factor alpha)	Fw: CCCAGGGACCTCTCTCTAATCA Rev: GGTTTGCTACAACATGGGCTACA Probe: CTCTGGCCCAGGCAGTCAGATCATCT
IL-1β (Interleukin 1 beta)	Fw: CCCTAAACAGATGAAGTGCTCCTT Rev: GGTGGTCGGAGATTCGTAGCT Probe: CTGGACCTCTGCCCTCTGGATGGC
IL-6 (Interleukin 6)	Fw: TTACAGGGAGAGGGAGCGAT Rev: TCAGACATCTCCAGTCCTCTT Pro: TGCAAGATGCCACAAGGTCCTCC
IL-10 (Interleukin 10)	Fw: TTGCTGGAGGACTTTAAGGGTTAC Rev: GTCTGGGTCTTGGTTCTCAGCTT Pro: TTGCCAAGCCTTGTCTGAGATGATCCA
CD34	Fw: AAGCACCAATCTGACCTGA Rev: CAGTGCAATCAGGGTCTT Pro: GCTGGGGATCCTAGATTTCACTGAGCAA
CD43	Fw: TCAAAGATGTACACCACTTCAA Rev: TGTTGGCTCAGGTAAAGG Pro: CCCTACCTCCCTCAACTTCCATCAA
CD45	Fw: GACTCTTTGGATAATGCTAGTG Rev: ATGTCTGCGTGTCAGTT Pro: ACAGGTGTTTCATCAGTACAGACGC
SOX2 (Sex-determining region Y-box 2)	Fw: TGCGAGCGCTGCACAT Rev: GCAGCGTGTACTTATCCTTCTTCA Probe: CCGGCGGAAAACCAAGACGCT
NANOG (Homeobox protein NANOG)	Fw: TGAAATCTAAGAGGTGGCAGAA Rev: CCTGGTGGTAGGAAGAGTAAAG Probe: TGGCCGAAGAATAGCAATGGTGTGA
OCT4 (Octamer-binding transcription factor 4 (POU5f1))	Fw: AAACCCACACTGCAGCAGATC Rev: CACACTCGGACCACATCCTTCT Probe: CCACATCGCCCAGCAGCTTGG
TDGF1 (Teratocarcinoma derived growth factor 1)	Fw: CTGTTTTGGCAATGACTCTGAATT Rev: CATGATCCAAATCACACTGTAAGAGA Probe: ATGCTAACGCCTCTTTTCCCCCTAATTGTT
DNM3TB (DNA-methyltransferase 3 beta)	Fw: CATGAAGGTTGGCGACAAGA Rev: ATGCTATCACGGGCCTGTTC Probe: TCTGCTGCTCACAGGGCCCGATA
Nurr-1a SYBR GREEN	Fw: CAGCAATTCTATGATCTCCTGACT Rev: TTCTGTATGCTAATCGAAGGACAAACAGT

2.9 iPSC culture and differentiation

2.9.1 Maintenance and subculture

General culture

iPSCs were cultured in TeSR-E8 complete media. Media was aliquoted into 50ml falcon tubes and stored at -20°C until required where it would then thaw at RT and kept in the fridge for up to 1 week. Before use, media was warmed to RT. Cells were cultured on Cultrex human Stem Cell Qualified reduced growth factor matrix. Cultrex was aliquoted into 100µl aliquots, stored at -20°C until required. Upon use, aliquots were thawed on ice at 4°C overnight before mixing with 9.9ml of ice cold DMEM-F12 (1:100). 4.5ml of the matrix was immediately added to a T25 flask, or 2ml to each well of a 6 well plate. The matrix was left to gel for 1h at RT before use or storage at 4°C for up to 2 weeks. Coated culture ware was warmed to RT for 1h before use, where it was then washed with 1xPBS and fresh TeSR-E8 media was added immediately.

Cryopreserved iPSCs were thawed quickly in a 37°C water bath, ensuring the vial was not completely submerged. 5ml of TeSR-E8 media was added to cells before they were completely defrosted, followed by a 5 min centrifuge at 300xg. The supernatant was aspirated, and the pellet resuspended in 1ml of fresh media which was then added to a Cultrex coated T25 flask to a total volume of 5ml, with 10µM ROCKi. Cells were kept in a 37°C incubator with 5% CO_2. TeSR-E8 media without ROCKi was refreshed every day.

Splitting

When cells reached ~70% confluency with most aggregates displaying the desired "cobblestone" morphology cells were split by one of two methods. For splitting into aggregates (most common)

T25 flasks were first washed with 1xPBS before 3ml of ReLeSR was added to the flask, left for 30s then aspirated, and the flask incubated at 37°C for 3.5 min. After incubation, 4ml of TeSR-E8 was added to the flask followed by gentle tapping from the back to dislodge aggregates. Depending on how concentrated the floating aggregates were, 0.5-4ml of the cell suspension was added to a new coated flask (or well) and media topped up to 5ml (2ml).

For single cell dissociation, T25 flasks were washed once with PBS, before the addition of 2.5ml Accutase. The flask was then incubated for 7.5 min at 37°C. Post incubation 7.5ml of DMEM-F12 (1:3) with 10μM ROCKi was added to the flask and pipetted up and down. The suspension was then transferred to a 15ml tube and centrifuged at 300xg for 5 min. The supernatant was aspirated and depending on the application cells were resuspended in the appropriate media with ROCKi (eg. Neuronal media, TeSR-E8). Often at this point cells were counted using a haemocytometer as seen in methods 2.3.4, and the appropriate density was seeded for the intended experiment.

Cryopreservation

Cells were cryopreserved from T25 flasks when they reached ~70% confluency. They were split using ReLeSR to generate aggregates. Depending on the confluency of the cells 1-5ml of Cryostor was used to resuspend the pellet. 1ml of this suspension was added per cryo tube, which was then placed in a Mr. Frosty at -20°C for 2h, followed by -80°C overnight and liquid nitrogen storage the following day.

2.9.2 Assessment of pluripotency

Pluripotency marker gene expression

The expression of iPSC pluripotency markers was investigated using RT-qPCR as in section 2.4.2. Primers and probes used can be found in Table 2.8-2.

Trilineage differentiation and ICC

Trilineage differentiation was carried out using STEMdiff Trilineage Differentiation Kit, following the manufacturer's instructions. To assess the differentiated 3 germ layers cells were first washed in 1xPBS twice, before fixation in 4% PFA in PBS for 20 min at RT. Cells were then washed thrice in washing buffer for 5 min followed by permeabilization and blocking for 45 min at RT. The cells were then incubated with the primary antibody (10µg/ml) overnight at 4°C and washed the next day in washing buffer three times before incubation with the secondary antibody (1:200 in washing buffer) for 1h in the dark. Cells were then washed twice for 5 min before incubation with DAPI (1:500 in 1xPBS) at RT for 2 min. Finally, after two washes cells were covered in 1xPBS and visualised using a Zeiss Exciter Wide field microscope.

Table 2.9-1 ICC reagents

Buffer	Recipe
Washing buffer	1% BSA in PBS
Permeabilization + blocking buffer	0.3% Triton X-100, 1% BSA, 10% donkey serum in PBS
Primary antibody dilutant	0.3% Triton X-100, 1% BSA, 10% donkey serum in PBS

Table 2.9-3 ICC antibodies

Antibody	Germ layer
Goat anti-human OTX2	Ectoderm
Goat anti-human Brachyury	Mesoderm
Goat anti-human SOX17	Endoderm
Anti-Goat 594	Secondary antibody

Genetic analysis

Genetic analysis of iPSCs was carried out using the Stemcell hPSC Genetic Analysis Kit according to the manufacturer's instructions. To obtain the genomic DNA from the iPSCs required for the kit, GeneJET genomic DNA purification kit was used to extract genomic DNA as per instructed.

2.9.3 Differentiation into haematopoietic (HP) cells

Two methods were used to differentiate iPSCs into HP cells:

STEMdiff Haematopoietic kit

iPSCs were differentiated into HP cells over 12 days using the STEMdiff Haematopoietic Kit as per the manufacturer's instructions.

Cytokine cocktail method

iPSCs were differentiated into HP cells using a cocktail of cytokines as described by Heo et al., (Heo et al., 2018). On day -1 iPSCs were dissociated using ReLeSR, centrifuged for 5 min at 300xg and resuspended in 2ml of DMEM-F12. Serial dilutions were performed and aggerate number counted so that 10-20 aggregates could be seeded per well of a Cultrex coated 6-well plate containing 2ml TeSR-E8 per well. The plate was swirled to ensure even distribution of aggregates and cells were incubated overnight at 37°C.

On day 0, optimal wells which contained ~4-10 aggregates were aspirated and replaced with 2ml media 1. This media refresh was repeated on days 1-3. On day 4 the media was replaced with 2ml media 2. On day 6 wells were replaced with 2ml media 3 and cultured for 11 days with 2ml of media added every 3 days.

Table 2.9-4 Media composition

Media	Recipe
Media 1	Stemline II Haematopoietic SFM, 1x ITS, TeSR-E8, 80ng/ml BMP4
Media 2	Stemline II haematopoietic SFM, 1x ITS 50ng/ml SCF, 40ng/ml VEGF
Media 3	Stemline II haematopoietic SFM, 1x ITS 50ng/ml SCF, 10ng/ml TPO, 50ng/ml IL3, 50ng/ml FLT3, 50ng/ml G-CSF

HP cell RT-qPCR

Haematopoietic cell identity was confirmed using RT-qPCR as in section 2.4.2. Primers and probes used can be found in Table 2.8-2.

2.9.3 Differentiation into microglia

HP cells were differentiated into microglia over 34 days using the STEMdiff Microglia Differentiation and Maturation Kit as per the manufacturer's instructions. On day 34, ICC was carried out as described previously for iPSCs in section 2.9.2. Antibodies can be found in Table 2.1-3.

2.9.4 Differentiation into dopaminergic neurons

Optimised protocol

On day 0 confluent iPSCs from T25 flasks were harvested in Accutase to generate a single cell suspension. Cells were resuspended in 1ml TeSR-E8 media + 10μM ROCKi and counted using a haemocytometer. $1x10^6$ cells were seeded per well of a Cultrex

coated 6 well plate in 2ml of TeSR-E8 media + 10μM ROCKi. Immediately, appropriate volumes of both TET-O-ALN and FUW-M2rtTA viruses were added to each well dropwise and swirled to distribute evenly. The plate was incubated overnight at 37°C.

The next day cell media was aspirated from each well and replaced with 2ml induction media + 1μg/ml doxycycline (Dox). This media change was repeated on days 2 and 3. On day 4 if most cells had begun to extend early processes (>70%), then the media was refreshed with the addition of 2μM Ara-C. However, if cells did not exhibit processes, then Ara-C addition was postponed up until day 6 at the latest. On day 5 the media was refreshed as in the previous step; this was repeated on day 7.

On day 9 the supernatant was aspirated and 2ml of neuron maturation media with reduced Ara-C (1μM/ml) was added to each well. Ara-C was stopped on day 11. Half media changes were carried out every other day until day 21 where ICC was performed.

Table 2.9-5 Neuronal induction reagents

Media	Recipe
Induction media	DMEM/F12, 25 μg ml^{-1} insulin, 50 μg ml^{-1} transferrin, 30 nM sodium selenite, 20 nM progesterone, 100 nM putrescine, 1μg/ml Dox, 4μM Ara-C
Neuronal media	DMEM/F12, 25 μg ml^{-1} insulin, 50 μg ml^{-1} transferrin, 30 nM sodium selenite, 20 nM progesterone, 100 nM putrescine, 1x B27

ICC

Cells were washed with 1xPBS, 500μl of 4%PFA was then added to each well and incubated at RT for 10 min followed by 3 washes in 1xPBS. Cells were permeabilised for 10 min at RT and washed thrice with 1xPBS. 500μL of the blocking solution was added to wells for a 1h incubation at RT. After 2 washes in 1xPBS, antibodies diluted in

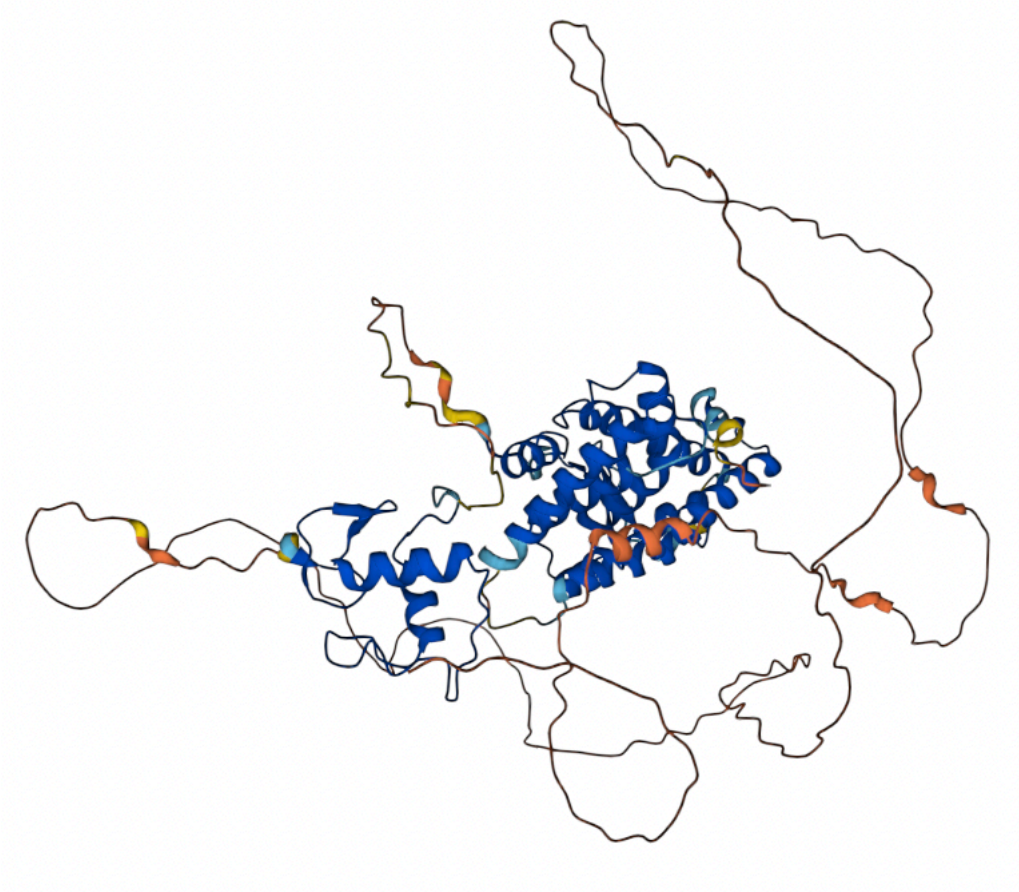
blocking buffer were added to each well and incubated overnight at 4°C. Wells were washed thrice in 1xPBS, followed by the addition of secondary antibodies in 1xPBS (1:500) and a 1h incubation in the dark at RT. Wells were washed thrice in 1xPBS. Finally, cells were incubated with DAPI (1:500 in 1xPBS) at RT for 1 min before visualised using a Zeiss Exciter Wide field microscope. The antibodies used can be found in Table 2.1-3.

Table 2.9.6 ICC reagents

Buffer	Recipe
Permeabilization solution	0.1% Triton-X-100 in 1xPBS
Blocking solution	1%BSA in 1xPBS

Chapter 3

SUMOylation of Nurr1 and Nurr-1a



(Human Nurr1 predicted structure from alpha fold Jumper et al., 2021)

3.1 Introduction

It is widely accepted that Nurr1 plays a vital role in the development, maintenance, and survival of dopaminergic (DA) neurons through the regulation of numerous genes. Many studies have highlighted this function through knockout studies in rodents or therapeutic manipulation (Saucedo-Cardenas and Conneely, 1996, Zetterström et al., 1997, Castillo et al., 1998a, Kim et al., 2016). Research has indicated that Nurr1 expression is decreased with age (Chu et al., 2002). This age-related decrease coupled with its role in DA neurons, highlights Nurr1 as a potential key player in the pathogenesis of PD.

Despite the therapeutic potential of Nurr1, research into many of its basic biological mechanisms is lacking. Such as the effect of PTMs on transcriptional regulation, or the functional role of variants produced by alternative splicing. Several isoforms of Nurr1 have been identified and are produced via alternative splicing, however further research is absent. One isoform, Nurr-1a, was first identified in 1997 through the screening of a mouse genomic phage library (Castillo et al., 1997). It was later shown to be expressed in human and rodent brain tissue during development, and then further identified in adult (33 years) substantia nigra (Ichinose et al., 1999, Michelhaugh et al., 2005).

Little is known about the function of Nurr-1a in the nervous system. Studies which have been performed show that it is minimally transcriptionally active compared to Nurr1, and therefore this has led to it being disregarded as a potentially important transcriptional regulator (Castillo et al., 1998b, Castillo et al., 1998a, Michelhaugh et al., 2005). However, a more recent report by Kim et al., demonstrated in HB1.F3 cells Nurr-1a was able to repress the basal activity of a 3xNBRE luciferase reporter greater than full length Nurr1

(Kim et al., 2013). Indicating a potentially important and unexplored role for Nurr-1a in the differential transcriptional regulation of Nurr1 related genes which may be dependent on cell type.

In addition to its neuronal role, Nurr1 has also been implicated in the regulation of inflammatory pathways (Lallier et al., 2016, Smith et al., 2015). It is now commonly accepted that Nurr1 regulates inflammation in a negative manner, decreasing the expression of pro-inflammatory cytokines in immune cells which therefore may offer some neuroprotection in disease processes with an overtly pro-inflammatory involvement such as PD and Alzheimer's disease (Li et al., 2018). This again highlights therapeutic potential of Nurr1 and raises the question as to what role Nurr-1a may play during inflammation?

The exact mechanism by which Nurr1 modulates inflammation requires further investigation. One hypothesis posited by Saijo et al., proposes that Nurr1 acts as part of a negative feedback loop to reduce inflammation. This regulation is achieved through Nurr1 transrepressing the activation of inflammatory promoters, reducing the expression of inflammatory mediators. SUMOylation is said to be a prerequisite for this transrepression, which is mediated through the E3 ligase activity of PIASg (Saijo et al., 2009). Currently, there is no research regarding the SUMOylation status of Nurr-1a.

SUMOylation is just one of many post-translational mechanisms which are responsible for the diverse regulation of biological processes. However, the precise molecular function of SUMOylation remains to be investigated. Protein inhibitors of activated STAT gamma (PIASg) has been identified as a key interaction partner of Nurr1 and is the E3 ligase responsible for SUMOylation, although a

further repressive SUMO-independent role of PIASg has also been reported (Galleguillos et al., 2004).

One topic which has sparked controversy is the site of which Nurr1 is SUMOylated. SUMOylation sites are lysine residues on target substrates which frequently reside in the same consensus motif Ψ-K-x-D/E (Johnson, 2004). It is noteworthy to add that not all SUMOylated sites conform to this motif, therefore SUMO modification can occur elsewhere (Hendriks et al., 2014, Rodriguez et al., 2001, Sampson et al., 2001). There are multiple different lysine's which are all reported to be the predominant site of Nurr1 SUMOylation. Through mutational studies of the residues in question, Galleguillos et al (2004) reported K91 to be the major site with K577 as a lesser secondary site. Whereas Saijo et al (2009) identified K558 and K576 to be the main sites (Galleguillos et al., 2004, Saijo et al., 2009). There are also discrepancies surrounding which of the SUMO isoforms is the predominant modifier of Nurr1, with some suggesting SUMO2/3 are interchangeable (Josa-Prado et al., 2019, Liu et al., 2021) and others stating SUMO2 is the principal isoform (Saijo et al., 2009, Arredondo et al., 2013). It is unclear why these data surrounding Nurr1 SUMOylation is so conflicting, however it is something we aim to clarify in this chapter.

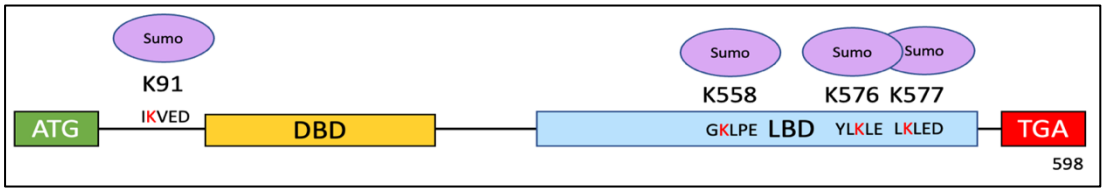


Figure 3.1-1 Nurr1 SUMOylation sites as reported in the literature

The main suggested sites of Nurr1 SUMOylation found in the literature (Saijo et al., 2009, Galleguillos et al., 2004, Arredondo et al., 2013).

In addition to the consensus SUMOylation sites, SUMO proteins can interact with other proteins through SUMO-interaction motifs (SIMs).

These are low affinity non-covalent interactions found on SUMO enzymes and substrate proteins (Henley et al., 2014, Namanja et al., 2012). These SIMs are not responsible for SUMOylation alone but are thought to aid or precede SUMO conjugation (Takahashi et al., 2005).

Nurr1 has been considered an 'orphan nuclear receptor' as it had no identified endogenous ligands. However increasing research suggests a potential role for fatty acids to regulate Nurr1 (Jang et al., 2021). Despite this many have developed or identified synthetic ligands reported to affect Nurr1, the majority focus on changing its transcriptional activity but few also focus on changing its expression (Kim et al., 2016, Ordentlich et al., 2003, Hammond et al., 2015, de Vera et al., 2016, Pan et al., 2005). There are ligands for nuclear receptors which have been shown to affect the level of SUMOylation for that specific receptor such as GW33965 increasing LXRβ SUMOylation (Ghisletti et al., 2007, Lee et al., 2009), however no ligands have been investigated in terms of Nurr1 SUMOylation or any effect they may have on the splice variant Nurr-1a.

This chapter aims to investigate the SUMOylation of Nurr1 and Nurr-1a. Clarifying any discrepancies surrounding the site of Nurr1 modification, in addition to providing novel insight into the SUMOylation status of Nurr-1a. Understanding this will help elucidate towards a potential role for Nurr-1a in inflammatory modulation. The transcriptional activity of Nurr-1a was also studied, despite previous reports showing it to have a minimal response. Finally, the effect, if any, that reported Nurr1 ligands may have on SUMOylation, and transcriptional regulation were also investigated. Which could ultimately lead to a potential candidate for the therapeutic manipulation of Nurr1 or Nurr-1a in Parkinson's disease.

3.2 Results

3.2.1 Cloning wild type Nurr1 and Nurr-1a

Prior to this work, our lab had cloned Nurr1 and Nurr-1a coding sequence from rat into pcDNA3.1(+)zeo vector with the addition of a FLAG tag; to enable the overexpression and detection of Nurr1/1a in mammalian cells (Figure 3.2-1). See appendix for detailed plasmid map.

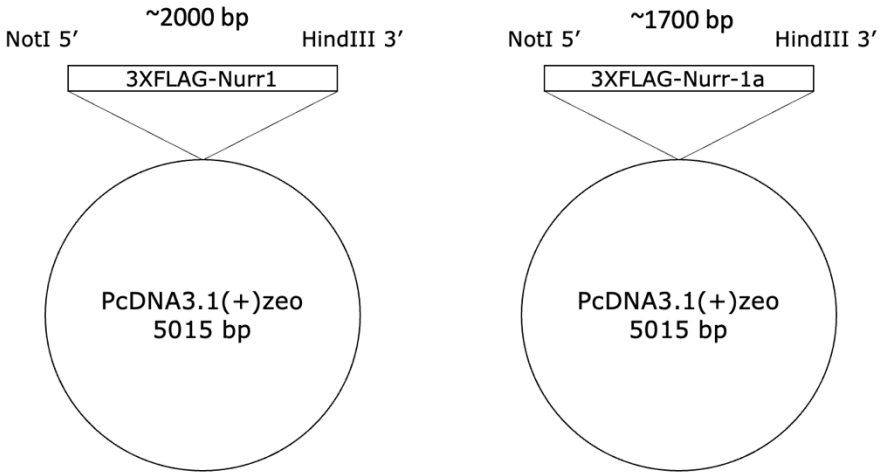


Figure 3.2-1 SUMO3 isoform SUMOylates Nurr1 and Nurr-1a the greatest

Nurr1 and Nurr-1a RNA was isolated from rat tissue, reverse transcribed and cloned into the above vector using the appropriate restriction enzymes, along with 3x FLAG tag. Sequences were analysed to ensure successful cloning (SourceBioscience).

3.2.2 SUMO isoforms of Nurr1 and Nurr-1a

To investigate the potential role of Nurr1 and Nurr-1a in the suggested transrepression mechanism, we needed to first confirm the SUMOylation of both isoforms. Previous reports concerning Nurr1 SUMOylation state SUMO2 and SUMO3 are interchangeable (Liu et al., 2021, Josa-Prado et al., 2019). However Arredondo et al., show through overexpression in COS-7 cells that SUMO2 was the most prominent modifier (Arredondo et al., 2013). We sought to evaluate

if Nurr-1a was capable of modification by SUMO, and if so which SUMO isoform caused the greatest modification of both Nurr1 and Nurr-1a receptors. The expression of the three SUMO isoforms were previously demonstrated in our lab to be comparable and reproducible, however this was not tested in the current study.

Following the SUMO pulldown method described by Pourcet et al., we overexpressed both FLAG-tagged receptor isoforms in HeLa cells along with His-tagged SUMO isoforms 1-3, PIASg and Ubc9 (Pourcet et al., 2013). Pulldown assays of the cell extracts were carried out using a Ni-NTA matrix to enrich SUMO conjugates, followed by western blotting with anti-FLAG and anti-βactin antibodies to detect proteins. Figure 3.2-2 A displays bands corresponding to unmodified (~63-kDa) and SUMOylated (~100-kDa) Nurr-1a. Multiple bands suggested Nurr-1a was poly-SUMOylated by all 3 isoforms, however SUMO3 modified the receptor the strongest; ~2-2.5 fold greater. Figure 3.2-2 B shows bands representing Nurr1 (~78-kDa), and faint bands representing modified Nurr1 (~110-kDa) samples. Previous reports state Nurr1 is modified by SUMO2/3 similarly. However, densitometry revealed a ~2-fold difference; suggesting SUMO3 modifies Nurr1 the greatest. SUMO1 modification of Nurr1 was nearly absent. These data clearly show Nurr-1a is SUMOylated to a greater level compared to Nurr1 and is capable of being modified by all 3 SUMO isoforms. It is also clear that SUMO3 modifies both Nurr1 and Nurr-1a significantly more than SUMOs 1 and 2.

It is noteworthy to mention that unmodified receptor is still detected in the SUMO enriched samples. As suggested by Sentis et al., nuclear receptors can be retained by the Ni-NTA matrix columns due to their zinc finger domain which comprises histidine residues (Sentis et al., 2005).

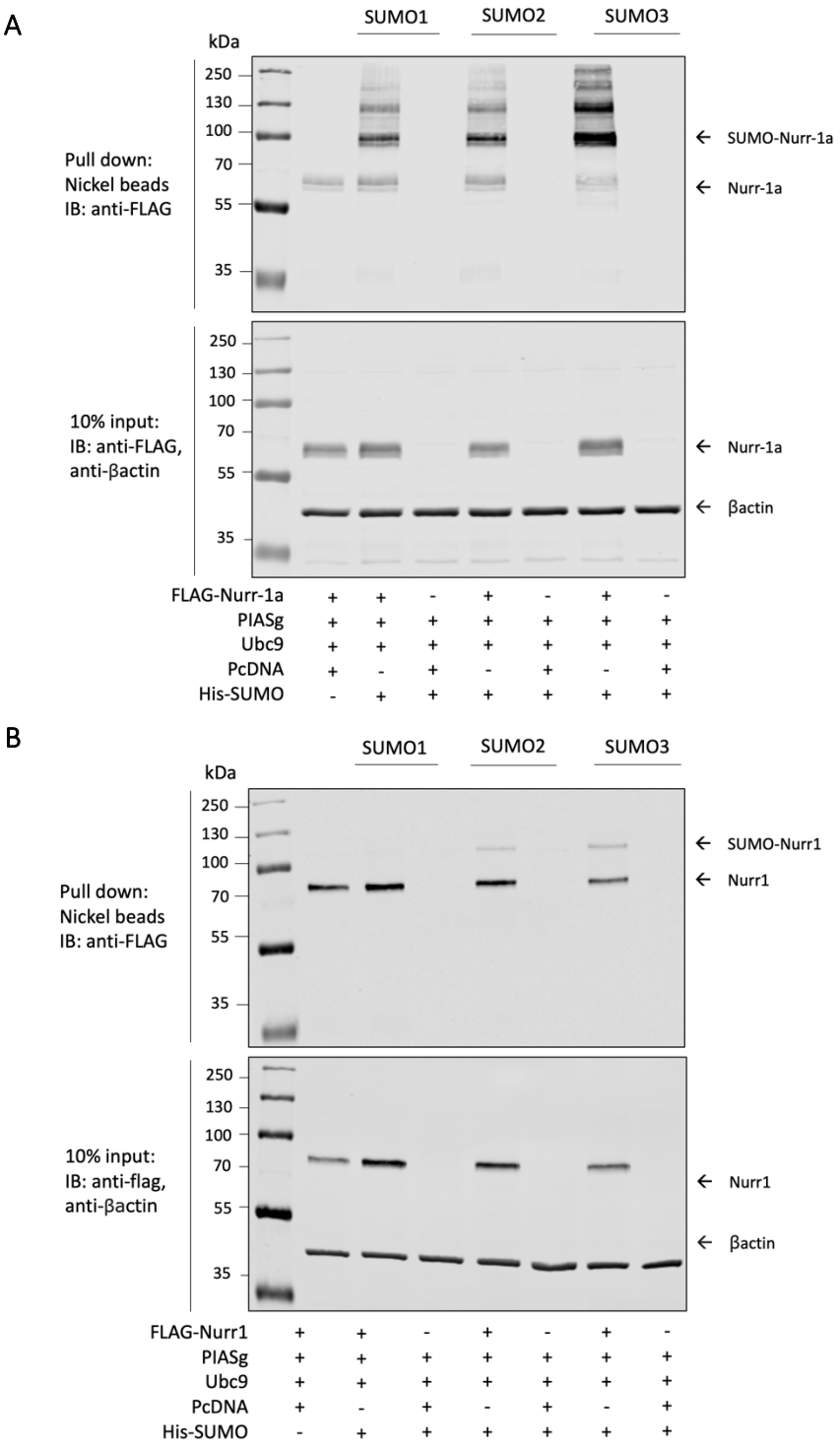


Figure 3.2-2 Nurr-1a is SUMOylated to a greater level than Nurr1

HeLa cells were transfected with plasmids expressing **(A)** FLAG-Nurr-1a, **(B)** FLAG-Nurr1, Ubc9, PIASg and either; His-SUMO1, 2 or 3. 90% of the total cell extract underwent purification with nickel beads before resolution on a 10% acrylamide SDS-PAGE gel. The remaining 10% was processed as a total input sample and electrophoresed similarly. Western blotting was performed with anti-FLAG (1:20,000) and anti-βactin (1:1000) antibodies. Data is representative of results from 3 independent experiments.

3.2.3 PIASg both SUMOylates Nurr-1a and stabilises its protein expression independent of its E3 ligase activity

PIASg is an interaction partner of Nurr1 and is reported to be the E3-SUMO ligase in the SUMOylation process (Arredondo et al., 2013, Galleguillos et al., 2004). After demonstrating Nurr-1a was capable of SUMO modification we wanted to determine the importance of PIASg as an interaction partner and E3 ligase.

Previous research identified a catalytically inactive PIASg mutant; C342A, which was unable to enhance Nurr1 SUMO modification (Arredondo et al., 2013). We transfected either C342A or wildtype PIASg in HeLa cells alongside FLAG-Nurr-1a, Ubc9, and His-SUMO3. Pulldown assays of the cell extracts followed by western blotting showed the highest levels of Nurr-1a protein when all SUMO machinery and wildtype PIASg was present (Figure 3.2-3). C342A generated reduced Nurr-1a expression; ~2-2.5 fold, however the level of SUMOylation remained consistent to overall expression. The absence of PIASg caused a significant reduction in Nurr-1a expression; ~3-5 fold. Indicating that PIASg is required for stable Nurr-1a expression, whilst C342A only altered the level of SUMOylation relative to total Nurr-1a expression.

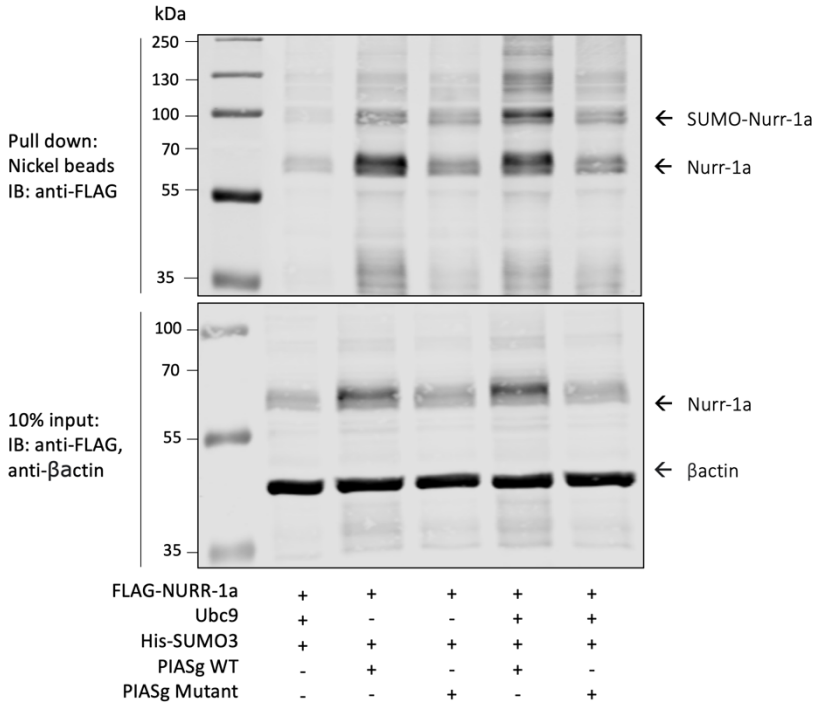


Figure 3.2-3 PIASg is required for stable Nurr-1a expression

Total extracts from HeLa cells transfected with plasmids expressing FLAG-Nurr-1a, Ubc9, His-SUMO3 and either wildtype or C342A PIASg were incubated with nickel beads overnight. 90% of the total cell extract underwent purification with nickel beads before resolution on a 10% acrylamide SDS-PAGE gel. The remaining 10% was processed as a total input sample and electrophoresed similarly. Western blotting was performed with anti-FLAG (1:20,000) and anti-βactin (1:1000) antibodies. Data is representative of results from 2 independent experiments.

We further investigated the C342A catalytic mutant to identify if the reduced Nurr-1a expression and subsequent SUMOylation was directly due to the catalytic function of the ligase, or if the mutation affected the stability and expression of PIASg itself. HeLa cells were overexpressed with either wildtype or C342A PIASg or an empty vector followed by western blotting with anti-PIASg antibody (Figure 3.2-4). Wildtype PIASg was seen at ~72-kDa, whilst C342A expression was significantly reduced by 8-11 fold. This suggests that the catalytically inactive C342A PIASg was less stable than the wildtype. These data show the reduction in the level of C342A may be responsible for the reduced levels of Nurr-1a, rather than a loss of catalytic activity.

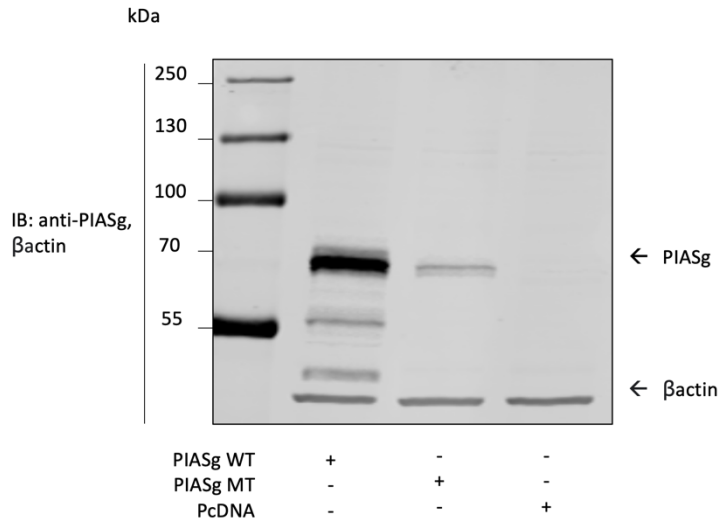


Figure 3.2-4 C342A PIASg protein expression is lower than the wildtype

HeLa cells were transfected with plasmids expressing either wildtype PIASg, C342A PIASg, or an empty vector. After 48h extracts were lysed in naturing conditions and 30µg of protein was resolved on a 10% SDS PAGE gel. Western blotting was performed using anti-PIASg (1:1000) and anti-βactin (1:1000) antibodies. Data is representative of results from 2 independent experiments.

3.2.4 K91 is the principal site of SUMOylation in both Nurr1 and Nurr-1a

The predominant SUMOylation sites of Nurr1 have been investigated and the published data are inconclusive and contradictory (Saijo et al., 2009, Galleguillos et al., 2004, Arredondo et al., 2013). Using SUMOylation site prediction software GPS-SUMO, JASSA and SUMO plot we identified potential SUMO sites in both human and rat Nurr1/1a sequences. It is noteworthy to add the SIM site identified in Nurr-1a was only picked up in GPS-SUMO and not in the other software. NCBI BLAST demonstrated that the amino acid coding sequence of rat and human Nurr1 and Nurr-1a are 93.60% and 92.76% homologous respectively.

Species	Isoform	Site	Sequences
Rat	Nurr1	K91	QSSIKVEDI
		K577	IFYLKLEDL
		K590	AIIDKLFLD
		K432	ADLPKADQD
	Nurr-1a	K91	QSSIKVEDI
		SIM site K448-452	LELFVLRLAYRI***
		K432	ADLPKADQD
Human	Nurr1	K91	QSSIKVEDI
		K577	IFYLKLEDL
		K590	AIIDKLFLD
		K432	ADLPKADQD
	Nurr-1a	K91	QSSIKVEDI
		SIM site K448-452	LELFVLRLAYRI***
		K432	ADLPKADQD

Figure 3.2-5 Predicted SUMO sites of Nurr1 and Nurr-1a

Nurr1 and Nurr-1a rat and human sequences were run through GPS-SUMO, JASSA and SUMO plot to identify predicted SUMO sites.

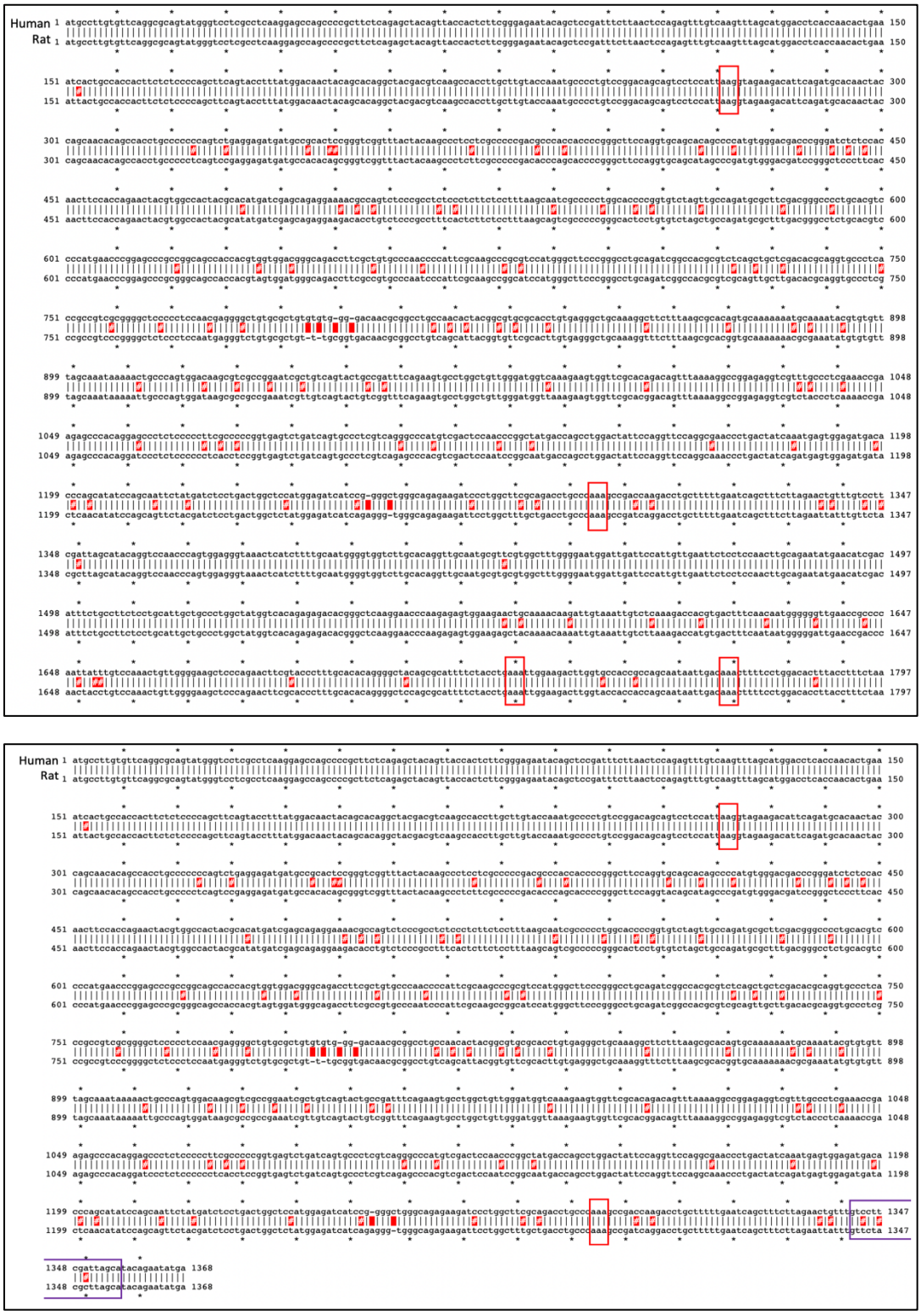


Figure 3.2-6 Alignment of Human and Rat Nurr1 and Nurr-1a sequences

Top panel aligns Human and Rat Nurr1, bottom aligns Nurr-1a. Red boxes outline predicted SUMOylation sites. Purple box outlines predicted SIM site.

We demonstrated that Nurr-1a is abundantly SUMOylated. Therefore, when investigating the main site of SUMOylation in Nurr1/1a we ruled out K577 and K590 in addition to those reported by Saijo et al., (K576 and K558) as these sites are absent in Nurr-1a due to its C-terminal truncation. SUMO prediction software scored K91 11-times higher than K432 suggesting it was a more probable site. To determine this, we used K91 mutants of Nurr1/1a which were previously made in our lab through site directed mutagenesis of lysine 91 (K91) to arginine to generate the K91R mutation.

Nurr1 and other nuclear receptors have been shown to move between the nucleus and cytoplasm in response to certain ligands or stimuli (Garcia-Yague et al., 2013, Zarraga-Granados et al., 2020, Andreou and Tavernarakis, 2009). Garcia-Yauge et al., reported Nurr1 to have two sites of nuclear localisation signals (NLS) within the DNA binding domain which are important for localisation into the nucleus and subsequent transcription of genes (Garcia-Yague et al., 2013). Exclusion from the nucleus renders nuclear receptors inactive in terms of transcriptional regulation. Some evidence suggests that SUMOylation can alter nuclear localisation, however Arredondo et al., demonstrates this is not the case for Nurr1 (Zarraga-Granados et al., 2020, Arredondo et al., 2013). Nevertheless, we wanted to investigate whether the K91 mutants are correctly localised and if the absence of SUMO machinery affected this.

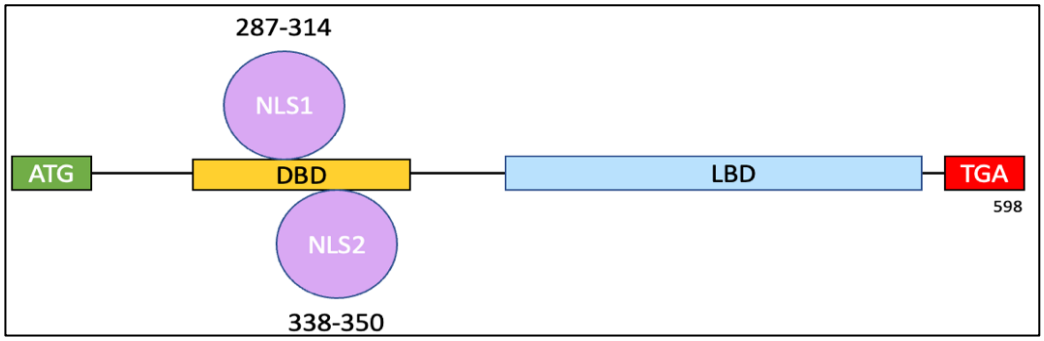


Figure 3.2-7 Reported Nuclear Localisation Signal sites of Nurr1

Schematic diagram of the two NLS sites reported by Garcia-Yague et al., (2013).

We transfected wildtype and K91 Nurr1 and Nurr-1a in HeLa cells, followed by immunocytochemistry using anti-FLAG and DAPI to observe the location of nuclear receptor in the cell 48h post transfection. As expected, both isoforms of Nurr1 are found almost exclusively in the nucleus, with levels of FLAG-Nurr1 or 1a positive nuclei remaining consistent regardless of wildtype or K91. These data clearly show that both the K91 mutation and the absence of SUMO machinery does not affect sub-cellular localisation.

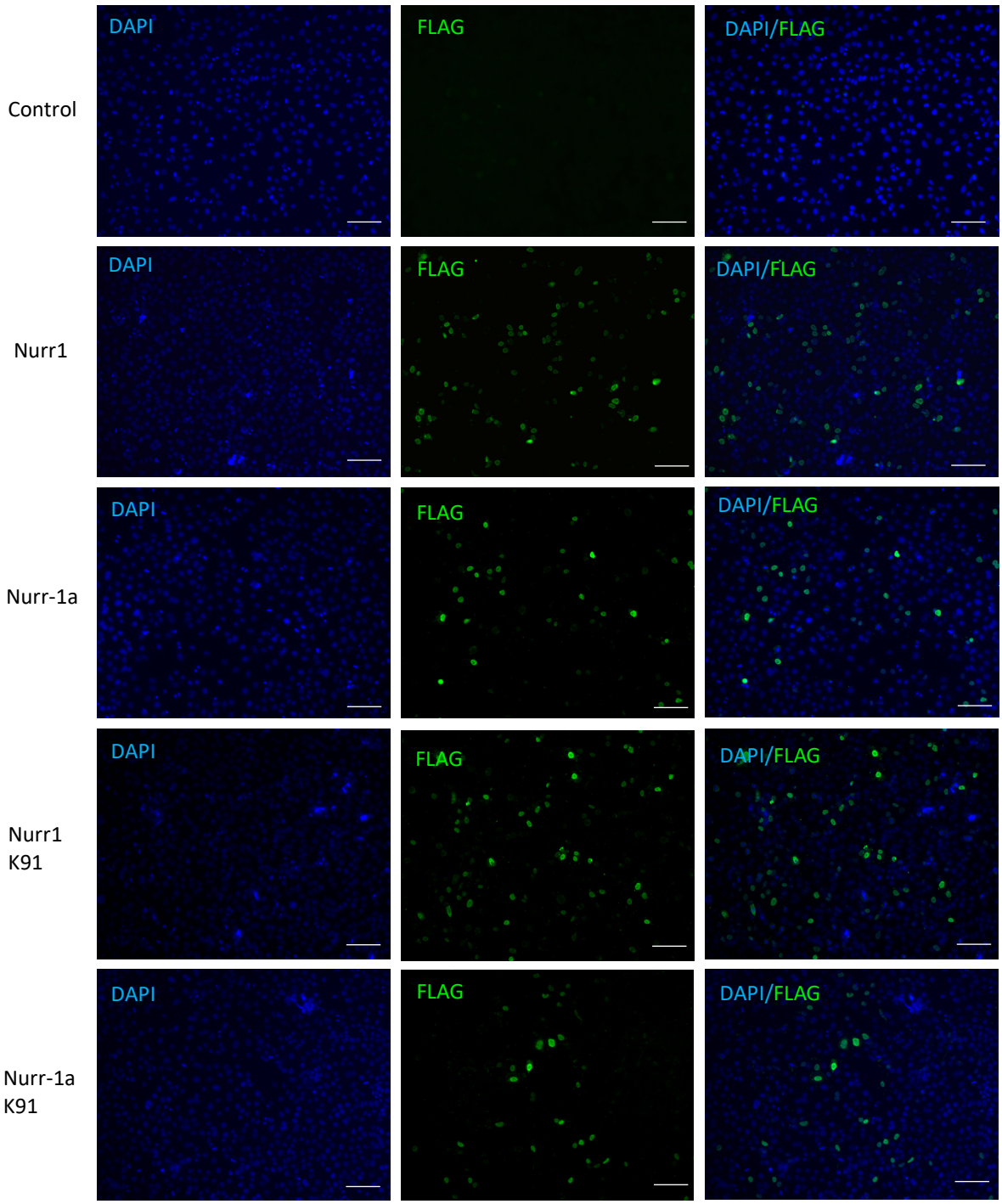


Figure 3.2-8 Subcellular localisation of Nurr1 and Nurr-1a K91 mutants

HeLa cells were transfected with either pcDNA3.1(+)zeo (control), FLAG-Nurr1, FLAG-Nurr-1a, FLAG-Nurr1 K91 and FLAG-Nurr-1a K91. ICC was carried out 48h after transfection with anti-FLAG (green) and DAPI nuclear staining (blue). Widefield microscope objective 10x. Data is representative of results from 2 independent experiments. Scale bar represents 100μm.

Since our previous results showed PIASg was required for stable expression of Nurr-1a, we investigated if the presence of this stabilising factor would affect cellular localisation. These data show the addition of PIASg did not alter localisation of Nurr1/1a. However, it did increase the number of Nurr-1a positive nuclei for both wildtype and K91, again confirming its role in Nurr-1a stability.

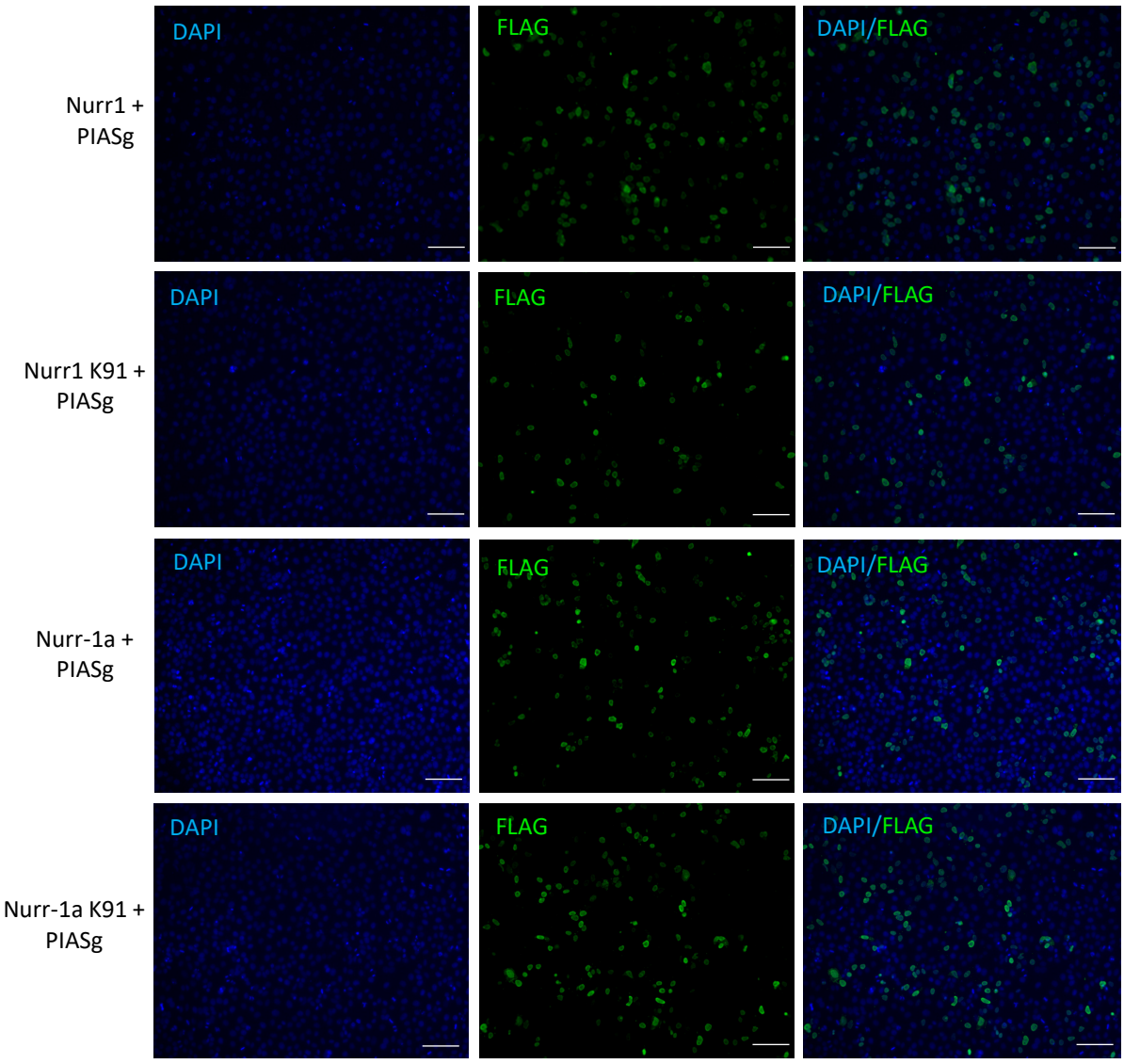


Figure 3.2-9 Subcellular localisation of Nurr1 and Nurr-1a K91 mutants with PIASg

HeLa cells were transfected with either FLAG-Nurr1, FLAG-Nurr-1a, FLAG-Nurr1 K91 and FLAG-Nurr-1a K91 with or without PIASg. ICC was carried out 48h after transfection with anti-FLAG (green) and DAPI nuclear staining (blue). Widefield microscope objective 10x. Data is representative of results from 2 independent experiments.

To evaluate the effect the K91 mutation would have on the SUMOylation of Nurr1 and Nurr-1a we overexpressed wildtype or K91 receptors along with His-SUMO2, Ubc9 and PIASg in HeLa cells. From this point on SUMO2 was used instead of SUMO3 as it is widely used in the literature, and we previously demonstrated (Figure 3.2-2) that both generate adequate and consistent levels of Nurr1/1a SUMOylation. SUMO pulldown assays of the cell extracts followed by western blotting with anti-FLAG antibody showed that K91 abolished the low level Nurr1 SUMOylation. The K91 mutation also markedly decreased the SUMO modification of Nurr-1a by ~2.5-4 fold, however it did not completely abolish it. This residual SUMOylation indicates there are other SUMO sites which are modified at a much lower level or may be a result of overexpressing SUMO machinery which can cause non-physiological SUMOylation of additional lysine's. This is typical of lysine mutagenesis experiments (Arredondo et al., 2013, Saijo et al., 2009).

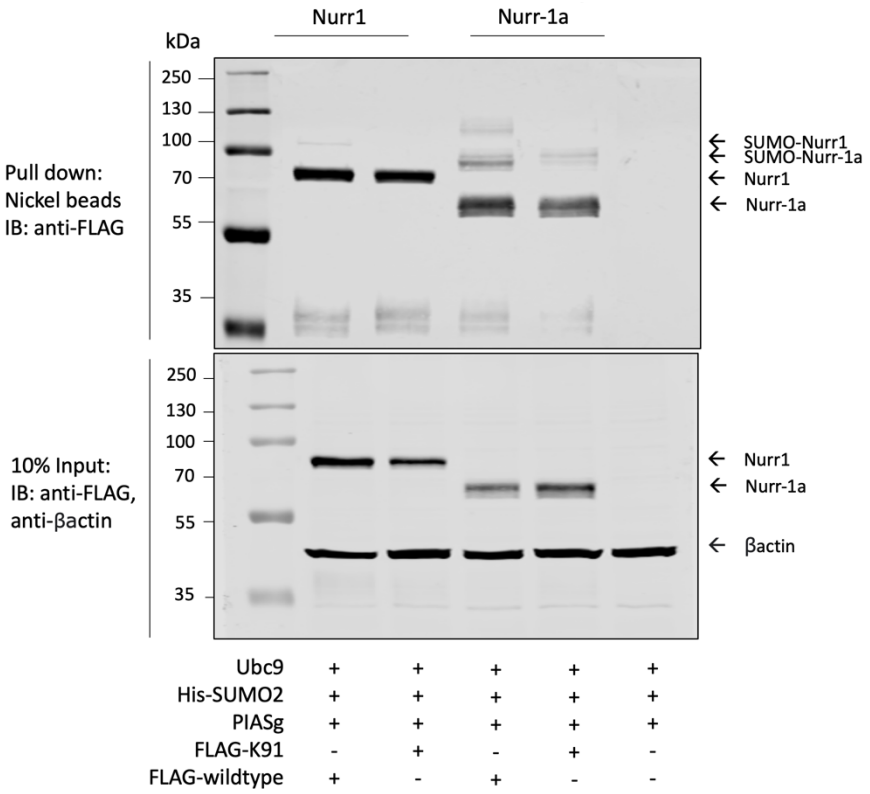


Figure 3.2-10 K91 is the major SUMOylation site of Nurr-1a

Total extracts from HeLa cells transfected with plasmids expressing either wildtype FLAG-Nurr1/K91R or wildtype Nurr-1a/K91R, Ubc9, His-SUMO2 and PIASg. 90% of the total cell extract underwent purification with nickel beads before resolution on a 10% acrylamide SDS-PAGE gel. The remaining 10% was processed as a total input sample and electrophoresed similarly. Western blotting was performed with anti-FLAG (1:20,000) and anti-βactin (1:1000) antibodies. Data is representative of results from 2 independent experiments.

3.2.5 Investigating the Nurr-1a SUMO Interaction Motif (SIM)

SIMs are known to aid in SUMO modified substrate recognition, enhancement of SUMOylation and promotion of complex assembly (Song et al., 2004, Meulmeester et al., 2008, Psakhye and Jentsch, 2012). GPS-SUMO software predicted a SIM site in Nurr-1a at k448-452. This site was not predicted in Nurr1, nor did other software predict this site. Site directed mutagenesis (SDM) following the 'Agilent QuikChange XL Site Directed Mutagenesis Kit' was used to create a Nurr-1a SIM mutant with 3-point mutation (V488A, L449A)

and is shown in Figure 3.2-10. Valine and Leucine were mutated to Arginine as Arginine is not SUMOylated and both Leucine and Arginine are positively charged. Additionally, these changes required only 3-point mutations.

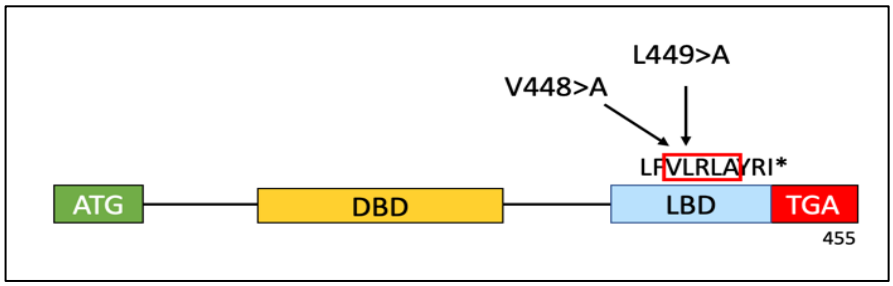


Figure 3.2-11 Mutating the Nurr-1a SIM site

Schematic representation of the Nurr-1a protein with the SIM site highlighted and mutations annotated.

Following mutagenesis and transformation, purified plasmids were sequenced, and identified to contain the mutated region (Figure 3.2-11).

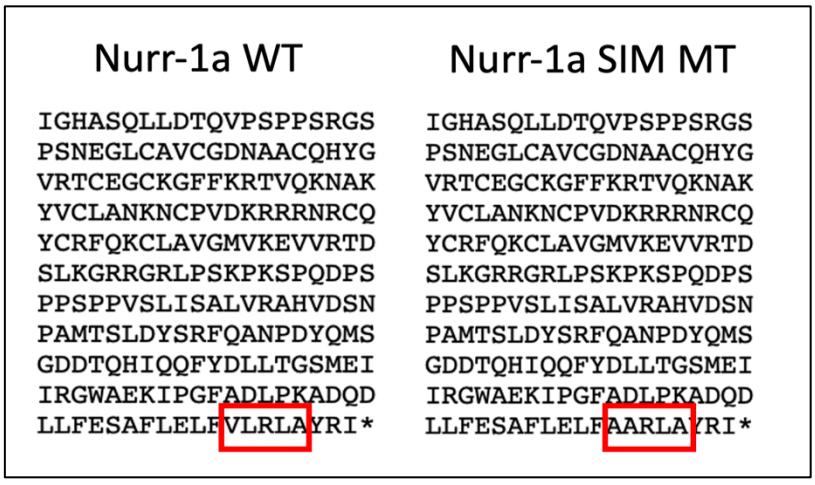


Figure 3.2-12 Nurr-1a SIM mutation sequence
Analyzed sequenced from wildtype and SIM mutant Nurr-1a plasmids (SourceBioscience) displaying successful site directed mutagenesis of amino acids V > A and L > A.

To determine the importance of this site on the overall level of Nurr-1a SUMOylation, we overexpressed this mutant in HeLa cells along with PIASg, His-SUMO2 and Ubc9, before performing a SUMO

pulldown assay and immunoblotting with anti-FLAG. The Nurr-1a SIM construct was not expressed as highly as the wildtype ~1.4-1.8 fold less; and any changes in SUMOylation reflected this. These data show that the SIM mutation affects Nurr-1a protein stability, but it does not directly affect the level of SUMOylation. Despite not altering SUMO modification it could still be an important site during transcriptional regulation.

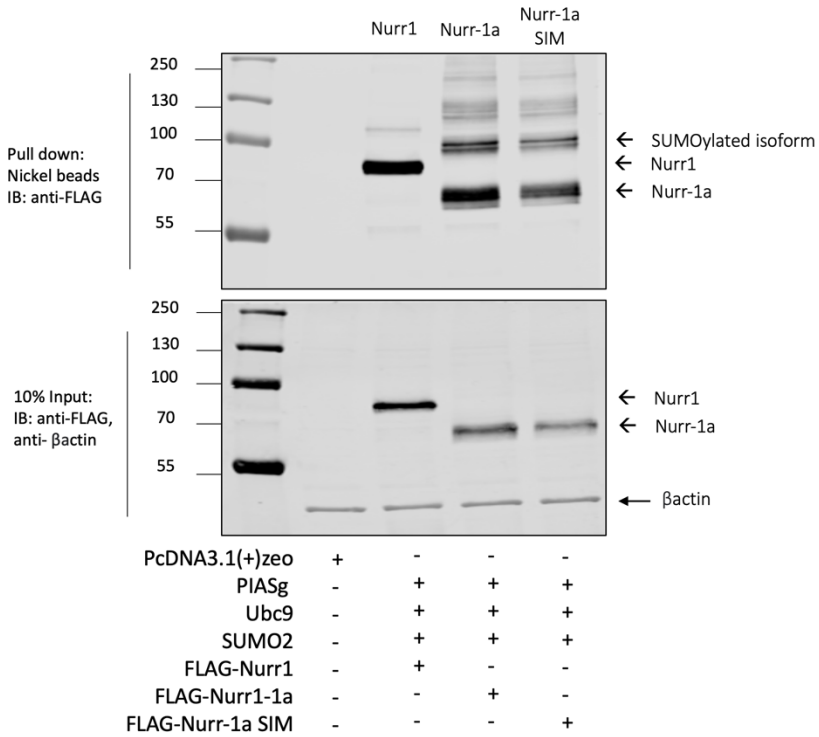


Figure 3.2-13 Nurr-1a SIM mutation reduces protein stability

Total extracts from HeLa cells transfected with plasmids expressing either WT Nurr1, WT-Nurr-1a or SIM MT-Nurr-1a and Ubc9, His-SUMO2 and PIASg. 90% of the total cell extract underwent purification with nickel beads before resolution on a 10% acrylamide SDS-PAGE gel. The remaining 10% was processed as a total input sample and electrophoresed similarly. Western blotting was performed with anti-Flag (1:20,000) and anti-βactin (1:1000) antibodies. Data is representative of results from 3 independent experiments.

3.2.6 Effect of ligands on Nurr1 and Nurr-1a

As Nurr1 is considered an orphan nuclear receptor with no known endogenous ligands; research has focused on the development of synthetic ligands and modulators which bind to sites other than the canonical binding pocket, which is situated in the LBD, and mediate the expression or activation of Nurr1. Although many of the previously investigated ligands have suggested mechanisms of action, none specifically address the effect these ligands have on Nurr1 SUMOylation. Additionally, the effects of ligands on Nurr-1a or on its SUMOylation have not yet been reported. We sought to investigate the effect various ligands had on the expression and SUMOylation of Nurr1 and Nurr-1a. Ligands used are listed in Table 3.2-1 below.

Table 3.2-1 Concentration of ligands

Ligand	Target	Model	Effect	Reference
DHA 50-100μm	LBD	HEK293T MN9D	Decreases Nurr1 transcriptional activity	(de Vera et al., 2016, de Vera et al., 2019)
AQ 5-20μm	LBD	Primary rat microglia BV-2	Increases Nurr1 transcriptional activity	(Kim et al., 2015, Kim et al., 2003a)
6-MP 10μm	AF-1	CV-1	Increases Nurr1 transcriptional activity	(Ordentlich et al., 2003)
C-DIM12 2.5-10μm	Coactivator binding site (LBD)	PC12 MPTP mice N2A N27 BV-2	Increases Nurr1 transcriptional activity	(Hammond et al., 2018, Hammond et al., 2015, De Miranda et al., 2015)
Pramipexole 1-10μm	D3 receptor	SH-SY5Y	Increases Nurr1 expression	(Pan et al., 2005) (Smits et al., 2003, Pan et al., 2005)

Nurr1 or Nurr-1a was overexpressed in HeLa cells along with His-SUMO2, Ubc9 and PIASg before samples were treated with one of five different ligands for 24h. Concentrations used were decided according to previous literature. His-tagged SUMO pulldown assays of the cell extracts were carried out followed by western blotting with anti-FLAG antibody and anti-βactin. It appeared the ligands had little effect on the expression or SUMOylation of Nurr1. Slight changes in expression of Nurr-1a were observed in response to ligands in Figure 3.2-14, but no specific changes in terms of SUMOylation. AQ and C-DIM12 (5μM) marginally reduced Nurr-1a expression by ~1.7 and ~1.3 fold respectively, whilst 6-MP, DHA and Pramipexole slightly increased expression in the total protein input blot compared to the DMSO and BSA controls ~1.2-1.4 fold. Demonstrating that the ligands, except possibly AQ, did not majorly change the expression or SUMOylation of Nurr1 or 1a in the SUMO pulldown experiments.

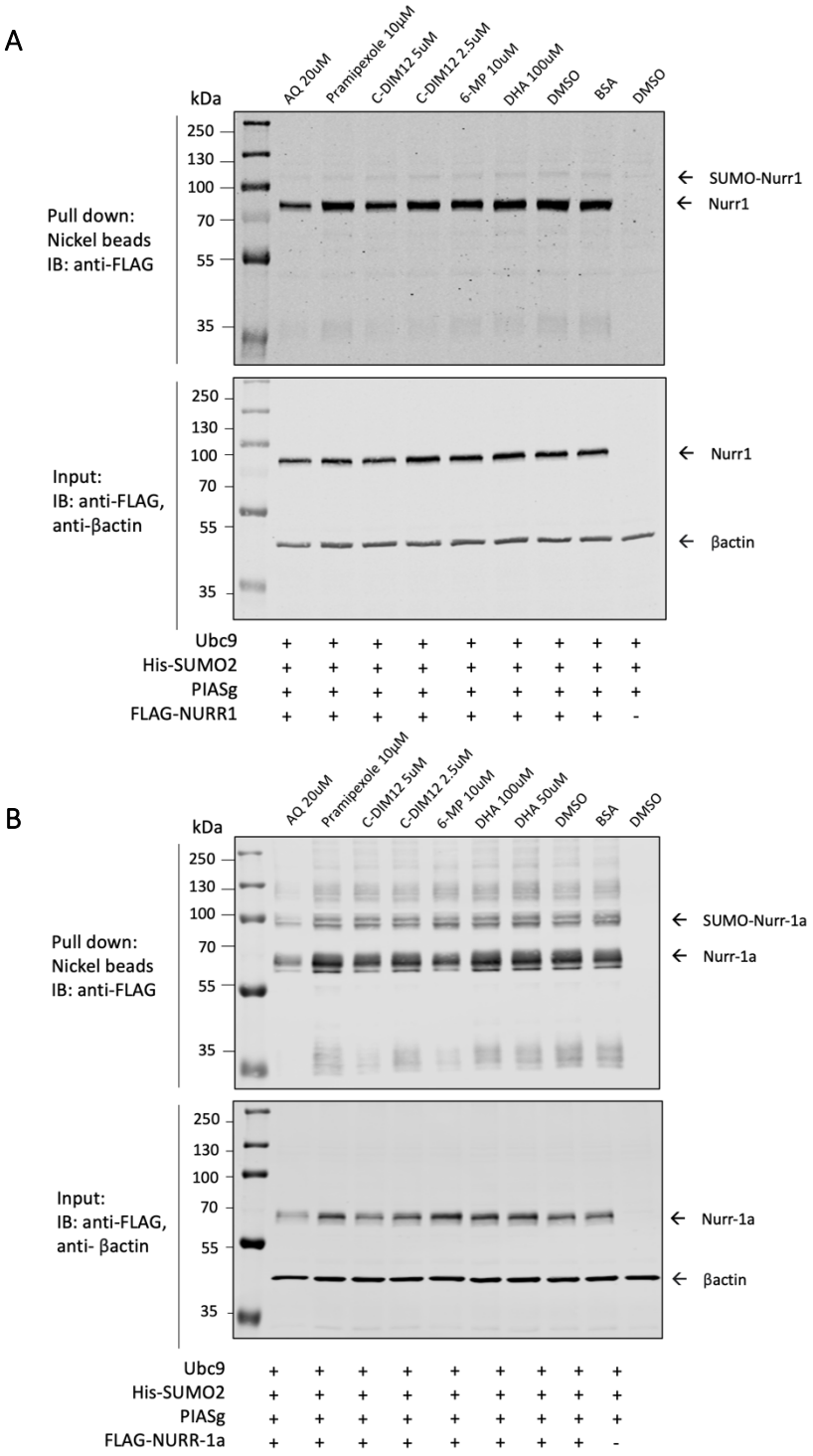


Figure 3.2-14 Ligands affect the expression of Nurr-1a

HeLa cells were transfected with plasmids expressing either FLAG-Nurr1 (A) or FLAG-Nurr1-1a (B) and Ubc9, His-SUMO2 and PIASg, followed by ligand treatment for 24h. 90% of the total cell extract underwent purification with nickel beads before resolution on a 10% acrylamide SDS-PAGE gel. The remaining 10% was processed as a total input sample and electrophoresed similarly. Western blotting was performed with anti-FLAG (1:20,000) and anti-βactin (1:1000) antibodies. Data is representative of results from 2 independent experiments.

The chosen ligands had minimal effects on the protein expression levels or SUMOylation of both Nurr1 and 1a. However, a previous report demonstrated that increasing the concentration of Pramipexole in SH-SY5Y cells increased Nurr1 expression as well as transcriptional activation (Pan et al., 2005). We did not observe any significant change in expression of Nurr1 treated with this ligand, but we did see a slight change in Nurr-1a expression (~1.2 fold), therefore we wanted to investigate if there was concentration dependent expression. Additionally, AQ was shown to decrease Nurr-1a expression (~1.7 fold), so we also investigated any dose dependent changes. SUMO machinery along with FLAG-Nurr-1a was expressed in HeLa cells for 24h followed by a 24h ligand treatment at varying concentrations (Figure 3.2-15). SUMO pulldown was carried out followed by western blotting. Pramipexole did modestly increase the Nurr-1a expression compared to the DMSO control in the input blot, however increasing the concentration did not change expression nor did it alter SUMOylation. Whilst increasing the concentration of AQ decreased the expression. These results suggest the ligands mildly influence the expression of Nurr-1a protein, however they do not significantly change the level of SUMOylation.

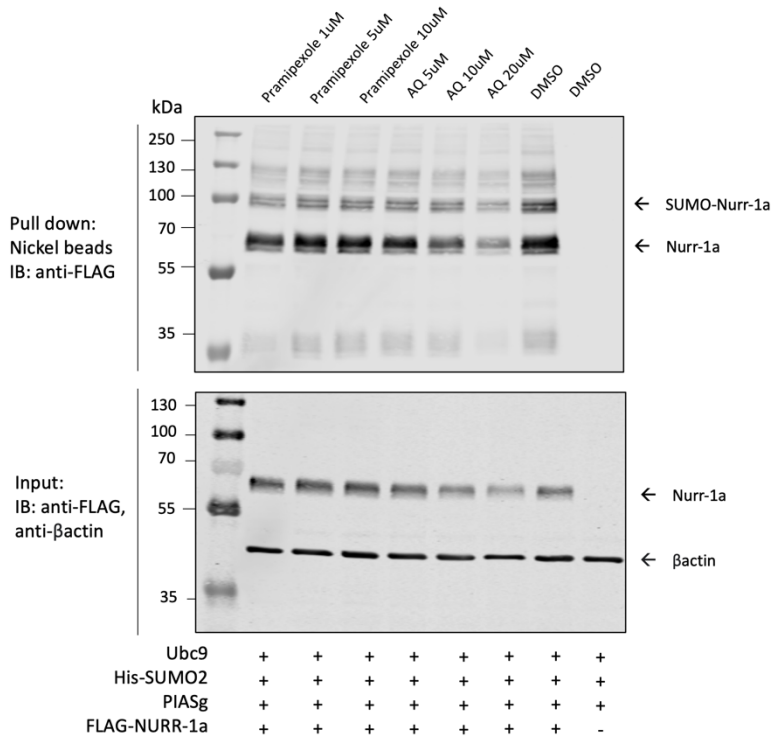


Figure 3.2-15 Concentration dependent effect of ligands upon Nurr-1a protein levels

HeLa cells were transfected with plasmids expressing FLAG-Nurr-1a alongside Ubc9, His-SUMO2 and PIASg, followed by ligand treatment for 24h. 90% of the total cell extract underwent purification with nickel beads before resolution on a 10% acrylamide SDS-PAGE gel. The remaining 10% was processed as a total input sample and electrophoresed similarly. Western blotting was performed with anti-FLAG (1:20,000) and anti-βactin (1:1000) antibodies. Data is representative of results from 2 independent experiments.

3.2.7 Evaluating the Nurr1/1a-SUMO interaction

To further confirm if Nurr1 and Nurr-1a are SUMOylated, we carried out a Proximity Ligase Assay (PLA) which can detect the interaction of two targets within close proximity of each other (40nm).

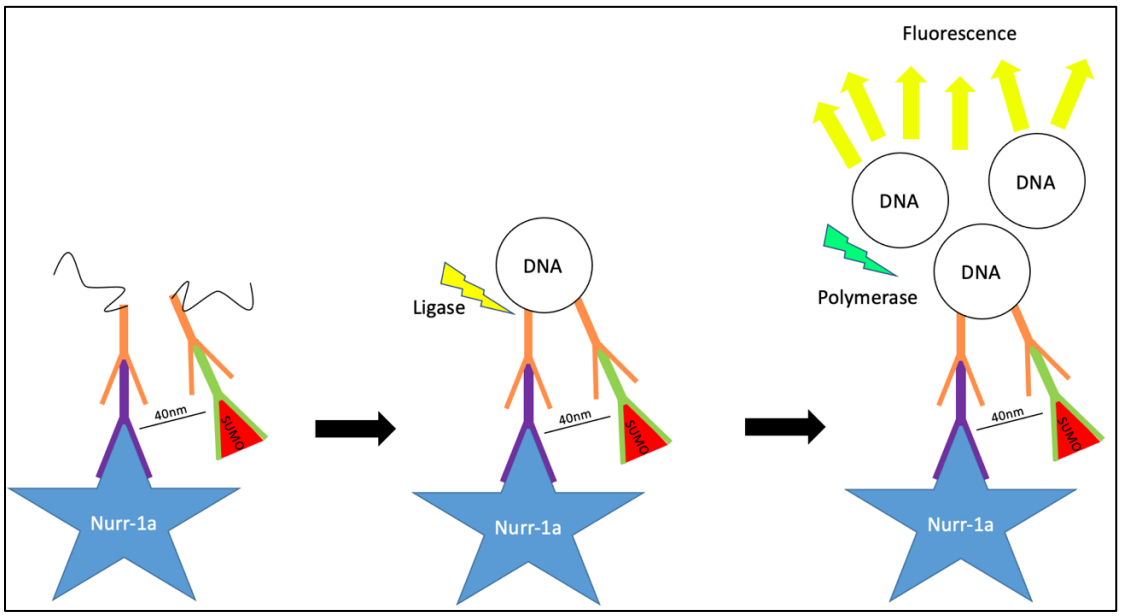


Figure 3.2-16 Schematic diagram of the Proximity Ligase assay

Schematic diagram depicting that close proximity (40nm) of two proteins (Nurr-1a and SUMO) allows secondary oligonucleotide labelled probes to ligate together to form circularised DNA. Polymerase then amplified the DNA followed by fluorescent detection.

The PLA assay was carried out in HeLa cells to evaluate Nurr1/1a-SUMO interactions. Results show that both wildtype and K91 Nurr1/1a were within close proximity of overexpressed SUMO. However, a large proportion of this signal was detected outside of the nucleus. This was surprising as our previous results showed the majority of Nurr to be detected in the nucleus, with minimal signal in the cytoplasm. Interestingly, we also saw similar levels of signal when cells were transfected with K91, which we have already shown to have significant less SUMOylation than the wildtype. A possibility is that the K91 mutant is in a complex with another SUMOylated protein which is less than 40nm away.

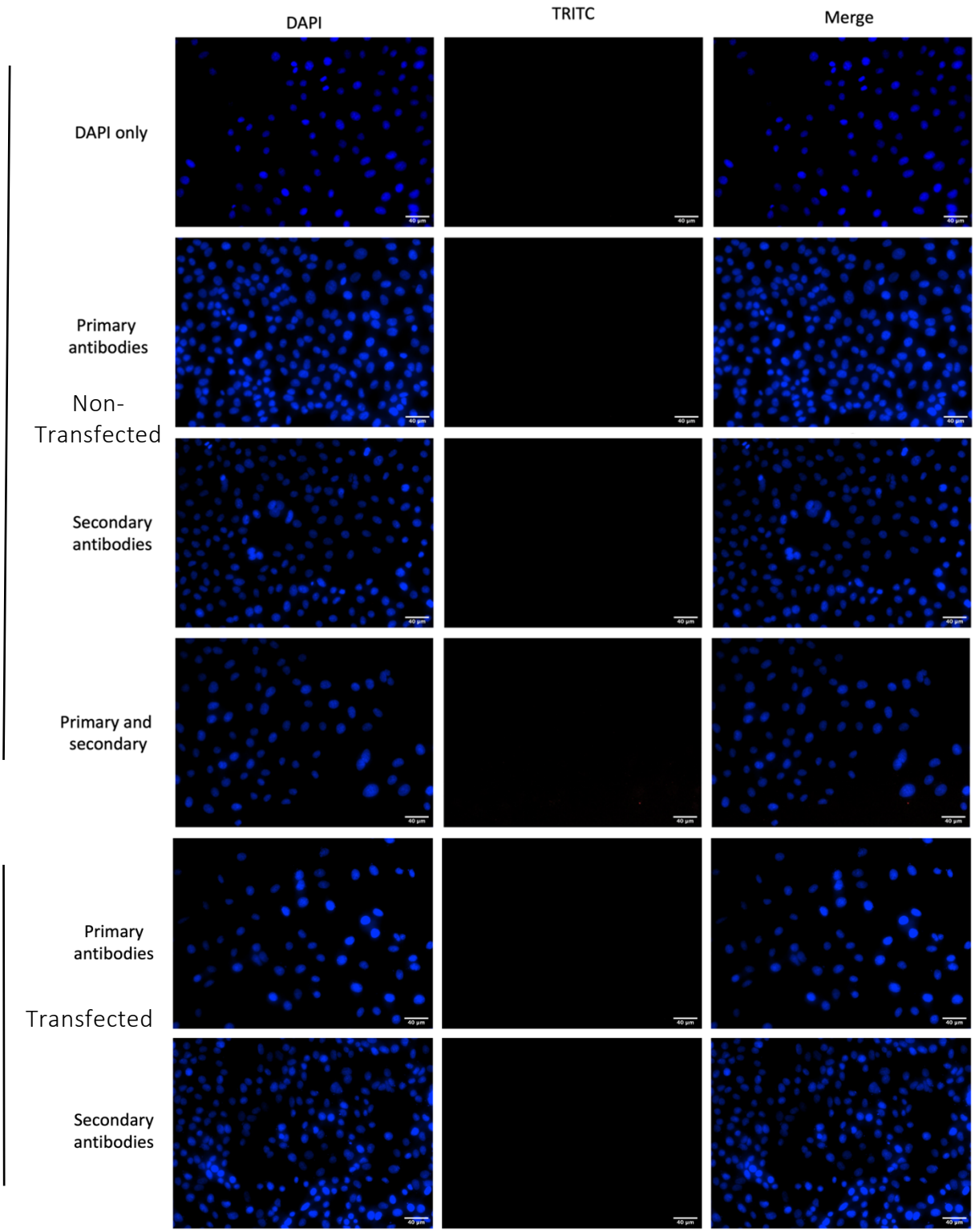


Figure 3.2-17 Controls used in the PLA

HeLa cells were either transfected with Nurr1 and SUMO or left un-transfected. Cells were subjected to immunocytochemistry using the combination of primary and secondary antibodies shown. TRITC (Red) signal was absent in controls indicating anti-SUMO and anti-Nurr1 were not within close proximity. DAPI was used for nuclear staining (blue). Widefield microscope objective 10x. Data is representative of results from 2 independent experiments.

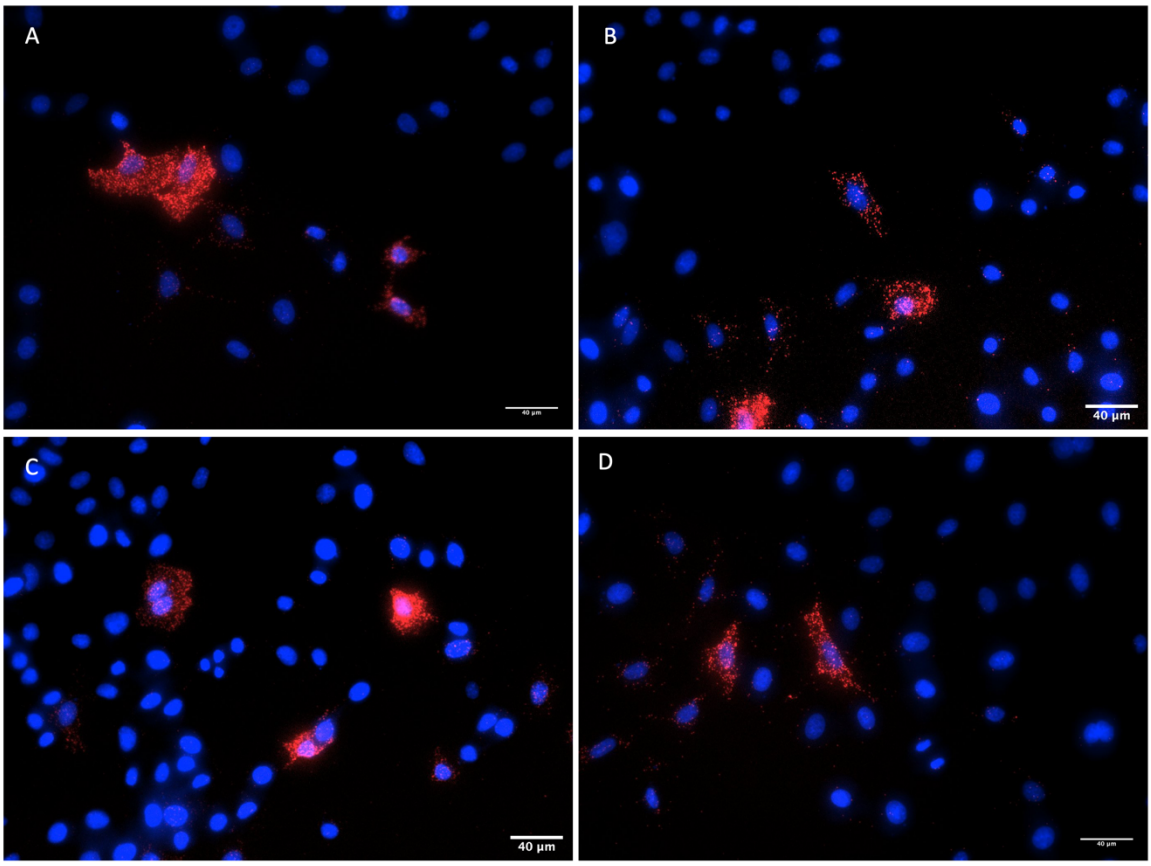


Figure 3.2-18 Proximity Ligase Assay investigating Nurr-SUMO interactions

HeLa cells were transfected with plasmids expressing either **(A)** FLAG-Nurr1, **(B)** FLAG-Nurr1-1a, **(C)** FLAG-Nurr1K91 or **(D)** FLAG-Nurr-1aK91 in addition to His-SUMO2 for 48h before subjection to the PLA. Close proximity of anti-Nurr1 and anti-SUMO indicated by red signal, nuclear staining observed using DAPI (blue). Widefield microscope objective 20x. Data is representative of results from 3 independent experiments.

We then hypothesised that transfecting SUMO alongside Nurr1/1a may cause translocation out of the nucleus into the cytoplasm and therefore why the PLA signal (red) could be observed there. Wildtype and K91 Nurr1/1a were transfected alongside SUMO2 and detected with immunocytochemistry using anti-FLAG and DAPI (Figure 3.2-19). These results reproduced our previous findings where Nurr1/1a was detected almost exclusively in the nucleus suggesting that co-transfecting with SUMO does not alter its cellular location. We do not have a definitive reason why in simple ICC Nurr appears exclusively

in the nucleus but in the PLA, signal is detected in both the cytoplasm and nucleus.

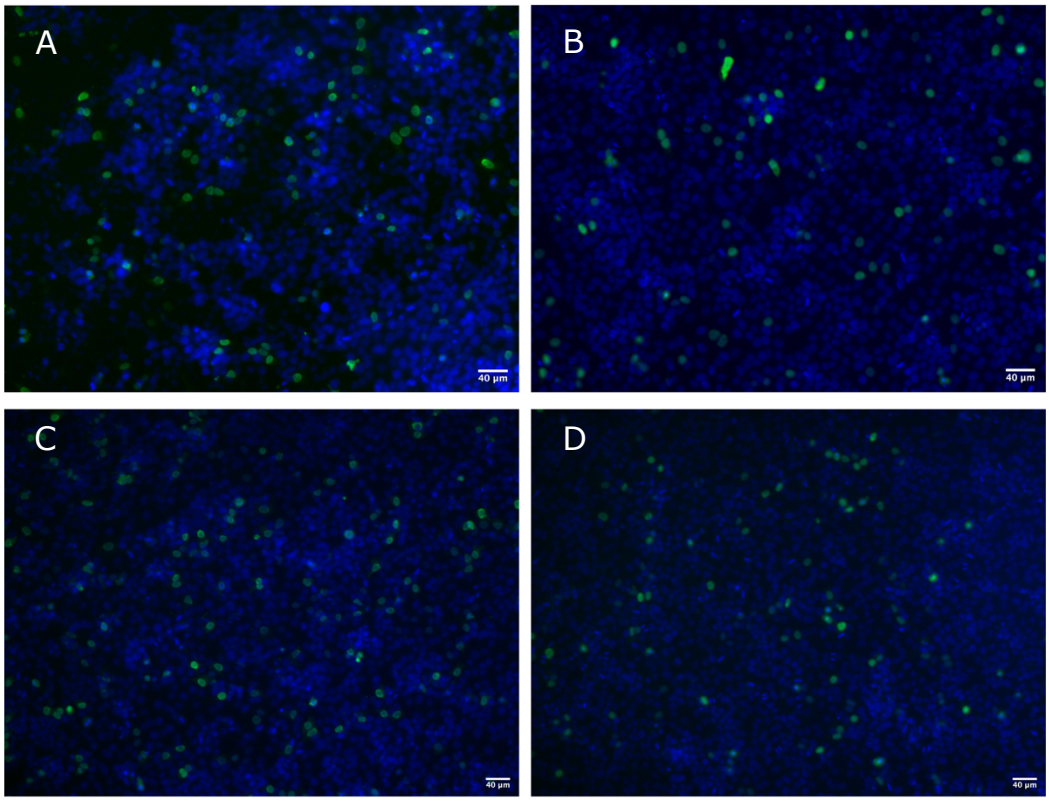


Figure 3.2-19 Co-transfection of Nurr1/1a and SUMO2 in HeLa cells

HeLa cells were transfected with plasmids expressing either **(A)** FLAG-Nurr1, **(B)** FLAG-Nurr1-1a, **(C)** FLAG-Nurr1K91 or **(D)** FLAG-Nurr-1aK91 in addition to His-SUMO2 for 48h before ICC was carried out using anti-FLAG (green) and nuclear staining observed using DAPI. Widefield microscope objective 10x.

3.2.8 Nurr1/1a transactivation of the TH promoter

Nurr1 is reported to regulate numerous genes involved in dopamine synthesis, such as Tyrosine Hydroxylase (TH) (Decressac et al., 2013, Zetterström et al., 1996, Zetterström et al., 1997, Chu et al., 2002). According to a report using SK-N-AS cells Nurr-1a has a significantly reduced (~50 fold) ability to transactivate Nurr1's canonical response element (NBRE) compared to its full length variant (Michelhaugh et al., 2005). A similar pattern was observed in NIH3T3 cells (Castillo et al., 1998b). However, one publication does discuss the ability of Nurr-1a to repress the TH promoter depending on cell type. They show that in HB1.F3 cells, Nurr-1a represses the basal activity of both a naturally occurring TH promoter region, in addition to a 3xNBRE reporter (Kim et al., 2013).

To examine the transactivation mediated by Nurr1/1a we first cloned the rat TH promoter region into a luciferase vector (PGL4.1 Luc2). Primers were designed to clone 1022bp of the promoter region including the 3 response elements: NL1, NL2 and NL3. NL3 has the same reported sequence as the canonical NBRE element, which Nurr1 is reported to bind to as a monomer (Kobayashi et al., 2020, Maira et al., 1999, Kim et al., 2003a). Additionally, when mutated, it is said to significantly reduce Nurr1 mediated transactivation of this promoter (Kim et al., 2013).

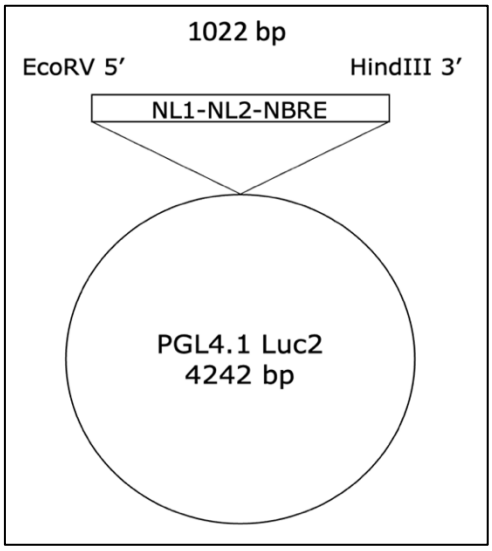


Figure 3.2-20 Schematic diagram of the cloned TH promoter

1022bp of the TH promoter region including the NBRE region was cloned into the PGL4.1 luciferase reporter vector using the indicated restriction enzymes.

SH-SY5Y cells were selected as a neuronal *in vitro* model to evaluate TH promoter activation. They are of neuroblastoma origin and endogenously express Nurr1-related genes such as TH, DAT and D2R (Kovalevich and Langford, 2013). Frequently they are used as a human dopaminergic-like cell line to study PD (Xicoy et al., 2017). Therefore, they provided an appropriate cellular background to assess transcription mediated by Nurr1 and Nurr-1a.

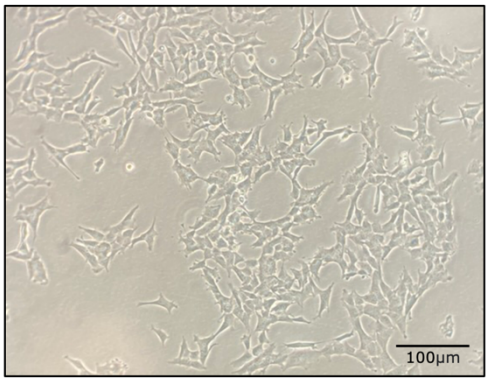


Figure 3.2-21 Morphology of SH-SY5Y cells

SH-SY5Y cells were cultured in complete media. Images were collected with an inverted light microscope.

We transfected either FLAG-Nurr1, FLAG-Nurr-1a, FLAG-Nurr1K91 or FLAG-Nurr-1aK91 in SH-SY5Y cells followed by immunoblotting 48h later with anti-FLAG and anti-βactin (Figure 3.2-22). These data show the K91 mutation reduced the level of Nurr1/1a detected. This may be due to reduced expression in this cell type, lack of stability or differences in protein turnover.

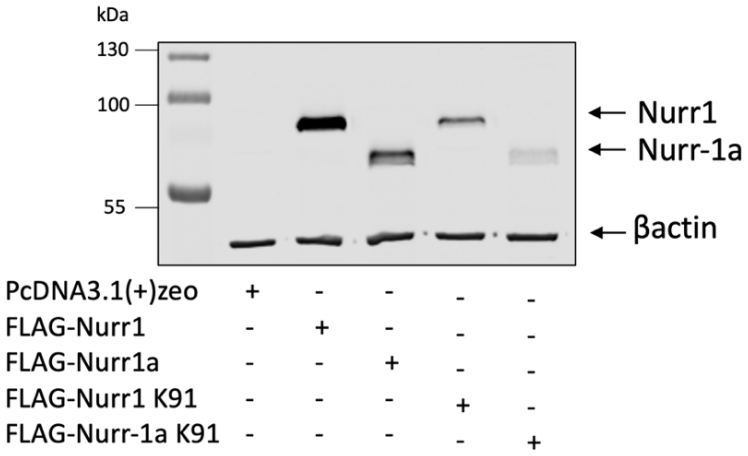


Figure 3.2-22 Protein expression in SH-SY5Y cells

SH-SY5Y cells were transfected with plasmids expressing either FLAG-Nurr1, FLAG-Nurr-1a, FLAG-Nurr1K91 or FLAG-Nurr-1aK91. 30µg of each sample was electrophoresed on a 10% SDS PAGE gel. Western blotting was performed with anti-Flag (1:20,000) and anti-βactin (1:1000) antibodies.

Luciferase assays are usually conducted 24-48h after transfection. We wanted to determine which time point was suitable for our experiments, and what ratio of Nurr1 plasmid DNA to X-tremeGENE transfection reagent was adequate. We co-transfected SH-SY5Y cells with Nurr1 and the TH-promoter using either 1:1 or 1:2 ratios of plasmid DNA: Transfection reagent (Figure 3.2-22). After 24 or 48 hours the cells were lysed, and their luciferase activity was measured. At both 24h **(A)** and 48h **(B)** increasing the ratio of X-tremeGENE transfection reagent increased the activation of the promoter (~1.8 and ~2.9 respectively). Promoter activity increased from 24h to 48h, however we concluded the activity at 24h mediated

by Nurr1 showed a sufficient increase compared to the empty plasmid. Therefore, a ratio of 1:2 at 24 hours was used for the following experiments unless stated otherwise.

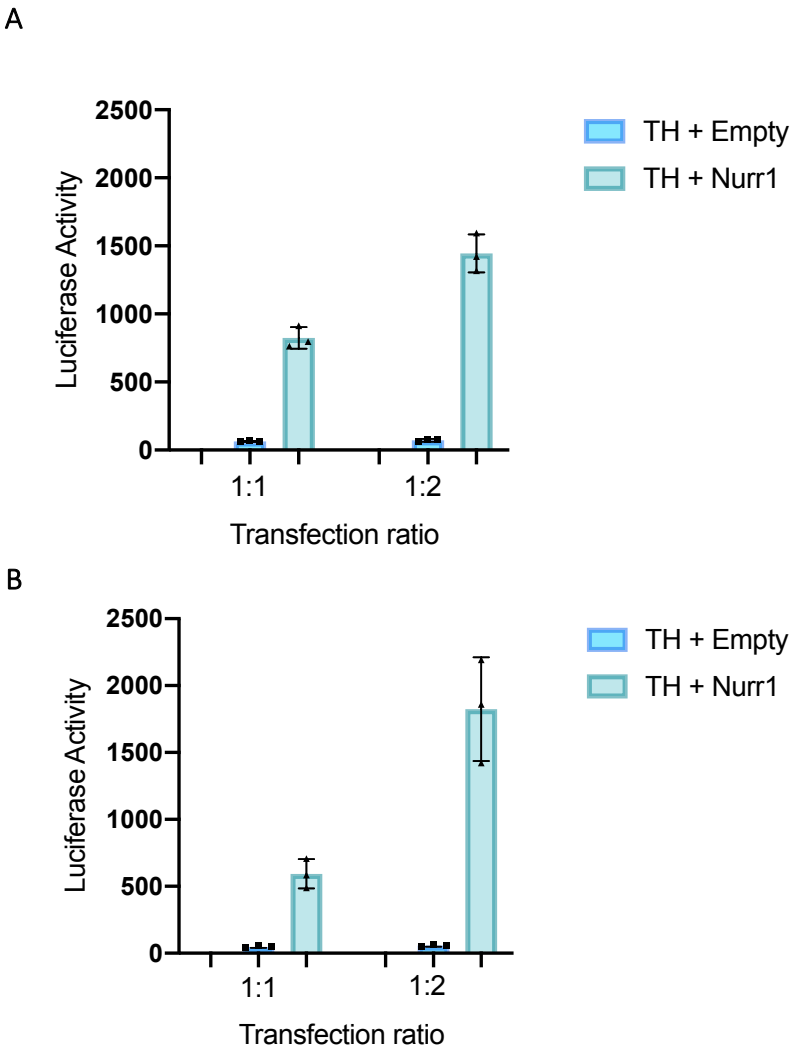


Figure 3.2-23 Plasmid expression in SH-SY5Y cells

SH-SY5Y cells were transfected with 300ng of TH-PGL4.1Luc2 plasmid and either FLAG-Nurr1 or PcDNA3.1(+) zeo at a transfection ratio of either 1:1 or 1:2 (plasmid DNA: X-tremeGENE transfection reagent), for **(A)** 24h or **(B)** 48h before cells were lysed with a passive lysis buffer and luciferase activity measured. Results expressed as arbitrary luminometric units. Error bars represent standard deviation from the mean. Data is representative of results from 2 independent experiments (N=3).

Our lab previously used a ratio of 6:1 promoter to receptor to elicit luciferase activity. We investigated this in terms of Nurr1 to identify

the optimal plasmid concentration. Cells were transfected and assayed as before, with increasing concentrations of Nurr1. These data clearly show that 50ng of Nurr1 plasmid significantly increased luciferase activity compared to the control (TH + Empty) shown in Figure 3.2-23. Increasing the concentration further did not significantly increase the luciferase activity. Therefore, 50ng of Nurr1 and 300ng of TH promoter plasmid were used for the following experiments unless stated otherwise.

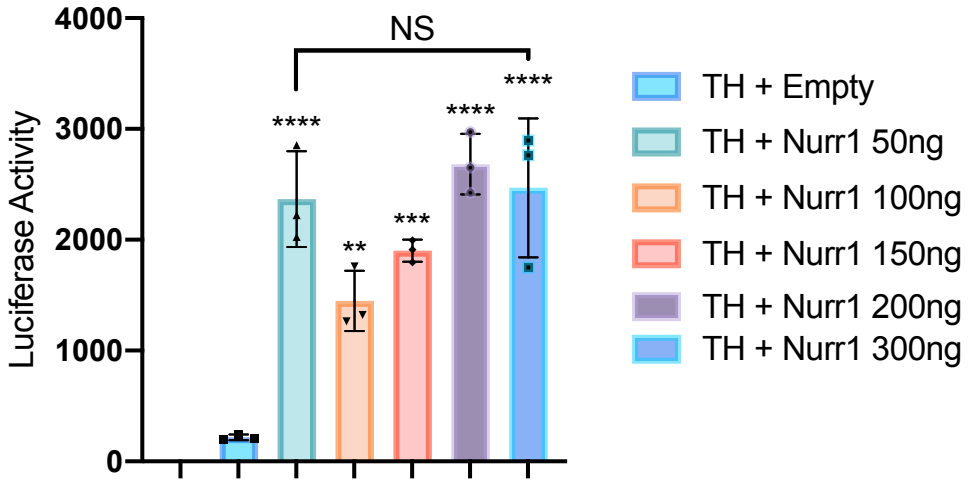


Figure 3.2-24 Nurr1 plasmid concentration alters luciferase activity

SH-SY5Y cells were transfected with 300ng of TH promoter and varying concentrations of FLAG-Nurr1 (50-300ng), at a 1:2 ratio of plasmid DNA:X-tremeGENE HP DNA transfection reagent for 24h before cells were lysed and luciferase activity measured. Graphs represent SD of the mean compared to the control group (TH + Empty). Data is representative of results from 2 independent experiments (N=3). Results expressed as arbitrary luminometric units. Statistically significant differences from all groups compared control (TH + Empty) were $^{**}p < 0.001$, $^{***}p < 0.0005$, **** $p < 0.0001$ (one-way ANOVA with Bonferroni post-test correction).

After optimising the experimental conditions for Nurr1 transactivation, we wanted to compare the transcriptional ability of Nurr-1a. Previous reports from Galleguillos et al., state that Nurr1 mediated transcriptional activity is repressed by PIASg in both SUMO

dependent and independent mechanisms (Galleguillos et al., 2004). Considering the importance of PIASg in Nurr-1a stability, we decided to investigate how Nurr-1a's transcriptional activity is affected by PIASg.

SH-SY5Y cells were transfected with the TH reporter plasmid and an empty expression vector (PcDNA3.1) or co-transfected with the TH promoter, FLAG-Nurr1/FLAG-Nurr-1a and PIASg. After 24 hours cells were lysed, and luciferase activity was measured. These results show that both Nurr1 and Nurr-1a significantly activate the TH promoter compared to the control, and PIASg represses the activity of both receptors in the absence of transfected SUMO.

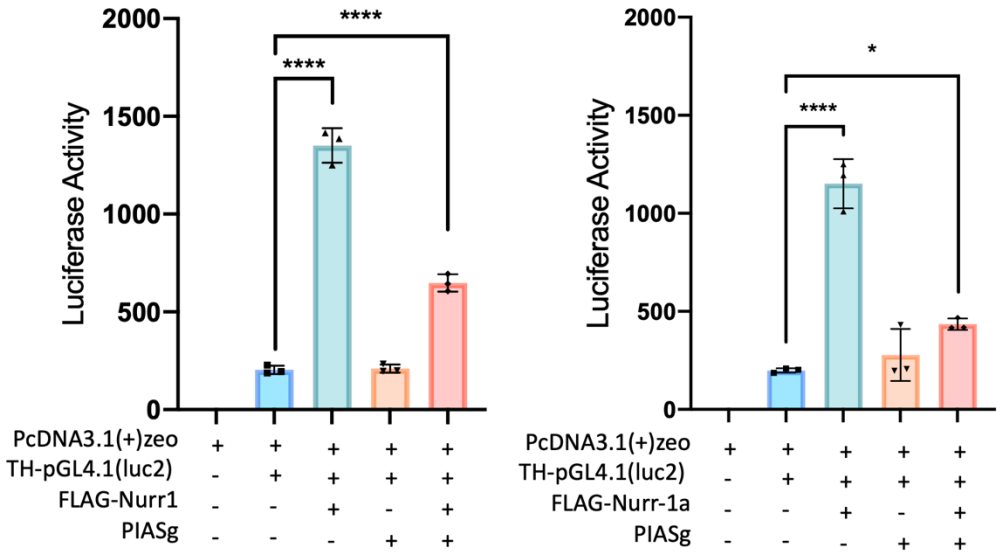


Figure 3.2-25 Nurr1 and Nurr-1a's transactivation of the TH promoter is repressed by PIASg

SH-SY5Y cells were transfected with: TH promoter, either FLAG-Nurr1 or FLAG-Nurr-1a, and either PIASg or Empty (PcDNA3.1(+)zeo), using X-tremeGENE HP DNA transfection reagent (1:2 DNA:X-tremeGENE). After 24h cells were lysed with a passive lysis buffer and luciferase activity was measured. Results expressed as arbitrary luminometric units and show standard deviation from the mean. Data is representative of results from three independent experiments. Statistically significant differences from control (TH + Empty) were *$p < 0.05$, **** $p < 0.0001$ (one-way ANOVA with Bonferroni post-test correction).

It was surprising to see that Nurr-1a was still able to activate the TH promoter in the absence of exogenous PIASg considering we previously demonstrated in HeLa cells that PIASg was required for stable expression (Figure 3.2-3). Therefore, we investigated the endogenous expression of PIASg in SH-SY5Y cells, alongside the stability of transfected Nurr-1a. Our results clearly show PIASg is endogenously expressed in SH-SY5Y cells. This may explain why Nurr-1a is able to activate the promoter in the absence of exogenous PIASg, however as Figure 3.2-25 **(A)** shows, the addition of PIASg and the other SUMO machinery does stabilise the protein further.

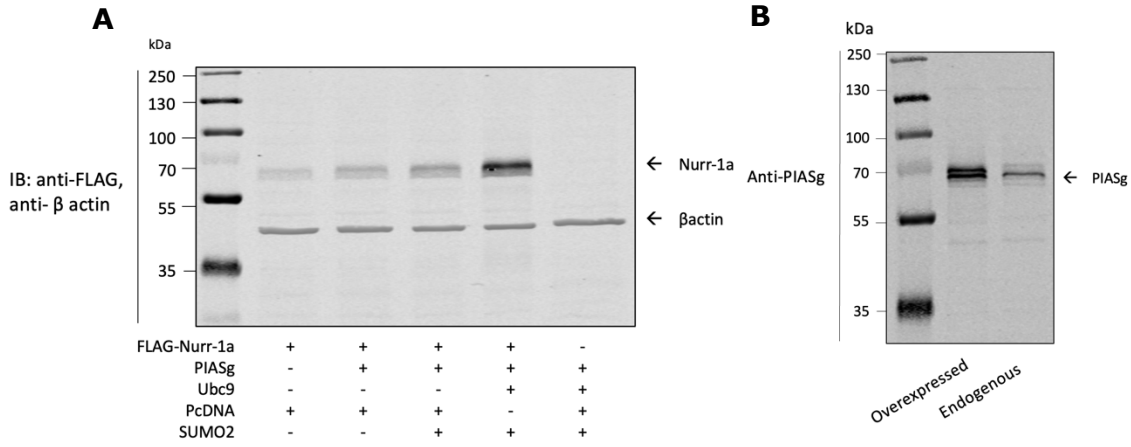


Figure 3.2-26 Nurr-1a is stabilized by endogenous PIASg in SH-SY5Y cells

(A) SH-SY5Y cells were transfected with plasmids expressing FLAG-Nurr-1a and different combinations of SUMO machinery plasmids. **(B)** SH-SY5Y cells were either transfected with PIASg or not transfected at all. After 48h extracts were lysed in naturing conditions and subjected to resolution (30µg) on a 10% acrylamide SDS-PAGE gel. Western blotting was performed with **(A)** anti-FLAG (1:20,000) and anti-βactin (1:1000) or **(B)** anti-PIASg (1:1000) antibodies.

To further validate PIASg's ability to repress the receptors in the absence of SUMO we repeated the previous experiment including the K91 SUMO mutants. A previous report using the Nurr1 K91 mutant described them to be more transcriptionally active at an NBRE promoter than the wild type in HEK293 cells (Galleguillos et al.,

2004). These results clearly show PIASg represses the activation mediated by the mutants similarly to the wildtype. Interestingly, we found both the K91 mutants activated the TH promoter less compared to the wildtype.

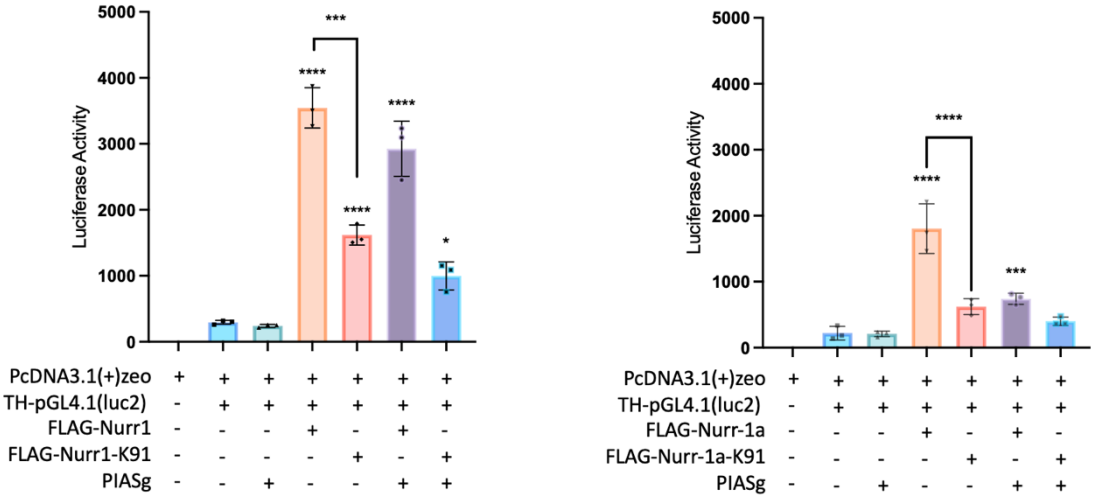


Figure 3.2-27 K91 mutants activate the TH promoter less than wildtype, and are similarly repressed by PIASg

SH-SY5Y cells were transfected with: TH promoter, either FLAG-Nurr1/K91, or FLAG-Nurr-1a/K91, and either PIASg/ Empty (PcDNA3.1(+)zeo), using X-tremeGENE HP DNA transfection reagent (1:2 DNA:X-tremeGENE). After 24h cells were lysed with a passive lysis buffer and luciferase activity was measured. Results expressed as arbitrary luminometric units and show standard deviation from the mean. Data is representative of results from three independent experiments. Statistically significant differences from control (TH + Empty), or between groups were *$p < 0.05$, **$p < 0.001$, ***$p < 0.0005$ **** $p < 0.0001$ (one-way ANOVA with Bonferroni post-test correction).

We next sought to evaluate the effect SUMO may have on Nurr1/1a transcriptional regulation. SH-SY5Y cells were transfected with the TH promoter driven luciferase reporter plasmid and an empty expression vector (PcDNA3.1(+)zeo) or co-transfected with the TH promoter, FLAG-Nurr1/FLAG-Nurr-1a (wildtype/K91) and SUMO2. After 24 hours cells were lysed, and luciferase activity was measured. These results clearly show that the addition of SUMO increased the activation mediated by Nurr1 and Nurr-1a. SUMO did

also increase the activation caused by the K91 mutants, however the increase is significantly less.

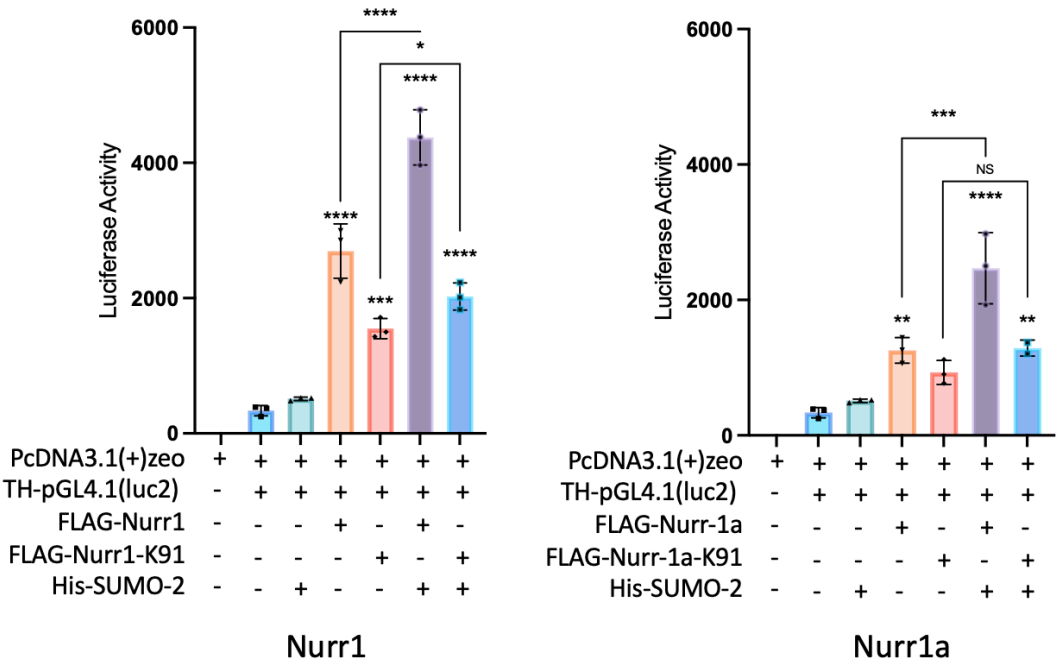


Figure 3.2-28 SUMO enhances Nurr1 and Nurr-1a mediated

SH-SY5Y cells were transfected with: TH promoter, either FLAG-Nurr1/K91 or FLAG-Nurr-1a/K91, and either SUMO2 or Empty (PcDNA3.1(+)zeo), using X-tremeGENE HP DNA transfection reagent (1:2 DNA:X-tremeGENE). After 24h cells were lysed with a passive lysis buffer and luciferase activity was measured. Results expressed as arbitrary luminometric units and show standard deviation from the mean. Data is representative of results from three independent experiments. Statistically significant differences from control (TH + Empty), or between groups were *$p < 0.05$, **$p < 0.001$, ***$p < 0.0005$ **** $p < 0.0001$ (one-way ANOVA with Bonferroni post-test correction).

3.2.9 SUMO enhanced transcriptional activation is cell specific

Galleguillos et al., reported in HEK293 cells the Nurr1 K91 mutant was more transcriptionally active at an 3xNBRE promoter than the wild type, and suggested that SUMOylation therefore repressed Nurr1's ability to activate the promoter (Galleguillos et al., 2004). Our results demonstrate the opposite; however, we used a neuronal cell type. Therefore, we proposed that these differences may be due to cell specific. Additionally, our assays were carried out at 24h, compared to the aforementioned report which used 48h, they also used a 1:1 ratio of reporter to Nurr1.

To determine if these differences were indeed due to cell type or alterations in experimental design, we repeated our experiment in both SH-SY5Y cells and HEK293 cells using 1:1 ratio of TH promoter to Nurr DNA and carried out luciferase assays at both 24h and 48h. Our results clearly show, like previously in Figure 3.2-26, that in SH-SY5Y cells wildtype Nurr1/1a activate the TH promoter more than K91 (Figure 3.2-28). Interestingly, at 48h Nurr-1a's activation of the promoter surpasses that of Nurr1 however this was not significant. In HEK293 cells endogenous promoter activity appeared very high however significant increases in activation were still seen when transfecting Nurr1/1a. Similarly, to SH-SY5Y cells at 24h wildtype Nurr1/1a increased promoter activity more than K91, but at 48h the Nurr1 K91 generated higher activation of the promoter than wildtype Nurr1; like reported in the literature (Galleguillos et al., 2004). These results suggest that the role of SUMO in Nurr1/1a TH promoter activation can differ depending on cell type, acting as an activator in neuronal cells and a repressor in non-neuronal cell types.

Additionally, the time at which the assay is carried out is important, this may affect protein turnover, receptor saturation or clearance.

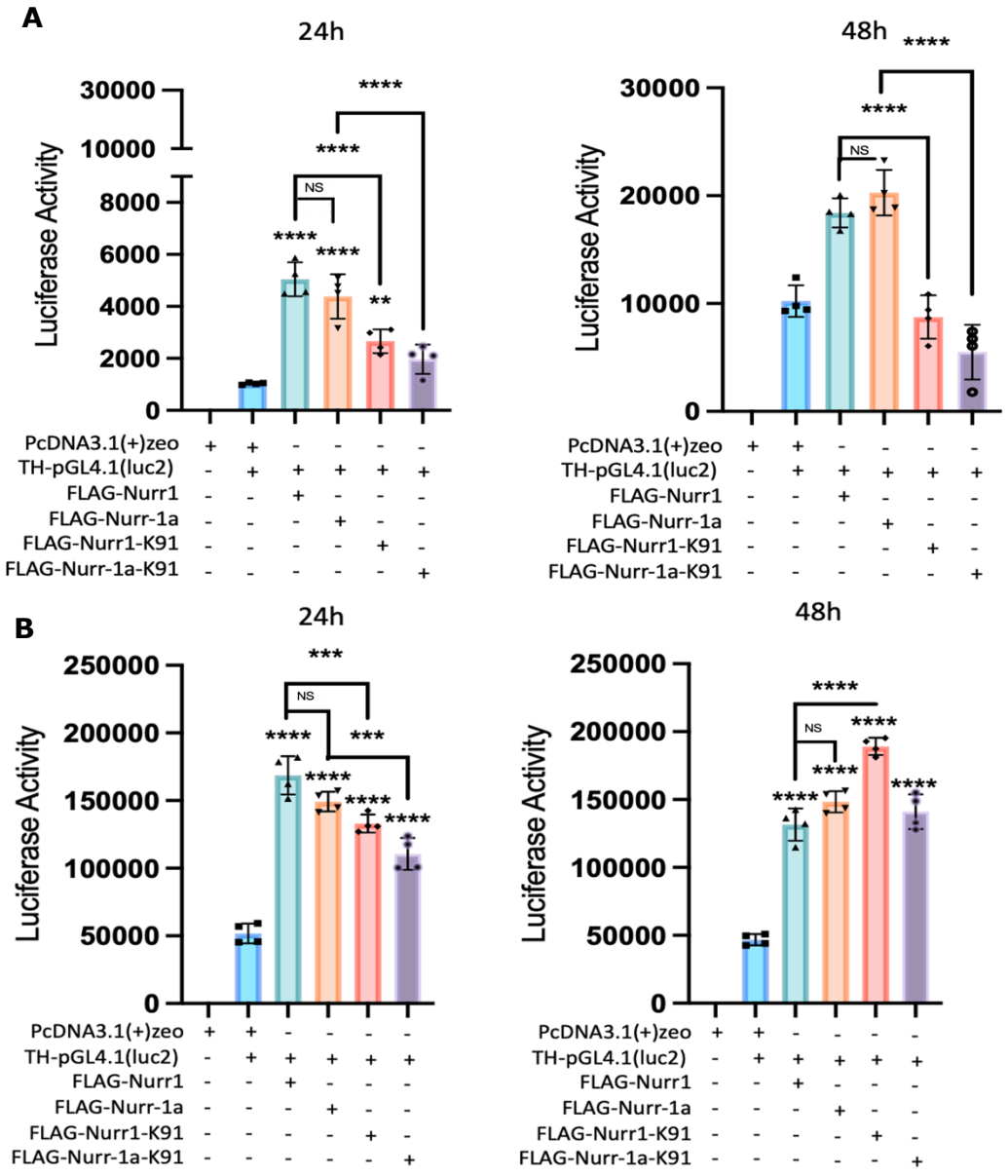


Figure 3.2-29 SUMO enhances Nurr1 and Nurr-1a mediated transactivation of the TH promoter

(A) SH-SY5Y or **(B)** HEK293 cells were transfected with 50ng TH promoter and 50ng of either FLAG-Nurr1/K91 or FLAG-Nurr-1a/K91, or Empty (PcDNA3.1(+)zeo), using X-tremeGENE HP DNA transfection reagent (1:2 DNA:X-tremeGENE). After 24h or 48h cells were lysed with a passive lysis buffer and luciferase activity was measured. Results expressed as arbitrary luminometric units and show standard deviation from the mean. Data is representative of results from three independent experiments. Statistically significant differences from control (TH + Empty), or between groups were *$p < 0.05$, **$p < 0.001$, ***$p < 0.0005$ **** $p < 0.0001$ (one-way ANOVA with Bonferroni post-test correction).

To ensure any changes observed in HEK293 cells were due to transcriptional ability and not expression of Nurr protein, we harvested representative samples and carried out a western blot to demonstrate Nurr expression. The level of expression was as seen previously in HeLa cells; Nurr1 expression was higher than Nurr-1a (~3.3 fold) with little change between wild type or mutant (<~1.2).

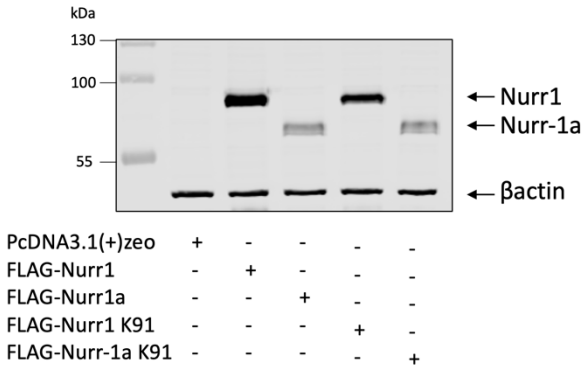


Figure 3.2-30 Nurr1 expression is greater than Nurr-1a in transfected HEK293 cells

HEK293 cells were transfected with plasmids expressing FLAG-Nurr1/1a or K91 mutants. After 48h extracts were lysed in naturing conditions and subjected to resolution (30µg) on a 10% acrylamide SDS-PAGE gel. Western blotting was performed with anti-FLAG (1:20,000) and anti-βactin (1:1000) antibodies. Data is representative of results from two independent experiments.

3.2.10 The effect of ligands on transactivation

Although we found the chosen ligands did not affect SUMOylation and had little effect on Nurr1/1a protein expression, we decided to investigate their effect on Nurr1/1a mediated activation of the TH promoter.

We repeated the luciferase assays as before in SH-SY5Y cells transfected with the TH reporter plasmid and either Nurr1 or Nurr-1a for 24h. Followed by a 24h ligand treatment using concentrations previously determined. These data clearly show that all but one ligand repressed Nurr1/1a mediated activation of the TH promoter.

This was unexpected as the ligands, except DHA, were all reported in the literature to be activators of Nurr1 (de Vera et al., 2016, Kim et al., 2015, Kim et al., 2016, Ordentlich et al., 2003, Hammond et al., 2015, Pan et al., 2005). DHA does appear to significantly reduce the luciferase activity measured however we found that 50µm caused a significant reduction in the protein content of the cell extract, indicating a possibility of cell death. 6-MP did appear to increase the activation mediated by Nurr-1a, but not that of Nurr1. Across three independent experiments the level of significance did vary, however the trend of the data remained the same.

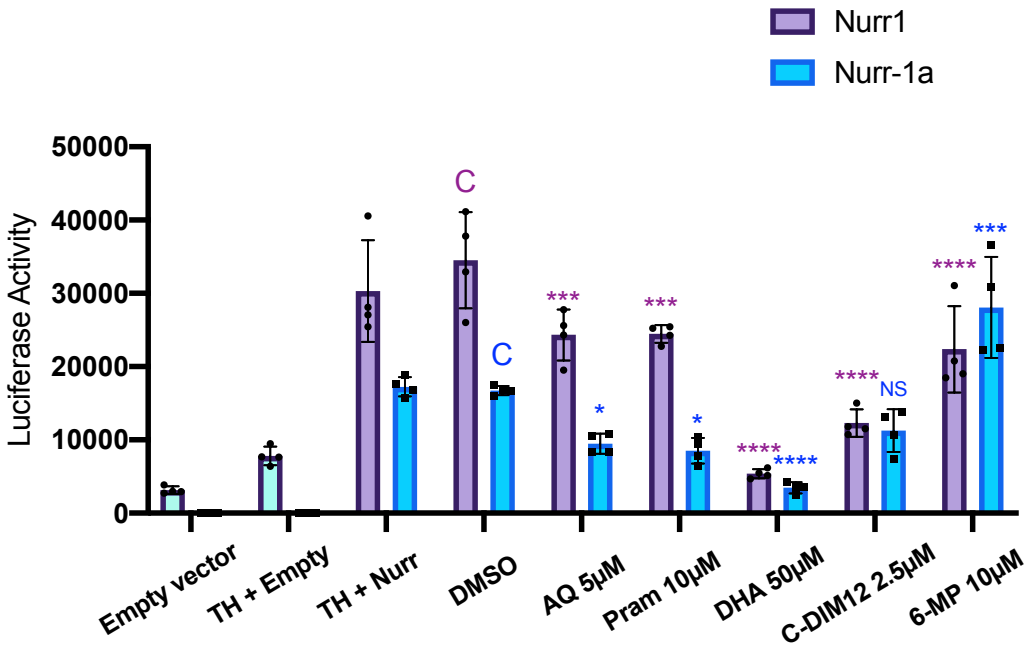


Figure 3.2-31 The effect of ligands on Nurr mediated transcriptional activation

SH-SY5Y cells were transfected with TH promoter and either FLAG-Nurr1 or FLAG-Nurr-1a. After 24h, cells were treated with ligands for a further 24h then lysed with a passive lysis buffer and luciferase activity was measured. Results expressed as arbitrary luminometric units and show standard deviation from the mean. Data is representative of results from three independent experiments. Statistically significant differences from DMSO control (Indicated as 'C') were *$p < 0.05$, **$p < 0.001$, ***$p < 0.0005$ **** $p < 0.0001$ (one-way ANOVA with Bonferroni post-test correction).

3.2 Discussion

Nurr-1a has received little research into its function despite the increasing attention Nurr1 has gained as a potential key player in PD (Chu et al., 2006, Dong et al., 2016b). This is due to previous studies denoting it to be minimally transcriptionally active in comparison to Nurr1 (Castillo et al., 1998b, Castillo et al., 1998a, Michelhaugh et al., 2005). In this chapter we show Nurr-1a is transcriptionally active and partakes in mechanisms that had previously only been described for Nurr1, such as PIASg mediated transcriptional repression (Galleguillos et al., 2004). We propose a novel role for SUMO as an enhancer of Nurr1/1a mediated transcriptional activation in a neuronal cell type, contrary to the majority of research which suggests SUMO modification acts as a repressor of transcription (Treuter and Venteclef, 2011, Saijo et al., 2009). Additionally, we demonstrated that Nurr-1a is SUMOylated far greater than Nurr1, whilst also confirming the main site of SUMOylation; previously contested in the literature (Saijo et al., 2009, Galleguillos et al., 2004, Arredondo et al., 2013). Saijo et al., suggested that SUMOylation underpins an inflammatory transrepression mechanism, which is how Nurr1 mediates its well-known anti-inflammatory effects (Saijo et al., 2009, Glass and Saijo, 2010, Bensinger and Tontonoz, 2009). Therefore, our data suggests Nurr-1a may facilitate more repression than Nurr1 at inflammatory promoters; due to its greater level of SUMOylation. Finally, we show that treatment with ligands did not enhance Nurr1 mediated transcriptional activation like reported in the literature (de Vera et al., 2016, Kim et al., 2015, Kim et al., 2016, Ordentlich et al., 2003, Hammond et al., 2015, Pan et al., 2005). Highlighting that Nurr1/1a mediated transcriptional regulation is cell type dependent, and that

there are clear transcriptional differences between the commonly used 3xNBRE promoter and the naturally occurring promoter.

Nurr-1a is SUMOylated more than Nurr1

Nurr1 is widely known for its role in neuronal gene regulation alongside a lesser investigated role in inflammation (Jeon et al., 2020, Bensinger and Tontonoz, 2009). It is accepted that Nurr1 works to reduce inflammation however the exact mechanism for how this occurs requires further investigation (Oh et al., 2020, Saijo et al., 2009, Lallier et al., 2016). Saijo et al., suggests a mechanism involving the SUMOylation of Nurr1 is responsible (Glass and Saijo, 2010, Saijo et al., 2009, Ghisletti et al., 2007, Pascual et al., 2005). Despite its reported existence in human midbrain (Ichinose et al., 1999, Michelhaugh et al., 2005), Nurr-1a has few studies which investigate its transcriptional activity and the role of SUMOylation remains completely unexplored (Castillo et al., 1998b, Castillo et al., 1998a, Michelhaugh et al., 2005). Therefore, this chapter began with investigations into the SUMOylation of Nurr1/1a.

The levels of SUMOylation were demonstrated to differ between the two isoforms. Nurr-1a appeared have significantly higher levels of SUMOylation and was capable of modification of by all three SUMO isoforms unlike Nurr1. As Nurr1 and Nurr-1a share near identical sequences besides a C-terminal truncation, it may be that the removal of this region allows Nurr-1a to adopt a conformation more facilitative of SUMOylation. The literature reports that Nurr1 is modified by SUMO2/3 similarly and not by SUMO1 (Arredondo et al., 2013). In agreement, we found little SUMO1 modification of Nurr1. However, we showed a two-fold difference between SUMO2/3 modification, nevertheless they both were capable of significantly modifying the protein. Our data shows that Nurr-1a is SUMOylated

far more than Nurr1. Suggesting; if Nurr1's ability to regulate inflammation is based upon SUMO modification, then Nurr-1a may have a more prolific role.

Multiple SUMO bands were observed throughout the Nurr-1a pulldown blots, likely due to poly-SUMOylation. Many reports state that SUMO1 does not readily create poly-SUMO chains as it does not contain the specific internal lysine (K11) required for conjugation (Hendriks et al., 2014, Tatham et al., 2001). However, a more recent proteomic analysis in HeLa cells stated that other internal lysine residues could be used, and even documented an inverted motif on SUMO1 which promoted chain formation (Hendriks et al., 2014, Hendriks and Vertegaal, 2016). Poly-SUMO chains can create a unique topology that can be further recognised by other proteins such as SUMO targeted Ubiquitin ligases (Hendriks and Vertegaal, 2016). Our results show that Nurr-1a is poly-SUMOylated by all three SUMO isoforms, unlike Nurr1 which appears to be mono-SUMOylated. Suggesting Nurr-1a may be tightly regulated though ubiquitination and can interact with other proteins, which Nurr1 may not, through recognition of its potentially unique topology consequent of poly-SUMOylation.

PIASg stabilises Nurr-1a protein expression

PIASg is a known interaction partner of Nurr1 and is the E3 ligase required in the SUMOylation cycle (Arredondo et al., 2013). Some proteins such as RanGAP1 do not require an E3 ligase for SUMOylation to occur, the presence of Ubc9 is sufficient (Bernier-Villamor et al., 2002). We investigated the requirement for PIASg in Nurr-1a SUMOylation using a catalytic mutant (C342A) previously shown to be incapable of SUMOylating Nurr1 in COS-7 cells (Arredondo et al., 2013). Our data showed that PIASg stabilised the

expression of Nurr-1a protein, however this stabilisation was not dependent on SUMOylation. Indicating that some other function of PIASg facilitates this stabilisation. Although there are no reports of PIASg stabilizing proteins through any other means than SUMOylation; a member of the same family PIAS1 was shown to stabilized P73 by directly binding to it (Munarriz et al., 2004). Therefore, PIASg may stabilize Nurr-1a by direct binding. In addition, we found C342A protein expression was less than the wildtype PIASg. Consequently, any reductions in Nurr-1a protein expression were likely due to reduced levels of C342A PIASg protein, not due to any changes in its catalytic activity. Although to a lesser extent, Nurr-1a SUMOylation was still observed even in the absence of PIASg therefore it is possible that, like RanGAP1, Ubc9 is sufficient for SUMOylation.

K91 is the main site of Nurr1/1a SUMOylation

The main site of Nurr1 SUMOylation has previously been investigated however reports differ in their results: Saijo et al., reported the main SUMOylation sites to be K558 and K576 in mouse (Saijo et al., 2009). Whilst Galleguillos et al., found in Rat the main sites to be K577 and K91 (Galleguillos et al., 2004). Similarly, Arredondo et al., suggest K91 is the main site (Arredondo et al., 2013). Sites K558, K576 and K577 are all located in the C-terminal truncation of Nurr-1a's sequence. Considering we previously demonstrated that Nurr-1a was SUMOylated more than Nurr1, it was unlikely that these were main sites of Nurr1/1a SUMOylation. Our results showed that mutating the K91 site abolished Nurr1 SUMOylation and significantly reduced Nurr-1a SUMOylation. Any residual Nurr-1a modification seen was thought to be due to additional less-SUMOylated sites or the overexpression of SUMO machinery resulting in aberrant SUMOylation. These mutational studies in

combination with our data showing Nurr-1a is highly SUMOylated suggests that the proposed C-terminal lysine's identified by Saijo et al., are not major SUMOylation sites.

The transrepression mechanism suggested by Saijo et al., states that inflammatory signals trigger Nurr1 SUMOylation at lysine's K576 and K558 which reside in the Ligand Binding Domain (LBD). This promotes Nurr1's recruitment to inflammatory promoters (NFκB) where it interacts with the P65 subunit. Subsequently, a co-repressor complex is recruited and binds to Nurr1 through its DNA binding domain (DBD) which ultimately represses the promoter. Our data shows that Nurr1/1a is not SUMOylated in its LBD but instead in its Activation Function 1 domain (AF-1), which would suggest this site is important in Nurr1 transrepression of inflammatory promoters. The absence of the AF-2 allow Nurr-1as AF-1 to form a conformation more facilitative of SUMOylation. The AF-1 domain has also been highlighted as a key region of SUMO modification and subsequent transcriptional repression in other NRs such as the androgen receptor and PPARγ (Poukka et al., 2000, Ohshima et al., 2004).

One piece of prediction software also suggested a SIM site in Nurr-1a not present in Nurr1. We thought this may be responsible for the greater level of SUMOylation. However, after mutating the site this result was not seen as the mutation only caused a decrease in Nurr-1a protein expression, no specific change to SUMOylation. This could be due to the SIM adversely affecting Nurr-1a's ability to interact and subsequently stabilised by PIASg. Although the site did not change levels of SUMOylation, it could still affect the transcriptional activity of Nurr-1a. However, this was not carried out in this study but could provide an interesting avenue for future work. Furthermore, prediction software suggests theoretical sites based on

pre-programmed sequence parameters, and therefore does not consider other requirements such as conformation.

Nurr1/1a and SUMO are within close proximity

Proximity Ligase Assays are carried out to detect close interactions between proteins. Therefore, it was used to further confirm Nurr1/1a-SUMO interactions. We found high levels of signal throughout the cell in both the nucleus and cytoplasm indicating close proximity of Nurr1/1a and SUMO. We had previously shown that Nurr1/1a mainly resides in the nucleus, therefore the signal in the cytoplasm was unexpected. Some reports do suggest that nuclear receptors can translocate in and out of the cytosol. Garcia-Yague et al., demonstrated in transfected HEK293 cells that Nurr1 was mostly found in the nucleus however there was some detected in the cytoplasm (Andreou and Tavernarakis, 2009, Garcia-Yague et al., 2013). It is suggested that SUMO can affect transcription through modifying receptors subsequently altering their subcellular localisation (Zárraga-Granados et al., 2020). We did not see any change in subcellular localisation when looking at the K91 SUMO mutants, and again to our surprise we detected the same level of signal as the wildtype, despite our previous western blots showing the K91 variants to have a lower level of SUMOylation. It is a possibility that the Nurr1/1a K91 mutants are in a complex with another SUMOylated protein, and therefore signal is still detected even though they are not directly SUMOylated. However, this would require further investigation as well as why we observe high levels of signal in the cytoplasm PLA experiments and not in the regular immunocytochemistry.

Ligands affect Nurr-1a protein levels, and their response is cell type specific

There are numerous synthetic ligands reported to affect Nurr1. Most are in reference to its transcriptional activity (de Vera et al., 2016, Kim et al., 2003a, Kim et al., 2015, Ordentlich et al., 2003), but some also affect Nurr1 protein expression (Hammond et al., 2015, Pan et al., 2005). We chose ligands which targeted Nurr1 in different ways; including one which interacted with the AF-1 domain, three with the LBD and one with a D3 dopamine receptor. None of these ligands had been studied in terms of Nurr1/1a SUMOylation or any effect they may have on Nurr-1a protein expression or transcriptional activity. Our results showed none of the ligands affected Nurr1/1a SUMOylation, and there was little effect on the protein expression of Nurr1. We did find a decrease in Nurr-1a protein expression in response to treatment with AQ, and there were modest (<1.5 fold) increases observed with 6-MP, DHA or Pramipexole treatment. Our data does not show increased Nurr1 protein expression in HeLa cells in response to Pramipexole like reported in the literature in SH-SY5Y cell (Pan et al., 2005). This is likely due to the use of different cell types. SH-SY5Y cells endogenously express Nurr1 and therefore possess the dopamine D2/D3 receptors which modulate its expression, unlike HeLa cells which are not dopaminergic. These data demonstrate that ligands can affect Nurr-1a protein levels, whether that be through protein expression, stabilisation or increased degradation. Additionally, it highlights cell specific responses to ligand treatments which should be considered when investigating Nurr1/1a further.

Nurr-1a is transcriptionally active

Nurr1 is known to regulate crucial genes involved in dopamine synthesis, including the rate limiting enzyme TH (TH) (Decressac et

al., 2013, Zetterström et al., 1996, Zetterström et al., 1997, Chu et al., 2002). To modulate gene expression Nurr1 is reported to bind as a monomer to the NGFI-B response element (NBRE) sequence, a homodimer to the inverted NurRE sequence, or as a heterodimer with RXRα to DR5 sequence (Maira et al., 1999). The TH promoter region has multiple reported NBRE-like sequences which differ by a single base pair from the classic NBRE sequence 5'-AAAGGTCA-3' (Kim et al., 2003a). Listed in Figure 3.2-32 are a series of NBRE-like sequences, within 2.5kb of the transcriptional start site (Oh et al., 2009), which have been investigated in terms of Nurr1 mediated TH promoter driven transcription. Reports differ in which exact NBRE sequence is most important for transcription (Kim et al., 2003a, Kim et al., 2013, Iwawaki et al., 2000, Maira et al., 1999). Therefore, we cloned 1kb region of the wildtype promoter into our TH driven luciferase reporter which included the most reported sequences; NL1, NL2/NBRE-A, NL3/NBRE-C and NBRE-B (Kim et al., 2003b). The full sequence of human versus rat TH promoter response elements can be found int the appendices.

Name	Sequence 5' > 3'	Reference
NL1	TGGCCTTT	(Kim et al., 2003a, Iwawaki et al., 2000)
NL2/NBRE-A	AAAGGTTA	(Kim et al., 2003a, Kim et al., 2013)
NL3	AAAGGTCA	(Kim et al., 2003a, Maira et al., 1999)
NBRE-B	AAAGGTCC	(Kim et al., 2003a, Kim et al., 2013)
NBRE-C	AAAGGTCT (Differing by 1 base pair from NL3)	(Kim et al., 2003a, Kim et al., 2013)

Figure 3.2-32. NGFI-B response element-like sequences which bind Nurr1

NGFI-B response element-like sequences reported in the literature to be important in Nurr1 mediated transcriptional regulation.

According to some reports, Nurr-1a has a significantly reduced ability to activate Nurr1's canonical response element (NBRE) compared to its full-length variant (Michelhaugh et al., 2005, Castillo et al., 1998b, Castillo et al., 1998a). As a result of this, little further research into Nurr-1a's transcriptional ability have been carried out, despite increasing research into Nurr1 and its role in Parkinson's (Li et al., 2018, Dong et al., 2016b, Chu et al., 2006). In agreement with previous literature, this study shows Nurr-1a activates a TH-driven luciferase promoter less than the full length Nurr1 although we did not find this difference to be significant. In addition, the data suggests that Nurr-1a partakes in the same PIASg transcriptional repression mechanism which has previously only been described for Nurr1 (Arredondo et al., 2013, Galleguillos et al., 2004).

The transcriptional activity of nuclear receptors is mediated through the AF-1 ligand independent domain and AF-2 ligand dependent domain (Wang et al., 2003). These domains can work independently or synergise together to mediate activity (Metivier et al., 2001). Since Nurr-1a has a part of its LBD/AF2 domain missing, our data could indicate that the absence of synergy due to this truncation may be responsible for Nurr-1a's diminished transcriptional activation of the TH promoter in comparison to Nurr1, an idea which has been suggested previously (Michelhaugh et al., 2005). Also, Nurr-1a appears to be less stable than Nurr1, which could contribute to the lower activity readout. Additionally, Wang et al., demonstrated through a two hybrid LBD assembly assay in HEK293 cells that the transcriptional activity of Nurr1 correlated with the LBD adopting a more stable conformation (Wang et al., 2003). Overall, this data alongside our previous results which show the SUMOylation of Nurr1/1a occurs at K91 within the AF-1 domain; suggests that the transcriptional activity of Nurr1/1a is mainly regulated through its

AF-1 domain, however synergic interactions with its AF-2 domain may also influence activity.

SUMO enhances Nurr1/1a mediated transcriptional activation in a neuronal cell type

Surprisingly, the K91 SUMO mutants activated the promoter less than the wild type, opposing previous reports. Galleguillos et al., demonstrated that K91 activated the TH promoter more than Nurr1 and therefore hypothesised that SUMOylation of Nurr1 would repress its ability to mediate activation (Galleguillos et al., 2004). Kim et al., reported that transcriptional regulation mediated by Nurr1 was in fact cell type specific. Where Nurr1 activity at the TH promoter in SH-SY5Y cells would increase activation even though activity at the same promoter in HB1.F3 cells would cause repression. Additionally, the report revealed that the repression of the promoter in HB1.F3 cells was actually higher when transfected with Nurr-1a compared to Nurr1. Making it the only study which considers the splice variant as a potentially important transcriptional regulator (Kim et al., 2013). The parallel transcriptional activation experiments carried out in this chapter in both HEK293 and SH-SY5Y cells confirm that Nurr1 mediated transcriptional regulation is cell specific and post translational mechanisms such as SUMOylation may also have differential roles depending on cell type.

One of the most interesting findings from this chapter suggests that in neuronal cell types, SUMO may act to enhance Nurr1/1a mediated transcriptional regulation. SUMOylation is largely considered to have a repressive role regarding nuclear receptors (Treuter and Venteclef, 2011, Saijo et al., 2009). Although there is growing evidence to suggest SUMO may also act as an activator (Lyst and Stancheva, 2007). This study demonstrates the addition of SUMO in SH-SY5Y

cells increased the Nurr1/1a mediated activation of the TH promoter. We did also see a slight increase in the K91 mutant activation however it was significantly less than the wildtype.

It is noteworthy to mention that these reporter assays were not normalised and the expression of the Nurr constructs did vary as demonstrated in the western blots. Therefore, future studies should be mindful of ensuring these factors are accounted for to generate the most robust results.

Composition of NBRE TH promoters affects transcriptional response to ligands

Most of the ligands used previously were reported to affect transcription. Therefore, they were applied to the same TH luciferase assay to investigate any effect they may have on Nurr1/1a mediated transcriptional activation. The results differed from the literature in that the majority of ligands decreased activation as opposed to increasing activation (Kim et al., 2015, Kim et al., 2003 (Ordentlich et al., 2003, Hammond et al., 2015). After highlighting cell type specific differences in the K91 mutational studies, we considered that the discrepancies in results may be due different cell lines used. Additionally, some studies used one or multiple copies of a singular NBRE motif, typically NL3 (Kim et al., 2015, Ordentlich et al., 2003). The TH promoter region used in this chapter used 1kb of the naturally occurring promoter which included NL1, NL2 and NL3/NBRE-A. Therefore, our results may represent a more physiologically relevant response than a promoter driven by three repeats of one sequence (3XNBRE).

Limitations and conclusions

One limitation throughout this chapter was the use of cellular models. Although well researched cell lines such as HEK293 or HeLa cells are important when investigating preliminary mechanisms, it is important to consider how endogenous expression of key proteins, or lack of, may affect transcriptional responses. In addition, overexpressing plasmid constructs in cell lines may not lead to reproducible results in *in vivo*, however due to the transient nature of SUMOylation there are few other alternatives. To confirm robust mechanisms, more representative humanised models should be used. This is something explored in the following chapters.

In conclusion, the chapter at present demonstrated that the splice variant Nurr-1a is transcriptionally active in a neuronal cell line and is capable of a far greater level of SUMOylation than its full-length variant. High levels of SUMOylation imply Nurr-1a may have a prominent role in SUMO dependent transrepression of inflammatory promoters, however this is something that needs to be investigated further. The data points towards the AF-1 domain as a key region for mediating Nurr1/1a's transcriptional activity, which aligns with the idea of ligand independent regulation of Nurr1. This research builds on the current mechanisms reported for Nurr1 SUMOylation, whilst revealing novel data surrounding Nurr-1a.

Chapter 4

The development of human based inflammatory and neuronal models to investigate the role of Nurr1 and Nurr-1a

4.1 Introduction: induced pluripotent stem cells

With limited knowledge surrounding the pathogenic mechanisms and the absence of effective treatment, neurodegenerative diseases such as PD pose a significant unmet medical requirement (Chang et al., 2020, Dong et al., 2016a). Disease pathology is usually complex, therefore immortalised cell lines and animal models are unable to fully capture the multifaceted and dynamic nature of the disease (Potashkin et al., 2010). Human induced Pluripotent Stem Cells (iPSCs) are a development which permit the generation of cells, such as those from the central nervous system (CNS), from an individual patient. Consequently, eliminating may problems which arise from species specificity (Chang et al., 2020).

iPSCs were initially developed through the reprogramming of fibroblasts using four key transcription factors: OCT4, SOX2, KLF4 and C-MYC to help induce and maintain the cells pluripotent state through viral transduction (Takahashi and Yamanaka, 2006, Takahashi et al., 2007). Any human somatic cell can be used for reprogramming however fibroblasts and peripheral blood mononuclear cells are the most frequent used due to their accessibility (Chlebanowska et al., 2020). There are various drawbacks to using iPSCs including cost, long development times, specific culture conditions and genetic instability. However there are methods developed to reduce genomic instability such as the use of non-integrating DNA like episomal vectors (Shi et al., 2017).

Frequently, *in vitro* attempts to model neuroinflammatory diseases use cell line or rodent co-culture systems (Peng et al., 2022). iPSCs provide a way of modelling the effect of inflammatory cells on neuronal cells in a human based model. This can be done either by

directly culturing the different cell types together, or by transferring the conditioned media from one cell culture to the other (Haenseler et al., 2017, Muffat et al., 2016). The direct method may be more advantageous for investigating bidirectional crosstalk between cell types; however, it is not without its difficulties as the media composition and culture method must facilitate the differentiation of two distinct cell types (Haenseler et al., 2017).

Microglia are the most abundant immune cells residing in the CNS. In resting physiological conditions, they partake in processes such as synaptic pruning and remodelling, however when pathologically activated they migrate to the required site and commence their inflammatory response (Ho, 2019). Activated microglia are suggested to be central to the inflammation seen in PD (Dzamko et al., 2017, Zheng and Zhang, 2021). Whereby the production of pro-inflammatory cytokines can damage nearby neurons and may in part be responsible for dopaminergic (DA) neuronal dysfunction (Le et al., 2001). Therefore, human based models which combine activated microglia and DA neurons are a valuable tool to model PD and evaluate the mechanisms at play.

Nurr1 is constituently expressed in DA neurons and is reported to be a vital transcription factor for neuronal development, maintenance, and survival (Shao et al., 2019, Chu et al., 2006). We have shown previously Nurr-1a is detected in human adult total brain RNA, however its function is unknown. The expression of Nurr1 in BV2 microglia was found to significantly increase in response to LPS, whereas knockdown or reduction of Nurr1 dramatically increased inflammation (Saijo et al., 2009). Therefore, research into the regulatory mechanisms of Nurr1 and Nurr-1a within these two pathways individually, and in combination, may reveal vital insight into PD disease pathology and targeting.

Protocols have been developed which allow the differentiation of human iPSCs into microglia and DA neurons. Although these methods are time consuming and costly, they may be necessary to understand disease pathogenesis in a human representative model of the CNS. In the first part of this chapter, we aim to optimise the culture and maintenance of iPSCs. We will differentiate iPSCs into DA neurons using Nurr1 as one of the key factors to drive this differentiation. In addition we attempt to differentiate iPSC's into microglia so that they can be subsequently used to model the effect of Nurr1 and Nurr-1a; in terms of their role during inflammation and the possible effect SUMOylation has in these processes.

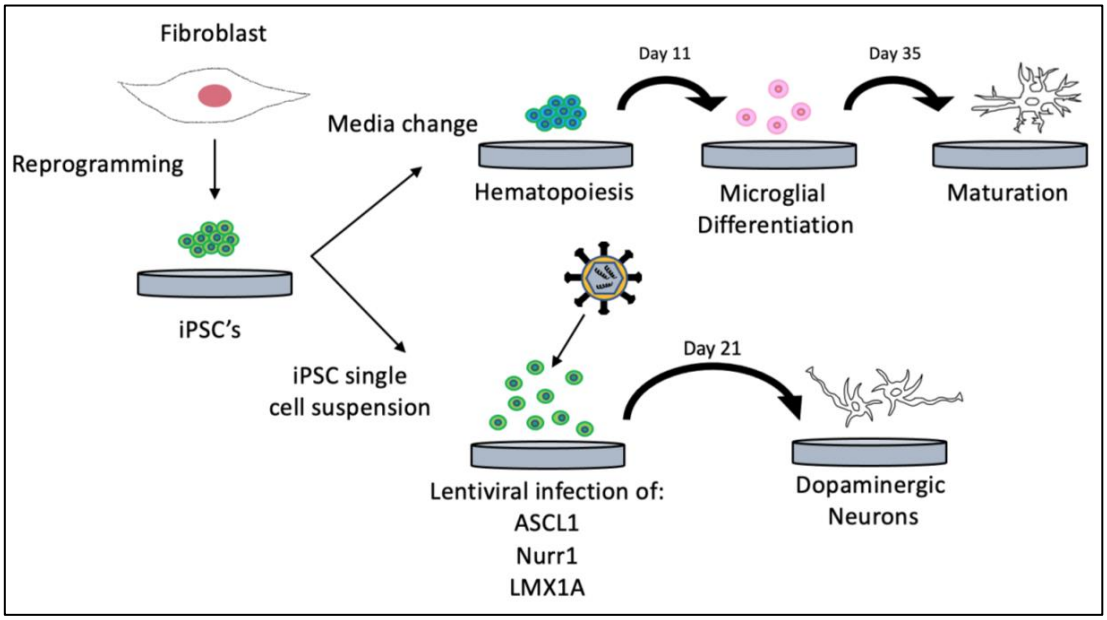


Figure 4.1-1 iPSC differentiation into Microglia and DA neurons
Schematic workflow of the differentiation of iPSC into microglia and DA neurons through developmental steps and viral induction respectively.

4.2 Results: iPSCs

4.2.1 Optimisation of iPSC culture

Traditionally pluripotent cells were cultured in serum-containing media on a monolayer of feeder cells such as mouse embryonic fibroblasts (Hoffman and Carpenter, 2005). Serum can interfere with numerous signalling pathways, therefore current methods to culture iPSCs use serum free Matrigel matrixes to ensure minimal variability between cultures (Ghasemi-Dehkordi et al., 2015).

iPSCs were initially cultured on Stem cell qualified Matrigel, derived from mouse sarcoma. However due to issues with supply this was switched to Cultrex, a matrix of the same origin. TeSR-E8 was used as a culture media. This combination facilitated the culture of iPSCs which retained a typical cobblestone morphology with a high nucleus to cytoplasm ratio and smooth edges a as indicated in Figure 4.2-1 below.

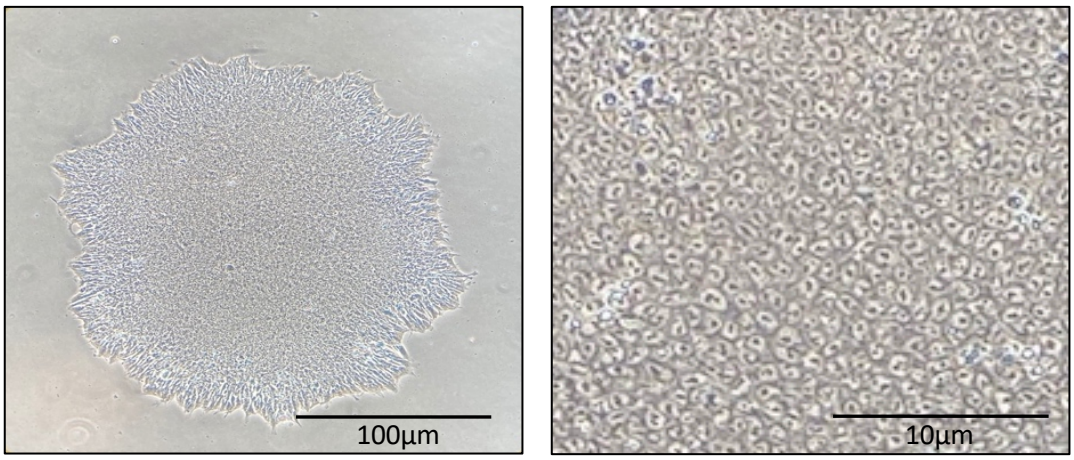


Figure 4.2-1 Assessment of typical iPSC morphology
Images taken of normal iPSC morphology in culture using TeSR-E8 media and Cultrex. Images were taken using an inverted light microscope.

Abnormal or differentiated iPSC morphology presented as disorganised heterogenous aggregates. Often outer cells extended

protrusions and had comparatively small nuclei as seen in Figure 4.2-2 below.

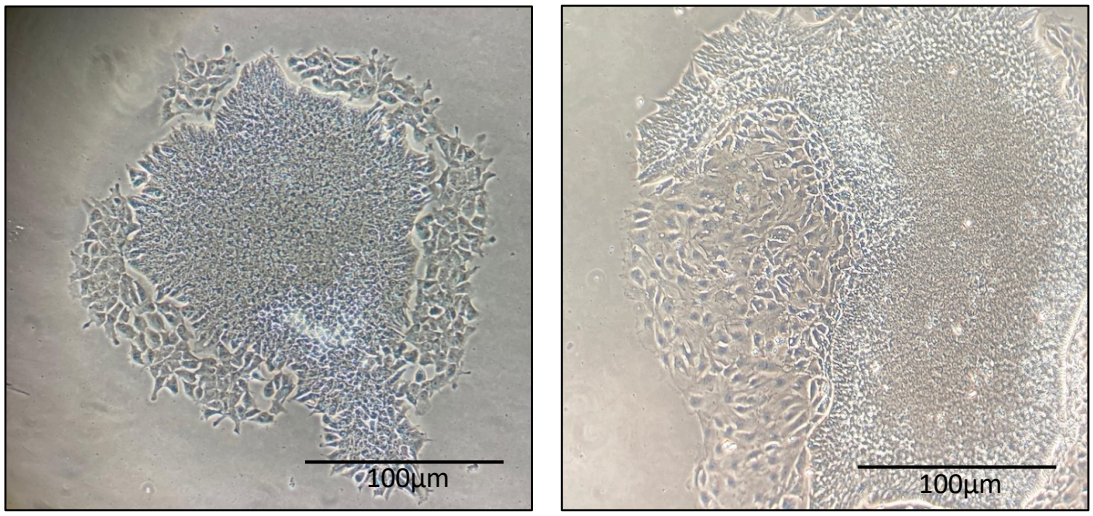


Figure 4.2-2 Example of differentiated cells within an iPSC culture

Differentiated iPSCs present a non-uniform morphology. Aggregates appear heterogenous with outer cells extending protrusions. Images were taken using an inverted light microscope.

Cell were routinely passaged using ReLeSR, an enzyme free dissociation reagent which takes advantage of the strong adherence differentiated cells have compared to undifferentiated cells. The optimal incubation time of cultures with ReLeSR was assessed visually using a light microscope. Cultures were incubated at 37°C, after every minute the flask was tapped and viewed to determine the time at which the greatest number of undifferentiated cells had detached, and the greatest number of differentiated cells remained adhered. We identified the optimal incubation with ReLeSR was 3.5 minutes.

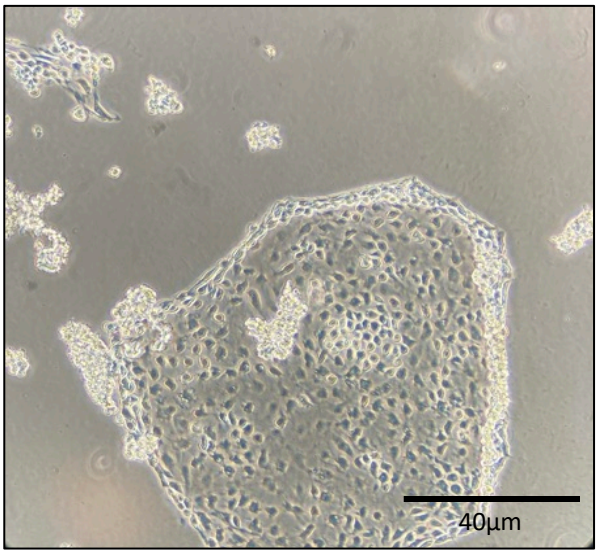


Figure 4.2-3 ReLeSR does not dislodge differentiated cell aggregates

Cells were passaged using ReLeSR for 3.5 minutes at 37°C. In these conditions undifferentiated iPSCs were dislodged whilst differentiated cells remained adherent.

In culture, human stem cells are vulnerable to apoptosis during cellular detachment and dissociation which is a requirement for passaging cells (Watanabe et al., 2007). Inhibition of Rho-associated protein kinase (ROCKi) activity is reported to promote the survival and subcloning efficiency of human stem cells during the recovery of cryopreserved stocks and routine passaging (Watanabe et al., 2007). However, not all reports suggest it is necessary to use ROCKi during every passage (Castro-Vinuelas et al., 2021). Therefore, we observed cultures post splitting with and without ROCKi after 24h and 48h. Our data clearly shows morphological differences between cultures after 24h. Cells treated with ROCKi present a spikey morphology and formed many small aggregates. Cultures without ROCKi appeared as typical iPSC aggregates, although fewer in number than the treated cells. After 48h both cultures adopted the same typical iPSC morphology and there were no noticeable differences between aggregate numbers.

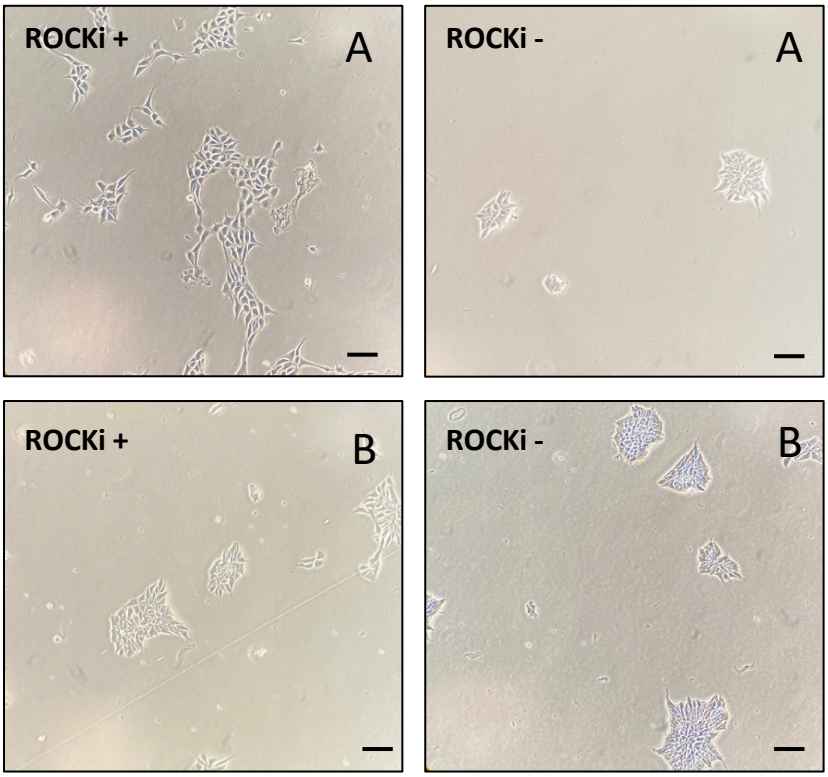


Figure 4.2-4 Passing with and without ROCKi

Images representative of cultures after passaging with ReLeSR, treated with and without ROCKi for 24h (A), followed by a further 24h without ROCKi (B). Scale bar is representative of 40μm.

4.2.2 Assessment of pluripotency

Pluripotency is the ability of a single cell to give rise to cells from all three germ layers (Feng et al., 2013). This can be assessed *in vivo* through teratoma formation or *in vitro* through trilineage differentiation (Singh et al., 2016). During trilineage differentiation, iPSCs are split into three individual cultures and supplemented with different germ layer inducing medias. Following this, cells are usually stained with antibodies specific to each germ layer: ectoderm, mesoderm and endoderm.

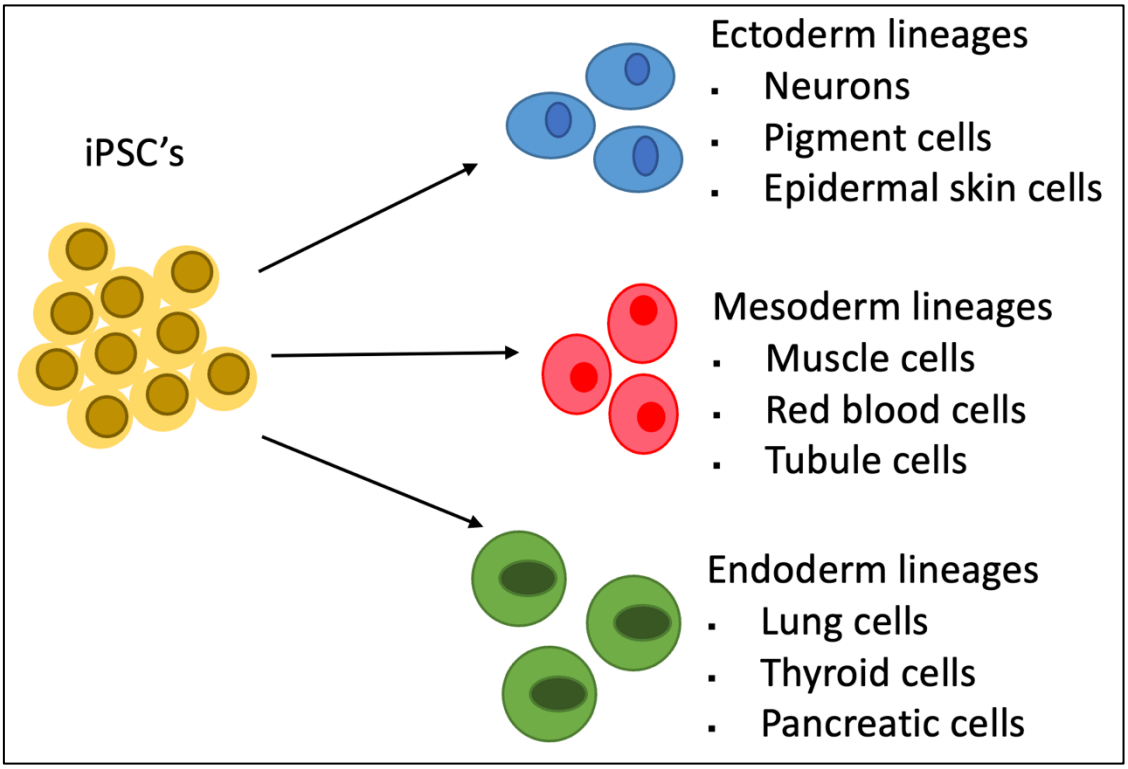


Figure 4.2-5 Schematic diagram of iPSC trilineage differentiation

A hallmark of pluripotency is the ability of a cell to differentiate into all three germ layers, which subsequently differentiate into further cell types.

Trilineage differentiation was carried out using the STEMdiff Trilineage Differentiation Kit following the manufacturer's instructions. Three antibodies were chosen specific to each germ layer: SOX17 is reported to be a key transcription factor during endoderm development (Kanai-Azuma et al., 2002), Brachyury is a transcription factor required for posterior mesoderm formation and differentiation (Barresi et al., 2014), and OTX2 is a regulator of ectoderm identity (Gammill and Sive, 2001). These data clearly show iPSCs were capable of differentiating into each germ layer. However cross reactivity of each antibody within the different germ layers was not assessed and so should be investigated in future experiments.

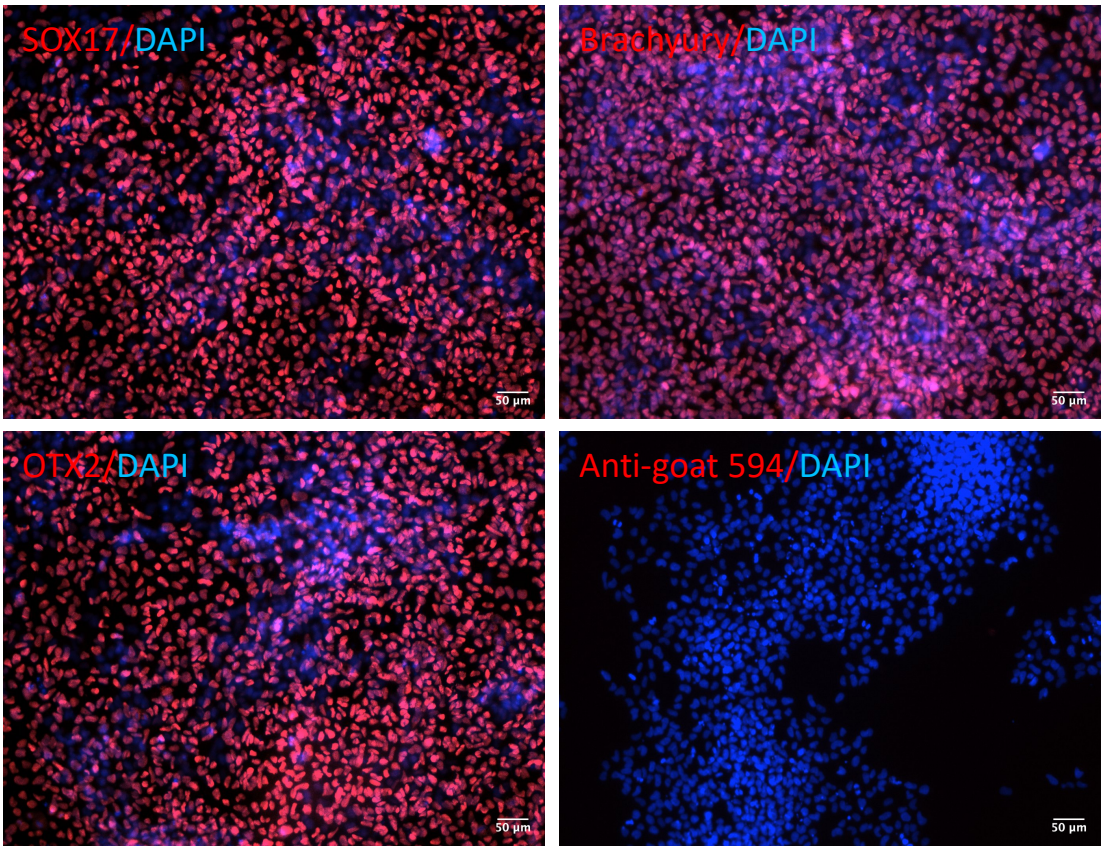


Figure 4.2-6 iPSCs differentiate into all three germ types

iPSCs were seeded and cultured in either endoderm or mesoderm differentiation media for 5 days, or ectoderm differentiation media for 7 days. Cells were fixed with 4% PFA before incubation with their respective primary antibodies overnight. The following day anti-goat 594 was used as a secondary antibody for a 1h room temperature incubation before a 2-minute incubation with DAPI nuclear stain (1:500). Control cells were incubated with the anti-goat 594 secondary only. Images were taken with a confocal widefield microscope at x10 and are representative of two independent experiments.

The pluripotency of cells is governed by molecular mechanisms which regulate gene expression responsible for their maintenance and suppression of differentiation (Singh et al., 2016). Following trilineage differentiation, we sought to investigate if the cells expressed key markers of pluripotency. In addition to if the expression of these markers was consistent throughout a number of passages. OCT4 and SOX2 are two of the four Yamanaka factors used to reprogramme somatic cells into pluripotent stem cells (Takahashi et al., 2007), NANOG directs the propagation of

undifferentiated cells (Chambers et al., 2003), DNMT3B is a methyltransferase reported to be highly specific for pluripotent cells (Gopalakrishna-Pillai and Iverson, 2011), and TDGF1 is a marker of undifferentiated stem cells (Bianco et al., 2010). 18 samples were randomly selected from passages 2-20 from two separate stocks of cyropreserved iPSCs. Our data clearly shows each sample expresses pluripotency genes.

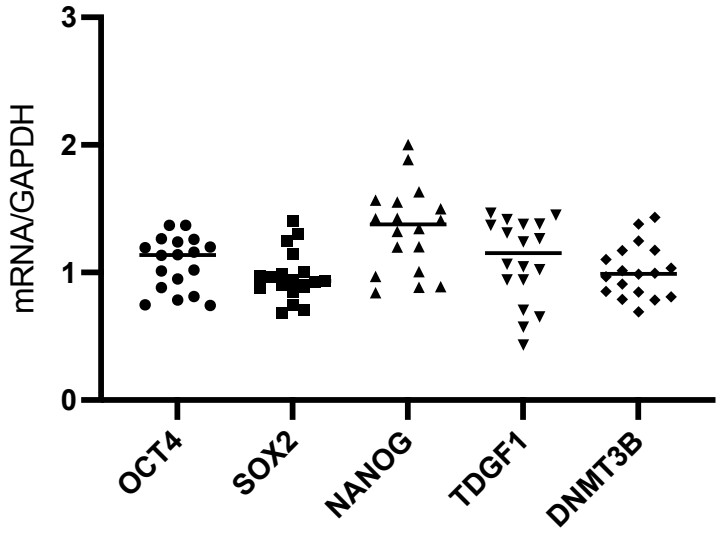


Figure 4.2-7 iPSCs express pluripotency markers

18 iPSC samples from two different cryovials were harvested between passage 2-20. The expression of key pluripotency genes were measured with RT-qPCR and normalised to GAPDH. Results show each individual data point. A Grubs analysis detected no outliers ($\alpha = 0.05$).

Genetic variants can influence cellular mechanisms and therefore lead to different phenotypic presentations in an organism. It is common in iPSCs to see a loss of genetic integrity which can cause variability in results, often compromising disease models (Kilpinen et al., 2017). Therefore, ensuring the genome of iPSCs remains consistent is a key factor in determining a healthy model. This is usually carried out through genetic testing and karyotyping.

We used the hPSC Genetic Analysis Kit (Stemcell technologies) which tests for the 8 most common mutations in iPSCs. The experiment was repeated twice using different passages and three samples from each. The results were analysed as recommended using the Stemcell genetic analysis software. Only one sample tested completely normal, another only had 'possible' amplifications. The remaining samples were reported to either have amplifications or deletions. Considering the large variation between three samples of the same passage, we concluded that the kit may not be sufficient for accurate prediction of stability. Therefore, future work should look to routine complete karyotype testing with G-banding analysis to confidently confirm the genomic status of the samples.

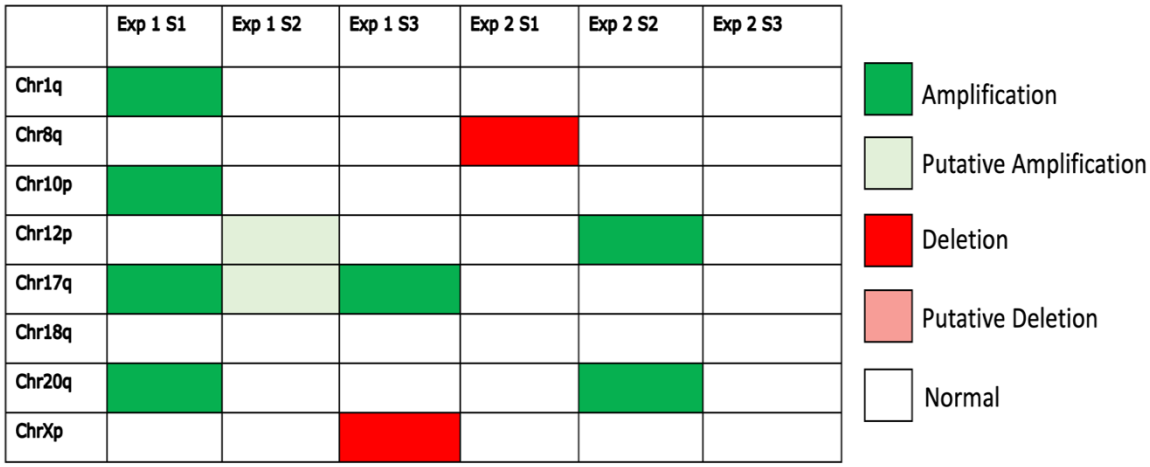


Figure 4.2-8 Analysis of 8 common chromosomal mutations in iPSCs generates varied results

Three iPSC samples from two different passages (Exp 1 and Exp 2) were tested using the Stemcell hPSC Genetic Analysis Kit for the 8 most common chromosome mutations. qPCR was used to measure gene expression normalised to Chr4p and compared to a genomic DNA control. Copy number < 1.8 or > 2.2 with a $p < 0.05$ indicates the presence of an abnormality within a sample.

4.2.3 iPSC derived dopaminergic neurons

Differentiating pluripotent stem cells into neurons can be achieved by sequential activation of signalling pathways or transcription factor programming (Ng et al., 2021). The difficulty with sequential activation is that it requires a multistep differentiation process which attempts to mimic the stages of embryonic development into mature neurons. Cultures are often asynchronous during this process and therefore can result in variable cultures with limited reproducibility. The use of transduced transcription factors has been shown to reduce this variability (Powell et al., 2021).

As aforementioned, Nurr1 is vital for the development of DA neurons. Exemplified by multiple knock out studies in mice which fail to generate DA neurons and die soon after death, or display a higher susceptibility to neurotoxins and obvious motor defects (Zetterström et al., 1997, Zetterström et al., 1996, Le et al., 1999). Thus, it is unsurprising that studies attempting to generate DA neurons often focus on the overexpression of Nurr1 alongside other key transcription factors to induce a DA phenotype. In combination with Nurr1, the transcription factors Ascl1 and LMX1B are reported to be sufficient for differentiating iPSC's into DA neurons (Powell et al., 2021, Theka et al., 2013). We overexpressed these three key transcription factors through the use of an inducible polycistronic vector to eliminate the variation caused by three independent viruses. The polycistronic vector obtained from Addgene (#43918 tetO-ALN was a gift from John Gearhart) did not encode the reverse tetracycline trans activator protein (rtTA) required for inducible expression of the Ascl1-LMX1B-Nurr1 (ALN) vector. Therefore, an additional vector was used which expressed rtTA.

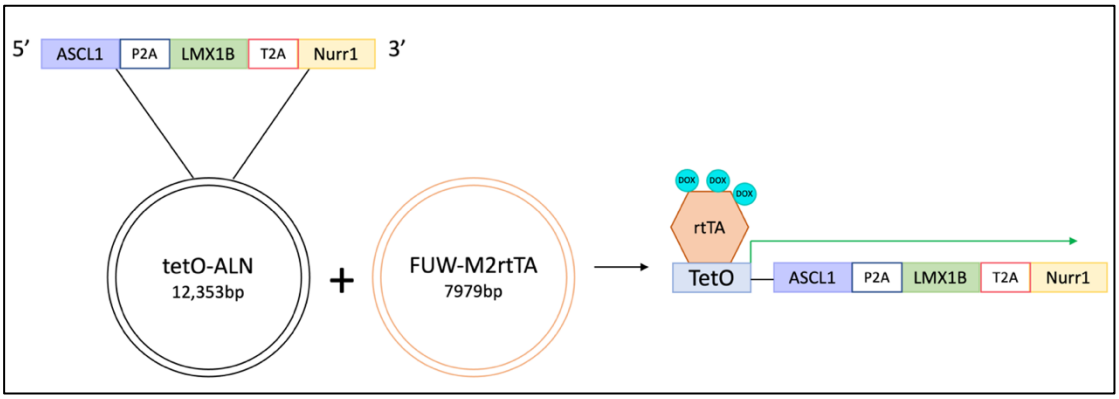


Figure 4.2-9 rtTA is required for transcription of ALN genes

Schematic of the tet-O-ALN and FUW-M2rtTA plasmids obtained from Addgene (accession numbers #43918 and #20342 respectively). Doxycycline binds to rtTA which is subsequently bound to the TetO promoter, allowing the transcription of the ALN genes.

Lentiviral transduction is a valuable method of introducing DNA into iPSC. It is an advantageous method of genetic modification because it has high cell viability and adequate efficiency compared to electroporation or lipofection (Cao et al., 2010). We sought to investigate the transduction efficiency of our iPSCs using pINDUCER20-GFP. Due to the sensitivity of iPSCs and their susceptibility to unwanted differentiation we tested both HEK293FT viral media (crude) and ultracentrifuged virus resuspended in PBS. Figure 4.2-10 clearly shows that ultracentrifuged virus was more effective at transducing iPSCs than crude virus. In addition, crude virus appeared to generate more cell death. Therefore, we decided to use ultracentrifuged virus for the subsequent experiments.

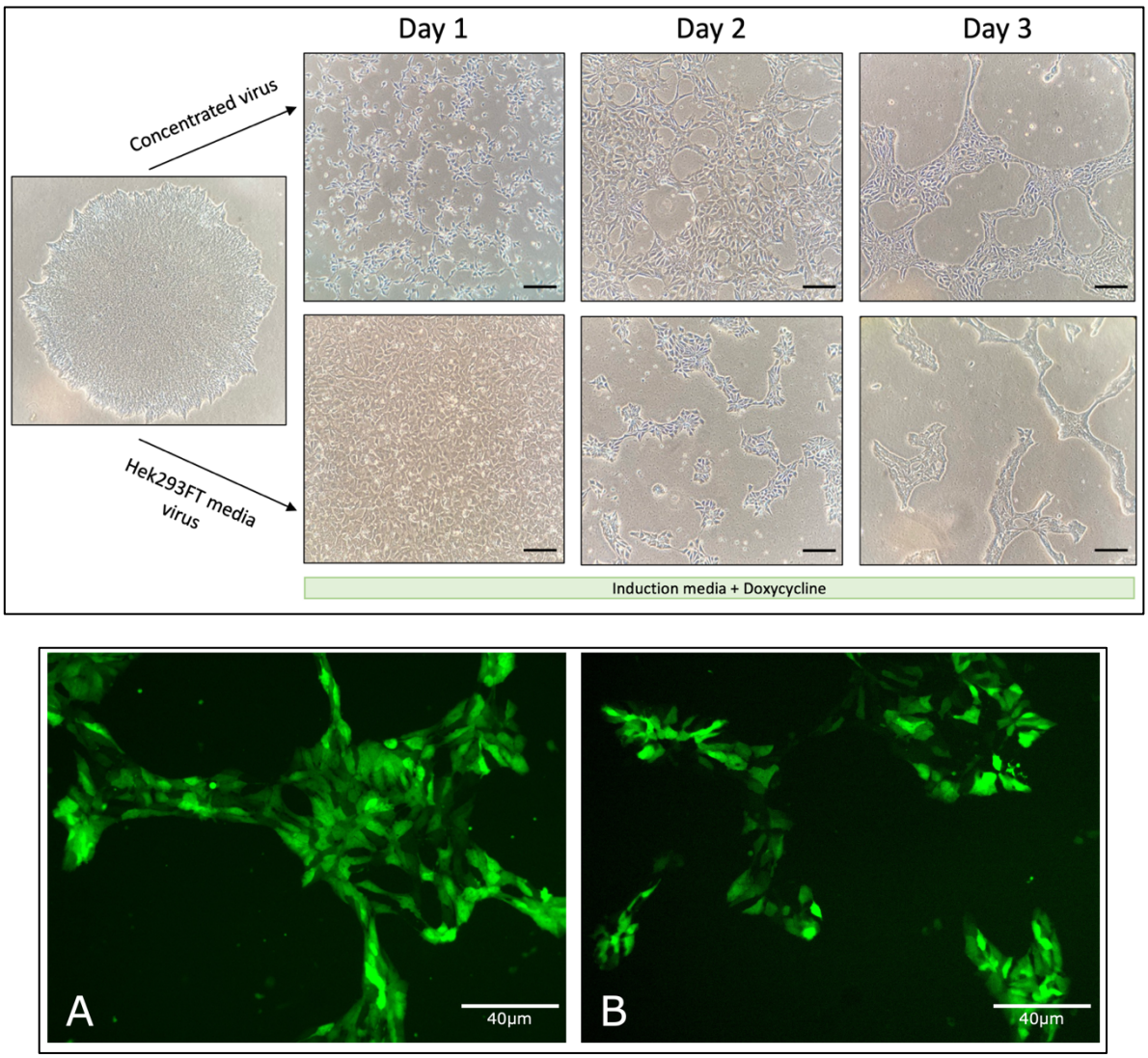


Figure 4.2-10 Ultracentrifuged virus transduce iPSCs efficiently

iPSCs dissociated into single cells were infected with GFP virus either produced in HEK293FT media (B) or ultraconcentrated in PBS (A). On day 1 induction media was added with 1µg/ml doxycycline. Cells were observed over 3 days before GFP was visualised using a confocal widefield microscope at x20 magnification. Scale bar represents approximately 40µm.

After establishing transduction efficiency, it was important to ascertain if transduction with the ALN virus produced stable protein expression. The Nurr1 gene is located at the 3' end of polycistronic sequence, therefore the detection of Nurr1 was considered an adequate indicator that transcription and translation of the whole

transgene sequence was successful. Our data clearly shows Nurr1 protein is expressed only when doxycycline was present.

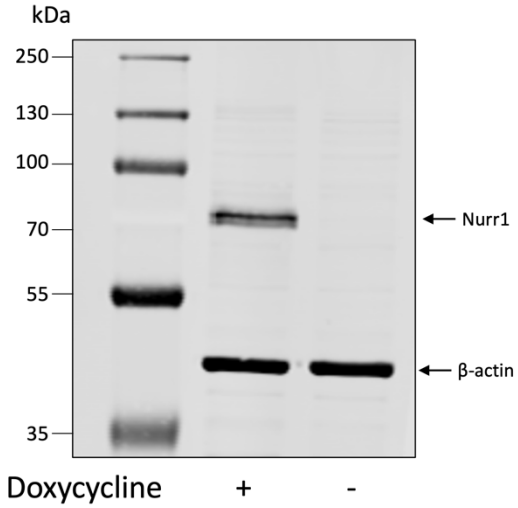


Figure 4.2-11 Doxycycline induces the expression of ALN

iPSCs dissociated into single cells were infected with equal amounts of ultraconcentrated ALN and rtTA viruses. After 24h, induction media with or without 1µg/ml doxycycline was added for 48h before cells were harvested, lysed and protein ran on a 10% SDS gel.

iPSCs were infected with ALN for 24h before induction media with 1µg/ml doxycycline was added. Cytosine arabinoside (Ara-C) is an antimitotic agent for dividing cells (Martin et al., 1990), used to inhibit the proliferation of glial cells, such as astrocytes, when used in low concentrations in neuronal cultures (Lesslich et al., 2022). After 9 days of neuronal induction media with doxycycline, clear cell process could be seen, some of which resembled axons. At this stage, if very few processes were observed then it was likely the viral transduction was not efficient and the experiment should be repeated. Neuron maturation media was then added which contained B27 without doxycycline. Ara-C was used up until day 11 at a reduced concentration. Half media changes were repeated every other day until day 21, where cells formed a complex network of processes, and it was at this point cells were fixed for immunocytochemistry.

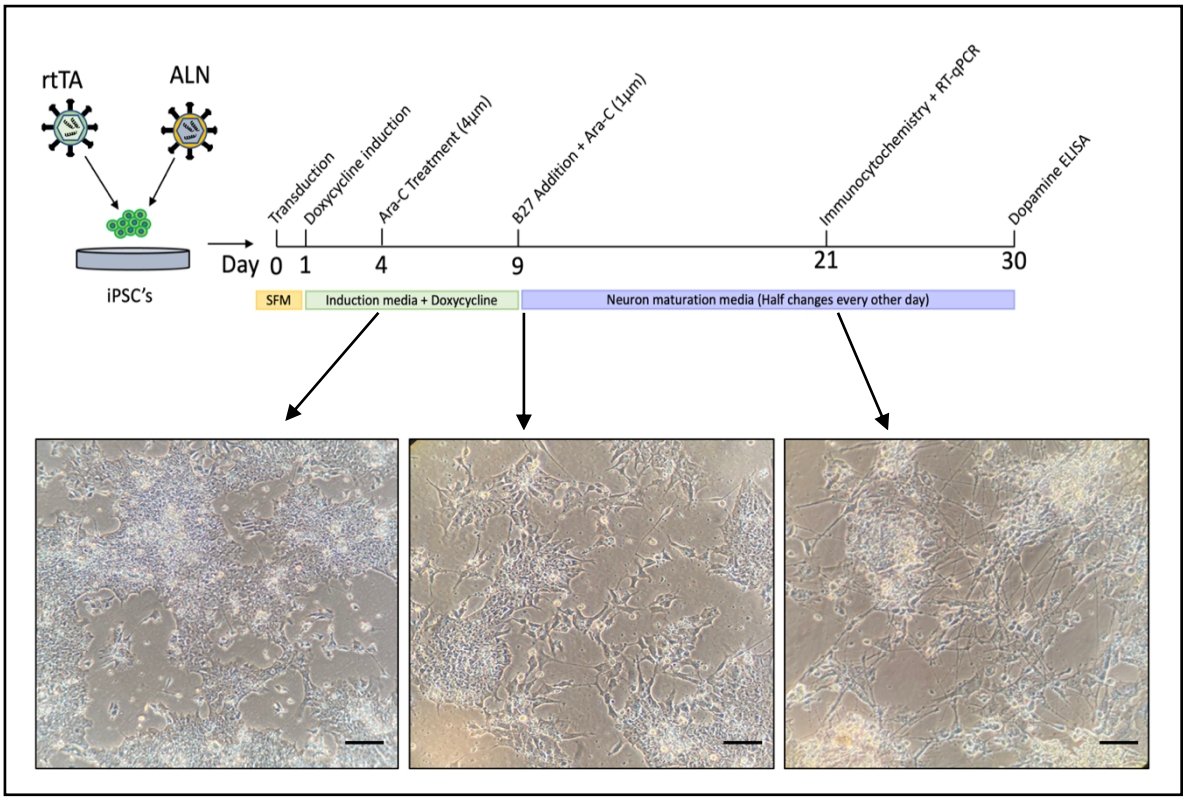


Figure 4.2-12 iPSC dopaminergic neuron differentiation timeline

Schematic diagram demonstrating the differentiation timeline, including key changes in media composition and representative images of days 4, 9 and 21 taken with an inverted light microscope. Scale bar represents approximately 40µm.

After 21 days in culture, neurons were assessed using immunocytochemistry to evaluate marker expression. We used NeuN and MAP2 as markers of mature neurons, TH as a key marker of DA neurons and GFAP as an astrocytic marker (Powell et al., 2021, Theka et al., 2013). Cells expressed each of the 3 neuronal markers but not GFAP. Unsuccessful cultures which presented flat cells and minimal processes expressed the marker GFAP.

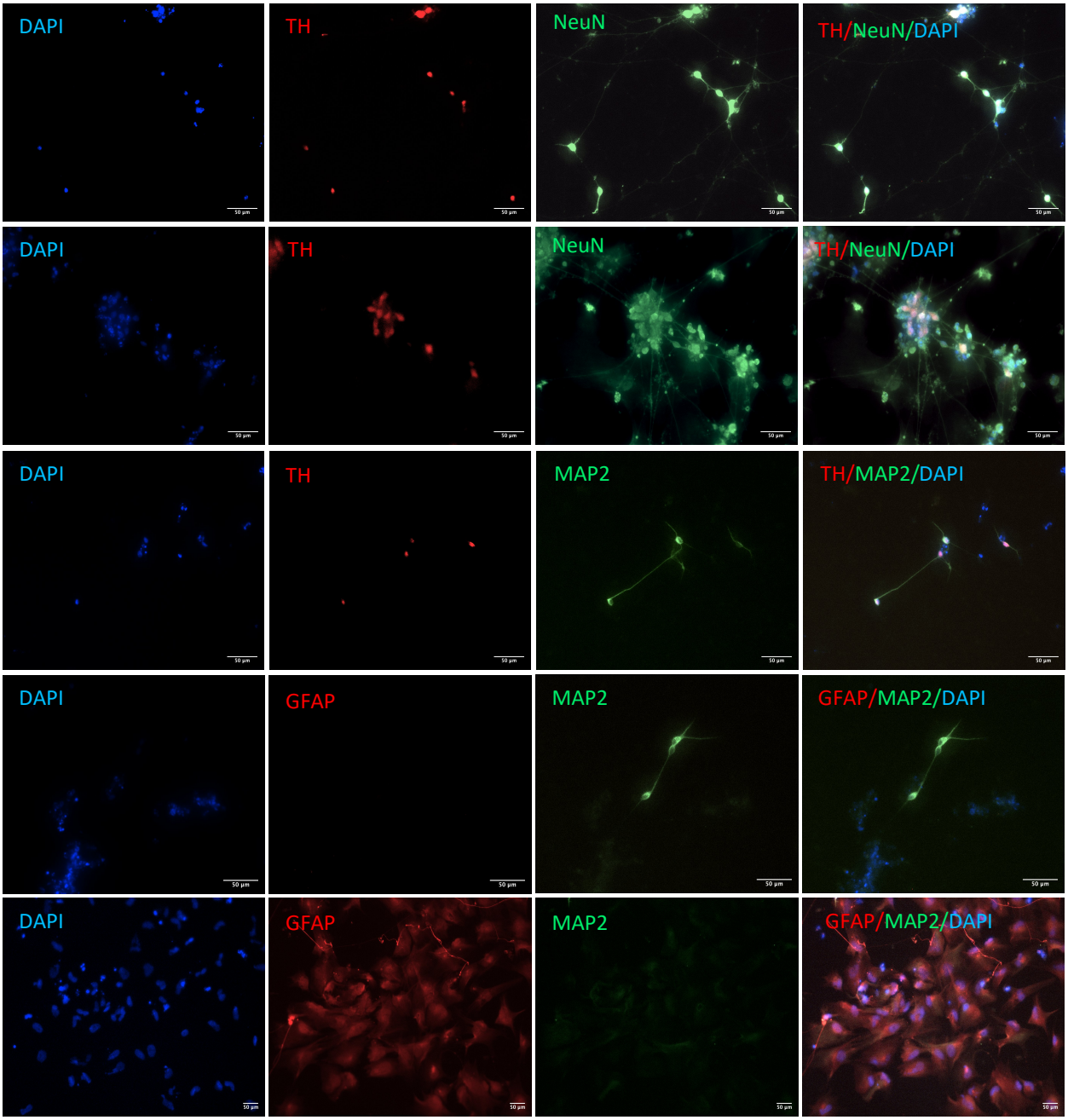


Figure 4.2-13 iPSC dopaminergic neurons express key markers

Immunocytochemistry was performed on DA neurons after 21 days in culture. Cells were fixed and stained with the indicated primary antibodies and appropriate secondaries, followed by DAPI nuclear staining (1:500). Images were collected with a widefield microscope at x10 and x20 magnification. Data are representative of results from two independent experiments.

From morphological and immunocytochemical assessment, it appeared the cells were successfully differentiated into DA neurons. However further characterisation is required to validate them as a

functional model. Next steps would assess the gene expression of key markers: TH, DAT, and VMAT2 (Powell et al., 2021, Theka et al., 2013). Followed by an ELISA assay to measure dopamine production. Finally, transduction efficiency of the differentiated neurons would need to be evaluated before investigations into dopaminergic gene regulation by transduced, or knocked out, Nurr1 and Nurr-1a could be carried out.

4.2.4 iPSC derived microglia

The differentiation of iPSCs into microglia can be achieved through stage specific expression of growth factors and cytokines which mimic extracellular signals during embryonic development. Commonly cultures begin with the expression of growth factors to induce the production of haematopoietic cells (HPs) over 12-20 days, which are then collected and sorted. The enriched HPs are then cultured for around 22-30 days in microglia differentiation media followed by a further 5-10 days in microglia maturation media (Abud et al., 2017, McQuade et al., 2018, Douvaras et al., 2017, Haenseler et al., 2017). The combination of cytokines and growth factors used at each stage differ between protocols. The complexity and lengthy process of this culture is the likely reason for the development of microglia differentiation kits, such as those provided by Stemcell Technologies.

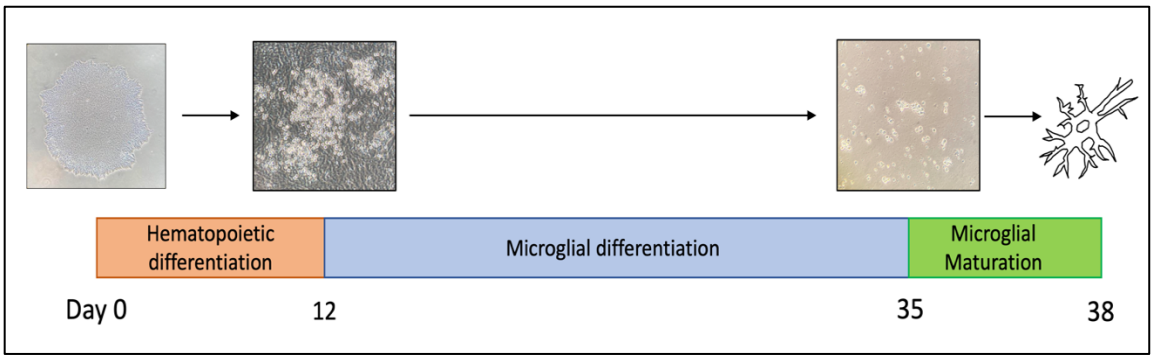


Figure 4.2-14 iPSC derived microglial differentiation timeline

Schematic representation of the process differentiating microglia from iPSCs, with representative morphology at each stage.

We used two different methods of differentiation to generate HPs from iPSCs. The first method utilised a kit purchased from Stemcell which consisted of media A to be used for 2 days and media B to be used for 10 days. Aggregates were seeded in TeSR-E8 medium so that on day 1 of differentiation there were approximately 20

aggregates (~100 cell) per well of a 6 well plate. The seeding density was important as too few aggregates would produce a poor yield and too many impaired proper differentiation (McQuade et al., 2018). The media was changed as per the manufacturer's instructions. After 4 days in culture the cells began to display mesoderm morphology, rapidly forming dense aggregates and an adherent monolayer. By day 10 floating haematopoietic cells could be observed, which increased in number until they were harvested on day 12. McQuade et al., reported similar observation using the same kit (McQuade et al., 2018).

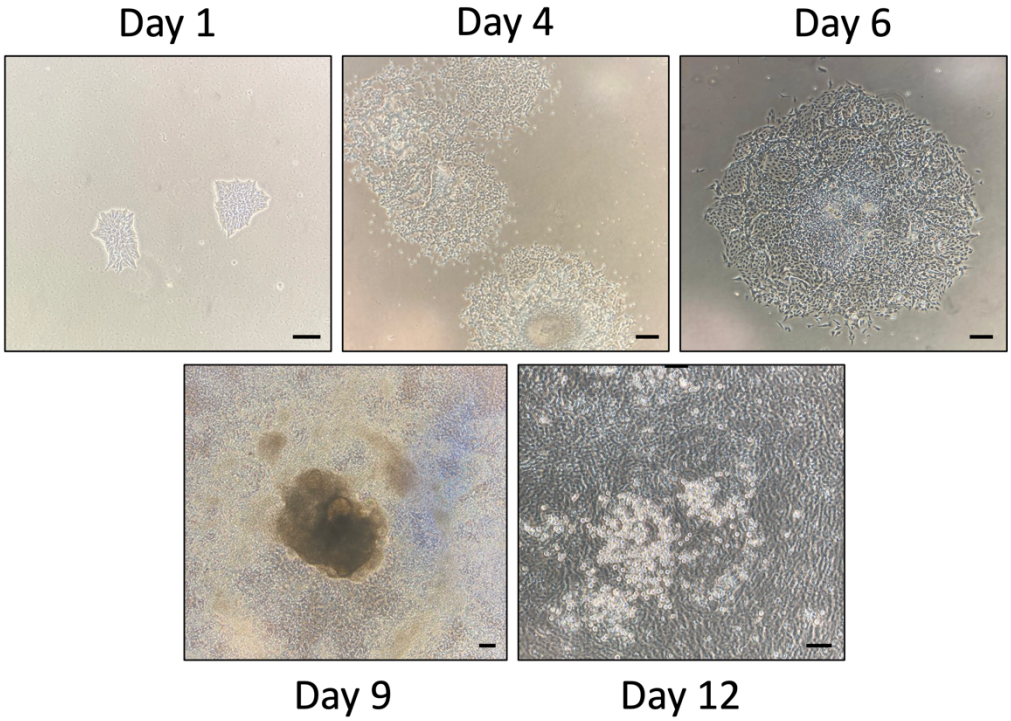


Figure 4.2-15 iPSCs were differentiated using the STEMdiff Hematopoietic Kit

The STEMdiff Hematopoietic Kit an be used to produce hematopoietic cells over 12 days. Representative images of days 1, 4, 6, 9 and 12 in culture were taken with an inverted light microscope. Scale bar represents approximately 40µm.

It is common after iPSC hematopoietic cell production to FACS sort into CD34+, CD43+ or CD45+ cells. However, McQuade et al., reported FACS was not necessary after using this specific Stemcell

kit, and that both sorted or un-sorted HPs generated virtually identical iPSC microglia (McQuade et al., 2018). To this end, we did not FACS sort our HPs, but further characterised them by analysing the gene expression of key hematopoietic genes. We found HPs expressed CD34, CD43 and CD45 whereas the undifferentiated iPSC control did not. Similarly, the iPSC control expressed SOX2 and OCT4 pluripotency markers unlike HPs. Our data clearly shows the HPs generated using the Stemcell kit have successfully differentiated away from a pluripotent state and express key hematopoietic markers.

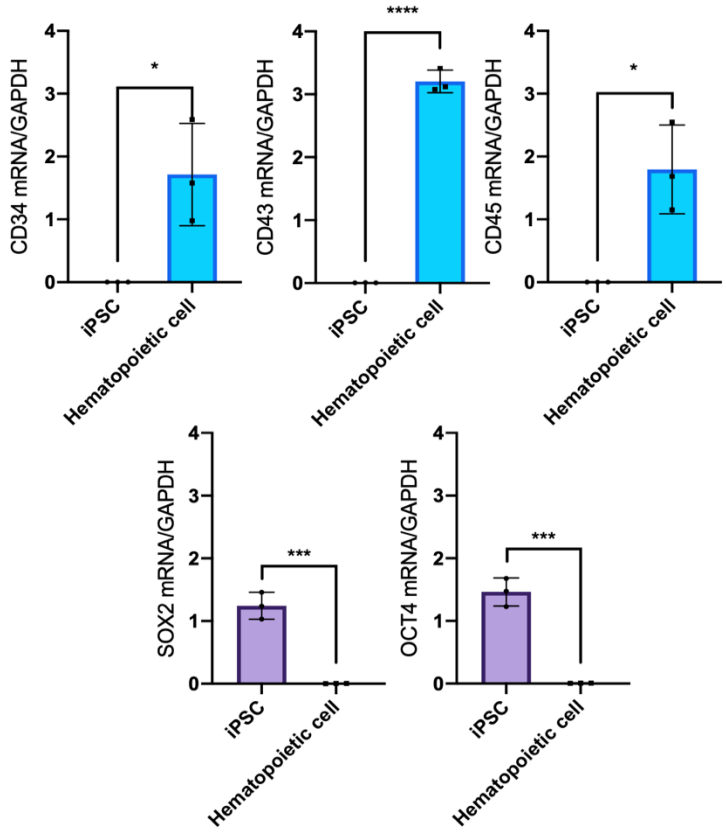


Figure 4.2-16 Hematopoietic cells express key markers

iPSCs were differentiated to hematopoietic cells using the Stemcell Hematopoietic Differentiation kit as per the manufacturer's instructions. The expression of key hematopoietic and pluripotency genes was measured with RT-qPCR and normalised to GAPDH. Data are presented as standard deviation from the mean and are representative of results from 2 independent experiments n=3. Statistically significant differences between indicated groups were *$p < 0.05$, ***$p < 0.0005$ **** $p < 0.0001$ (one-way ANOVA with Bonferroni post-test correction).

The second method used to generate HPs used a cocktail of cytokines over 18 days, as described by Heo et al., (Heo et al., 2018). The morphology observed was similar to that of the Stemcell kit, however on the day of harvest many of the cells remained adherent which generated an extremely low yield unable to be processed for gene expression. This culture method was repeated twice with the same disappointing results therefore this method was not used in subsequent experiments.

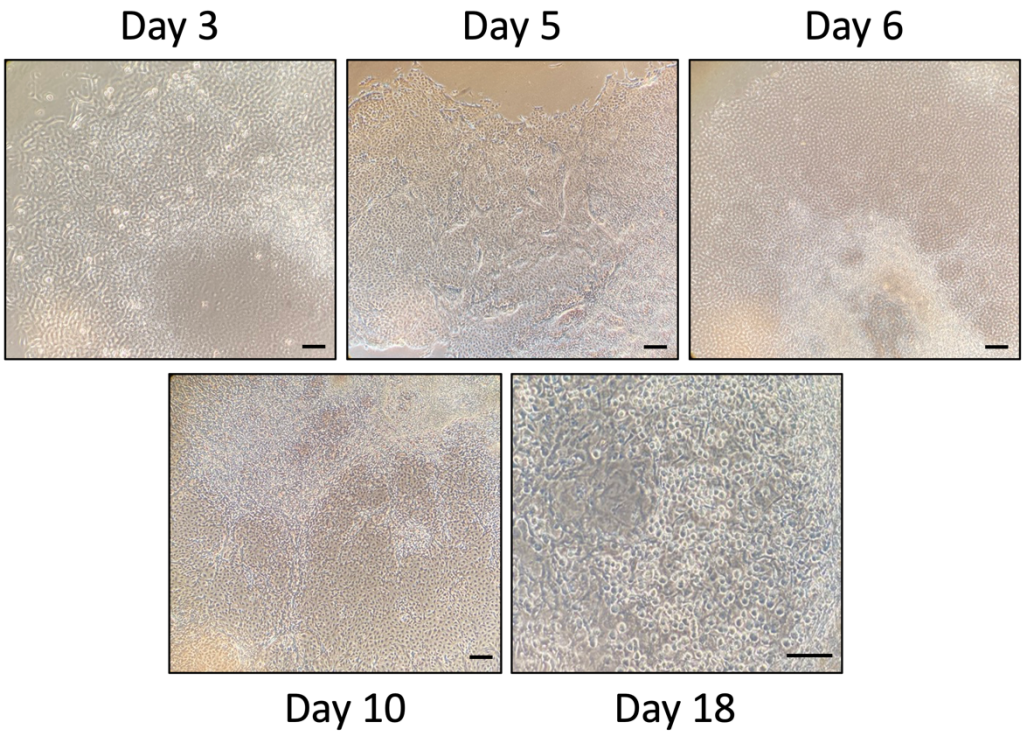


Figure 4.2-17 iPSCs were unable to differentiate into hematopoietic cells using a cytokine cocktail method

iPSCs were cultured in Stemline II serum-free medium containing insulin-transferrin-selenium and BMP4 (20ng/ml) for 4 days, followed by treatment with SCF (50ng/ml) and VEGF (40ng/ml) for 2 days. On day 6 a cocktail of cytokines including SCF, IL-3, G-CSF, FLT3 (each 50ng/ml) and TPO (10ng/ml), were added to fresh Stemline II SF media and cultured until day 18. Scale bar represents approximately 40μm.

We next attempted to differentiate the HPs into microglia using the STEMdiff Microglia Differentiation Kit and the STEMdiff Microglia Maturation Kit (Stemcell Technologies). Across the 34 days of culture cells were not adherent and there were minimal changes in cell

morphology. As seen on day 10 in Figure 4.2-18, cells occasionally formed aggregates which were indicative of cell death as described previously (McQuade and Blurton-Jones, 2022).

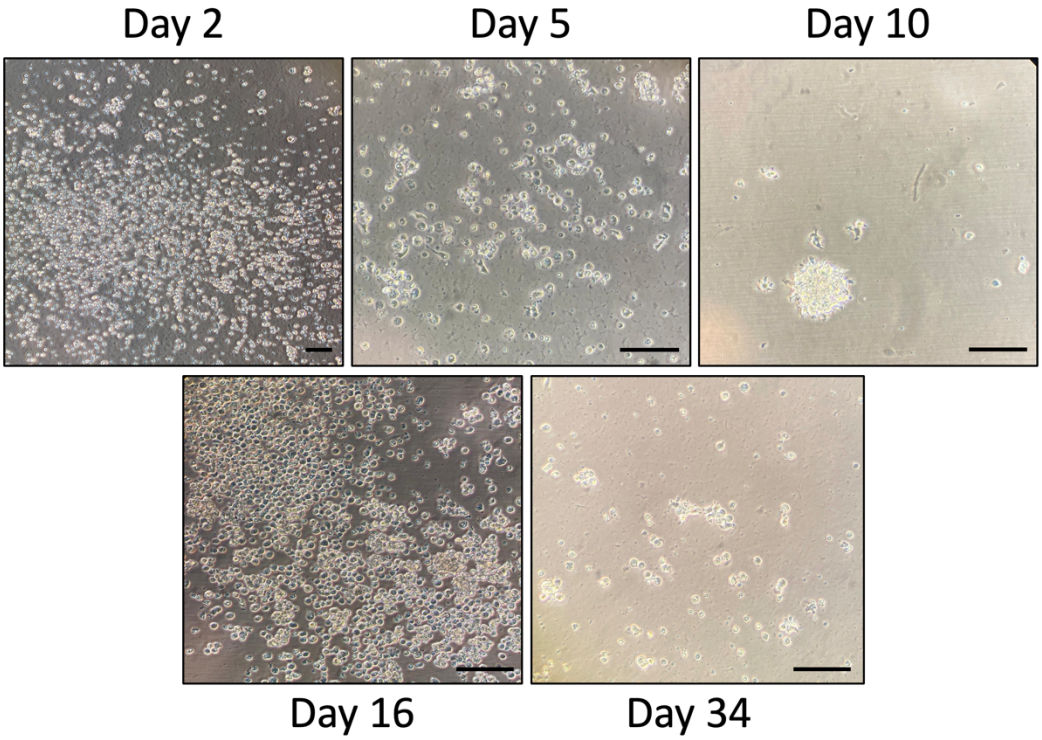


Figure 4.2-18 The differentiation of hematopoietic cells using STEMdiff microglia differentiation kits did not morphologically resemble microglia

Hematopoietic cells were subjected to differentiation using the STEMdiff Microglia Differentiation Kit for 24 days, followed by the STEMdiff Microglia Maturation Kit for a further 10 days. Scale bar represents approximately 40µm.

Despite the unexpected morphology, cells were fixed and subjected to immunocytochemistry. Many cells were lost during the washes as they were not adherent. Our results show the remaining cells expressed both Iba1 and TMEM119. However, there was an abundance of debris which also stained for these markers indicating there could be non-specific staining. This was a singular experiment due to the lengthy culture time (~50 days) and lack of cells however future work should look repeating the experiment before any

meaningful conclusions can be drawn about the cell's identity and viability.

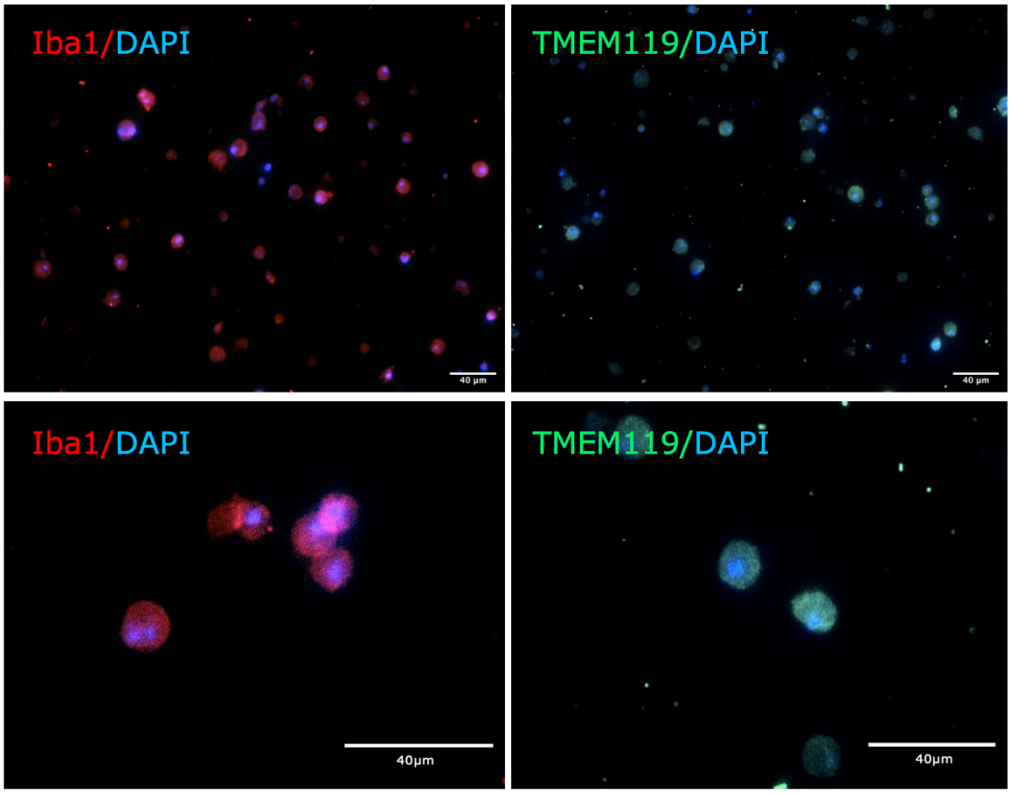


Figure 4.2-19 iPSC derived microglia express Iba1 and TMEM119

Hematopoietic cells subjected to differentiation using the STEMdiff Microglia Differentiation Kit for 24 days, followed by the STEMdiff Microglia Maturation Kit for a further 10 days. Cells were fixed and stained with Iba1 (1:200) or TMEM119 (1:500) followed by appropriate secondary antibodies and DAPI nuclear staining (1:500).

4.2 Discussion: iPSCs

Methods to generate dopaminergic neurons from iPSC have previously been explored, which frequently involve multiple stages of complex media compositions yielding variable and inconsistent results. In the first part of this chapter, we describe an inexpensive method, based upon the overexpression of Nurr1, Ascl1 and LMX1B, in which to generate DA neurons expressing key markers after 21 days of culture. To validate the functionality of these DA neurons they will need to be assayed further to ensure dopamine production and gene expression of key markers. Nevertheless, initial results appear promising. Additionally, we attempted to differentiate iPSCs into mature microglia with limited success, albeit we were able to validate a method of producing the intermediate haematopoietic cells.

Methods to culture and maintain iPSCs vary greatly due to the media used, matrixes, passaging methods and downstream intention (Chatterjee et al., 2016, Gilmozzi et al., 2021, McQuade et al., 2018, Powell et al., 2021). We generated a method using enzyme free passaging which eliminated potentially damaging effects of enzymatic reagents on the cell surface (Beers et al., 2012). In combination with TeSR-E8 media and RGF Stem Cell Qualified Cultrex, consistent non-differentiated cultures were produced. These cells were validated by assessment of key pluripotency markers alongside successful differentiation into the three germ layers (Takahashi et al., 2007, Chambers et al., 2003) (Gopalakrishna-Pillai and Iverson, 2011), (Bianco et al., 2010). Genetic analysis was completed using the hPSC Genetic Analysis Kit (Stemcell technologies), however the results varied greatly between samples of the same passage suggesting potential issues with the accuracy of the assay or preparation of samples. Further work will look to

routine full karyotypic analysis with G-banding to ensure the genetic stability of iPSC cultures.

Generating human based dopaminergic neuronal models are vital for understanding neuroinflammation in PD. Reports have suggested that Nurr1 plays a neuroprotective role (Smith et al., 2015). However, the role, if any, of Nurr-1a remains unidentified. Powell et al., and Theka et al., published methods to generate functional dopaminergic neurons from human iPSCs (Theka et al., 2013, Powell et al., 2021). Both reports overexpress the key transcription factors Ascl1, LMX1a/b and Nurr1 through lentiviral transduction. However, Powell et al., used a polycistronic vector to eliminate the variability of co-transduction with multiple viruses. Although different isoforms of LMX1a and LMX1b were used, reports suggest they function cooperatively and can act to compensate each other (Yan et al., 2011). Our methods use a polycistronic vector similar to Powell et al., in a simplified method, see Figure 4.2-10 below, which required no neuronal splitting halfway through and a simplified basic media regime. The only alterations to the media composition was the addition of doxycycline, Ara-C and B27 on the respective days indicated in Figure 4.2-12. After 21 days of culture cells exhibited typical neuronal morphology: small cell somas with long axons forming a complex network. DA neurons expressed mature neuronal markers MAP2 and NeuN, in addition to TH a key dopaminergic marker. These cells did not express the astrocytic marker GFAP, however morphologically unsuccessful cultures with enlarged flat cells absent of processes did express GFAP. Neurons were validated by morphology and immunocytochemical marker expression only. Therefore, further assessments are required before they can be used confidently as a dopaminergic model, but initial data is promising.

Day	Stage	Task
0	Seeding & transduction	• iPSC's from a T25 flask were harvested in Accutase to generate a single cell suspension. • Cells resuspended in TeSR-E8 media with 10μM ROCKi, counted and seeded at $1x10^6$ cells per well of a 6 well plate in 2ml of TeSR-E8 media + 10μM ROCKi. • Immediately appropriate volumes of both TET-O-ALN and FUW-M2rtTA viruses were added dropwise to each well, swirled and incubated overnight at 37°C.
1	Feed induction media	• Media was aspirated from each well and replaced with 2ml of induction media + 1μg/ml doxycycline (dox).
2 & 3	Feed induction media	• Media was aspirated from each well and replaced with 2ml of induction media + 1μg/ml dox.
4 & 5	Feed induction media	• If cells (>70%) cells extended early processes, then the media was aspirated and replaced with induction media + 1μg/ml dox + 2μM Ara-C. • If cells did not extend processes, the addition of Ara-C was postponed.
6	Feed induction media	• The media was aspirated and replaced with induction media + 1μg/ml dox + 2μM Ara-C. • If at this point many (<70%) cells did not extend processes the culture had failed and would be discarded.
7	Feed induction media	• The media was aspirated and replaced with induction media + 1μg/ml dox + 2μM Ara-C.
9	Feed maturation media	• The media was aspirated and 2ml of neuron maturation media was added with reduced Ara-C 1μM.
11	Feed maturation	• From this point half media changes were carried out every other day with maturation media only.
21	Harvest	• Culture is harvested/fixed/used for functional assay.
Media recipes		
Induction media		DMEM/F12, 25 μg ml^{-1} insulin, 50 μg ml^{-1} transferrin, 30 nM sodium selenite, 20 nM progesterone, 100 nM putrescine, 1μg/ml Dox, 4μM Ara-C
Maturation media		DMEM/F12, 25 μg ml^{-1} insulin, 50 μg ml^{-1} transferrin, 30 nM sodium selenite, 20 nM progesterone, 100 nM putrescine, 1x B27

Figure 4.2-10 Protocol to differentiate iPSC into Dopaminergic neurons.

Activated microglia are suggested to be culpable for much of the neuroinflammation seen during PD (Dzamko et al., 2017, Zheng and Zhang, 2021). Generating a human iPSC derived model would allow us to mimic neuroinflammation through treatment of iPSC microglia with aggregated or mutant alpha-synuclein to produce conditioned media more physiologically relevant of a neuroinflammatory response. This could then be applied to neurons and its effects on survival and degeneration could be studied. Additionally, the regulation of inflammation and neuroprotection by Nurr1 and Nurr-1a could be evaluated (Smith et al., 2015, Saijo et al., 2009). Due to the long and complicated nature of differentiating iPSCs into microglia, a variety of kits have been developed. These kits sequentially force the cells through different differentiation stages; however, they eliminate the variability of multi-cytokine media compositions. The first stage of differentiation is the generation of HPs. We attempted two methods to generate HPs however only the kit produced an adequate yield of cells which were confirmed to express key HP markers. These HPs were subjected to microglial differentiation and maturation using kits purchased from Stemcell Technologies. After 34 days in culture the cells did not resemble typical ramified microglia morphology. They were instead round, and many cells were floating which could be indicative of an activated state or cell death. Despite the unexpected morphology the cells expressed Iba1 and 'microglial specific' marker TMEM119. Further analysis is required to ensure these cells have the correct gene expression and can phagocytose. Our data suggests that despite the initial high cost, kits of pre-made medias may be preferential over optimising multiple cytokine cocktail's.

In conclusion, the first part of this chapter revealed a simplified method of differentiating iPSCs into dopaminergic neurons. Although the final cells produced through this method require further

validation, we are confident this method is a cost and time effective way forward to generate DA neurons. The process of differentiating iPSCs into microglia was not as promising. Due to our inability to generate functional microglia and the extremely time intensive nature of the process, we sought investigate alternative methods to generate inflammatory cells in which to investigate the role of Nurr1 and Nurr-1a.

4.3 Introduction: monocyte derived macrophages and microglial-like cells

Multiple mechanisms are suggested to underly the progressive death of dopaminergic neurons in PD (Surmeier, 2018). Whether these mechanisms are mutually exclusive with a singular driver of neuronal death or are synergic at mediating disease pathology remains unclear. Mitochondrial dysfunction, Lewy body formation and neuroinflammation are all commonly accepted theories accompanied by substantial evidence (Surmeier, 2018). A more recent concept is the gut-brain axis; suggesting gut dysbiosis is linked to an inflammatory environment which may contribute to the initiation or progression of PD (Houser and Tansey, 2017, Romano et al., 2021).

A problematic aspect of treating PD is that symptoms do not usually occur until striatal dopamine levels and nigral neurons are reduced by 80% and 50% respectively (Fearnley and Lees, 1991). Therefore, early detection and diagnosis is key to attempt to protect the remaining functional neurons. A meta-analysis of 71 studies revealed that inflammatory cytokines TGF-ß, IL-1ß and TNFα were all increased in the cerebral spinal fluid of PD patients compared to controls (Chen et al., 2018). Suggesting not only a strong association between the inflammatory response and PD but also highlights a potential role for cytokine levels in the CSF to be used as an early biomarker. In addition to CSF, elevated cytokines have been reported in the PBMCs of patients with PD, accompanied by a decrease (~61%) in Nurr1 expression (Li et al., 2018). This correlation similarly suggests inflammation is a key part of PD pathogenesis and Nurr1 may be involved in this response.

Nurr1 is reported to act in a negative feedback loop during inflammation (Saijo et al., 2009). Whereby the gene expression of

Nurr1 itself is induced via the NFκB pathway in inflammatory cells (Lilley et al., 2022, Saijo et al., 2009). Similarly, NFκB induces the production of proinflammatory cytokines which are subsequently repressed by Nurr1 reportedly binding to NFκB on inflammatory gene promoters, recruiting the co-repressor complex CoREST and repressing gene expression (Saijo et al., 2009). We hypothesise Nurr1 acts in a protective braking mechanism which allows inflammation to initially proceed but prevents it from becoming excessive or chronic. An alternative splice variant of Nurr1, termed Nurr-1a, differing only by a C-terminal truncation has been reported in brain tissue, however its function remains unknown. Considering the similar nature of the coding sequence, Nurr-1a may also have a repressive role during inflammation, or perhaps the truncation removes this ability. Nevertheless, Nurr-1a's role at inflammatory promoters is something we sought to reveal.

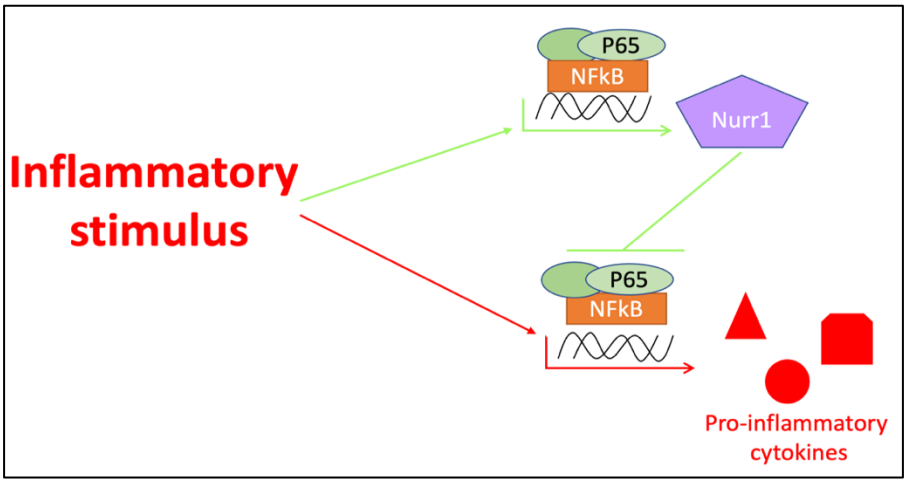


Figure 4.3-1 Schematic representation Nurr1's repressive role during inflammation

Inflammatory stimulus induces the NFκB mediated expression of Nurr1 in addition to pro-inflammatory cytokines. Nurr1 subsequently represses the expression of pro-inflammatory cytokines, preventing excessive inflammation from occurring.

Pivotal to CNS inflammation is microglial activation. During this state, microglia can secrete pro-inflammatory cytokines including IL-1ß, IL-6, TNFα and IFNy (Dai et al., 2019, Smith et al., 2012). If this

process becomes dysregulated or chronic then it can lead to neuronal damage or death. A study which grafted embryonic DA neurons into the striatum of PD patients found that invasion of activated microglia was present several years before α-synuclein accumulated (Olanow et al., 2019). This data, in line with supporting reports, suggests that microglial activation and inflammation may precede PD neuronal pathology (Dzamko et al., 2017, Zheng and Zhang, 2021).

Similar to microglia, macrophages can also adopt an activated state and release pro-inflammatory cytokines such as IL-1ß, IL-6, TNFα. More recently, there is evidence to suggest that macrophages in the peripheral immune system may be associated with PD pathogenesis. Mouse models of PD have shown the reduction of activated macrophages in the peripheral immune system, through intraperitoneal injections of Clodronate Liposomes, reduced the level of inflammatory cytokines released subsequently ameliorating microglia activation in the SN (Yan et al., 2018, Qin et al., 2007). Additionally, there are reports which suggest the gut-brain axis may be partly responsible for α-synuclein aggregation and neuroinflammation (Sampson et al., 2016). However, the idea of peripheral signals crossing the blood brain barrier remains controversial (Oberg et al., 2021).

Immune tolerance is now being investigated in the context of neuroinflammation and disease (Wendeln et al., 2018, Yao et al., 2022). Immune tolerance is the reduced responsiveness of the immune response when the body is repeatedly exposed to stimuli such as PAMPs or DAMPs through its TLRs (Chen and Ivashkiv, 2010). It is described as a protective mechanism whereby pro-inflammatory cytokine production is decreased and anti-inflammatory factors are increased to protect the body from excessive inflammation. A study using mice found that tolerizing the

mice through a LPS peripheral pre-treatment inhibited the activation of microglia induced by following LPS treatments (Yao et al., 2022). Suggesting that inducing peripheral immune tolerance is neuroprotective. Nurr1 has not been investigated in the context of immune tolerance, despite its suggested importance in inflammatory regulation (Saijo et al., 2009). A report suggests that TLR induced genes fall into two categories based on chromatin modifications; those which are silenced such as pro-inflammatory genes and those which are primed (Foster et al., 2007). Moreover, it would be interesting to evaluate what category Nurr1 falls into and any potential role it may have in this inflammatory protective mechanism.

IFNy plays a major role in inflammatory cell types by regulating cytokine production, activating immune cells and inducing cell death (Lee et al., 2017). IFNy has been associated with the death of DA neurons in PD (Barcia et al., 2011), in addition to its elevated presence in the blood of PD patients (Diaz et al., 2022). Mount et al., used a mouse model to demonstrate that through the regulation of microglia, IFNy is implicated in DA neuronal death (Mount et al., 2007). Additionally, IFNy is reported to enhance or repress different subsets of LPS induced genes, although there is some controversy as to which genes are increased and which are decreased (Kang et al., 2019, Hoeksema et al., 2015). Most interestingly however, is the ability of IFNy to abrogate immune tolerance and restore repressed cytokine levels. This has been demonstrated in tolerance induced monocyte models in addition to cells derived from patients suffering with sepsis induced immunosuppression (Chen and Ivashkiv, 2010, Allantaz-Frager et al., 2013). Little is known about the effect of IFNy on Nurr1 and vice versa. However, it may have an opposing role as Nurr1 is considered neuroprotective.

Much of the research into microglia and macrophage activation in PD is carried out in rodent models or cell lines, despite PD being an exclusively human disease (Potashkin et al., 2010). Models which use toxins such as MPTP to damage the nigrostriatal pathway do not fully recapitulate human disease. This is evident in studies using neuroprotective agents found to be successful in animal models, but do not translate the same protection when used in human patients (Investigators, 2008, Investigators, 2015). Therefore, the development of human models is increasingly important.

Models of human microglia commonly use cell lines, post-mortem examinations, and iPSC differentiation (Rai et al., 2020). Which unfortunately can change cellular phenotypes over several passages, give limited data, and are extremely labour intensive respectively. However human macrophages have been routinely differentiated from PBMCs (Nielsen et al., 2020), and some recent studies have demonstrated a similar protocol can be used to induce a microglial-like phenotype through the addition of key cytokines which attempt to mimic the CNS microenvironment (Ohgidani et al., 2014, Banerjee et al., 2021).

We aimed to use the methods described by Banerjee et al., as a guide to produce functional microglia and macrophage models. These models could then be used to investigate the interplay of Nurr1 and IFNy during inflammation and immune tolerance. Additionally, we sought to use an inducible lentiviral system to evaluate the effect overexpressed Nurr-1a would have on LPS induced inflammation in a primary inflammatory model. These data will aid in the understanding of Nurr1's role during inflammation and reveal a potentially unidentified role for Nurr-1a.

4.4 Results: monocyte derived macrophages and microglial-like cells

4.4.1 Isolation and differentiation of peripheral blood derived monocytes into macrophages and microglial-like cells

Peripheral blood monocyte cells (PBMC) were isolated from fresh human blood using histopaqe-1077 density centrifugation to obtain the PBMC containing layer. This was followed by plastic adherence to isolate monocytes from other cell types. We then used a cocktail of IL-34 (100ng/ml) and GM-CSF (100ng/ml) as described previously (Banerjee et al., 2021, Ohgidani et al., 2014, Bruzelius et al., 2021) to generate induced microglial-like cells (iMGL). Similarly, we used GM-CSF (10ng/ml) in combination with 10% FBS to produce macrophages.

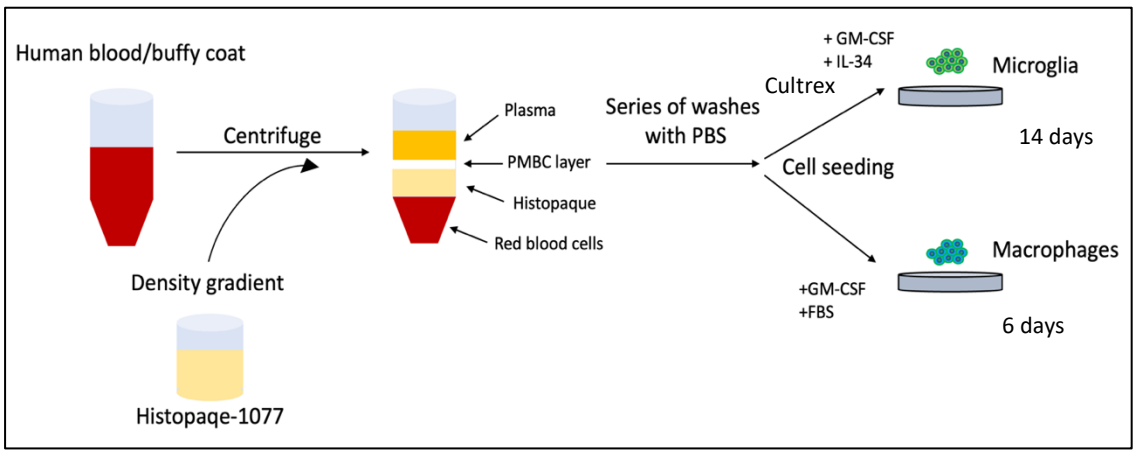


Figure 4.4-1 Schematic representation of human monocyte isolation and differentiation into macrophage and iMGL cells

Human blood separated into density dependent phases via centrifugation with Histopaqe-1077. The PMBC layer was then washed, and cells were differentiated into desired cell types with their respective cytokines.

After a 2h incubation at 37°C in cell seeding media (10% FBS) on either non-coated (macrophage) or Cultrex-coated (iMGL) plates, non-adherent cells were washed off. Few red blood cells, platelets and debris remained however this was removed in subsequent media changes. The adherent monocytes displayed a round morphology shown in Figure 4.4-2.

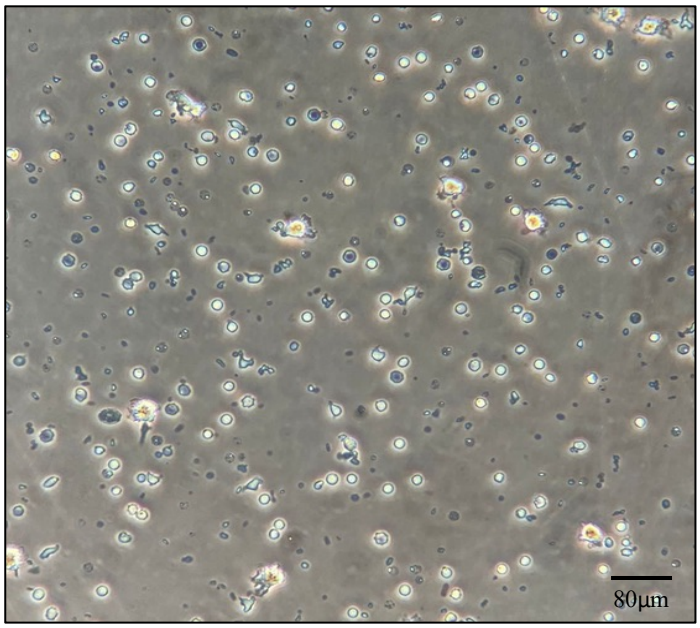


Figure 4.4-2 Isolated untreated monocytes

Monocytes were isolated from human blood using a density gradient followed by a 2h incubation in 10% FBS at 37°C to allow adherence. Non-adherent cells were washed off leaving adherent monocytes alongside some debris and few red blood cells.

After 4 days in Macrophage differentiation media cells displayed the typical 'fried egg' morphology, consistent with previous descriptions (Jin and Kruth, 2016), demonstrated in Figure 4.2-3. Macrophages were ready for downstream assays on day 6 and were cultured for up to 10 days.

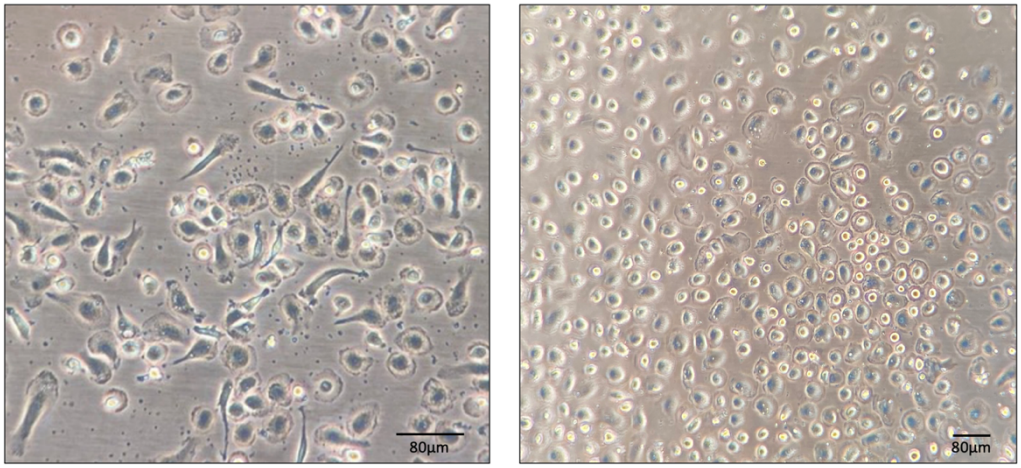


Figure 4.4-3 Morphology of monocyte derived macrophages

Isolated human monocytes were differentiated into macrophage cells using differentiation media (GM-CSF 10ng/ml and 10% FBS), refreshed every 3 days. Morphology is shown at day 4 & 6 in culture under a light microscope at x10 and x20 magnification.

Early iMGL cells could be observed on day 4, with morphology resembling typical microglia cells by day 12. After 14 days in culture, 3 distinct morphologies were observed; amoeboid, semi-ramified and ramified. Similar to those described by Bruzelius et al., in bone marrow derived microglia (Bruzelius et al., 2021) These are indicated by arrows (blue: Amoeboid, red: semi-ramified, and green: ramified) in Figure 4.4-4.

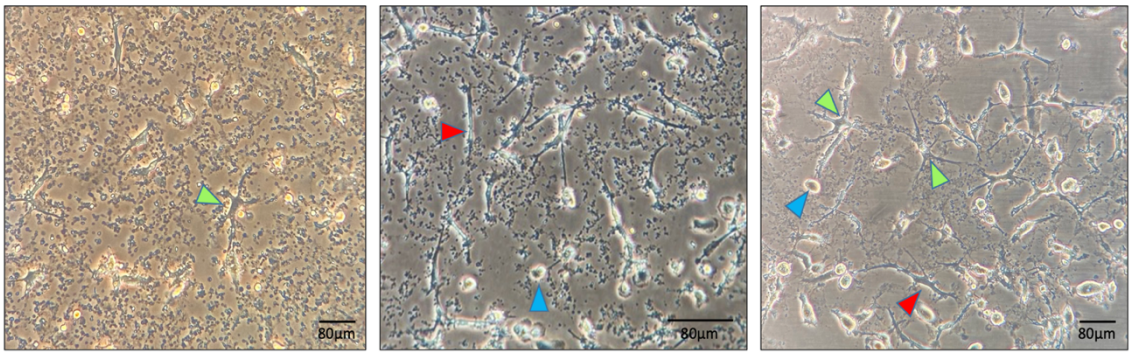


Figure 4.4-4 Morphology of monocyte derived iMGL cells

Monocytes were differentiated into iMGL cells over 14 days using differentiation media (IL-34 100ng/ml and GM-CSF 10ng/ml), refreshed every 3 days. Morphology shown under a light microscope at x10 and x20 magnification. Three distinct morphologies were observed and indicated by different arrow heads: blue: amoeboid, red: semi-ramified, green: ramified.

4.4.2 Markers expressed by macrophage and iMGL cells

Microglia and macrophages share many common markers, such as Iba1, TREM2 or PU.1, which has previously made it difficult to distinguish between cell types. However more recent research has suggested that transmembrane protein 119 (TMEM119) and purinergic receptor P2RY12 are unique markers for microglia (Bruzelius et al., 2021, Banerjee et al., 2021, Zhu et al., 2017, Satoh et al., 2016). We used both a common myeloid marker Iba1 as well as the mentioned microglial specific markers to verify the identity and specificity of the monocyte differentiated cells. These data clearly show that both iMGL cells and macrophages express Iba1 as expected, and P2RY12 is only expressed in iMGL cells. Surprisingly, we found TMEM119 expression in both cell types. This could suggest that the antibody is not specific or TMEM119 is also expressed in macrophages but at a lower level than microglia.

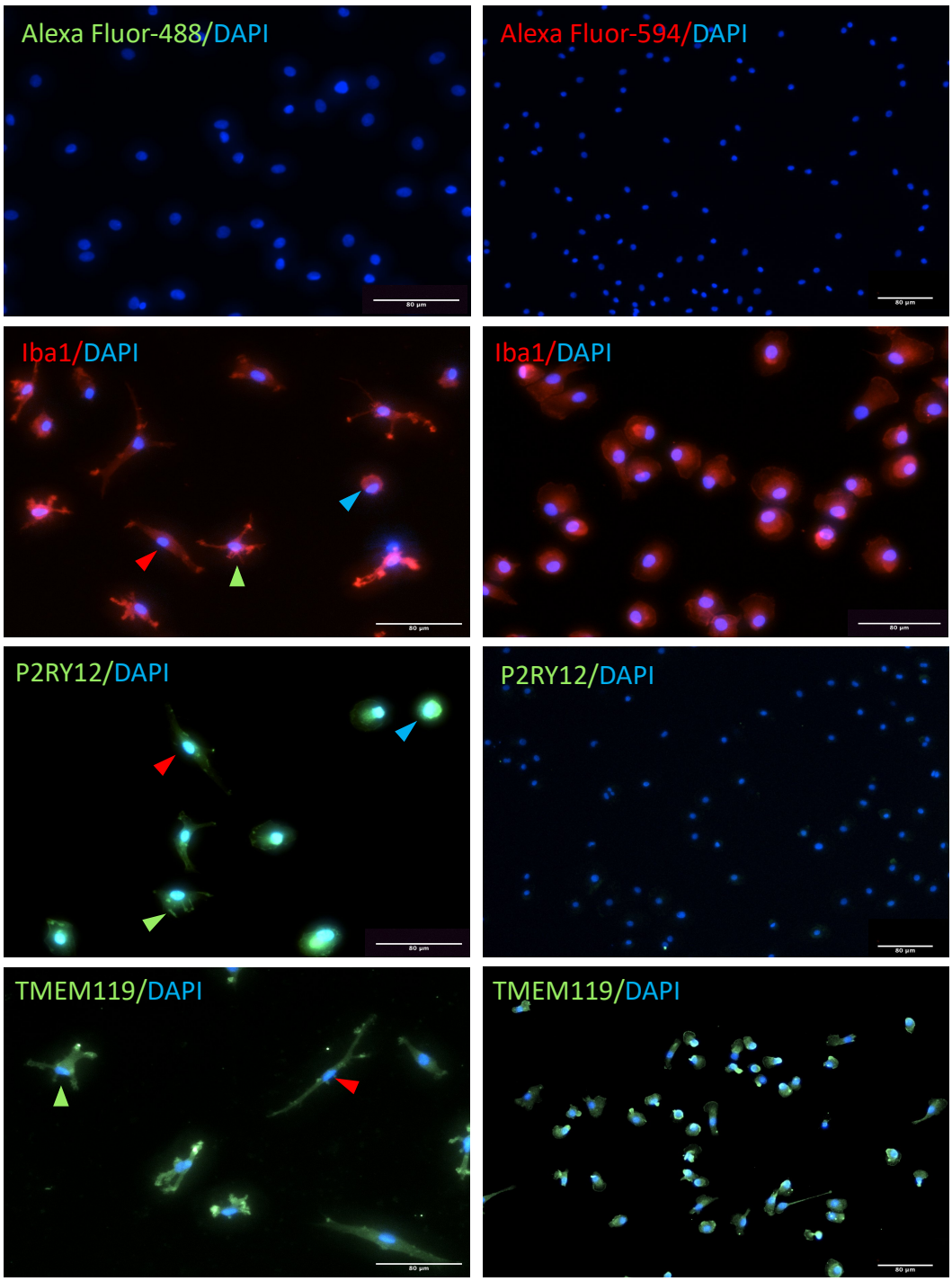


Figure 4.4-5 Macrophage and iMGL cells express typical cell surface markers

Expression of cell surface markers on monocyte differentiated macrophage (right) and iMGL cells (left) were assessed with immunocytochemistry. Anti-Iba1, anti-P2RY12 and anti-TMEM119 were used as primary antibodies incubated overnight. Secondary antibodies were tested for non-specific binding. The iMGL cultures displayed three distinct morphologies indicated by different arrow heads: blue: amoeboid, red: semi-ramified, green: ramified. Images were captured using a widefield microscope at 10x or 20x. Data is representative of images from 3 independent experiments.

The cells were further validated by confirming mRNA expression of key markers. CD45, a receptor-like tyrosine phosphatase expressed on all haematopoietic nucleated cells (Jurga et al., 2020), and Transmembrane 2 Family (TREM2) expressed widely throughout cells of the myeloid lineage but not in monocytes (Gratuze et al., 2018, Schmid et al., 2002, Liu et al., 2020), were used alongside P2RY12 and TMEM119. Monocytes were harvested directly after the adherence stage, whilst macrophage and iMGL cells were harvested on days 6 and 14 respectively before gene expression was validated with RT-qPCR.

These data clearly show that both macrophages and iMGL express common myeloid markers CD45 and TREM2. Macrophages do not express microglial specific markers TMEM119 and P2RY12, however we did observe similar levels of P2RY12 in iMGL and monocytes. Similarly, the Human Protein Atlas does report P2RY12 expression in some subsets of bone marrow derived cells, specifically monocytes. Using this combination of markers, we can conclude that the iMGL, macrophages and monocytes express different markers and thus can be distinguished by their gene expression patterns.

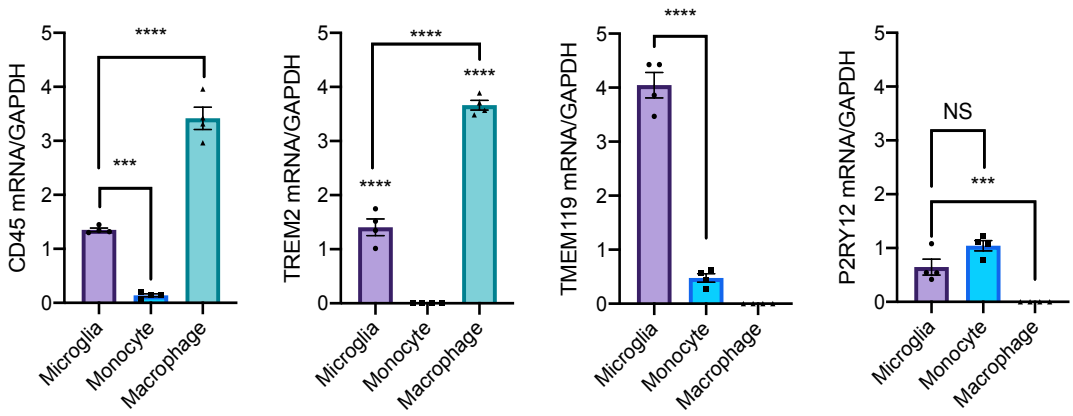


Figure 4.4-6 Macrophage and iMGL cells express key markers

PBMCs were plated in 6-well plates at a density of $1.8x10^6$ cells/well. Adherent monocytes were harvested after 2h of incubation at 37°C, macrophages after 6 days of differentiation (10ng/ml GM-CSF + 10% FBS) and iMGL cells after 14 days of differentiation (10ng/ml GM-CSF + 100ng/ml IL-34). The expression of key markers was determined by real-time qPCR normalised to GAPDH mRNA expression. Data are presented as standard error of the mean and are representative of results from 2 independent experiments (N=4). Statistically significant differences between indicated groups were *$p < 0.05$, **$p < 0.001$, ***$p < 0.0005$ **** $p < 0.0001$ (one-way ANOVA with Bonferroni post-test correction).

4.4.3 Phagocytosis assay in monocyte derived macrophages and iMGL cells

A vital function in both microglia and macrophages is the ability to phagocytose. In macrophages phagocytosis is vital for the removal of pathogens and the immune response (Hirayama et al., 2017). Whilst in microglia it is important for the removal of damaged or dying neurons, in addition to eliminating infiltrating non-neuronal cells such as activated neutrophils (Brown and Neher, 2014). Therefore, it was essential that the monocyte derived macrophage and iMGL cells not only expressed key markers but were also functionally active.

On days 6 and 14 for macrophage and iMGL cells respectively, we incubated cells with GFP tagged latex beads for 24h at 37°C to allow

phagocytosis to proceed. Cells were then fixed and stained with Iba1 which is reported to participate in membrane ruffling and phagocytosis, therefore it was used to ensure the beads were physically engulfed inside the cells (Ohsawa et al., 2000). iMGL cells, shown in Figure 4.4-8A, appeared to change cell morphology from ramified to amoeboid after the addition of beads; consistent with previous reports (Ohgidani et al., 2014). Macrophages, shown in Figure 4.4-8B, also phagocytosed the beads. Their morphology became more compact than the typical 'fried egg' structures previously seen in Figures 4.4-3 and 4.4-5.

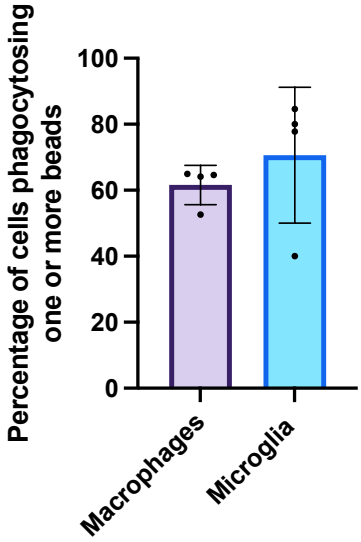


Figure 4.4-7 Macrophage and iMGL cells phagocytose GFP latex beads

On day 14 and 6 of culture, for iMGL cells and macrophages respectively, GFP-tagged beads opsonised in FBS were added to the culture medium to reach a final concentration of 0.05% per ml of media. Cells were incubated for 24h at 37°C before they were fixed in 4% PFA and stained with anti-Iba1 (1:200) and DAPI (1:500) nuclear staining. Images were analysed for percentage of cells phagocytosing 1 or more beads. Data is representative of images from 2 independent experiments (N=2) using 2 different donors and presented as standard deviation.

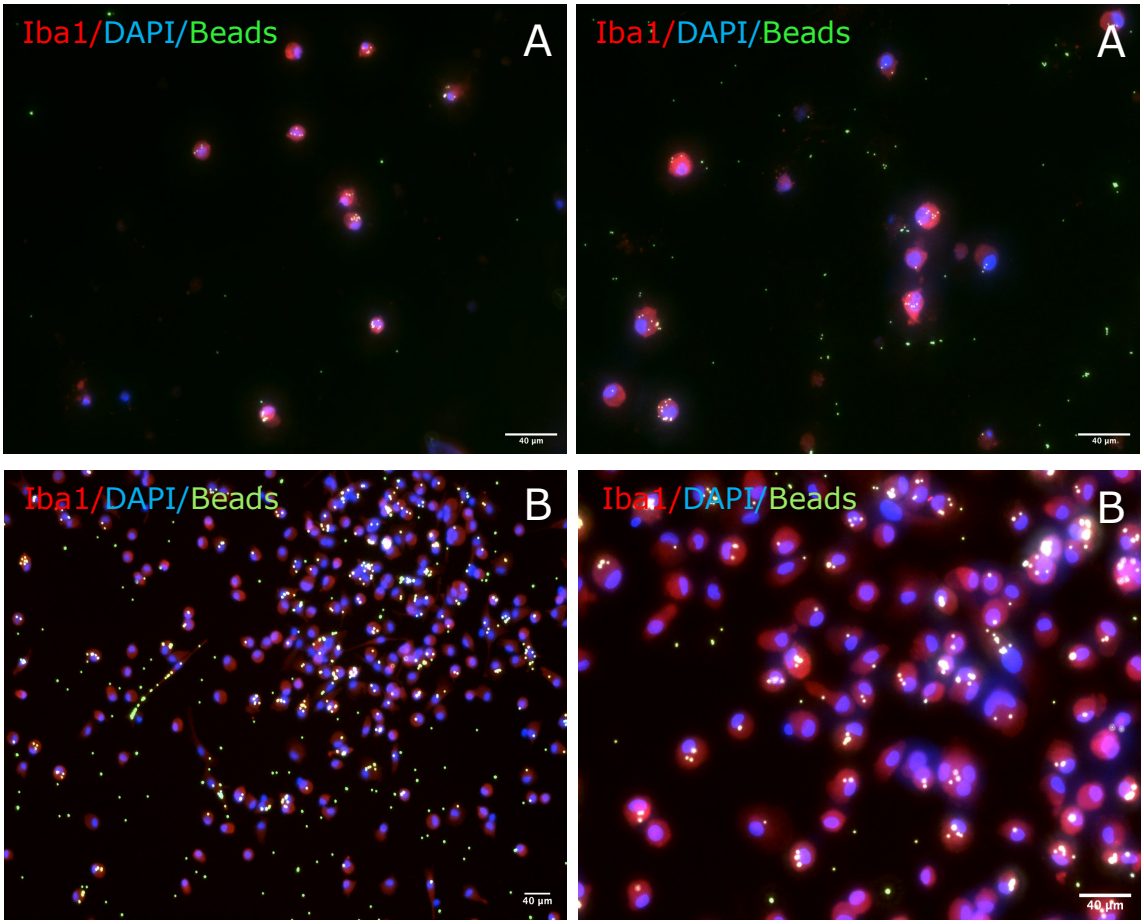


Figure 4.4-8 Macrophage and iMGL cells phagocytose GFP latex beads

On day 14 and 6 of culture, for iMGL cells (A) and macrophages (B) respectively, GFP-tagged beads opsonised in FBS were added to the culture medium to reach a final concentration of 0.05% per ml of media. Cells were incubated for 24h at 37°C before they were fixed in 4% PFA and stained with anti-Iba1 (1:200) and DAPI (1:500) nuclear staining. Images were captured using a widefield microscope at 10x or 20x. Data is representative of images from 2 independent experiments (N=2) using 2 different donors.

4.4.4 Macrophages and iMGL can function as inflammatory models

To evaluate if the differentiated macrophages and iMGL cells were able to function as inflammatory models we stimulated the cells and evaluated the gene expression of inflammatory cytokines. Unfortunately, at this time we were unable to analyse Nurr-1a due to primer and probe design. RT-qPCR probes must cross an exon boundary and the only differing exon boundary between Nurr1 and

Nurr-1a is the alternatively spliced exon 7. Exon 7 creates an early stop codon in Nurr-1a, hence why a probe could not be designed to cross exon 7 followed by a reverse primer as the sequence following the junction had been truncated. This issue was ramified in further experiments by using SYBR green primers which did not require the generation of a probe.

Nevertheless, we proceeded to investigate inflammatory gene expression. Our data clearly shows the LPS treatment of the iMGL was sufficient to elicit an inflammatory phenotype and induce the expression of key inflammatory markers IL-1β, IL-6, TNFα, IL-10. Additionally, the expression of Nurr1 was also increased which aligns with previous reports (Mahajan et al., 2015).

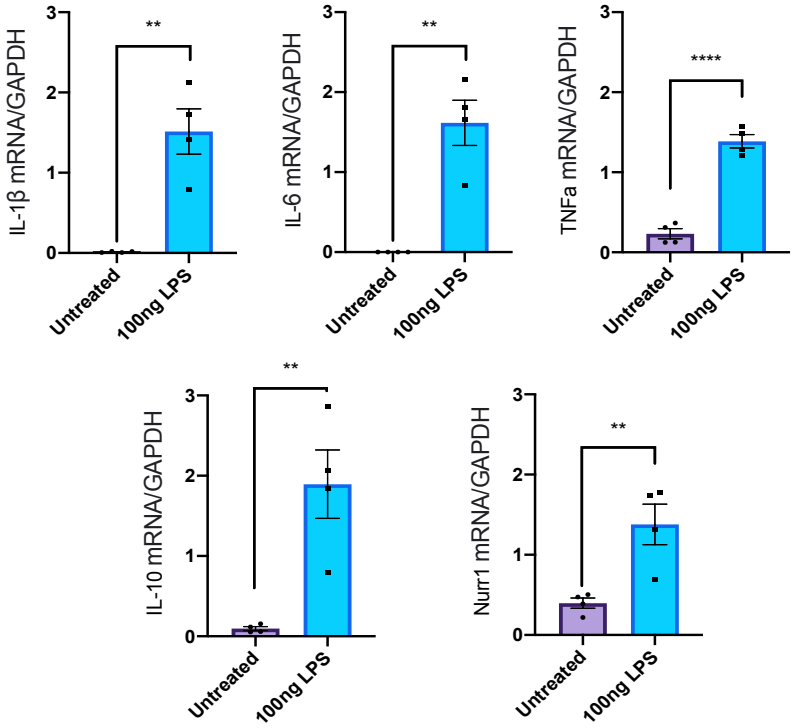


Figure 4.4-9 iMGL cells express inflammatory mediators

iMGL cells were treated with 100ng/ml LPS for 24h. The expression of IL-1β, IL-6, TNFα, IL-10 and Nurr1 was determined by real-time qPCR normalized to GAPDH expression. Data is representative of 2 independent experiments (N=4) and are presented as standard error of the mean. Statistically significant differences between indicated groups were $**p < 0.001$, **** $p < 0.0001$ (unpaired t-test).

Macrophages are dynamic cells that can differentiate across a spectrum of states in response to inflammatory signals including IFNy and LPS (Lawrence and Natoli, 2011). Interestingly, IFNy alone does not increase the expression of cytokine levels, yet in combination with LPS it is reported to potentiate the activation of some LPS induced genes whilst diminishing that of others (Kang et al., 2019, Hoeksema et al., 2015). LPS can induce cytokine expression on its own, however for proof of concept and to ensure the cells could tolerate the combination we used both IFNy and LPS to induce inflammation in the PMBC derived macrophages. Our data clearly shows the macrophages were induced into an inflammatory-like state by the addition of IFNy and LPS. Pro-inflammatory markers IL-1β, IL-6, and TNFα were all increased in addition to Nurr1. However, macrophages exhibited relatively high levels of IL-10 in untreated cells compared to treated cells. This may be due to the kinetics of pro and anti-inflammatory responses or indicate the cells had a more anti-inflammatory phenotype prior to stimulation (Hobbs et al., 2018).

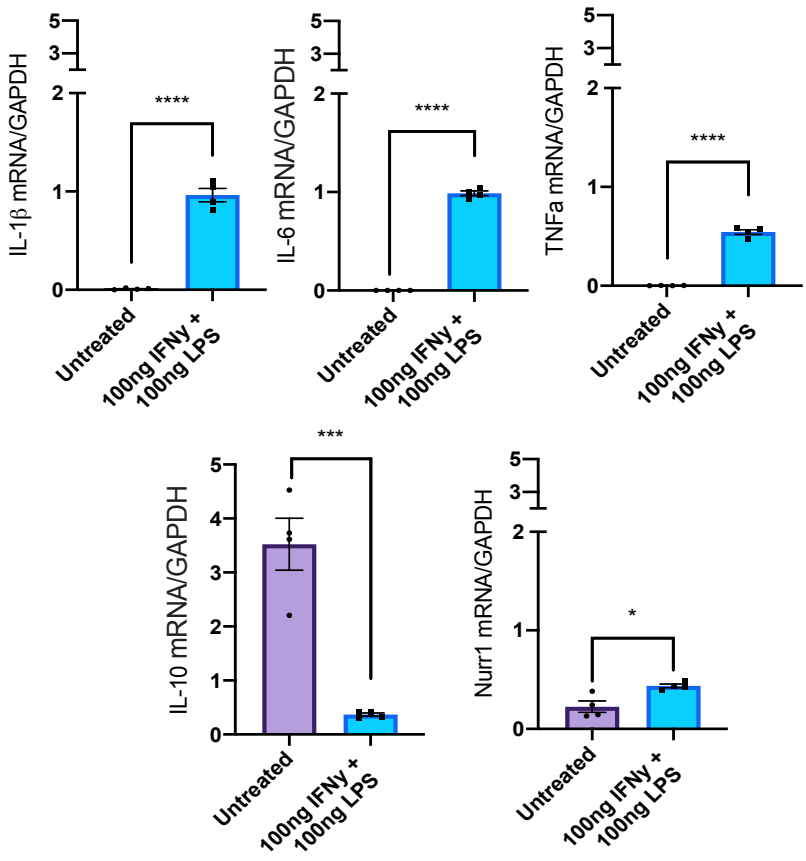


Figure 4.4-10 Macrophages express inflammatory mediators

Macrophages were treated with 100ng/ml LPS + 100ng/ml IFNy for 24h. The expression of IL-1β, IL-6, TNFα, IL-10 and Nurr1 was determined by real-time qPCR normalized to GAPDH expression. Data is representative of 3 independent experiments (N=4) and are presented as standard error of the mean. Statistically significant differences between indicated groups were *$p < 0.05$, ***$p < 0.0005$ **** $p < 0.0001$ (unpaired t-test).

Following this set of experiments, we were unable to consistently generate iMGL cells using our culture methods. Therefore, the following experiments are conducted in macrophages only. It was later discovered that the cause of the inconsistent iMGL cell cultures was likely due to lot variability of IL-34 cytokine activity. After changing supplier this was no longer an issue. Future work aims to repeat the experiments carried out in macrophages in the iMGL cells.

4.4.5 The role of Nurr1 in immune tolerance

The role, if any, of Nurr1 in immune tolerance has not yet been investigated. Immune tolerance presents as a protective mechanism to decrease the levels of pro-inflammatory cytokines produced upon repeated exposure of its TLRs to a stimulus (Chen and Ivashkiv, 2010). Similarly, Nurr1 is suggested to act in a protective mechanism, applying a brake to excessive inflammation through the repression of inflammatory gene promoters (Saijo et al., 2009). Therefore, Nurr1 may also have a role in immune tolerance, furthering the protective effects.

After identifying monocyte-derived macrophages could be used as an inflammatory model, the time point at which gene expression was to be measured required optimisation. Macrophages were stimulated with LPS alone and evaluated the gene expression of inflammatory cytokines in addition to Nurr1 at 1h, 3h and 6h post stimulation. All three pro-inflammatory cytokines show a clear peak at 3h. Overall IL-10 appeared to increase after the peak of pro-inflammatory cytokines, consistent with previous (Hobbs et al., 2018). Conversely, Nurr1 expression peaked at 1h before decreasing, reinforcing the concept that Nurr1 is an immediate early gene that is rapidly induced. Therefore, we determined that gene expression assays would be carried out at 3h for inflammatory cytokines, and a 1h for Nurr1.

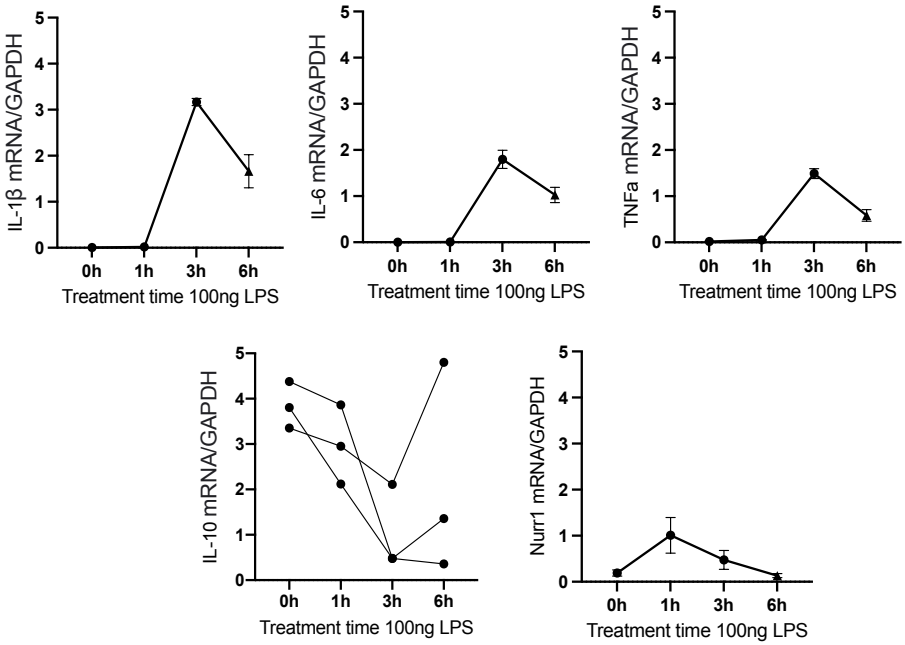


Figure 4.4-11 Macrophage temporal expression of inflammatory mediators

Macrophages were treated with 100ng/ml LPS for 1h, 3h or 6h. The expression of IL-1β, IL-6, TNFα, IL-10 and Nurr1 was determined by real-time qPCR normalized to GAPDH expression. Data are representative of 3 independent experiments and presented as standard deviation from the mean. IL-10 data shows 3 independent experiments plotted.

As mentioned, IFNy is reported to enhance or repress different subsets of LPS induced genes, however current studies are contradictory in their results (Kang et al., 2019, Hoeksema et al., 2015). We have previously shown, in Figure 4.4-11, that LPS alone could induce inflammatory cytokine expression in addition to Nurr1. Similarly in comparison to the untreated cells the combination of IFNy and LPS also increased gene expression in Figure 4.4-10. Therefore, we sought to investigate the difference between LPS treatment alone and in combination with IFNy pre-treatment (Chen and Ivashkiv, 2010), and any effect this may have on Nurr1 expression.

Our data clearly shows that IL-1β, IL-6 and IL-10 expression is decreased when LPS is used in combination with IFNγ compared to LPS alone. Interestingly, the expression of TNFα and Nurr1 are both increased after the combination treatment compared to LPS only. Our data aligns with that reported by Hoeksema et al., who suggest that the difference in expression is due to IFNγ selectively priming gene expression to regulate inflammation.

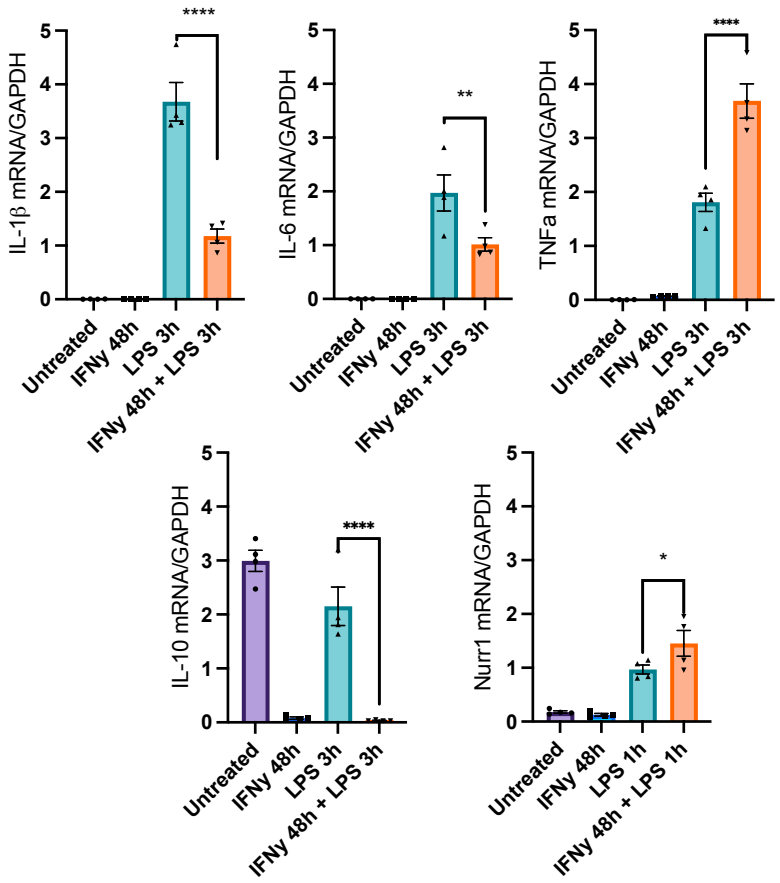


Figure 4.4-12 IFNγ enhances and supresses different LPS induced genes

Macrophages were treated with 100ng/ml LPS and/or 100ng/ml IFNγ as indicated. The expression of IL-1β, IL-6, TNFα, IL-10 and Nurr1 was determined by real-time qPCR normalized to GAPDH expression. Data are representative of results from 3 independent experiments (N=4) and presented as standard error of the mean. Statistically significant differences between indicated groups were *$p < 0.05$, **$p < 0.001$, ***$p < 0.0005$ **** $p < 0.0001$ (one-way ANOVA with Bonferroni post-test correction).

Immune tolerance is the reduced response to repeated exposure of a cells TLR to a PAMP or DAMP stimulus. We induced tolerance through two sequential LPS treatments as described previously (Chen and Ivashkiv, 2010). As expected, our data clearly shows that tolerisation decreases the expression of inflammatory cytokines IL-1β, IL-6, TNFα and IL-10. Most interestingly however, we found that tolerisation causes a super induction of Nurr1 expression.

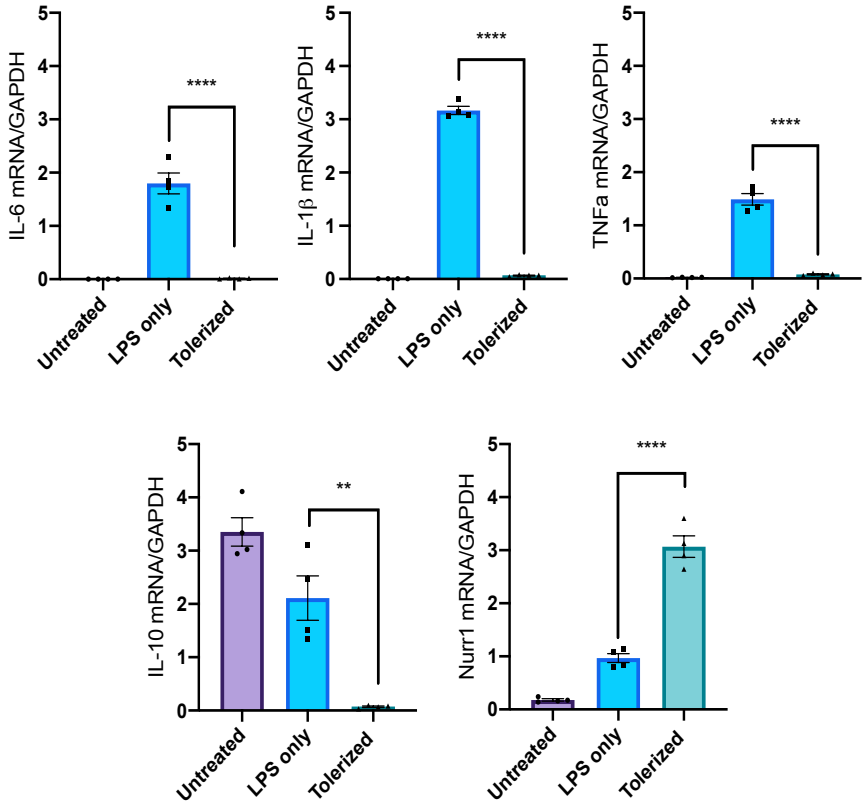


Figure 4.4-13 Tolerisation superinduces Nurr1 whilst repressing inflammatory cytokines

Macrophages were treated with either 100ng/ml LPS for 3h (LPS only) or for 24h with 100ng/ml LPS followed by a second 3h 100ng/ml LPS stimulation (Tolerized). The expression of IL-1β, IL-6, TNFα, IL-10 and Nurr1 was determined by real-time qPCR normalized to GAPDH expression. Data are representative of results from 3 independent experiments (N=4) and presented as standard error of the mean. Statistically significant differences between indicated groups were *$p < 0.05$, **$p < 0.001$, ***$p < 0.0005$ **** $p < 0.0001$ (one-way ANOVA with Bonferroni post-test correction).

IFNy has been associated with the death of DA neurons in PD and is also found in the blood of PD patients (Diaz et al., 2022). Previous reports demonstrate that pre-treating inflammatory cells with IFNy before induction of immune tolerance allows inflammatory cytokine production to proceeded (Chen and Ivashkiv, 2010). This could suggest increased IFNy expression may contribute to neuroinflammation in PD. We have shown during immune tolerance Nurr1 is superinduced which may further the protective effects. In addition, we revealed that IFNy in combination with LPS can increase Nurr1 gene expression. Therefore, we sought to identify the effect IFNy has on Nurr1 gene expression during tolerisation.

In support of the literature, Figure 4.4-14 clearly shows that IFNy pre-treatment restored some of the proinflammatory cytokine expression (Chen and Ivashkiv, 2010). We found no significant change in IL-10 expression. Unexpectedly, we found IFNy pre-treatment significantly reduced the expression of Nurr1. Although this reduction removed the super inductive effect on Nurr1, the expression was still higher than treatment with LPS alone. Overall these data suggest IFNy pre-treatment of tolerized cells promotes a proinflammatory phenotype.

Future work will look to the effect on Nurr-1a expression, in addition to investigating tolerance in iMGL cells using inflammatory stimuli or α-synuclein to better model PD (Dzamko et al., 2017).

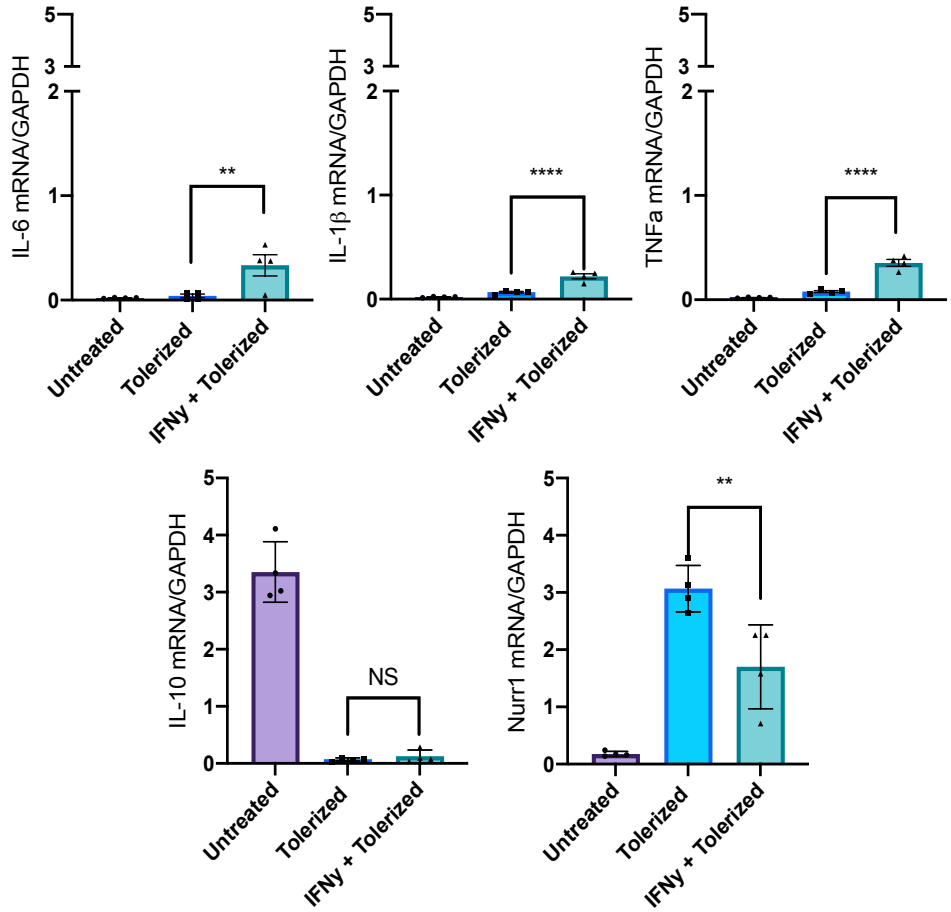


Figure 4.4-14 IFNy treatment of tolerized cells promotes a pro-inflammatory phenotype

Macrophages were either tolerized with 100ng/ml LPS followed by a second 3h 100ng/ml LPS stimulation (Tolerized) or treated with 100ng/ml IFNy for 48h before Tolerisation as described (IFNy + Tolerized). The expression of IL-1β, IL-6, TNFα, IL-10 and Nurr1 was determined by real-time qPCR normalized to GAPDH expression. Data are representative of results from 3 independent experiments (N=4) and presented as standard error of the mean. Statistically significant differences between indicated groups were *$p < 0.05$, **$p < 0.001$, ***$p < 0.0005$ **** $p < 0.0001$ (one-way ANOVA with Bonferroni post-test correction).

4.4.6 Cloning human Nurr-1a from total brain RNA

Previous experiments in HeLa and SH-SY5Y cells used Nurr1 and Nurr-1a expressing plasmids cloned from rat. Considering we had developed human derived macrophages to model inflammation more representative to human physiology, we decided to generate human Nurr1 and Nurr-1a plasmids. A human Nurr1 inducible lentiviral plasmid was purchased from Genocopia, however a plasmid for Nurr-1a was absent. Nurr-1a's human sequence has been described (Ichinose et al., 1999) however currently there is no GenBank entry. The sequences of both variants are identical up 444 amino acids, at this point alternative splicing at exon 7 generates a frameshift mutation and consequently an early stop codon which produces the truncated Nurr-1a isoform. This is depicted below in Figure 4.4-15.

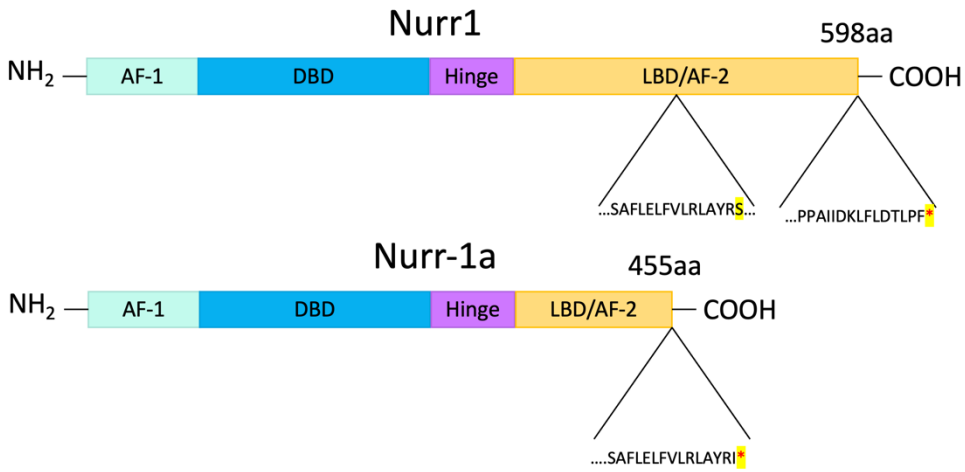


Figure 4.4-15 Schematic diagram of a Nurr1 frameshift mutation which generates Nurr-1a

Diagram depicting classic nuclear receptor domain structure. Nurr1 and Nurr-1a have the same sequences until alternative splicing of Nurr1 causes a frameshift mutation and an early stop codon which generates the truncated Nurr-1a. Sequence represents amino acid (aa) arrangement.

Additionally, it was important to show the presence of both Nurr1 and 1a variants in human brain tissue, in addition to cloning the Nurr-1a variant. Reverse transcription (RT) was used to show the isoforms present in human total brain RNA (Thermo Fisher Scientific

#AM7962). Using random primers only generated the full length Nurr1 variant, most likely because it is in high abundance compared to Nurr-1a. To observe both isoforms, we developed gene specific (GS) reverse primers which spanned the frameshift in Nurr-1a and the C terminus of Nurr1 which is absent from Nurr-1a. Primers and sequence alignment can be found in the appendix. These primers were used to carry out RT followed by PCR amplification using a common forward primer and the GS reverse primers. The open reading frame for Nurr1 is reported to be 1794 bases (Jankovic et al., 2005). Nurr-1a's sequence is 455 residues long, therefore its ORF should be 1365 bases. Our data clearly shows that both Nurr1 and Nurr-1a are present in human total brain RNA. There are a number of additional bands present on the gel which may represent additional variants or primer dimers.

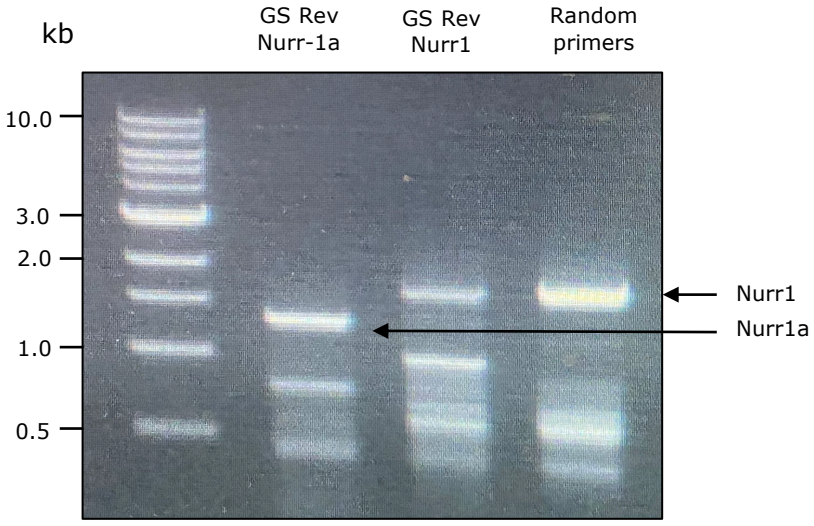


Figure 4.4-16 Nurr1 and Nurr-1a are present in human total brain RNA

Total human brain RNA was reverse transcribed with either Nurr1/1a gene specific reverse primers or random primers before subjection to PCR amplification (35 cycles) using gene specific reverse primers and a common forward primer. This was followed by separation on a 1% w/v agarose gel via electrophoresis and visualised with UV light. 0.5-10kb ladder was used as a size reference.

PCR amplification yields blunt ended fragments. Considering the Nurr-1a primer spanned the C-terminus sequence with no additional bases on the end, restriction enzymes which generate sticky ends for ligation could not be used as they would cut through the coding sequence. Therefore, we used a restriction enzyme which generated blunt ends to digest the vector resulting in phosphorylated ends. For ligation to occur, ends must be phosphorylated. To prevent the vector from re-ligating without the insert, we dephosphorylated the vector and phosphorylated the insert PCR fragment. After ligation, competent bacteria were transformed, plasmids purified and sent for sequencing to confirm correct orientation and sequence. This process is depicted in Figure 4.4-17 below.

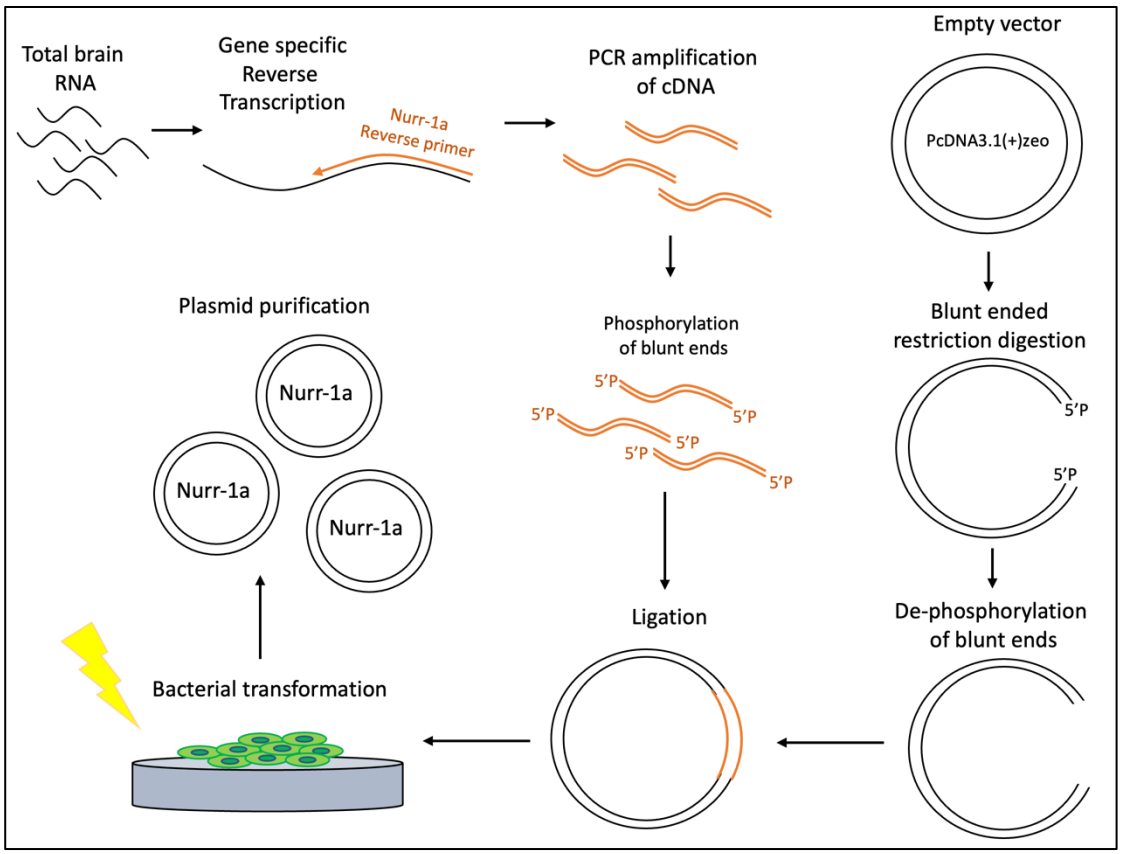


Figure 4.4-17 Cloning human Nurr-1a from total brain RNA

Schematic diagram showing the workflow of cloning human Nurr-1a from total brain RNA into a PcDNA3.1(+)zeo empty plasmid.

4.4.7 Lentiviral cloning and expression of Nurr1 and Nurr-1a

Primary human macrophages are notoriously difficult to transfect (Keller et al., 2018, Dokka et al., 2000, Dong et al., 2020). There have been reports demonstrating the success of infecting macrophages with lentivirus (Leyva et al., 2011). We cloned the human Nurr1/1a plasmids into tetracycline dependent lentiviral vectors (pINDUCER20) using the "One-Tube" Gateway Clonase II system described in methods section 2.7. After cloning and bacterial transformation colony PCR was carried out using pINDUCER20 primers LNCX and PIND20 to ensure the insert was present in the colony. Plasmids were purified and then sent for sequencing.

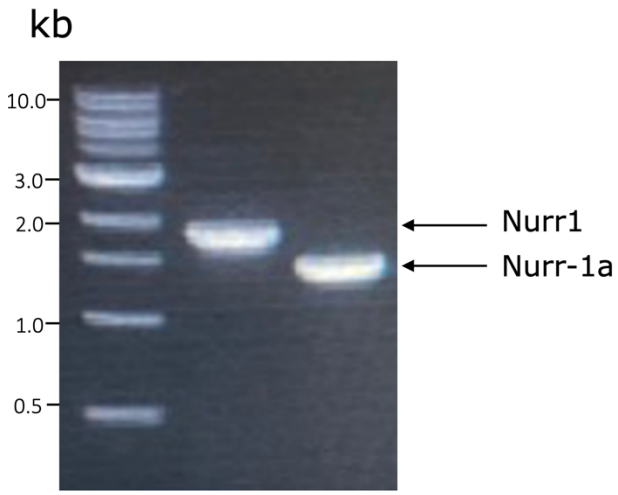


Figure 4.4-18 Human Nurr1 and Nurr-1a inserts were present in pINDUCER20 viral vector after cloning

Colony PCR was carried out after cloning with pINDUCER20 primers LNCX and PIND20, followed by separation on a 1% w/v agarose gel via electrophoresis. Nurr1 and Nurr-1a inserts were visualised with UV light. 0.5-10kb ladder was used as a size reference.

HEK293FT cells were used to produce the human Nurr1 and Nurr-1a viruses alongside a GFP expressing virus as described in methods section 2.7. Non concentrated viruses were tested in HeLa cells as they are an easy to infect cell line. These data clearly show HeLa

cells were infected by GFP expressing lentivirus. In addition, doxycycline was able to successfully induce the lentiviral expression of Nurr1 and Nurr-1a protein in HeLa cells at varying concentrations. However, it appeared the most protein was produced when 200µl of unconcentrated virus was used.

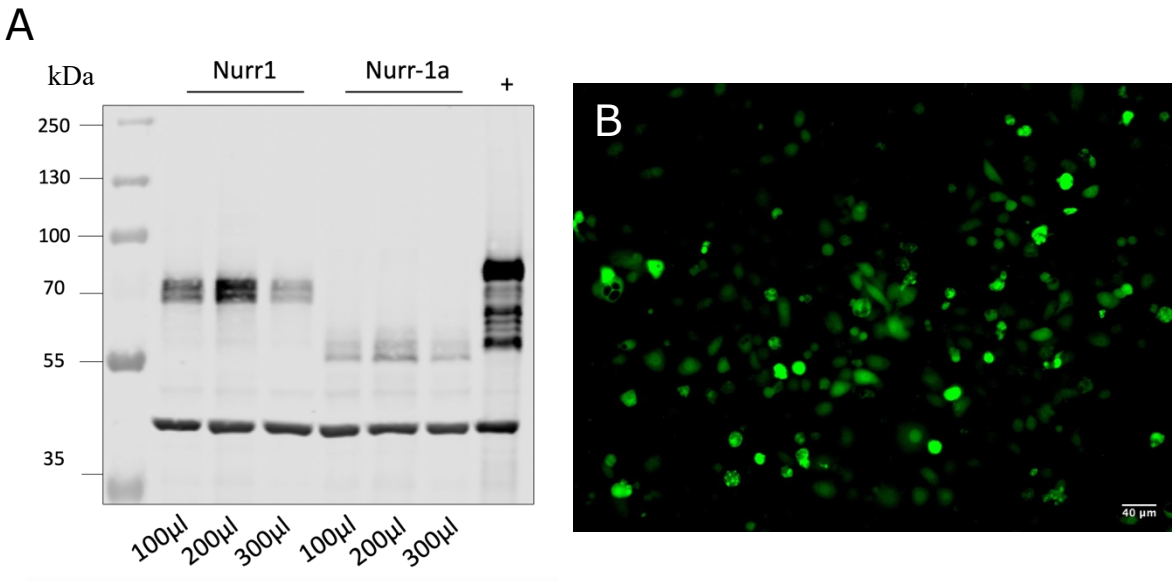


Figure 4.4-19 Human Nurr1 and Nurr-1a lentiviruses transduce HeLa cells

HeLa cells were transduced with 10µg/ml polybrene and either pINDUCER20-GFP (200µl), pINDUCER20-Nurr1 (100µl-300µl) or pINDUCER20-Nurr-1a (100µl-300µl), before they were induced with doxycycline 1µg/ml for 48h. **(A)** cells were lysed, and protein extracted before separation on a 10% SDS polyacrylamide gel. Western blotting was performed using anti-Nurr1 (1:1000) and anti-βactin (1:1000). A transfected HeLa Rat Nurr1 sample was used as a positive control (+). **(B)** GFP was observed using a widefield fluorescent microscope.

We next sought to transduce PBMC macrophages with pINDUCER20-GFP, to ensure the cells could be infected and induced with doxycycline. Polybrene can enhance the efficiency of lentiviral infection (Davis et al., 2002), however it can also be toxic to some cells and is usually recommended between 2-10µg/ml. Therefore, a low concentration of 4µg/ml was used for initial viral transduction, followed by 48h of induction with 1µg/ml doxycycline. Our data

shows these cells are capable of transduction, however the efficiency is very low. The addition of polybrene did not increase efficiency and appeared to reduce the cell number.

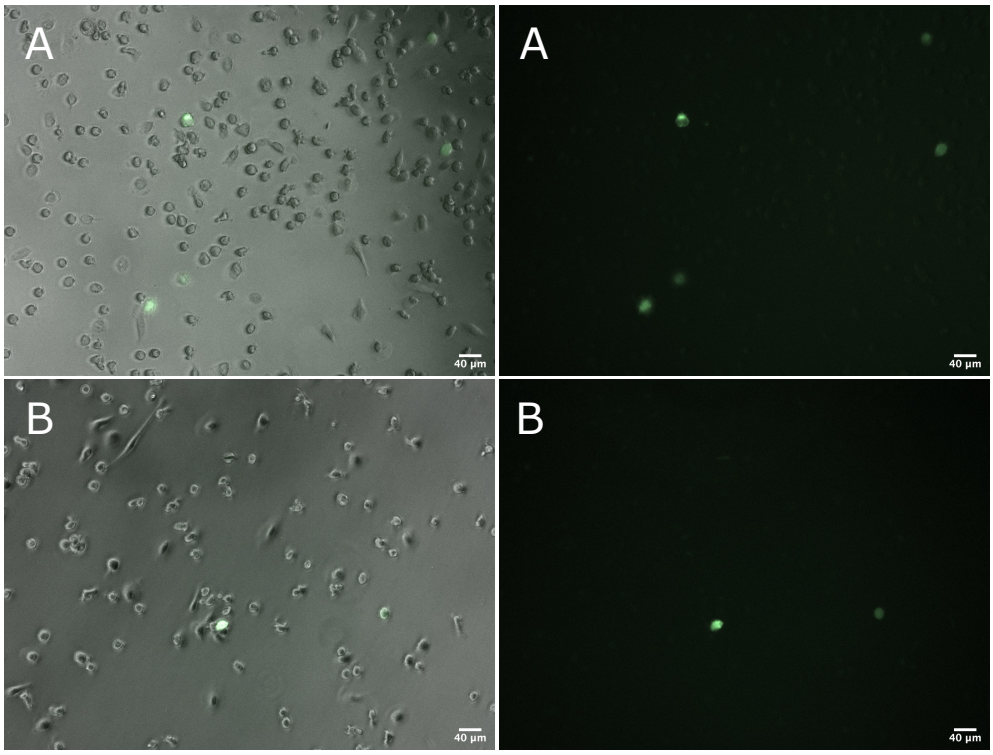


Figure 4.4-20 Human PBMC differentiated macrophages are minimally transduced by GFP

Macrophages were transduced with pINDUCER20-GFP (400µl) with **(B)** and without **(A)** polybrene 4µg/ml. GFP was observed using a widefield fluorescent microscope.

The protein expression of pINDUCER20-Nurr1 and pINDUCER-Nurr-1a was also investigated. A very faint band representing Nurr1 was detected, however no band was detected for Nurr-1a. Weak protein expression was most likely a reflection of the low transduction efficiency. Further optimisation of the viral infection should look to increasing the amount of virus, polybrene concentration and also the time at which the cells are transduced (Leyva et al., 2011).

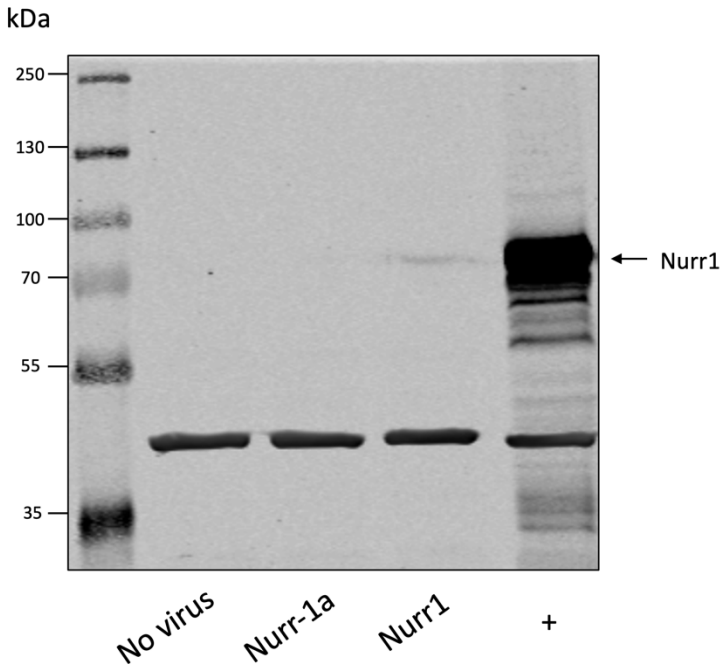


Figure 4.4-21 Human PBMC differentiated macrophages are minimally transduced by Nurr1 and Nurr-1a viruses

Macrophages were transduced with pINDUCER20-Nurr1 or pINDUCER20-Nurr-1a (400µl) for 24h, before induction with 1µg/ml doxycycline for 48h. Cells were harvested, lysed and subjected to western blotting with anti-Nurr1 (1:1000) and anti-βactin (1:1000). Nurr1 transfected HeLa cells used as a positive control (+).

As an inducible lentiviral system was used to express Nurr1 and Nurr-1a. It was important to ensure that doxycycline addition did not change inflammatory gene expression in macrophages and therefore any results were due to the variables we were investigating. Our data clearly showed that doxycycline alone did not significantly change the expression of any of the pro-inflammatory cytokines or Nurr1, it did however increase IL-10 expression significantly. This could be due to the nature of doxycycline as an antibiotic with anti-inflammatory properties (Krakauer and Buckley, 2003).

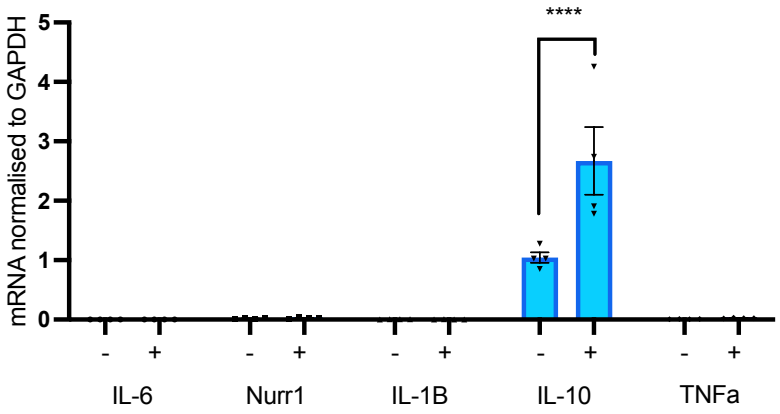


Figure 4.4-22 Doxycycline significantly increases IL-10 expression in macrophages

Macrophages were treated with (+) or without (-) 1µg/ml doxycycline for 48h. Gene expression was determined by RT-qPCR normalised to GAPDH. Data are presented as standard deviation and is representative of results from three independent experiments. Statistically significant differences between indicated groups were $p < 0.0001$ (one-way ANOVA with Bonferroni post-test correction).

4.4.8 Investigating the effect Nurr1/1a has on inflammation

The current macrophage transduction method yielded low infection efficiency as demonstrated by immunocytochemistry and western blotting. However RT-qPCR is more sensitive than these techniques (Wong and Medrano, 2005), thus we proceeded to evaluate inflammatory gene expression after transduction and LPS stimulation.

Macrophages were transduced as before either Nurr1 or Nurr-1a virus. Cells were harvested before RNA isolation and reverse transcription was carried out. Previously we were unable to measure Nurr-1a gene expression by RT-qPCR. For the following experiments we measured the expression of each gene by RT-qPCR, except for Nurr-1a for which we use SYBR green. Our data clearly shows that the addition of Nurr1/1a lentivirus significantly increases the mRNA expression of both variants compared to the non-transduced cells.

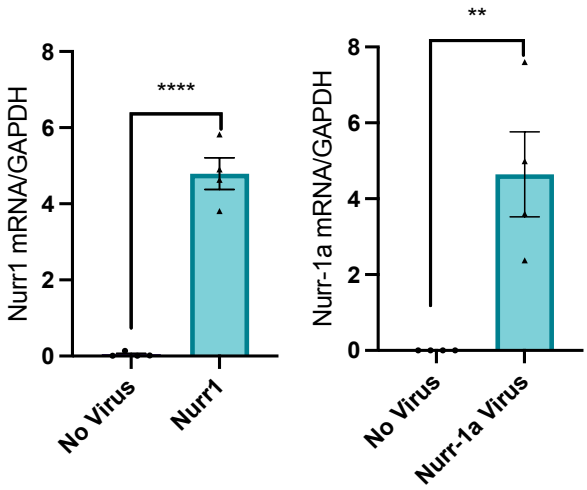


Figure 4.4-23 Human PBMC differentiated macrophages show Nurr1 and Nurr-1a gene expression after lentiviral transduction

Macrophages were transduced with pINDUCER20-Nurr1 or pINDUCER20-Nurr-1a (400µl) for 24h, before induction with 1µg/ml doxycycline for 48h. The expression of Nurr1 mRNA was determined by RT-qPCR, whilst Nurr-1a expression was determined by SYBR green, both normalised to GAPDH. Data are presented as standard error of the mean and is representative of results from three independent experiments (N=4). Statistically significant differences between indicated groups were $**p < 0.001$ (unpaired t-test).

As a significant increase in Nurr1/1a gene expression was observed, we proceeded to measure inflammatory gene expression after inflammation was induced and investigated the effect Nurr1/1a would have on expression levels.

Unfortunately, our data was inconclusive. After three independent experiments we found no significant difference in inflammatory gene expression between cells stimulated with LPS and those transduced with Nurr1 before LPS stimulation, bar one IL-10 experiment. One reason for this may be the dose of LPS is too high to see subtle effects of Nurr1 on gene expression. Another could be due to temporal differences. Nurr1 acts as a break on inflammation so although 3h was initially considered the optimal timepoint to evaluate peak inflammatory expression as shown in Figure 4.4-11; looking at a wider timescale may reveal effects of Nurr1 not otherwise seen at 3h alone. Furthermore, an additional explanation

is due to inadequate levels of Nurr1 protein expression. Viral transduction itself likely induces inflammatory gene expression which masks any effect the small amount of Nurr1 has on LPS induced inflammation. We did find a pattern of increased inflammatory gene expression in cells transduced with Nurr-1a before LPS stimulation compared to LPS alone. Although the level of significance did vary from no significance to *** $p < 0.0005$. This data suggests that the proportion of cells transduced with the Nurr1-a virus was not sufficient to elicit any effect on LPS induced inflammation, and the increase in inflammatory markers seen was due to viral transduction itself.

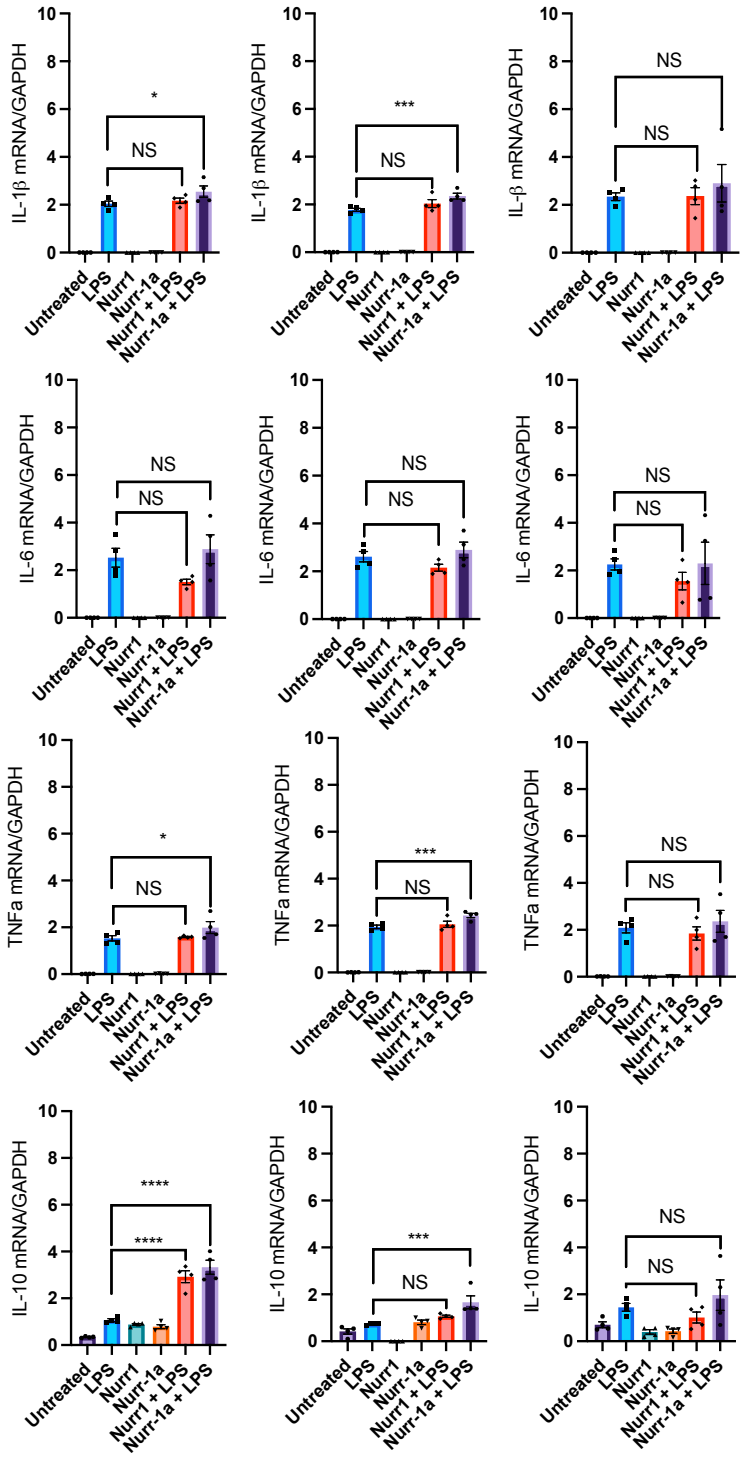


Figure 4.4-24 Viral transduction has no clear effect on inflammatory gene expression

Macrophages were transduced with either pINDUCER20-Nurr1 or pINDUCER20-Nurr-1a for 48h with 1µg/ml doxycycline before stimulation with 100ng/µl LPS for 3h. Gene expression was determined by real-time qPCR normalized to GAPDH expression. Data shows three independent experiments (N=4) with standard error of the mean. Statistically significant differences between indicated groups were *$p < 0.05$, **$p < 0.001$, ***$p < 0.0005$ **** $p < 0.0001$ (one-way ANOVA with Bonferroni post-test correction).

Although the initial experiments using the Nurr1 and Nurr-1a virus did not yield the expected results, it outlined key areas of the experiment which required optimisation before continuing. Nevertheless, for future research to evaluate the extent to which SUMO affects Nurr1 and Nurr-1a mediated inflammatory regulation, SUMO mutants would be required. Therefore, we used Site Directed Mutagenesis to mutate the K91 SUMOylation site in the Nurr1 and Nurr-1a pINDUCER20 plasmids. Lysine 91 was mutated to arginine to create the K91 mutation. The products were transformed in bacteria, purified and sent for sequencing.

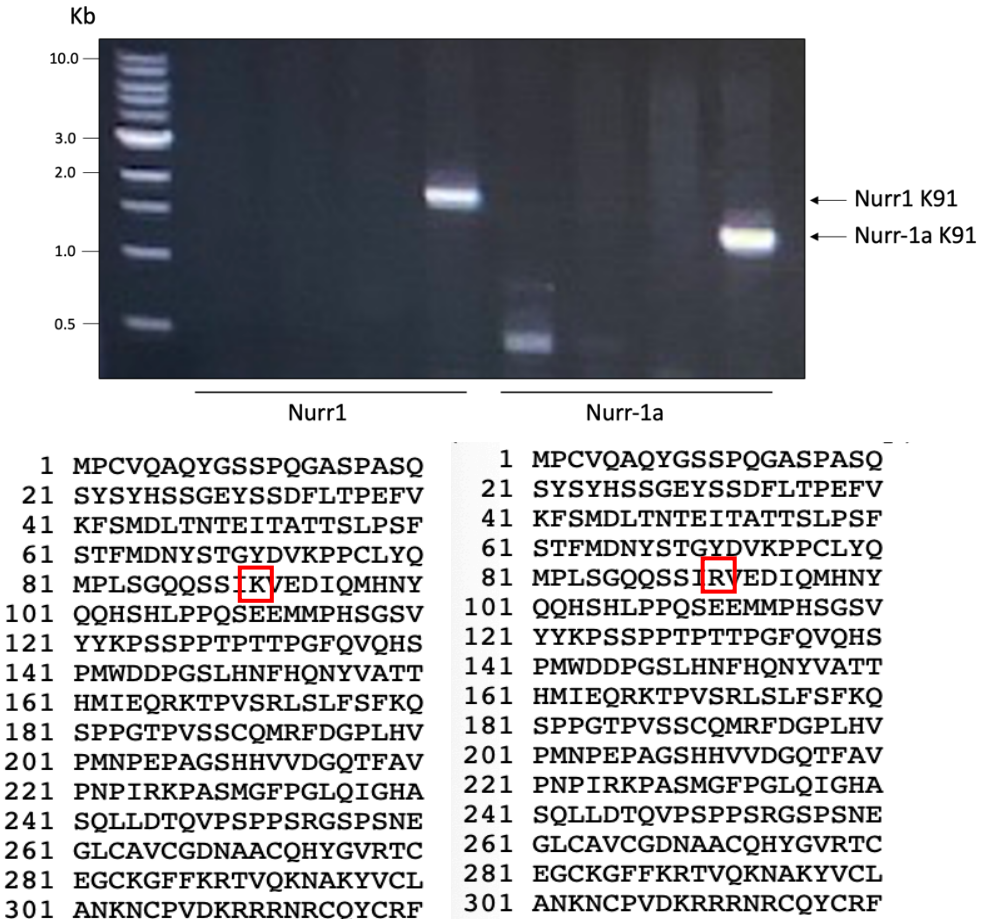


Figure 4.4-25 Site Directed Mutagenesis of K91 in lentiviral vectors

Colony PCR was carried out after mutagenesis of K91>R91 in both pINDUCER20-Nurr1 and pINDUCER20-Nurr-1a followed by separation on a 1% w/v agarose gel via electrophoresis. Plasmids with inserts were visualised with UV light. 0.5-10kb ladder was used as a size reference. Sequencing data from SourceBioscience confirmed the mutation.

Future work will look to optimising viral transduction of macrophages to yield a better protein expression, in addition to a wider timeframe and titrated LPS doses. Lastly the experiment will be expanded to incorporate the SUMO Nurr1/1a mutants so that the role of SUMO in Nurr1/1a inflammatory repression can be properly investigated.

4.5 Discussion: monocyte derived macrophages and microglial-like cells

Nurr1 is reported to be an important regulator of inflammation (Saijo et al., 2009, Oh et al., 2020). However, reports investigating Nurr1's mechanisms in human inflammatory models are lacking. In addition, research into Nurr-1a's potential role during inflammation is absent. In the second part of this chapter, we developed two primary human models of inflammation which express the expected inflammatory cytokine mRNA's upon stimulation as well as rapidly inducing the gene expression of Nurr1. The human macrophage model was used further to identify a potentially novel role for Nurr1 in the regulation of immune tolerance. In addition, Nurr1 was identified as a LPS inducible gene selectively primed by IFNy with differing fates dependent on tolerisation state. Furthermore, an inducible lentiviral system was developed to overexpress human Nurr1 and Nurr-1a. However, transduction of these viruses into the primary human models requires further optimisation.

The use of PBMCs to generate macrophages is not uncommon (Nielsen et al., 2020) . Reports suggest macrophages can be induced into 'M1 or M2' phenotypes via the expression of GM-CSF/IFNy or M-CSF/IL-4 respectively (Mia et al., 2014). However more recent data suggests that macrophage phenotype falls within a spectrum, where a flux occurs between activated or resting states in response to cytokines and their microenvironment (Nahrendorf and Swirski, 2016). This is similarly reported for microglia (Guo et al., 2022). Microglia originate from erythro-myeloid progenitors in the yolk sac (Alliot et al., 1999). However, there are reports which describe a method where microglial-like cells can be differentiated from blood or bone marrow derived monocytes (Bruzelius et al., 2021, Ohgidani et al., 2014, Banerjee et al., 2021).

Using a cocktail of GM-CSF and IL-34 we were able to generate human blood derived microglial-like cells which expressed microglia specific markers TMEM119 and P2RY12, alongside the ability to phagocytose and express inflammatory markers upon LPS stimulation. It is unsurprising that IL-34 is required to induce these cells, considering it is expressed by neurons and reported to enhance the proliferation of microglia (Mizuno et al., 2011). In addition it is a cytokine listed in methods to differentiate iPSCs into microglia (McQuade et al., 2018). Nurr1 gene expression was significantly induced by stimulation with LPS, in addition to IL-1ß, IL-6, TNFα and IL-10. This aligns with the literature and subsequently validates these microglial-like cells as an appropriate model in which to investigate inflammation (Dai et al., 2019, Smith et al., 2012).

Macrophages were generated using GM-CSF and FBS as described previously (Nielsen et al., 2020). Similarly, they expressed key markers, retained the ability to phagocytose, and expressed inflammatory markers upon stimulation. Unexpectedly, macrophages had high levels of IL-10 in the absence of stimulation. This could indicate an anti-inflammatory phenotype at rest which further supports the concept of a phenotype spectrum (Nahrendorf and Swirski, 2016). Pre-treating macrophages with IFNy before LPS stimulation revealed that IFNy can both enhance and repress different TLR-LPS stimulated genes. This has been reported previously however not in the context of Nurr1 (Kang et al., 2019, Hoeksema et al., 2015). Similar to what was reported by Hoeksema et al., pre-treatment with IFNy followed by LPS enhanced the expression of TNFα whilst repressing the expression of IL-1ß and IL-6 compared to no pre-treatment. In addition, the pre-treatment also enhanced Nurr1 expression, highlighting how the selective priming by IFNy can in turn regulate the inflammatory response. Although

TNFα and Nurr1 behave in contradicting roles, in human physiology the selective enhancement of both molecules by IFNγ may work to stimulate apoptosis at the site of inflammation whilst also preventing the excessive production of cytokines respectively (Idriss and Naismith, 2000).

Immune tolerisation was induced in the macrophages by two sequential LPS stimulations. Concurrent with the literature, tolerisation abolished the expression of pro-inflammatory cytokines IL-6, IL-1ß and TNFα, in addition to IL-10 (Chen and Ivashkiv, 2010). Interestingly, tolerisation appeared to superinduce the expression of Nurr1. Chromatin remodelling is suggested to be responsible for the silencing of these pro-inflammatory genes during tolerisation (Foster et al., 2007). This remodelling prevents transcription factors such as NFκB from binding to inflammatory gene promoters. This may increase the likelihood of NFκB binding to the promoter of Nurr1 superinducing its transcription. Nurr1 is reported to repress IL-6, IL-1ß and TNFα during inflammation by binding to NFκB on inflammatory promoters (Saijo et al., 2009). Our data proposes Nurr1 may act in an mechanism to further inflammatory repression during immune tolerance. Whereby superinduction of the Nurr1 gene results in increased Nurr1 protein binding to the promoters of pro-inflammatory genes and consequent gene repression.

Reports have previously shown pre-treatment with IFNγ abrogates immune tolerance in macrophages, restoring the expression of inflammatory cytokines. Data concerning the role of Nurr1 in immune tolerance is absent. Pre-treating tolerized macrophages with IFNγ, we accordingly found the expression of pro-inflammatory cytokines was reintroduced, however the expression of IL-10 was not. Unexpectedly, the expression of Nurr1 was actually decreased

after IFNy pre-treatment. Therefore, IFNy has differential effects on Nurr1 expression, where in non-tolerised cells it increases Nurr1 expression, but in tolerized cells it decreases Nurr1 expression. This data suggests that in tolerized cells IFNy promotes a pro-inflammatory phenotype; where pro-inflammatory gene expression is induced but a reduction in Nurr1 removes the protective braking mechanism. Increased IFNy is found in the blood of PD patients, alongside decreased Nurr1, and is associated with damaged neurons (Diaz et al., 2022). It may be that increased IFNy coupled with decreased Nurr1 can lead to chronic inflammation causing more damage to nearby cells.

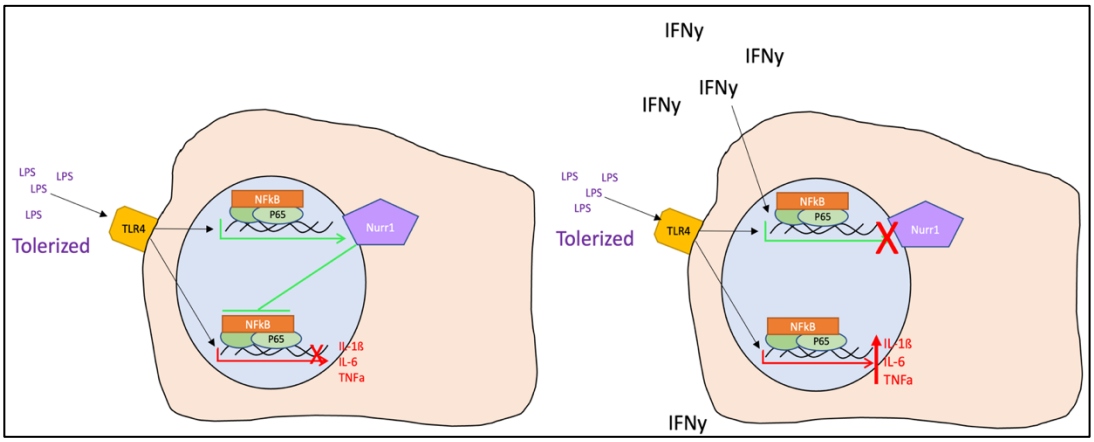


Figure 4.5-1 Immune tolerized cells vs pre-treatment with IFNy

Schematic representation of tolerized cells (Left) IFNy pre-treated tolerized cells (right). Tolerisation induces the expression Nurr1 whilst decreasing the expression of pro-inflammatory cytokines. Subsequently Nurr1 expression can feed back and repress the inflammatory cytokine production further to prevent excessive inflammation. In tolerized cells IFNy pre-treatment reduces the expression of Nurr1, whilst relieving the repression caused by tolerisation. Leading to an increase in pro-inflammatory cytokines with a reduced Nurr1 braking mechanism.

The transduction efficiency of the Nurr1 and Nurr-1a viruses in macrophages was low. Therefore, the likely reason for high levels of mRNA gene expression was due to detection of remaining vector itself with the Nurr inserts, not true macrophage expression. In addition viral transduction is likely to induce some level of

inflammation in macrophages as they are surveillance immune cells. Transducing the cells with the minimal level of Nurr1 produced unchanged, or minimally decreased, pro-inflammatory gene expression. There are multiple reasons for this including LPS dose, temporal regulation or a low level of functional Nurr1 protein produced which is only capable of repressing the inflammation induced by viral infection itself and not that of the LPS. Therefore, we predict that with a better transduction efficiency, a titrated LPS dose and multiple timepoints we would see a greater reduction in pro-inflammatory cytokine production, similar to what is reported in the literature (Saijo et al., 2009).

There are two likely reasons for the increase in pro-inflammatory gene expression when cells were transduced with Nurr-1a. Firstly, the level of Nurr-1a present was too low to elicit any effect and therefore the increase in inflammatory cytokines was due to viral transduction itself. This is supported by the lack of protein detected in the western blot. The other possibility is that Nurr-1a does not repress the production of proinflammatory cytokines. Suggesting an interesting concept whereby if Nurr-1a does not repress inflammation, even though it is SUMOylated greater than Nurr1, then the repression induced by Nurr1 may not be dependent on SUMOylation. However further research with an optimised transduction efficiency is undoubtably required to confirm or deny either possibility.

In conclusion, the second part of this chapter validates a method of producing functional human macrophage and microglial-like cells within 6 and 14 days respectively. Presenting an alternative time and cost-effective method to investigate human *in vitro* inflammatory pathways. We suggest a novel role for Nurr1 during immune tolerisation, which aids in our understanding of the

mechanisms by which tolerisation works. In addition to identifying a potential pathway induced by IFNy dysregulation which furthers chronic inflammation in PD. Understanding the role Nurr1 plays in these pathways reveals potential ways of controlling inflammation in PD by therapeutically targeting Nurr1 and IFNy. Lastly, although requiring further optimisation, we provide the framework to investigate the role of Nurr1, Nurr-1a and SUMO during inflammation.

Chapter 5

Significant findings, general discussion, and future work

5.1 Summary of Significant findings

New/Original findings
1. The level of Nurr-1a SUMOylation is significantly higher than Nurr1 2. SUMO3 isoform shows preference over SUMO2 3. K91 is the major site of Nurr1 and Nurr-1a SUMOylation 4. SUMO enhances Nurr1 and Nurr-1a mediated transcriptional activation 5. Nurr-1a acts in the same transcriptional mechanisms as Nurr1 6. Nurr1 and Nurr-1a transcriptional activity is cell specific and dependent on reporter construct 7. IFNy primes LPS induced Nurr1 expression 8. Nurr1 is superinduced during immune tolerance 9. Development of quick simplified method to generate iPSC DA neurons
Confirmed previously published findings
1. Nurr-1a activates the TH promoter less than Nurr1 2. Generation of microglial-like cells from peripheral blood mononuclear cells 3. Generation of Hematopoietic cells using a StemCell Technologies kit

5.2 General discussion

In the present study we aimed to investigate the role of SUMOylation in Nurr1 transcriptional regulation and provide insight into the possible function of the splice variant Nurr-1a. Although a mechanism for the role of Nurr1 SUMOylation in inflammatory repression has been described by Saijo et al., the present work focused on the mechanism of SUMOylation itself, clarifying isoform specificity, SUMOylation site and implication in neuronal regulation (Saijo et al., 2009). In addition, we investigated Nurr-1a comparatively to reveal similarities in receptor mechanisms.

To investigate levels of Nurr1 and Nurr-1a SUMOylation a cell-based protocol, previously described for PPAR SUMOylation, was used which relies on the purification of 6xHis-SUMO from cell lysates to enrich SUMO conjugates under denaturing conditions followed by probing for FLAG-tagged Nurr1 or Nurr-1a (Pourcet et al., 2013). A method dissimilar from immunoprecipitation studies previously reported to evaluate Nurr1 SUMOylation (Saijo et al., 2009,

Galleguillos et al., 2004, Arredondo et al., 2013). Purifying conjugates under denaturing conditions inhibits enzymes responsible for SUMO deconjugation whilst not disrupting the iso-peptide bond and decreases non-covalent interactions (Tatham et al., 2009).

This study revealed the SUMOylation of Nurr-1a was greater and more versatile than Nurr1. Nurr-1a was capable of modification by all three isoforms and displayed poly-SUMO chains which are known to create a unique topology recognised by other factors including SUMO targeted ubiquitin ligases (Hendriks and Vertegaal, 2016). Nurr1 was SUMOylated by SUMO2/3 only, had no poly-SUMOylation and, like Nurr-1a, showed preference towards SUMO3. This opposes previous reports which state SUMO2 is the principal modifier of Nurr1, however these studies did not use the same SUMO enrichment protocol (Saijo et al., 2009, Arredondo et al., 2013). Overall this suggests Nurr-1a has greater versatility in its regulation by SUMOylation, including that by SUMO1 which is uniquely distributed to the nuclear envelope and nucleolus (Ayaydin and Dasso, 2004). Additionally, conjugation of SUMO2/3 is suggested to be involved in the cellular stress response. Comparatively high levels of Nurr-1a SUMO2/3 SUMOylation compared to Nurr1 was the first evidence to suggest that Nurr-1a may have an important SUMO-regulated role in the response to cellular stress.

The post translational modification of nuclear receptors can occur throughout different regions of the receptor, including the AF-1 domain, LBD and hinge region (Germain et al., 2006, Walther et al., 2005). PTMs can affect transcriptional regulation through coregulator recruitment, dissociation and by influencing subcellular localisation. The SUMOylation of Nurr1 is reported to affect its transcriptional activity through 1) the recruitment of a corepressor

complex in a transrepression mechanism, 2) PIASg mediated direct repression of Nurr1 transcriptionally activating target genes (Saijo et al., 2009, Arredondo et al., 2013). However, the site at which this SUMOylation occurs has been contested in the literature with some reports suggesting the AF-1 domain and others suggesting the LBD/AF-2 domain (Arredondo et al., 2013, Saijo et al., 2009, Galleguillos et al., 2004). As Nurr-1a was shown to be SUMOylated greater than Nurr1 it established the AF-2 domain proposed previously and absent in Nurr-1a, was not the main site of SUMOylation (Glass and Saijo, 2010, Saijo et al., 2009). To this end K91, within the AF-1 domain, was confirmed as the major site of SUMOylation for both Nurr1 and Nurr-1a through site directed mutagenesis experiments. In line with previous reports (Arredondo et al., 2013, Galleguillos et al., 2004) this result suggests the AF-1 domain is critical to the transcriptional activity mediated by Nurr1 and Nurr-1a. Furthermore, we speculate the truncation of the AF-2 region in Nurr-1a may allow it to adopt a conformation more facilitative of SUMOylation and hence the greater levels seen with this isoform.

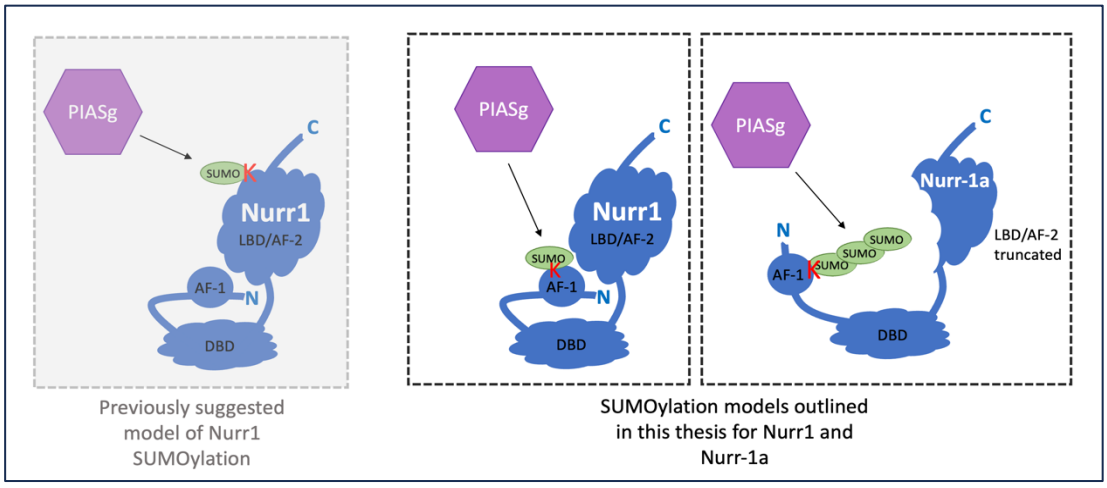


Figure 5.2-1 Previous and current suggested models of Nurr1 and Nurr-1a SUMOyaltion.

Schematic of a previously suggested model whereby PIASg SUMOylates Nurr1 in its AF-2/LBD. Versus current model where PIASg SUMOylates Nurr1/1a in its AF-1 domain, and the AF2/LBD truncation in Nurr-1a allows it to adopt a conformation where AF-1 can be more readily SUMOylated.

The transrepression mechanism reported by Saijo et al., holds Nurr1 LBD SUMOylation at its core. The authors show using CHIP that Nurr1 is recruited to LPS responsive promoters such as TNFα after LPS treatment in BV2 cells. In HeLa cells they demonstrate key SUMOylation sites in Nurr1s LBD, and mutation of these same sites in RAW264.7 cells shows a significantly reduced ability of Nurr1 to repress an iNOS driven luciferase reporter in response to LPS. The authors suggest it is this LBD SUMOyaltion which facilitates the association of its DBD with CoREST and the subsequent clearance of p65 from the promoter of NFκB responsive genes to restore a repressed state (Saijo et al., 2009). Our data clearly opposes the LBD as the main site of SUMOylation and is not alone in its support for AF-1 as the mediator of Nurr1 based transcriptional repression instead of the LBD (Kim et al., 2013). This highlights the importance of the AF-1 domain during inflammatory repression and therefore proposes a site that may be a pivotal therapeutic target during neuroinflammation and subsequent disease. To further confirm our results, future experiments should look to repeating CHIP experiments described by Saijo et al., using the K91 Nurr1/1a mutants firstly in the BV2 cell line described followed by the primary inflammatory models developed in this thesis.

SUMOylation of nuclear receptors is largely considered a repressive function and, until this study, had only been reported in association with Nurr1 in terms of repression (Glass and Saijo, 2010) (Gill, 2005, Saijo et al., 2009). This report demonstrated SUMO can enhance Nurr1 and Nurr-1a mediated transcriptional activation of a natural TH promoter in neuronal cells through two lines of evidence. Firstly, K91 mutants activated the TH promoter less than the wild type. Secondly, overexpression of SUMO enhanced the wildtype mediated activation of the promoter. Opposing literature states K91 SUMO mutants were able to activate a NBRE driven promoter more than

the wild type in HEK293 cells, suggesting SUMOylation of this site is repressive. The difference in result is likely due to the use of different cell lines and promoter regions. Kim et al., has highlighted differences such as these in parallel studies of Nurr1 in F3 and SH-SY5Y cell lines which result in opposite effects on transcription on the same promoter (Kim et al., 2013). It is possible that this differential SUMOylation of Nurr1 and Nurr-1a dependent on cell type, may be responsible for the variable transcriptional activities in specific cells.

In line with the literature, Nurr-1a was found to transcriptionally activate an NBRE driven promoter less than Nurr1 in a neuronal cell type (Castillo et al., 1998b, Michelhaugh et al., 2005, Kim et al., 2013). However, this is not to say that Nurr-1a is not an important transcriptional regulator. The data in this study highlights the ability of Nurr-1a to partake in the same mechanisms as Nurr1 but at different strengths. Including PIASg mediated repression, transcriptional activation, and SUMO mediated regulation. Kim et al., reported that Nurr-1a exhibited greater repression of an NBRE reporter in a neural stem cell line (HB1.F3) than full length Nurr1 (Kim et al., 2013). Considering Nurr-1a has a higher level of SUMOylation, this may support the idea of SUMOylation as a prerequisite for Nurr1/1a mediated transcriptional repression in certain cell types.

Nurr1 has many reported synthetic ligands and more recently suggested natural ligands (de Vera et al., 2019, Kim et al., 2015, Ordentlich et al., 2003, Hammond et al., 2015, Pan et al., 2005). These ligands have largely been used in *in vitro* cell based studies with reporter constructs derived from the classically reported 3xNBRE motif (5'-AAAGGTCA-3'). One of which, AQ, was shown to enhance the transrepressive role of Nurr1, reducing the expression

of pro-inflammatory cytokines in microglia (Kim et al., 2015). However, using the concentration we found no change in Nurr1 or Nurr-1a SUMOylation, which may reflect the difference in cell choice or could suggest AQ mediates its effects through a mechanism alternate to SUMO dependent Nurr1 transrepression. To evaluate the effect of ligands on Nurr1 and Nurr-1a transcriptional regulation a natural TH promoter was used. 'Natural' refers to a cloned region of the promoter encompassing the NBRE and NBRE-like motifs which reside in this region. As opposed to a 3xNBRE reporter construct which incorporates three synthetic repeats of the same canonical NBRE motif Nurr1 is reported to bind to. The ligands chosen did not mimic the results described in the literature and the likely reason for this is due to the difference in reporter. Kim et al., also highlighted this difference using both a naturally occurring TH promoter in addition to a 3xNBRE promoter. The authors show that the other NBRE-like motifs that reside in the promoter region bind to monomeric Nurr1 and contribute to transcriptional activity (Kim et al., 2013). Moreover, the data emphasises the importance of carefully selecting the promoter and cell type which best reflects the transcriptional environment of interest when investigating the effect of Nurr1 ligands on transcriptional activity.

IFNy is reported to have a major role in inflammation; activating immune cells, regulating cytokine production and inducing cell death (Lee et al., 2017). Although considered a pro-inflammatory mediator, IFNy can enhance or supress different subsets of LPS induced genes (Kang et al., 2019, Hoeksema et al., 2015). Treatment of macrophages with IFNy and LPS revealed enhanced Nurr1 expression. Suggesting a mechanism to promote inflammation whilst retaining the inflammatory brake of Nurr1 to ensure inflammation is not excessive. Similarly, tolerized macrophages superinduced the expression of Nurr1 which may suggest a new role

for Nurr1 in a negative feedback mechanism to mediate or further the protective effects of tolerisation. Increased IFNy has been found in the blood of PD patients (33.0±4.1% $p < 0.01$) and is associated with DA neuronal death (Barcia et al., 2011, Diaz et al., 2022, Mount et al., 2007). In tolerized macrophages, pre-treatment with IFNy restores inflammatory cytokine production whilst reducing the expression of Nurr1, which could lead to excessive inflammation with limited protection from Nurr1. Nurr1 is shown to be reduced in PD patients whilst IFNy levels are higher. Therefore, a low level of Nurr1 could lead to a reduction in inflammatory tolerisation and coupled with increased IFNy may result in chronic inflammation. The experiments in this study used macrophages and whilst the relationship between the peripheral immune system and the CNS in PD remains under investigation (Yan et al., 2018, Yao et al., 2022), it would be pertinent to investigate this mechanism in cells of the CNS. Therefore, future work should look to investigating immune tolerance in microglia, which was part of the rational for optimising the generation of iMGL cells.

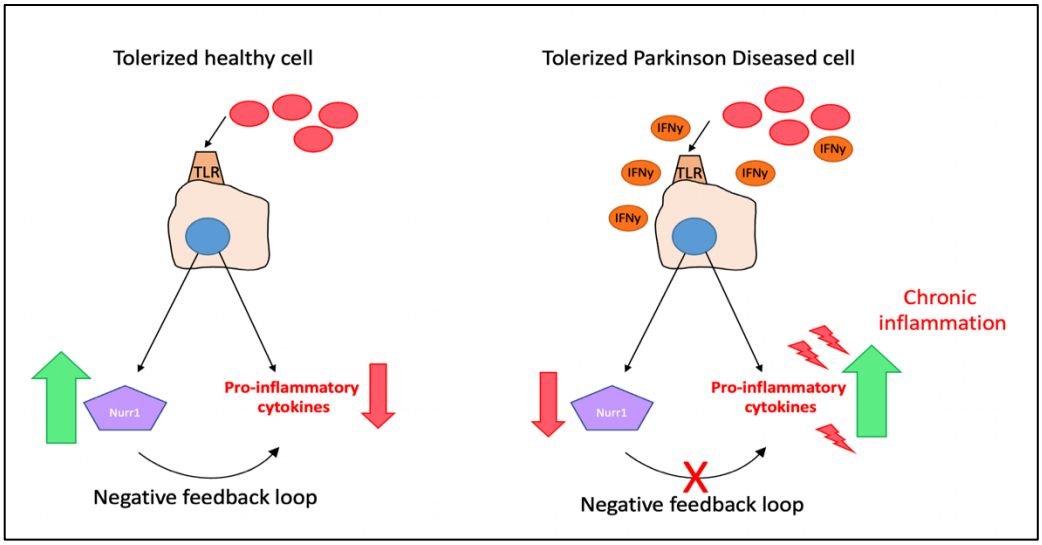


Figure 5.2-2 Nurr1 inflammatory feedback mechanism in healthy and diseased states

In tolerized macrophages Nurr1 expression is increased which feeds back to repress the expression of pro-inflammatory cytokines. In diseased tolerized cells with increased IFNy, Nurr1 expression is decreased whilst pro-inflammatory cytokine expression is increased, leading to chronic and excessive inflammation.

Nurr1 is well documented as a key regulator of DA neuronal development (Zetterström et al., 1996, Zetterström et al., 1997, Hermanson et al., 2003). Therefore, it is unsurprising that Nurr1 has been used as a key transcription factor in the differentiation of *in vitro* cells to DA neurons (Andersson et al., 2007, Lee et al., 2010, Park et al., 2008). More recent advancements revealed a one-step method using Nurr1 alongside two other key transcription factors to differentiate human iPSCs into DA neurons; without the need to transition cells through multiple developmental stages (Theka et al., 2013, Powell et al., 2021). Using viral transduction and a relatively simplistic neuronal induction media cells were differentiated into DA neurons which displayed characteristic morphology and cell surface markers. The method developed in this thesis differed from published data in the simplification of multiple steps and media composition. Developing DA neuronal cells through this method provides a quick and simple way of generating a human model in which to investigate Nurr1 and Nurr-1a transcriptional activity, alongside neuroprotective capabilities when exposed to inflammatory insult.

In summary Nurr-1a is regulated by mechanisms similar to those identified for Nurr1. Including the ability to be SUMOylated, to an even greater level than the full-length variant. The role of Nurr1 and Nurr-1a SUMOylation appears to have differential effects dependent upon cell type, and this may in part contribute to the variable transcriptional activity mediated through its AF-1 domain. Nurr1 is an important regulator of inflammation in both the peripheral immune system and the CNS, however to what extent mechanisms of the peripheral immune system translate to the CNS remains to be investigated. Future experiments using human based models are required to further clarify the functional significance of Nurr1/1a

SUMOylation in microglia and DA neurons. In addition to any protection imparted by the receptors during PD pathology.

6.3 Limitations and future work

The most physiologically representative method in which to investigate Nurr1 SUMOylation would involve immunoprecipitation of SUMO modified proteins followed by western blotting for endogenously expressed Nurr1 in primary cells (Barysch et al., 2014). However, this method would require high cell number as only a small fraction of a proteins cellular pool is SUMOylated at steady state, as well as a large volume of antibody. Additionally, detection of endogenous nuclear receptors using antibodies is notoriously challenging due to low abundance and efforts to do so with Nurr1 in our lab previously failed. Therefore, this study relied on the overexpression of SUMOylation machinery in the HeLa cell line to demonstrate protein expression. The overexpression of SUMOylation machinery is not sufficient to definitively investigate the function of SUMOylation, however it was an important preliminary step to confirm the SUMOylation status of Nurr1 and Nurr-1a. An additional method in which to study SUMOylation is the proximity ligase assay which can detect SUMO-target protein interactions up to 40nm. However, a positive signal does not necessarily reflect SUMOylated Nurr1 or Nurr-1a. A signal can still be seen if Nurr1 is within 40nm distance from another SUMOylated protein, which is the likely reason that a signal was still detected in the K91 SUMO mutant samples. Future experiments in PBMC derived microglia and macrophages infected with Nurr1/1a wildtype and K91 SUMO mutant lentiviruses will clarify the importance of SUMOylation in Nurr1/1a mediated transcriptional repression and reveal any potential role for Nurr-1a in this process.

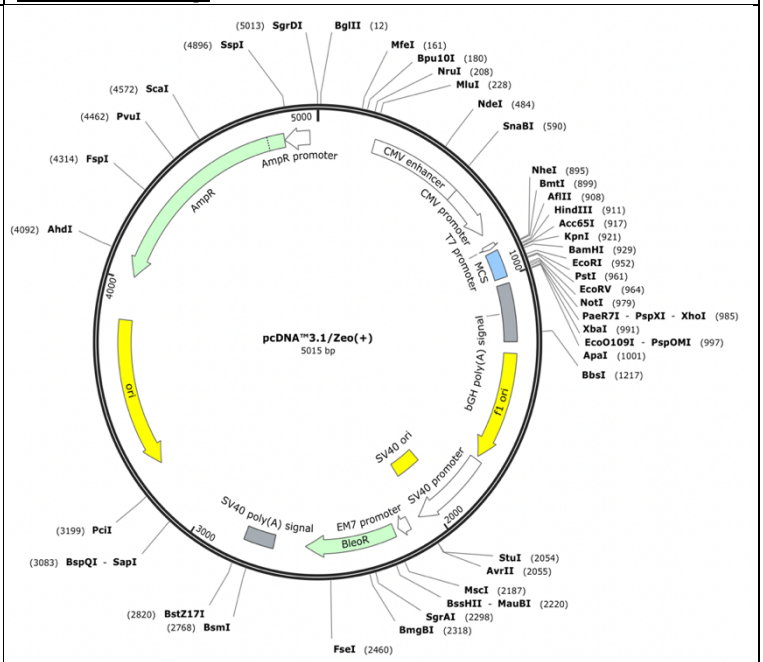
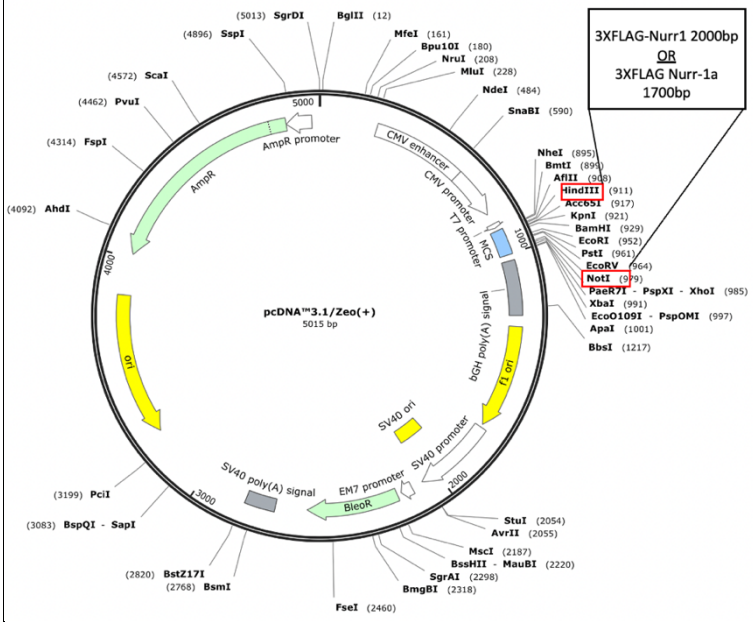
To what extent the peripheral immune system interacts with the CNS requires further investigation (Kortekaas et al., 2005, Rite et al., 2007). In terms of inflammation in PD, it would be most relevant to study the role of Nurr1 in microglia and how this impacts DA neurons (Olanow et al., 2019, Saijo et al., 2009). However due to the complexity and time constraints of differentiating iPSCs into microglia or the further optimisation of the PBMC derived microglial-like cells, initial experiments used PBMC derived macrophages as an inflammatory model. Nurr1 expression is rapidly induced by LPS in macrophages through a similar pathway as in microglia (Pei et al., 2005). The mechanism proposed for the role of Nurr1 in immune tolerance is limited to the peripheral immune system, as the study only used macrophages and therefore cannot be fully translated to microglia in PD. Efforts to differentiate PBMC to microglial-like cells were successful after optimisation. However, it is noteworthy to add that physiologically, microglia develop from the fetal yolk-sac, therefore microglia derived from monocytes cannot be considered true microglia (Lenz and Nelson, 2018). Future experiments using the microglia-like cells will reveal to what extent the Nurr1 immune tolerance mechanism can be applied to PD.

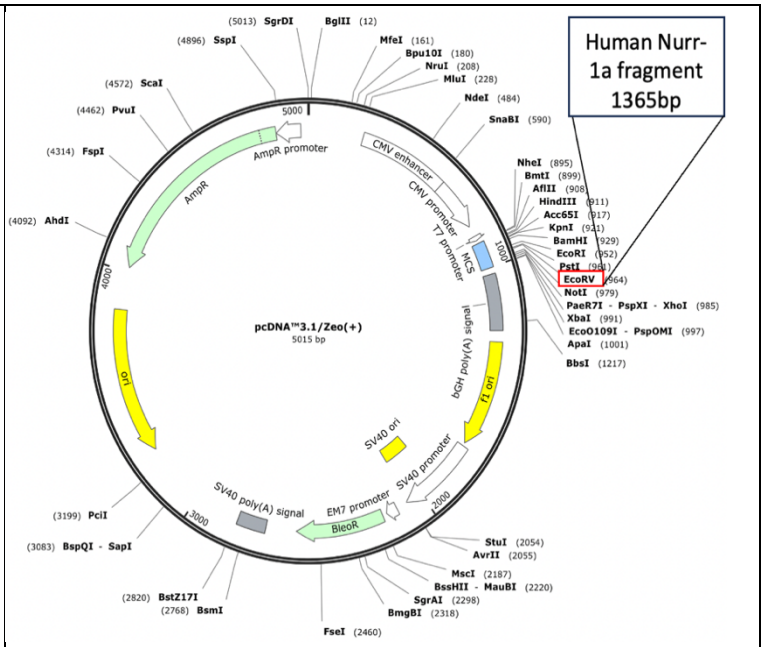
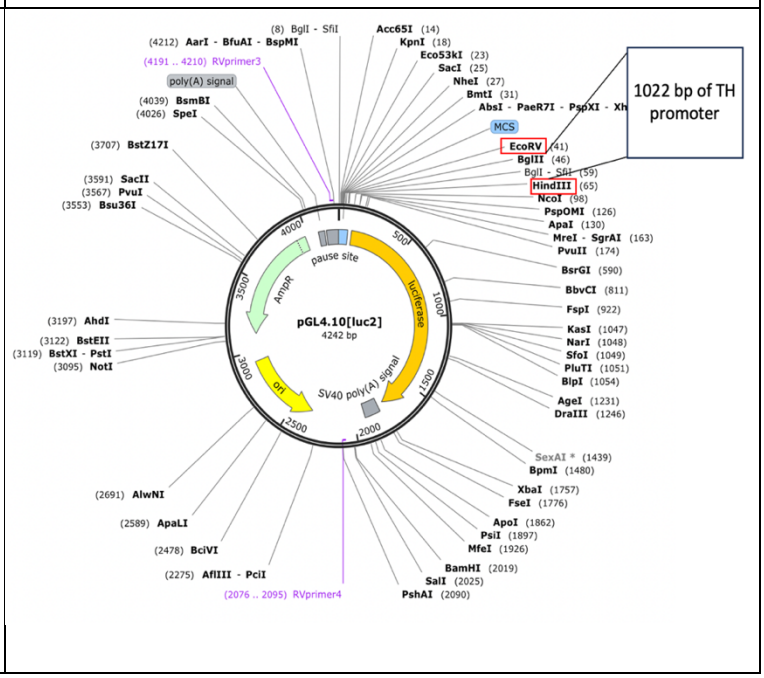
The use of cell lines and specific response element constructs to evaluate transcriptional activity have already been highlighted as a limitation of this work. The variability between cell type and reporter construct has also been demonstrated by Kim et al., (Kim et al., 2013). This suggests the most relevant way to investigate the transcriptional activity of Nurr1 and Nurr-1a in DA neurons would be to use DA neurons themselves. DA neurons have been successfully differentiated from iPSCs using key transcription factors, including Nurr1, previously (Theka et al., 2013, Powell et al., 2021). The DA neurons generated in this thesis morphologically resembled DA neurons and were immuno positive for multiple key markers.

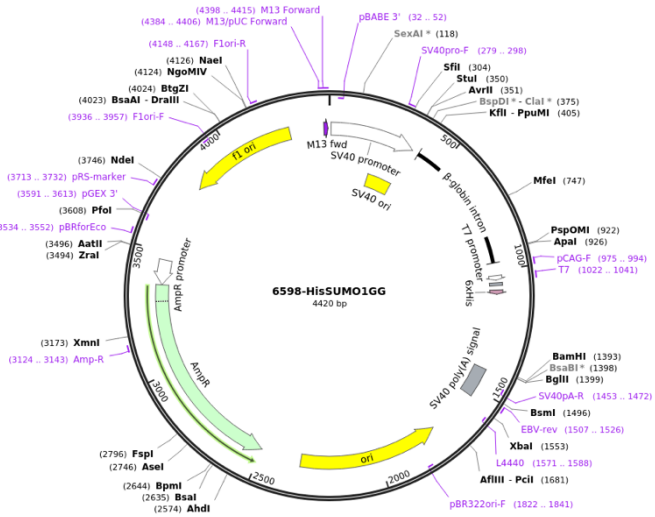
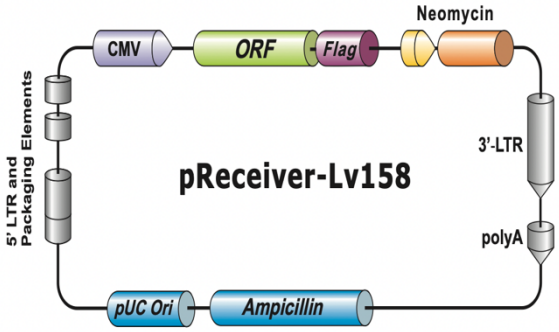
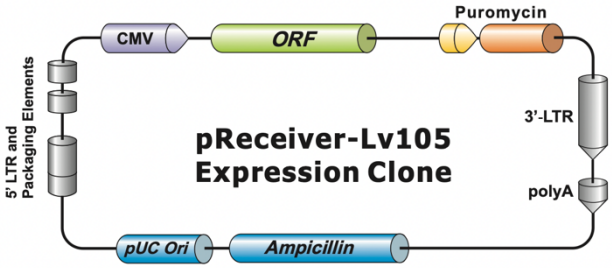
However, cells were not tested for their ability to produce dopamine. Future experiments using fully validated DA neurons will provide insight into the transcriptional activity of Nurr1 and Nurr-1a through the use of RNA-Seq and natural reporter constructs. In addition, DA neurons can be used in combination with microglial-like cells to model inflammatory insult and reveal any protective effects Nurr1 and Nurr-1a may have during this process.

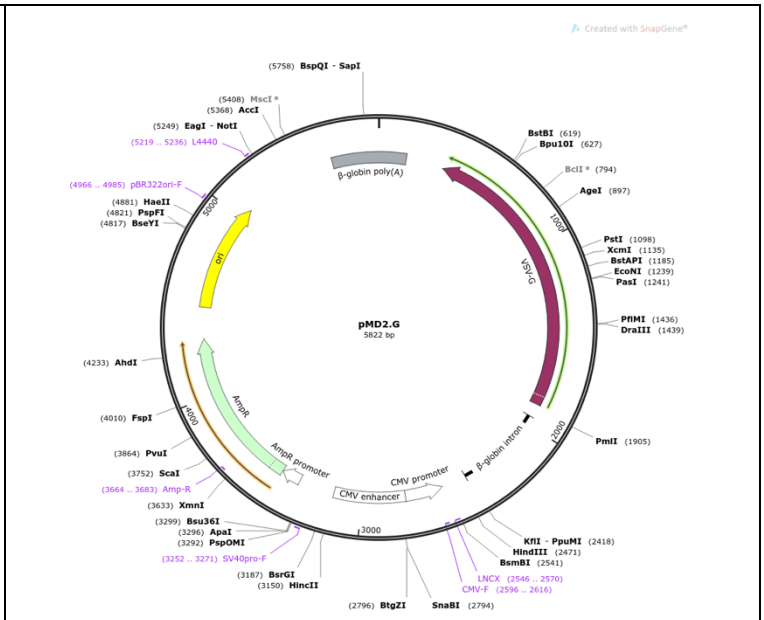
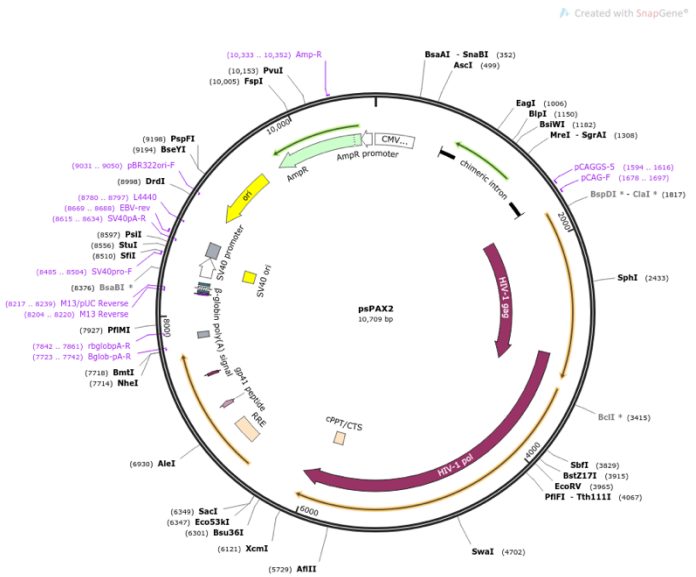
Collectively future experiments will hopefully reveal the significance of Nurr-1a in transcriptional regulation, and further confirm the function of SUMOylation in DA neurons and microglia. Contributing to what is already known about DA neurons and microglia in PD and highlighting potential therapeutic targets.

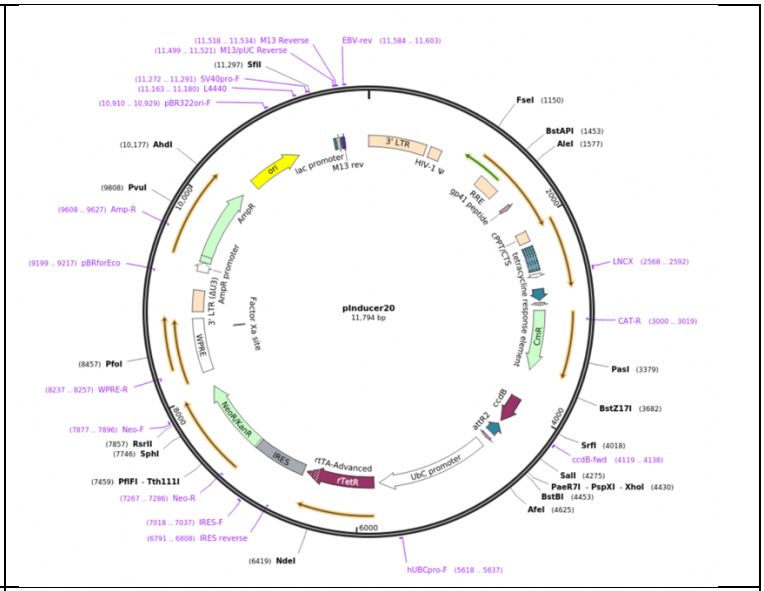
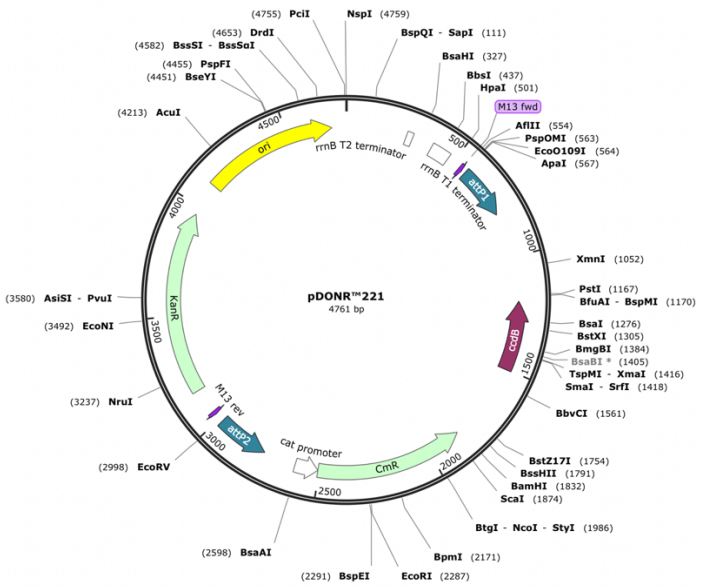
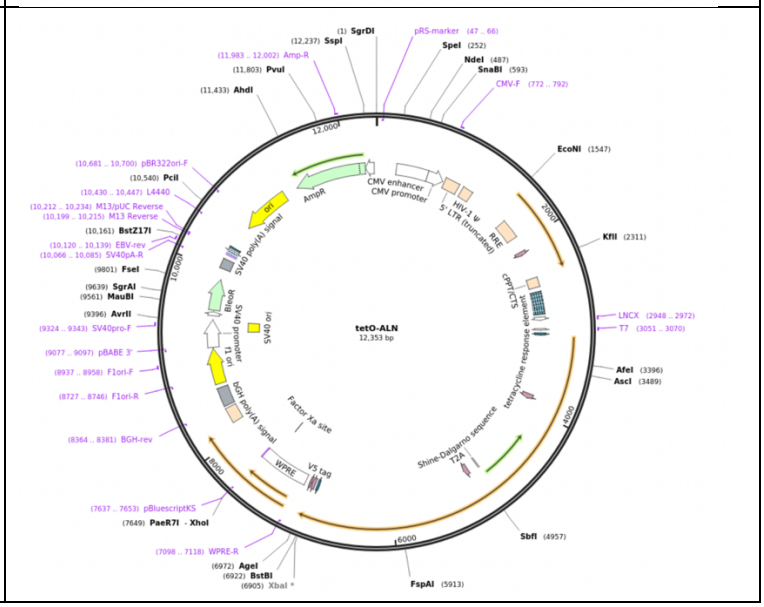
Appendices

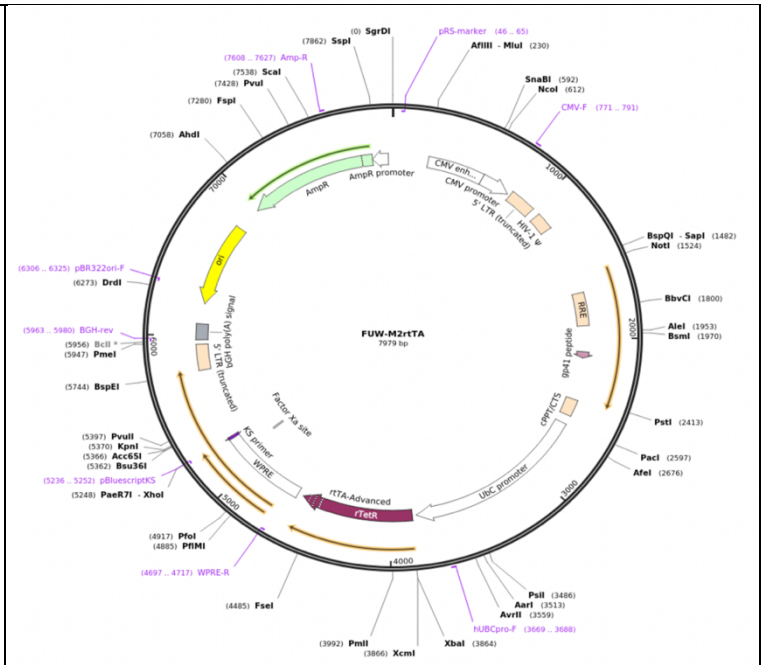
Name	Description	Plasmid map
pcDNA3.1 zeo (+)	pcDNA3.1 (+) Mamalian expression vector Invitrogen V86020	
FLAG-Nurr1 **FLAG Nurr-1a** **FLAG Nurr1-K91** **FLAG Nurr-1a-K91** **FLAG Nurr-1a-SIM**	Representative construct comprised of pcDNA3.1 (+) Mamalian expression vector (Invitrogen V86020) with either wild type, SIM or K91 mutant Nurr1 or Nurr-1a Rat inserts cloned between RE sites indicated.	

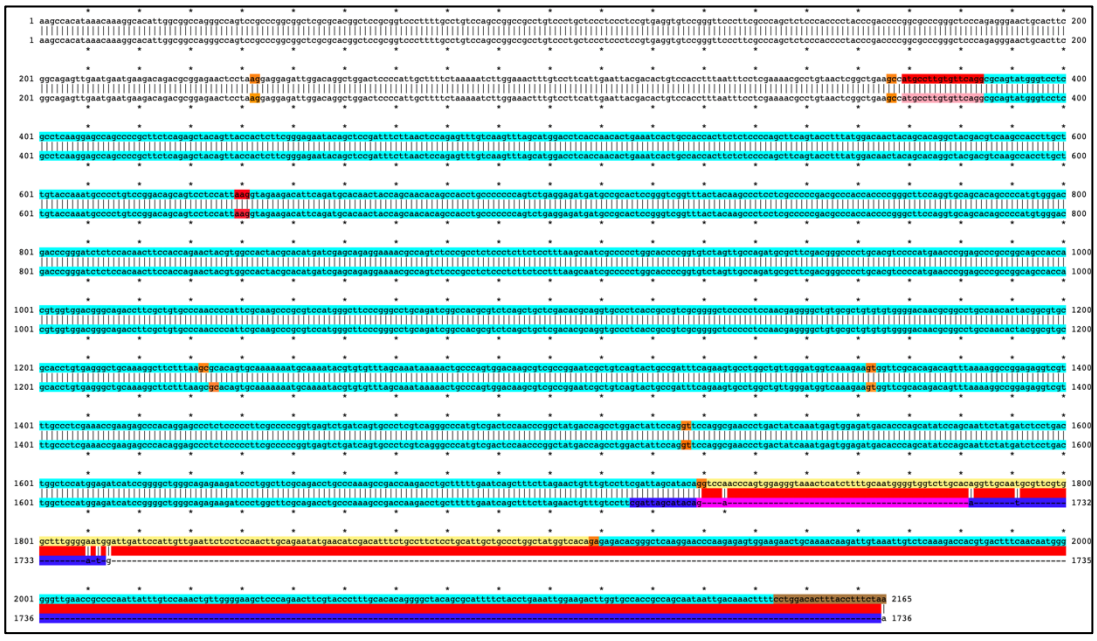
Human Nurr-1a	Human Nurr-1a coding sequence obtained from reverse transcribing human total RNA cloned into empty vector through blunt ended cloning.	
TH-Luc Reporter	pGL4.1 (Luc2) vector with 1022bp of the TH promoter cloned in between RE sites indicated. Vector kindly provided by Dr. Dawson (University of Nottingham)	

6XHis-SUMO1GG	6598-HisSUMO1GG was a gift from Anne Dejean (Addgene plasmid # 13376 ; http://n2t.net/addgene:13376 ; RRID:Addgene_13376)	
Human Nurr1 **Human Nurr1-K91**	pReceiver-Lv158 lentiviral human Nurr1 vector obtained from GeneCopoeia. Site directed mutagenesis used to generate Nurr1 K91.	
Human PIASg	pReceiver-Lv105 lentiviral human PIASg vector obtained from GeneCopoeia.	

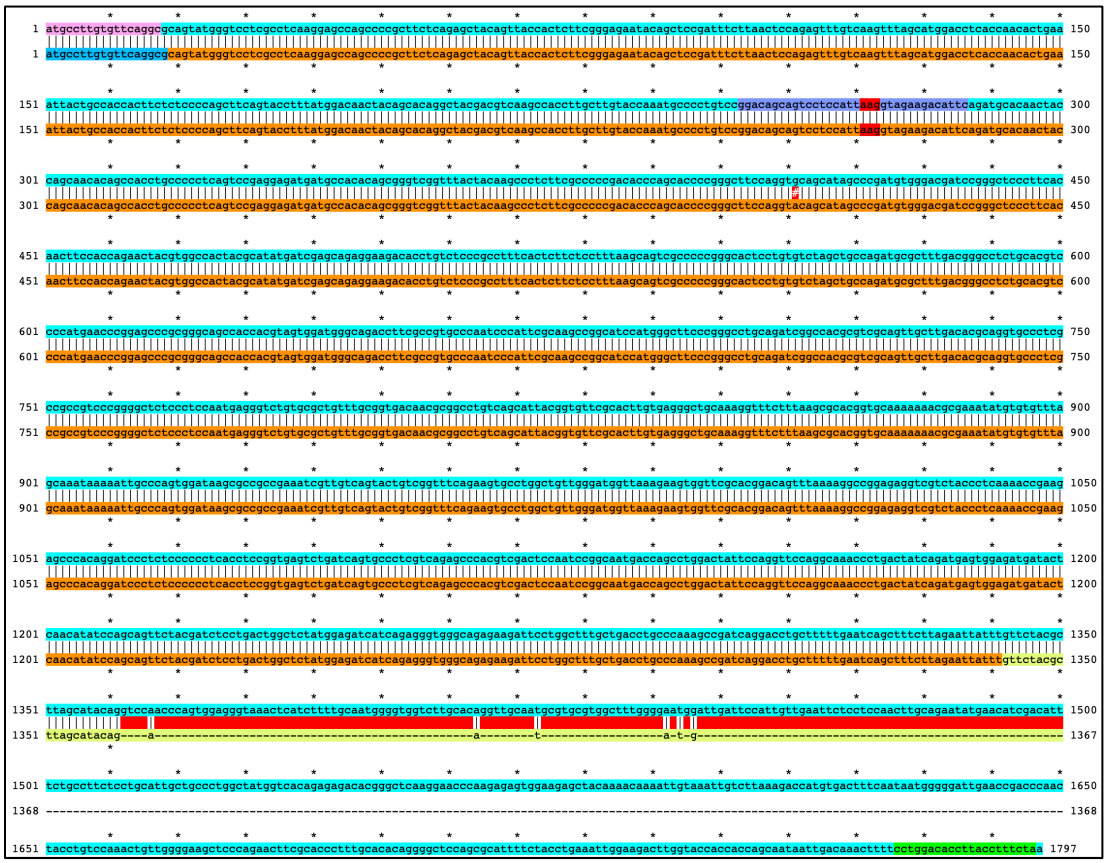
PMD2.G	pMD2.G was a gift from Didier Trono (Addgene plasmid # 12259 ; http://n2t.net/addgene:12259 ; RRID:Addgene_12259)	
psPAX2	psPAX2 was a gift from Didier Trono (Addgene plasmid # 12260 ; http://n2t.net/addgene:12260 ; RRID:Addgene_12260)	

pINDUCER20 **GFP** **Human Nurr-1a** **Human Nurr-1a-K91**	Inducible lentiviral expression plasmid. Gateway Clonase system used to insert human Nurr-1a and human Nurr-1a-K91 between att sites.	
Doner vector	pDONR221 used in the gateway Clonase cloning Invitrogen 12536017	
Tet-O-ALN	Ascl1, LMX1B and Nurr1 polycistronic vector. Tet-O-ALN was a gift from John Gearhart 43918.	

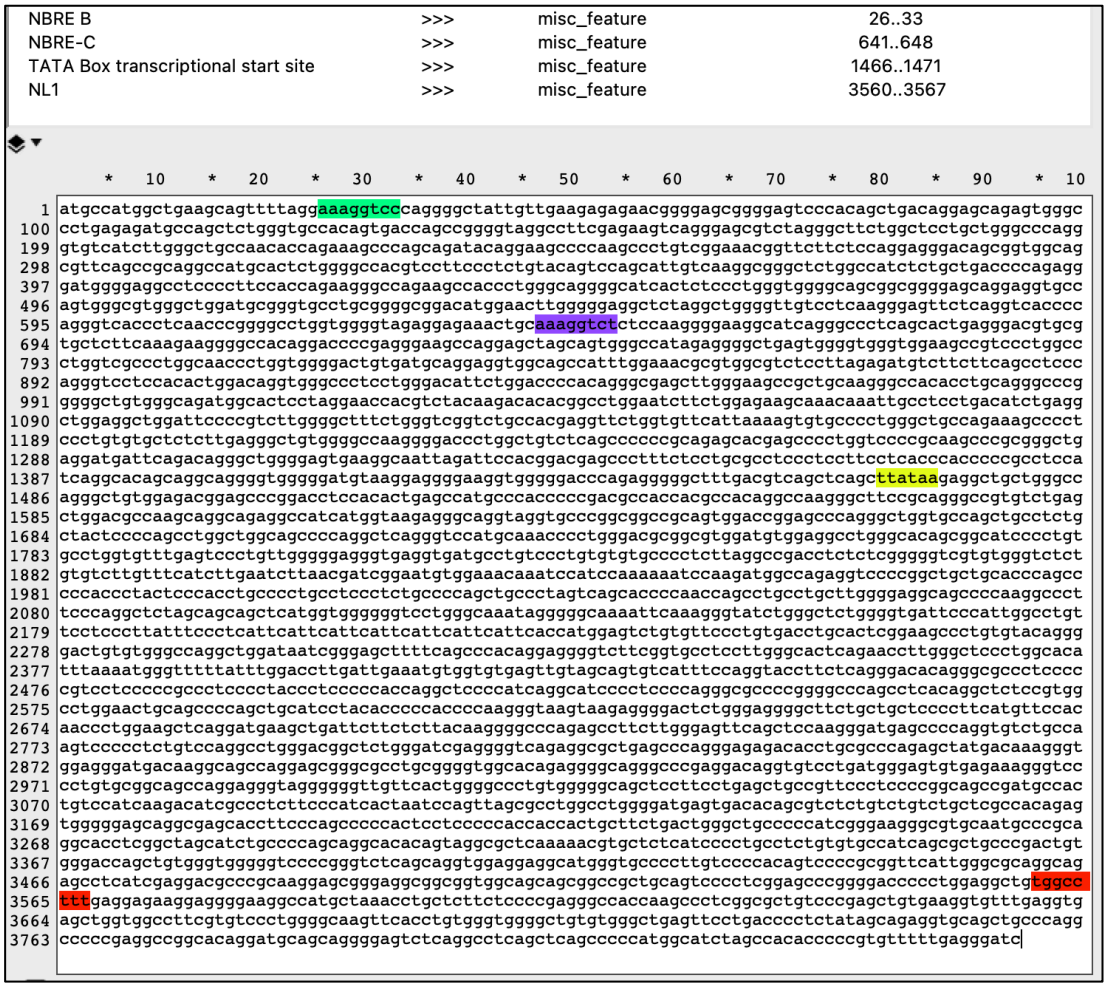
FUW-M2rtTA	Reverse transcription trans-activator protein. FUW-M2rtTA was a gift from Rudolf Jaenisch 20342	



Human Nurr1 (Upper) and Nurr-1a (lower) sequence alignment. Colour reference: CDS, exon junctions, Exon 7 alternatively spliced from Nurr-1a sequence, Nurr1 Fw primer, Nurr1 Rev primer, Nurr-1a Fw primer, Nurr-1a rev primer.



Rat Nurr1 and Nurr-1a sequence alignment.
Nurr1 (upper) and Nurr-1a (lower) sequences were obtained from NCBI and aligned using APE software. K91 site highlighted in red and respective primers in purple. Nurr1 forward and reverse primers are highlighted in pink and green. Nurr-1a forward and reverse primers are highlighted in blue and yellow.



Sections of the Human TH promoter (upper) and Rat TH promoter (lower) with respective NBRE/NL response elements and TATA box highlighted. NBRE-B, NBRE-C (NL3 differs by one bp), NL2, and NL1. As reported by (Kim et al., 2003b, Kim et al., 2003a).

Bibliography:

AARNISALO, P., KIM, C. H., LEE, J. W. & PERLMANN, T. 2002. Defining requirements for heterodimerization between the retinoid X receptor and the orphan nuclear receptor Nurr1. *J Biol Chem,* 277**,** 35118-23.

ABUD, E. M., RAMIREZ, R. N., MARTINEZ, E. S., HEALY, L. M., NGUYEN, C. H. H., NEWMAN, S. A., YEROMIN, A. V., SCARFONE, V. M., MARSH, S. E., FIMBRES, C., CARAWAY, C. A., FOTE, G. M., MADANY, A. M., AGRAWAL, A., KAYED, R., GYLYS, K. H., CAHALAN, M. D., CUMMINGS, B. J., ANTEL, J. P., MORTAZAVI, A., CARSON, M. J., POON, W. W. & BLURTON-JONES, M. 2017. iPSC-Derived Human Microglia-like Cells to Study Neurological Diseases. *Neuron,* 94**,** 278-293.e9.

AHN, J. H., LEE, J. S., CHO, J. H., PARK, J. H., LEE, T. K., SONG, M., KIM, H., KANG, S. H., WON, M. H. & LEE, C. H. 2018. Age-dependent decrease of Nurr1 protein expression in the gerbil hippocampus. *Biomed Rep,* 8**,** 517-522.

ALARID, E. T. 2006. Lives and times of nuclear receptors. *Mol Endocrinol,* 20**,** 1972-81.

ALLANTAZ-FRAGER, F., TURREL-DAVIN, F., VENET, F., MONNIN, C., DE SAINT JEAN, A., BARBALAT, V., CERRATO, E., PACHOT, A., LEPAPE, A. & MONNERET, G. 2013. Identification of biomarkers of response to IFNg during endotoxin tolerance: application to septic shock. *PLoS One,* 8**,** e68218.

ALLIOT, F., GODIN, I. & PESSAC, B. 1999. Microglia derive from progenitors, originating from the yolk sac, and which proliferate in the brain. *Brain Res Dev Brain Res,* 117**,** 145-52.

AMELIO, A. L., CAPUTI, M. & CONKRIGHT, M. D. 2009. Bipartite functions of the CREB co-activators selectively direct alternative splicing or transcriptional activation. *EMBO J,* 28**,** 2733-47.

ANDERSSON, E. K., IRVIN, D. K., AHLSIO, J. & PARMAR, M. 2007. Ngn2 and Nurr1 act in synergy to induce midbrain dopaminergic neurons from expanded neural stem and progenitor cells. *Exp Cell Res,* 313**,** 1172-80.

ANDREOU, A. M. & TAVERNARAKIS, N. 2009. SUMOylation and cell signalling. *Biotechnol J,* 4**,** 1740-52.

ARREDONDO, C., ORELLANA, M., VECCHIOLA, A., PEREIRA, L. A., GALDAMES, L. & ANDRÉS, M. E. 2013. PIASγ enhanced SUMO-2 modification of Nurr1 activation-function-1 domain limits Nurr1 transcriptional synergy. *PLoS One,* 8**,** e55035.

ASHBURNER, B. P., WESTERHEIDE, S. D. & BALDWIN, A. S. 2001. The p65 (RelA) subunit of NF-kappaB interacts with the histone deacetylase (HDAC) corepressors HDAC1 and HDAC2 to negatively regulate gene expression. *Mol Cell Biol,* 21**,** 7065-77.

AUPHAN, N., DIDONATO, J. A., ROSETTE, C., HELMBERG, A. & KARIN, M. 1995. Immunosuppression by glucocorticoids: inhibition of NF-kappa B activity through induction of I kappa B synthesis. *Science,* 270**,** 286-90.

AYAYDIN, F. & DASSO, M. 2004. Distinct in vivo dynamics of vertebrate SUMO paralogues. *Mol Biol Cell,* 15**,** 5208-18.

AZEEZ, J. M., SUSMI, T. R., REMADEVI, V., RAVINDRAN, V., SASIKUMAR SUJATHA, A., AYSWARYA, R. N. S. & SREEJA, S. 2021. New insights into the functions of

progesterone receptor (PR) isoforms and progesterone signaling. *Am J Cancer Res,* 11**,** 5214-5232.

AZIZI, S. M., SARHANGI, N., AFSHARI, M., ABBASI, D., AGHAEI MEYBODI, H. R. & HASANZAD, M. 2019. Association Analysis of the HNF4A Common Genetic Variants with Type 2 Diabetes Mellitus Risk. *Int J Mol Cell Med,* 8**,** 56-62.

BACHILLER, S., JIMENEZ-FERRER, I., PAULUS, A., YANG, Y., SWANBERG, M., DEIERBORG, T. & BOZA-SERRANO, A. 2018. Microglia in Neurological Diseases: A Road Map to Brain-Disease Dependent-Inflammatory Response. *Front Cell Neurosci,* 12**,** 488.

BACZYK, D., AUDETTE, M. C., DREWLO, S., LEVYTSKA, K. & KINGDOM, J. C. 2017. SUMO-4: A novel functional candidate in the human placental protein SUMOylation machinery. *PLoS One,* 12**,** e0178056.

BANERJEE, A., LU, Y., DO, K., MIZE, T., WU, X., CHEN, X. & CHEN, J. 2021. Validation of Induced Microglia-Like Cells (iMG Cells) for Future Studies of Brain Diseases. *Front Cell Neurosci,* 15**,** 629279.

BANNON, M. J. & WHITTY, C. J. 1997. Age-related and regional differences in dopamine transporter mRNA expression in human midbrain. *Neurology,* 48**,** 969-77.

BAPTISTA, M. J., O'FARRELL, C., DAYA, S., AHMAD, R., MILLER, D. W., HARDY, J., FARRER, M. J. & COOKSON, M. R. 2003. Co-ordinate transcriptional regulation of dopamine synthesis genes by alpha-synuclein in human neuroblastoma cell lines. *J Neurochem,* 85**,** 957-68.

BARCIA, C., ROS, C. M., ANNESE, V., GOMEZ, A., ROS-BERNAL, F., AGUADO-YERA, D., MARTINEZ-PAGAN, M. E., DE PABLOS, V., FERNANDEZ-VILLALBA, E. & HERRERO, M. T. 2011. IFN-gamma signaling, with the synergistic contribution of TNF-alpha, mediates cell specific microglial and astroglial activation in experimental models of Parkinson's disease. *Cell Death Dis,* 2**,** e142.

BARRESI, V., IENI, A., BRANCA, G. & TUCCARI, G. 2014. Brachyury: a diagnostic marker for the differential diagnosis of chordoma and hemangioblastoma versus neoplastic histological mimickers. *Dis Markers,* 2014**,** 514753.

BARYSCH, S. V., DITTNER, C., FLOTHO, A., BECKER, J. & MELCHIOR, F. 2014. Identification and analysis of endogenous SUMO1 and SUMO2/3 targets in mammalian cells and tissues using monoclonal antibodies. *Nat Protoc,* 9**,** 896-909.

BASTIEN, J. & ROCHETTE-EGLY, C. 2004. Nuclear retinoid receptors and the transcription of retinoid-target genes. *Gene,* 328**,** 1-16.

BEERS, J., GULBRANSON, D. R., GEORGE, N., SINISCALCHI, L. I., JONES, J., THOMSON, J. A. & CHEN, G. 2012. Passaging and colony expansion of human pluripotent stem cells by enzyme-free dissociation in chemically defined culture conditions. *Nat Protoc,* 7**,** 2029-40.

BENECKE, A., CHAMBON, P. & GRONEMEYER, H. 2000. Synergy between estrogen receptor alpha activation functions AF1 and AF2 mediated by transcription intermediary factor TIF2. *EMBO Rep,* 1**,** 151-7.

BENSINGER, S. J. & TONTONOZ, P. 2009. A Nurr1 pathway for neuroprotection. *Cell,* 137**,** 26-8.

BERNIER-VILLAMOR, V., SAMPSON, D. A., MATUNIS, M. J. & LIMA, C. D. 2002. Structural basis for E2-mediated SUMO conjugation revealed by a complex between ubiquitin-conjugating enzyme Ubc9 and RanGAP1. *Cell,* 108**,** 345-56.

BERRABAH, W., AUMERCIER, P., LEFEBVRE, P. & STAELS, B. 2011. Control of nuclear receptor activities in metabolism by post-translational modifications. *FEBS Lett,* 585**,** 1640-50.

BIANCO, C., RANGEL, M. C., CASTRO, N. P., NAGAOKA, T., ROLLMAN, K., GONZALES, M. & SALOMON, D. S. 2010. Role of Cripto-1 in stem cell maintenance and malignant progression. *Am J Pathol,* 177**,** 532-40.

BILOTTA, M. T., PETILLO, S., SANTONI, A. & CIPPITELLI, M. 2020. Liver X Receptors: Regulators of Cholesterol Metabolism, Inflammation, Autoimmunity, and Cancer. *Front Immunol,* 11**,** 584303.

BOILLÉE, S., VANDE VELDE, C. & CLEVELAND, D. W. 2006. ALS: a disease of motor neurons and their nonneuronal neighbors. *Neuron,* 52**,** 39-59.

BOITIER, E., GAUTIER, J. C. & ROBERTS, R. 2003. Advances in understanding the regulation of apoptosis and mitosis by peroxisome-proliferator activated receptors in pre-clinical models: relevance for human health and disease. *Comp Hepatol,* 2**,** 3.

BONTA, P. I., VAN TIEL, C. M., VOS, M., POLS, T. W., VAN THIENEN, J. V., FERREIRA, V., ARKENBOUT, E. K., SEPPEN, J., SPEK, C. A., VAN DER POLL, T., PANNEKOEK, H. & DE VRIES, C. J. 2006. Nuclear receptors Nur77, Nurr1, and NOR-1 expressed in atherosclerotic lesion macrophages reduce lipid loading and inflammatory responses. *Arterioscler Thromb Vasc Biol,* 26**,** 2288-94.

BOURGUET, W., GERMAIN, P. & GRONEMEYER, H. 2000. Nuclear receptor ligand-binding domains: three-dimensional structures, molecular interactions and pharmacological implications. *Trends Pharmacol Sci,* 21**,** 381-8.

BROWN, G. C. & NEHER, J. J. 2014. Microglial phagocytosis of live neurons. *Nat Rev Neurosci,* 15**,** 209-16.

BRUNING, J. M., WANG, Y., OLTRABELLA, F., TIAN, B., KHOLODAR, S. A., LIU, H., BHATTACHARYA, P., GUO, S., HOLTON, J. M., FLETTERICK, R. J., JACOBSON, M. P. & ENGLAND, P. M. 2019. Covalent Modification and Regulation of the Nuclear Receptor Nurr1 by a Dopamine Metabolite. *Cell Chem Biol,* 26**,** 674-685.e6.

BRUZELIUS, A., HIDALGO, I., BOZA-SERRANO, A., HJELMER, A. G., TISON, A., DEIERBORG, T., BENGZON, J. & RAMOS-MORENO, T. 2021. The human bone marrow harbors a CD45(-) CD11B(+) cell progenitor permitting rapid microglia-like cell derivative approaches. *Stem Cells Transl Med,* 10**,** 582-597.

BURNS, K. A., LI, Y., ARAO, Y., PETROVICH, R. M. & KORACH, K. S. 2011. Selective mutations in estrogen receptor alpha D-domain alters nuclear translocation and non-estrogen response element gene regulatory mechanisms. *J Biol Chem,* 286**,** 12640-9.

BUTCHER, S. K., O'CARROLL, C. E., WELLS, C. A. & CARMODY, R. J. 2018. Toll-Like Receptors Drive Specific Patterns of Tolerance and Training on Restimulation of Macrophages. *Front Immunol,* 9**,** 933.

BÄCKMAN, C., PERLMANN, T., WALLÉN, A., HOFFER, B. J. & MORALES, M. 1999. A selective group of dopaminergic neurons express Nurr1 in the adult mouse brain. *Brain Res,* 851**,** 125-32.

CAO, F., XIE, X., GOLLAN, T., ZHAO, L., NARSINH, K., LEE, R. J. & WU, J. C. 2010. Comparison of gene-transfer efficiency in human embryonic stem cells. *Mol Imaging Biol,* 12**,** 15-24.

CAPILI, A. D. & LIMA, C. D. 2007. Taking it step by step: mechanistic insights from structural studies of ubiquitin/ubiquitin-like protein modification pathways. *Curr Opin Struct Biol,* 17**,** 726-35.

CARATTI, G., MATTHEWS, L., POOLMAN, T., KERSHAW, S., BAXTER, M. & RAY, D. 2015. Glucocorticoid receptor function in health and disease. *Clin Endocrinol (Oxf),* 83**,** 441-8.

CASTILLO, S. O., BAFFI, J. S., PALKOVITS, M., GOLDSTEIN, D. S., KOPIN, I. J., WITTA, J., MAGNUSON, M. A. & NIKODEM, V. M. 1998a. Dopamine biosynthesis is selectively abolished in substantia nigra/ventral tegmental area but not in hypothalamic neurons in mice with targeted disruption of the Nurr1 gene. *Mol Cell Neurosci,* 11**,** 36-46.

CASTILLO, S. O., XIAO, Q., KOSTROUCH, Z., DOZIN, B. & NIKODEM, V. M. 1998b. A divergent role of COOH-terminal domains in Nurr1 and Nur77 transactivation. *Gene Expr,* 7**,** 1-12.

CASTILLO, S. O., XIAO, Q., LYU, M. S., KOZAK, C. A. & NIKODEM, V. M. 1997. Organization, sequence, chromosomal localization, and promoter identification of the mouse orphan nuclear receptor Nurr1 gene. *Genomics,* 41**,** 250-7.

CASTRO, D. S., ARVIDSSON, M., BONDESSON BOLIN, M. & PERLMANN, T. 1999. Activity of the Nurr1 carboxyl-terminal domain depends on cell type and integrity of the activation function 2. *J Biol Chem,* 274**,** 37483-90.

CASTRO-VINUELAS, R., SANJURJO-RODRIGUEZ, C., PINEIRO-RAMIL, M., RODRIGUEZ-FERNANDEZ, S., LOPEZ-BALTAR, I., FUENTES-BOQUETE, I., BLANCO, F. J. & DIAZ-PRADO, S. 2021. Tips and tricks for successfully culturing and adapting human induced pluripotent stem cells. *Mol Ther Methods Clin Dev,* 23**,** 569-581.

CHALKIADAKI, A. & TALIANIDIS, I. 2005. SUMO-dependent compartmentalization in promyelocytic leukemia protein nuclear bodies prevents the access of LRH-1 to chromatin. *Mol Cell Biol,* 25**,** 5095-105.

CHAMBERS, I., COLBY, D., ROBERTSON, M., NICHOLS, J., LEE, S., TWEEDIE, S. & SMITH, A. 2003. Functional expression cloning of Nanog, a pluripotency sustaining factor in embryonic stem cells. *Cell,* 113**,** 643-55.

CHANG, C. Y., TING, H. C., LIU, C. A., SU, H. L., CHIOU, T. W., LIN, S. Z., HARN, H. J. & HO, T. J. 2020. Induced Pluripotent Stem Cell (iPSC)-Based Neurodegenerative Disease Models for Phenotype Recapitulation and Drug Screening. *Molecules,* 25.

CHATTERJEE, I., LI, F., KOHLER, E. E., REHMAN, J., MALIK, A. B. & WARY, K. K. 2016. Induced Pluripotent Stem (iPS) Cell Culture Methods and Induction of Differentiation into Endothelial Cells. *Methods Mol Biol,* 1357**,** 311-27.

CHATTERJEE, V. K., LEE, J. K., RENTOUMIS, A. & JAMESON, J. L. 1989. Negative regulation of the thyroid-stimulating hormone alpha gene by thyroid

hormone: receptor interaction adjacent to the TATA box. *Proc Natl Acad Sci U S A,* 86**,** 9114-8.
CHEN, J. & IVASHKIV, L. B. 2010. IFN-gamma abrogates endotoxin tolerance by facilitating Toll-like receptor-induced chromatin remodeling. *Proc Natl Acad Sci U S A,* 107**,** 19438-43.
CHEN, J. D. & EVANS, R. M. 1995. A transcriptional co-repressor that interacts with nuclear hormone receptors. *Nature,* 377**,** 454-7.
CHEN, X., HU, Y., CAO, Z., LIU, Q. & CHENG, Y. 2018. Cerebrospinal Fluid Inflammatory Cytokine Aberrations in Alzheimer's Disease, Parkinson's Disease and Amyotrophic Lateral Sclerosis: A Systematic Review and Meta-Analysis. *Front Immunol,* 9**,** 2122.
CHENG, J., BAWA, T., LEE, P., GONG, L. & YEH, E. T. 2006. Role of desumoylation in the development of prostate cancer. *Neoplasia,* 8**,** 667-76.
CHLEBANOWSKA, P., SUŁKOWSKI, M., SKRZYPEK, K., TEJCHMAN, A., MUSZYŃSKA, A., NOROOZI, R. & MAJKA, M. 2020. Origin of the Induced Pluripotent Stem Cells Affects Their Differentiation into Dopaminergic Neurons. *Int J Mol Sci,* 21.
CHU, Y., KOMPOLITI, K., COCHRAN, E. J., MUFSON, E. J. & KORDOWER, J. H. 2002. Age-related decreases in Nurr1 immunoreactivity in the human substantia nigra. *J Comp Neurol,* 450**,** 203-14.
CHU, Y., LE, W., KOMPOLITI, K., JANKOVIC, J., MUFSON, E. J. & KORDOWER, J. H. 2006. Nurr1 in Parkinson's disease and related disorders. *J Comp Neurol,* 494**,** 495-514.
CHUNG, S., SONNTAG, K. C., ANDERSSON, T., BJORKLUND, L. M., PARK, J. J., KIM, D. W., KANG, U. J., ISACSON, O. & KIM, K. S. 2002. Genetic engineering of mouse embryonic stem cells by Nurr1 enhances differentiation and maturation into dopaminergic neurons. *Eur J Neurosci,* 16**,** 1829-38.
COLÓN-CESARIO, W. I., MARTÍNEZ-MONTEMAYOR, M. M., MORALES, S., FÉLIX, J., CRUZ, J., ADORNO, M., PEREIRA, L., COLÓN, N., MALDONADO-VLAAR, C. S. & PEÑA DE ORTIZ, S. 2006. Knockdown of Nurr1 in the rat hippocampus: implications to spatial discrimination learning and memory. *Learn Mem,* 13**,** 734-44.
CONSTANTINO, A. E. & HONIG, L. S. 2001. Parkinson's disease. *Sci Aging Knowledge Environ,* 2001**,** dn4.
CUADROS, M. A. & NAVASCUES, J. 1998. The origin and differentiation of microglial cells during development. *Prog Neurobiol,* 56**,** 173-89.
DAI, D., YUAN, J., WANG, Y., XU, J., MAO, C. & XIAO, Y. 2019. Peli1 controls the survival of dopaminergic neurons through modulating microglia-mediated neuroinflammation. *Sci Rep,* 9**,** 8034.
DAVIES, T. F., ANDO, T., LIN, R. Y., TOMER, Y. & LATIF, R. 2005. Thyrotropin receptor-associated diseases: from adenomata to Graves disease. *J Clin Invest,* 115**,** 1972-83.
DAVIS, H. E., MORGAN, J. R. & YARMUSH, M. L. 2002. Polybrene increases retrovirus gene transfer efficiency by enhancing receptor-independent virus adsorption on target cell membranes. *Biophys Chem,* 97**,** 159-72.
DE MIRANDA, B. R., POPICHAK, K. A., HAMMOND, S. L., JORGENSEN, B. A., PHILLIPS, A. T., SAFE, S. & TJALKENS, R. B. 2015. The Nurr1 Activator 1,1-Bis(3'-Indolyl)-

1-(p-Chlorophenyl)Methane Blocks Inflammatory Gene Expression in BV-2 Microglial Cells by Inhibiting Nuclear Factor κB. *Mol Pharmacol,* 87**,** 1021-34.
DE VERA, I. M., GIRI, P. K., MUNOZ-TELLO, P., BRUST, R., FUHRMANN, J., MATTA-CAMACHO, E., SHANG, J., CAMPBELL, S., WILSON, H. D., GRANADOS, J., GARDNER, W. J., CREAMER, T. P., SOLT, L. A. & KOJETIN, D. J. 2016. Identification of a Binding Site for Unsaturated Fatty Acids in the Orphan Nuclear Receptor Nurr1. *ACS Chem Biol,* 11**,** 1795-9.
DE VERA, I. M. S. 2018. Advances in Orphan Nuclear Receptor Pharmacology: A New Era in Drug Discovery. *ACS Pharmacol Transl Sci,* 1**,** 134-137.
DE VERA, I. M. S., MUNOZ-TELLO, P., ZHENG, J., DHARMARAJAN, V., MARCIANO, D. P., MATTA-CAMACHO, E., GIRI, P. K., SHANG, J., HUGHES, T. S., RANCE, M., GRIFFIN, P. R. & KOJETIN, D. J. 2019. Defining a Canonical Ligand-Binding Pocket in the Orphan Nuclear Receptor Nurr1. *Structure,* 27**,** 66-77.e5.
DECRESSAC, M., VOLAKAKIS, N., BJÖRKLUND, A. & PERLMANN, T. 2013. NURR1 in Parkinson disease--from pathogenesis to therapeutic potential. *Nat Rev Neurol,* 9**,** 629-36.
DELEIDI, M. & GASSER, T. 2013. The role of inflammation in sporadic and familial Parkinson's disease. *Cell Mol Life Sci,* 70**,** 4259-73.
DELMOTTE, M. H., TAHAYATO, A., FORMSTECHER, P. & LEFEBVRE, P. 1999. Serine 157, a retinoic acid receptor alpha residue phosphorylated by protein kinase C in vitro, is involved in RXR.RARalpha heterodimerization and transcriptional activity. *J Biol Chem,* 274**,** 38225-31.
DESTERRO, J. M., RODRIGUEZ, M. S. & HAY, R. T. 1998. SUMO-1 modification of IkappaBalpha inhibits NF-kappaB activation. *Mol Cell,* 2**,** 233-9.
DIAZ, K., KOHUT, M. L., RUSSELL, D. W. & STEGEMOLLER, E. L. 2022. Peripheral inflammatory cytokines and motor symptoms in persons with Parkinson's disease. *Brain Behav Immun Health,* 21**,** 100442.
DING, L., YANG, L., WANG, Z. & HUANG, W. 2015. Bile acid nuclear receptor FXR and digestive system diseases. *Acta Pharm Sin B,* 5**,** 135-44.
DOHMEN, R. J. 2004. SUMO protein modification. *Biochim Biophys Acta,* 1695**,** 113-31.
DOKKA, S., TOLEDO, D., SHI, X., YE, J. & ROJANASAKUL, Y. 2000. High-efficiency gene transfection of macrophages by lipoplexes. *Int J Pharm,* 206**,** 97-104.
DONG, J., CUI, Y., LI, S. & LE, W. 2016a. Current Pharmaceutical Treatments and Alternative Therapies of Parkinson's Disease. *Curr Neuropharmacol,* 14**,** 339-55.
DONG, J., LI, S., MO, J. L., CAI, H. B. & LE, W. D. 2016b. Nurr1-Based Therapies for Parkinson's Disease. *CNS Neurosci Ther,* 22**,** 351-9.
DONG, S. X. M., CABALLERO, R., ALI, H., ROY, D. L. F., CASSOL, E. & KUMAR, A. 2020. Transfection of hard-to-transfect primary human macrophages with Bax siRNA to reverse Resveratrol-induced apoptosis. *RNA Biol,* 17**,** 755-764.
DORVAL, V. & FRASER, P. E. 2006. Small ubiquitin-like modifier (SUMO) modification of natively unfolded proteins tau and alpha-synuclein. *J Biol Chem,* 281**,** 9919-24.
DORVAL, V., MAZZELLA, M. J., MATHEWS, P. M., HAY, R. T. & FRASER, P. E. 2007. Modulation of Abeta generation by small ubiquitin-like modifiers does not require conjugation to target proteins. *Biochem J,* 404**,** 309-16.

DOUVARAS, P., SUN, B., WANG, M., KRUGLIKOV, I., LALLOS, G., ZIMMER, M., TERRENOIRE, C., ZHANG, B., GANDY, S., SCHADT, E., FREYTES, D. O., NOGGLE, S. & FOSSATI, V. 2017. Directed Differentiation of Human Pluripotent Stem Cells to Microglia. *Stem Cell Reports,* 8**,** 1516-1524.

DUVAL, D., DUVAL, G., KEDINGER, C., POCH, O. & BOEUF, H. 2003. The 'PINIT' motif, of a newly identified conserved domain of the PIAS protein family, is essential for nuclear retention of PIAS3L. *FEBS Lett,* 554**,** 111-8.

DZAMKO, N., GYSBERS, A., PERERA, G., BAHAR, A., SHANKAR, A., GAO, J., FU, Y. & HALLIDAY, G. M. 2017. Toll-like receptor 2 is increased in neurons in Parkinson's disease brain and may contribute to alpha-synuclein pathology. *Acta Neuropathol,* 133**,** 303-319.

ECKERMANN, K. 2013. SUMO and Parkinson's disease. *Neuromolecular Med,* 15**,** 737-59.

EL-KHAIRI, R. & ACHERMANN, J. C. 2012. Steroidogenic factor-1 and human disease. *Semin Reprod Med,* 30**,** 374-81.

FAN, X., LUO, G., MING, M., PU, P., LI, L., YANG, D. & LE, W. 2009. Nurr1 expression and its modulation in microglia. *Neuroimmunomodulation,* 16**,** 162-70.

FANG, W., BI, D., ZHENG, R., CAI, N., XU, H., ZHOU, R., LU, J., WAN, M. & XU, X. 2017. Identification and activation of TLR4-mediated signalling pathways by alginate-derived guluronate oligosaccharide in RAW264.7 macrophages. *Sci Rep,* 7**,** 1663.

FEARNLEY, J. M. & LEES, A. J. 1991. Ageing and Parkinson's disease: substantia nigra regional selectivity. *Brain,* 114 (Pt 5)**,** 2283-301.

FEI, E., JIA, N., YAN, M., YING, Z., SUN, Q., WANG, H., ZHANG, T., MA, X., DING, H., YAO, X., SHI, Y. & WANG, G. 2006. SUMO-1 modification increases human SOD1 stability and aggregation. *Biochem Biophys Res Commun,* 347**,** 406-12.

FENG, C., JIA, Y. D. & ZHAO, X. Y. 2013. Pluripotency of induced pluripotent stem cells. *Genomics Proteomics Bioinformatics,* 11**,** 299-303.

FLOTHO, A. & WERNER, A. 2012. The RanBP2/RanGAP1*SUMO1/Ubc9 complex: a multisubunit E3 ligase at the intersection of sumoylation and the RanGTPase cycle. *Nucleus,* 3**,** 429-32.

FORMAN, B. M., UMESONO, K., CHEN, J. & EVANS, R. M. 1995. Unique response pathways are established by allosteric interactions among nuclear hormone receptors. *Cell,* 81**,** 541-50.

FOSTER, S. L., HARGREAVES, D. C. & MEDZHITOV, R. 2007. Gene-specific control of inflammation by TLR-induced chromatin modifications. *Nature,* 447**,** 972-8.

FUSCO, G., CHEN, S. W., WILLIAMSON, P. T. F., CASCELLA, R., PERNI, M., JARVIS, J. A., CECCHI, C., VENDRUSCOLO, M., CHITI, F., CREMADES, N., YING, L., DOBSON, C. M. & DE SIMONE, A. 2017. Structural basis of membrane disruption and cellular toxicity by α-synuclein oligomers. *Science,* 358**,** 1440-1443.

GALLEGUILLOS, D., VECCHIOLA, A., FUENTEALBA, J. A., OJEDA, V., ALVAREZ, K., GÓMEZ, A. & ANDRÉS, M. E. 2004. PIASgamma represses the transcriptional activation induced by the nuclear receptor Nurr1. *J Biol Chem,* 279**,** 2005-11.

GAMMILL, L. S. & SIVE, H. 2001. otx2 expression in the ectoderm activates anterior neural determination and is required for Xenopus cement gland formation. *Dev Biol,* 240**,** 223-36.

GARCIA-YAGUE, A. J., RADA, P., ROJO, A. I., LASTRES-BECKER, I. & CUADRADO, A. 2013. Nuclear import and export signals control the subcellular localization of Nurr1 protein in response to oxidative stress. *J Biol Chem,* 288**,** 5506-17.

GAREAU, J. R. & LIMA, C. D. 2010. The SUMO pathway: emerging mechanisms that shape specificity, conjugation and recognition. *Nat Rev Mol Cell Biol,* 11**,** 861-71.

GERHARD, A. 2016. TSPO imaging in parkinsonian disorders. *Clin Transl Imaging,* 4**,** 183-190.

GERHARD, A., PAVESE, N., HOTTON, G., TURKHEIMER, F., ES, M., HAMMERS, A., EGGERT, K., OERTEL, W., BANATI, R. B. & BROOKS, D. J. 2006. In vivo imaging of microglial activation with [11C](R)-PK11195 PET in idiopathic Parkinson's disease. *Neurobiol Dis,* 21**,** 404-12.

GERMAIN, P., KAMMERER, S., PEREZ, E., PELUSO-ILTIS, C., TORTOLANI, D., ZUSI, F. C., STARRETT, J., LAPOINTE, P., DARIS, J. P., MARINIER, A., DE LERA, A. R., ROCHEL, N. & GRONEMEYER, H. 2004. Rational design of RAR-selective ligands revealed by RARbeta crystal stucture. *EMBO Rep,* 5**,** 877-82.

GERMAIN, P., STAELS, B., DACQUET, C., SPEDDING, M. & LAUDET, V. 2006. Overview of nomenclature of nuclear receptors. *Pharmacol Rev,* 58**,** 685-704.

GHASEMI-DEHKORDI, P., ALLAHBAKHSHIAN-FARSANI, M., ABDIAN, N., MIRZAEIAN, A., SAFFARI-CHALESHTORI, J., HEYBATI, F., MARDANI, G., KARIMI-TAGHANAKI, A., DOOSTI, A., JAMI, M. S., ABOLHASANI, M. & HASHEMZADEH-CHALESHTORI, M. 2015. Comparison between the cultures of human induced pluripotent stem cells (hiPSCs) on feeder-and serum-free system (Matrigel matrix), MEF and HDF feeder cell lines. *J Cell Commun Signal,* 9**,** 233-46.

GHISLETTI, S., HUANG, W., OGAWA, S., PASCUAL, G., LIN, M. E., WILLSON, T. M., ROSENFELD, M. G. & GLASS, C. K. 2007. Parallel SUMOylation-dependent pathways mediate gene- and signal-specific transrepression by LXRs and PPARgamma. *Mol Cell,* 25**,** 57-70.

GILL, G. 2005. Something about SUMO inhibits transcription. *Curr Opin Genet Dev,* 15**,** 536-41.

GILMOZZI, V., GENTILE, G., RIEKSCHNITZ, D. A., VON TROYER, M., LAVDAS, A. A., KERSCHBAMER, E., WEICHENBERGER, C. X., ROSATO-SIRI, M. D., CASAROSA, S., CONTI, L., PRAMSTALLER, P. P., HICKS, A. A., PICHLER, I. & ZANON, A. 2021. Generation of hiPSC-Derived Functional Dopaminergic Neurons in Alginate-Based 3D Culture. *Front Cell Dev Biol,* 9**,** 708389.

GLASS, C. K. & SAIJO, K. 2010. Nuclear receptor transrepression pathways that regulate inflammation in macrophages and T cells. *Nat Rev Immunol,* 10**,** 365-76.

GONG, L., MILLAS, S., MAUL, G. G. & YEH, E. T. 2000. Differential regulation of sentrinized proteins by a novel sentrin-specific protease. *J Biol Chem,* 275**,** 3355-9.

GONZALEZ DE AGUILAR, J. L., ECHANIZ-LAGUNA, A., FERGANI, A., RENÉ, F., MEININGER, V., LOEFFLER, J. P. & DUPUIS, L. 2007. Amyotrophic lateral sclerosis: all roads lead to Rome. *J Neurochem,* 101**,** 1153-60.

GOPALAKRISHNA-PILLAI, S. & IVERSON, L. E. 2011. A DNMT3B alternatively spliced exon and encoded peptide are novel biomarkers of human pluripotent stem cells. *PLoS One,* 6**,** e20663.

GRATUZE, M., LEYNS, C. E. G. & HOLTZMAN, D. M. 2018. New insights into the role of TREM2 in Alzheimer's disease. *Mol Neurodegener,* 13**,** 66.

GRESCHIK, H., WURTZ, J. M., SANGLIER, S., BOURGUET, W., VAN DORSSELAER, A., MORAS, D. & RENAUD, J. P. 2002. Structural and functional evidence for ligand-independent transcriptional activation by the estrogen-related receptor 3. *Mol Cell,* 9**,** 303-13.

GRETER, M., LELIOS, I., PELCZAR, P., HOEFFEL, G., PRICE, J., LEBOEUF, M., KUNDIG, T. M., FREI, K., GINHOUX, F., MERAD, M. & BECHER, B. 2012. Stroma-derived interleukin-34 controls the development and maintenance of langerhans cells and the maintenance of microglia. *Immunity,* 37**,** 1050-1060.

GRIMES, D. A., HAN, F., PANISSET, M., RACACHO, L., XIAO, F., ZOU, R., WESTAFF, K. & BULMAN, D. E. 2006. Translated mutation in the Nurr1 gene as a cause for Parkinson's disease. *Mov Disord,* 21**,** 906-9.

GUO, S., WANG, H. & YIN, Y. 2022. Microglia Polarization From M1 to M2 in Neurodegenerative Diseases. *Front Aging Neurosci,* 14**,** 815347.

HAENSELER, W., SANSOM, S. N., BUCHRIESER, J., NEWEY, S. E., MOORE, C. S., NICHOLLS, F. J., CHINTAWAR, S., SCHNELL, C., ANTEL, J. P., ALLEN, N. D., CADER, M. Z., WADE-MARTINS, R., JAMES, W. S. & COWLEY, S. A. 2017. A Highly Efficient Human Pluripotent Stem Cell Microglia Model Displays a Neuronal-Co-culture-Specific Expression Profile and Inflammatory Response. *Stem Cell Reports,* 8**,** 1727-1742.

HAMMER, G. D., KRYLOVA, I., ZHANG, Y., DARIMONT, B. D., SIMPSON, K., WEIGEL, N. L. & INGRAHAM, H. A. 1999. Phosphorylation of the nuclear receptor SF-1 modulates cofactor recruitment: integration of hormone signaling in reproduction and stress. *Mol Cell,* 3**,** 521-6.

HAMMOND, S. L., POPICHAK, K. A., LI, X., HUNT, L. G., RICHMAN, E. H., DAMALE, P. U., CHONG, E. K. P., BACKOS, D. S., SAFE, S. & TJALKENS, R. B. 2018. The Nurr1 Ligand,1,1-bis(3'-Indolyl)-1-(*J Pharmacol Exp Ther,* 365**,** 636-651.

HAMMOND, S. L., SAFE, S. & TJALKENS, R. B. 2015. A novel synthetic activator of Nurr1 induces dopaminergic gene expression and protects against 6-hydroxydopamine neurotoxicity in vitro. *Neurosci Lett,* 607**,** 83-89.

HARDELAND, U., STEINACHER, R., JIRICNY, J. & SCHAR, P. 2002. Modification of the human thymine-DNA glycosylase by ubiquitin-like proteins facilitates enzymatic turnover. *EMBO J,* 21**,** 1456-64.

HENDRIKS, I. A., D'SOUZA, R. C., YANG, B., VERLAAN-DE VRIES, M., MANN, M. & VERTEGAAL, A. C. 2014. Uncovering global SUMOylation signaling networks in a site-specific manner. *Nat Struct Mol Biol,* 21**,** 927-36.

HENDRIKS, I. A. & VERTEGAAL, A. C. 2016. A comprehensive compilation of SUMO proteomics. *Nat Rev Mol Cell Biol,* 17**,** 581-95.

HENEKA, M. T., KUMMER, M. P. & LATZ, E. 2014. Innate immune activation in neurodegenerative disease. *Nat Rev Immunol,* 14**,** 463-77.

HENLEY, J. M., CRAIG, T. J. & WILKINSON, K. A. 2014. Neuronal SUMOylation: mechanisms, physiology, and roles in neuronal dysfunction. *Physiol Rev,* 94**,** 1249-85.

HEO, H. R., SONG, H., KIM, H. R., LEE, J. E., CHUNG, Y. G., KIM, W. J., YANG, S. R., KIM, K. S., CHUN, T., LEE, D. R. & HONG, S. H. 2018. Reprogramming mechanisms influence the maturation of hematopoietic progenitors from human pluripotent stem cells. *Cell Death Dis,* 9**,** 1090.

HERMANSON, E., JOSEPH, B., CASTRO, D., LINDQVIST, E., AARNISALO, P., WALLÉN, A., BENOIT, G., HENGERER, B., OLSON, L. & PERLMANN, T. 2003. Nurr1 regulates dopamine synthesis and storage in MN9D dopamine cells. *Exp Cell Res,* 288**,** 324-34.

HICKEY, C. M., WILSON, N. R. & HOCHSTRASSER, M. 2012. Function and regulation of SUMO proteases. *Nat Rev Mol Cell Biol,* 13**,** 755-66.

HIRAYAMA, D., IIDA, T. & NAKASE, H. 2017. The Phagocytic Function of Macrophage-Enforcing Innate Immunity and Tissue Homeostasis. *Int J Mol Sci,* 19.

HO, M. S. 2019. Microglia in Parkinson's Disease. *Adv Exp Med Biol,* 1175**,** 335-353.

HOBBS, S., REYNOSO, M., GEDDIS, A. V., MITROPHANOV, A. Y. & MATHENY, R. W., JR. 2018. LPS-stimulated NF-kappaB p65 dynamic response marks the initiation of TNF expression and transition to IL-10 expression in RAW 264.7 macrophages. *Physiol Rep,* 6**,** e13914.

HOCHSTRASSER, M. 2001. SP-RING for SUMO: new functions bloom for a ubiquitin-like protein. *Cell,* 107**,** 5-8.

HOEKSEMA, M. A., SCICLUNA, B. P., BOSHUIZEN, M. C., VAN DER VELDEN, S., NEELE, A. E., VAN DEN BOSSCHE, J., MATLUNG, H. L., VAN DEN BERG, T. K., GOOSSENS, P. & DE WINTHER, M. P. 2015. IFN-gamma priming of macrophages represses a part of the inflammatory program and attenuates neutrophil recruitment. *J Immunol,* 194**,** 3909-16.

HOFFMAN, L. M. & CARPENTER, M. K. 2005. Characterization and culture of human embryonic stem cells. *Nat Biotechnol,* 23**,** 699-708.

HOPPE, J. B., RATTRAY, M., TU, H., SALBEGO, C. G. & CIMAROSTI, H. 2013. SUMO-1 conjugation blocks beta-amyloid-induced astrocyte reactivity. *Neurosci Lett,* 546**,** 51-6.

HOUSER, M. C. & TANSEY, M. G. 2017. The gut-brain axis: is intestinal inflammation a silent driver of Parkinson's disease pathogenesis? *NPJ Parkinsons Dis,* 3**,** 3.

HUANG, W. & GLASS, C. K. 2010. Nuclear receptors and inflammation control: molecular mechanisms and pathophysiological relevance. *Arterioscler Thromb Vasc Biol,* 30**,** 1542-9.

HUNTER, T. & SUN, H. 2008. Crosstalk between the SUMO and ubiquitin pathways. *Ernst Schering Found Symp Proc***,** 1-16.

ICHINOSE, H., OHYE, T., SUZUKI, T., SUMI-ICHINOSE, C., NOMURA, T., HAGINO, Y. & NAGATSU, T. 1999. Molecular cloning of the human Nurr1 gene: characterization of the human gene and cDNAs. *Gene,* 230**,** 233-9.

IDRISS, H. T. & NAISMITH, J. H. 2000. TNF alpha and the TNF receptor superfamily: structure-function relationship(s). *Microsc Res Tech,* 50**,** 184-95.

INVESTIGATORS, N. E. T. I. P. D. F.-Z. 2015. Pioglitazone in early Parkinson's disease: a phase 2, multicentre, double-blind, randomised trial. *Lancet Neurol,* 14**,** 795-803.

INVESTIGATORS, N. N.-P. 2008. A pilot clinical trial of creatine and minocycline in early Parkinson disease: 18-month results. *Clin Neuropharmacol,* 31**,** 141-50.

ISHIZUKA, T. & LAZAR, M. A. 2003. The N-CoR/histone deacetylase 3 complex is required for repression by thyroid hormone receptor. *Mol Cell Biol,* 23**,** 5122-31.
IWAWAKI, T., KOHNO, K. & KOBAYASHI, K. 2000. Identification of a potential nurr1 response element that activates the tyrosine hydroxylase gene promoter in cultured cells. *Biochem Biophys Res Commun,* 274**,** 590-5.
JANG, Y., KIM, W., LEBLANC, P., KIM, C. H. & KIM, K. S. 2021. Potent synthetic and endogenous ligands for the adopted orphan nuclear receptor Nurr1. *Exp Mol Med,* 53**,** 19-29.
JANKOVIC, J., CHEN, S. & LE, W. D. 2005. The role of Nurr1 in the development of dopaminergic neurons and Parkinson's disease. *Prog Neurobiol,* 77**,** 128-38.
JARDIN, C., HORN, A. H. & STICHT, H. 2015. Binding properties of SUMO-interacting motifs (SIMs) in yeast. *J Mol Model,* 21**,** 50.
JEON, S. G., YOO, A., CHUN, D. W., HONG, S. B., CHUNG, H., KIM, J. I. & MOON, M. 2020. The Critical Role of Nurr1 as a Mediator and Therapeutic Target in Alzheimer's Disease-related Pathogenesis. *Aging Dis,* 11**,** 705-724.
JIA, C., QI, H., CHENG, C., WU, X., YANG, Z., CAI, H., CHEN, S. & LE, W. 2020. α-Synuclein Negatively Regulates Nurr1 Expression Through NF-κB-Related Mechanism. *Front Mol Neurosci,* 13**,** 64.
JIN, X. & KRUTH, H. S. 2016. Culture of Macrophage Colony-stimulating Factor Differentiated Human Monocyte-derived Macrophages. *J Vis Exp*.
JOHNSON, E. S. 2004. Protein modification by SUMO. *Annu Rev Biochem,* 73**,** 355-82.
JOHNSON, E. S. & GUPTA, A. A. 2001. An E3-like factor that promotes SUMO conjugation to the yeast septins. *Cell,* 106**,** 735-44.
JOHNSON, E. S., SCHWIENHORST, I., DOHMEN, R. J. & BLOBEL, G. 1997. The ubiquitin-like protein Smt3p is activated for conjugation to other proteins by an Aos1p/Uba2p heterodimer. *EMBO J,* 16**,** 5509-19.
JOSA-PRADO, F., LUO, J., RUBIN, P., HENLEY, J. M. & WILKINSON, K. A. 2019. Developmental profiles of SUMOylation pathway proteins in rat cerebrum and cerebellum. *PLoS One,* 14**,** e0212857.
JUMPER, J., EVANS, R., PRITZEL, A., GREEN, T., FIGURNOV, M., RONNEBERGER, O., TUNYASUVUNAKOOL, K., BATES, R., ŽÍDEK, A., POTAPENKO, A., BRIDGLAND, A., MEYER, C., KOHL, S. A. A., BALLARD, A. J., COWIE, A., ROMERA-PAREDES, B., NIKOLOV, S., JAIN, R., ADLER, J., BACK, T., PETERSEN, S., REIMAN, D., CLANCY, E., ZIELINSKI, M., STEINEGGER, M., PACHOLSKA, M., BERGHAMMER, T., BODENSTEIN, S., SILVER, D., VINYALS, O., SENIOR, A. W., KAVUKCUOGLU, K., KOHLI, P. & HASSABIS, D. 2021. Highly accurate protein structure prediction with AlphaFold. *Nature,* 596**,** 583-589.
JURGA, A. M., PALECZNA, M. & KUTER, K. Z. 2020. Overview of General and Discriminating Markers of Differential Microglia Phenotypes. *Front Cell Neurosci,* 14**,** 198.
KADKHODAEI, B., ITO, T., JOODMARDI, E., MATTSSON, B., ROUILLARD, C., CARTA, M., MURAMATSU, S., SUMI-ICHINOSE, C., NOMURA, T., METZGER, D., CHAMBON, P., LINDQVIST, E., LARSSON, N. G., OLSON, L., BJÖRKLUND, A., ICHINOSE, H. & PERLMANN, T. 2009. Nurr1 is required for maintenance of maturing and adult midbrain dopamine neurons. *J Neurosci,* 29**,** 15923-32.

KANAI-AZUMA, M., KANAI, Y., GAD, J. M., TAJIMA, Y., TAYA, C., KUROHMARU, M., SANAI, Y., YONEKAWA, H., YAZAKI, K., TAM, P. P. & HAYASHI, Y. 2002. Depletion of definitive gut endoderm in Sox17-null mutant mice. *Development,* 129**,** 2367-79.

KANG, K., BACHU, M., PARK, S. H., KANG, K., BAE, S., PARK-MIN, K. H. & IVASHKIV, L. B. 2019. IFN-gamma selectively suppresses a subset of TLR4-activated genes and enhancers to potentiate macrophage activation. *Nat Commun,* 10**,** 3320.

KAWAI, T. & AKIRA, S. 2007. Signaling to NF-kappaB by Toll-like receptors. *Trends Mol Med,* 13**,** 460-9.

KELLER, A. A., MAESS, M. B., SCHNOOR, M., SCHEIDING, B. & LORKOWSKI, S. 2018. Transfecting Macrophages. *Methods Mol Biol,* 1784**,** 187-195.

KERSCHER, O. 2007. SUMO junction-what's your function? New insights through SUMO-interacting motifs. *EMBO Rep,* 8**,** 550-5.

KHORASANIZADEH, S. & RASTINEJAD, F. 2001. Nuclear-receptor interactions on DNA-response elements. *Trends Biochem Sci,* 26**,** 384-90.

KILPINEN, H., GONCALVES, A., LEHA, A., AFZAL, V., ALASOO, K., ASHFORD, S., BALA, S., BENSADDEK, D., CASALE, F. P., CULLEY, O. J., DANECEK, P., FAULCONBRIDGE, A., HARRISON, P. W., KATHURIA, A., MCCARTHY, D., MCCARTHY, S. A., MELECKYTE, R., MEMARI, Y., MOENS, N., SOARES, F., MANN, A., STREETER, I., AGU, C. A., ALDERTON, A., NELSON, R., HARPER, S., PATEL, M., WHITE, A., PATEL, S. R., CLARKE, L., HALAI, R., KIRTON, C. M., KOLB-KOKOCINSKI, A., BEALES, P., BIRNEY, E., DANOVI, D., LAMOND, A. I., OUWEHAND, W. H., VALLIER, L., WATT, F. M., DURBIN, R., STEGLE, O. & GAFFNEY, D. J. 2017. Common genetic variation drives molecular heterogeneity in human iPSCs. *Nature,* 546**,** 370-375.

KIM, C. H., HAN, B. S., MOON, J., KIM, D. J., SHIN, J., RAJAN, S., NGUYEN, Q. T., SOHN, M., KIM, W. G., HAN, M., JEONG, I., KIM, K. S., LEE, E. H., TU, Y., NAFFIN-OLIVOS, J. L., PARK, C. H., RINGE, D., YOON, H. S. & PETSKO, G. A. 2015. Nuclear receptor Nurr1 agonists enhance its dual functions and improve behavioral deficits in an animal model of Parkinson's disease. *Proc Natl Acad Sci U S A,* 112**,** 8756-61.

KIM, J. I., JEON, S. G., KIM, K. A., KIM, Y. J., SONG, E. J., CHOI, J., AHN, K. J., KIM, C. J., CHUNG, H. Y., MOON, M. & CHUNG, H. 2016. The pharmacological stimulation of Nurr1 improves cognitive functions via enhancement of adult hippocampal neurogenesis. *Stem Cell Res,* 17**,** 534-543.

KIM, K. S., KIM, C. H., HWANG, D. Y., SEO, H., CHUNG, S., HONG, S. J., LIM, J. K., ANDERSON, T. & ISACSON, O. 2003a. Orphan nuclear receptor Nurr1 directly transactivates the promoter activity of the tyrosine hydroxylase gene in a cell-specific manner. *J Neurochem,* 85**,** 622-34.

KIM, T. E., PARK, M. J., CHOI, E. J., LEE, H. S., LEE, S. H., YOON, S. H., OH, C. K., LEE, B. J., KIM, S. U., LEE, Y. S. & LEE, M. A. 2003b. Cloning and cell type-specific regulation of the human tyrosine hydroxylase gene promoter. *Biochem Biophys Res Commun,* 312**,** 1123-31.

KIM, T. E., SEO, J. S., YANG, J. W., KIM, M. W., KAUSAR, R., JOE, E., KIM, B. Y. & LEE, M. A. 2013. Nurr1 represses tyrosine hydroxylase expression via SIRT1 in human neural stem cells. *PLoS One,* 8**,** e71469.

KOBAYASHI, S., ASAKAWA, T., NOZAKI, T., SUGIYAMA, K., SAMESHIMA, T. & KUROZUMI, K. 2020. Development of a novel gripping test for the evaluation of the finger fine motor ability in MPTP-treated monkeys. *J Integr Neurosci,* 19**,** 209-215.

KORTEKAAS, R., LEENDERS, K. L., VAN OOSTROM, J. C., VAALBURG, W., BART, J., WILLEMSEN, A. T. & HENDRIKSE, N. H. 2005. Blood-brain barrier dysfunction in parkinsonian midbrain in vivo. *Ann Neurol,* 57**,** 176-9.

KOVALEVICH, J. & LANGFORD, D. 2013. Considerations for the use of SH-SY5Y neuroblastoma cells in neurobiology. *Methods Mol Biol,* 1078**,** 9-21.

KRAKAUER, T. & BUCKLEY, M. 2003. Doxycycline is anti-inflammatory and inhibits staphylococcal exotoxin-induced cytokines and chemokines. *Antimicrob Agents Chemother,* 47**,** 3630-3.

KUMAR, V., GREEN, S., STAUB, A. & CHAMBON, P. 1986. Localisation of the oestradiol-binding and putative DNA-binding domains of the human oestrogen receptor. *EMBO J,* 5**,** 2231-6.

LAFERLA, F. M., GREEN, K. N. & ODDO, S. 2007. Intracellular amyloid-beta in Alzheimer's disease. *Nat Rev Neurosci,* 8**,** 499-509.

LALLIER, S. W., GRAF, A. E., WAIDYARANTE, G. R. & ROGERS, L. K. 2016. Nurr1 expression is modified by inflammation in microglia. *Neuroreport,* 27**,** 1120-7.

LAW, S. W., CONNEELY, O. M., DEMAYO, F. J. & O'MALLEY, B. W. 1992. Identification of a new brain-specific transcription factor, NURR1. *Mol Endocrinol,* 6**,** 2129-35.

LAWRENCE, T. & NATOLI, G. 2011. Transcriptional regulation of macrophage polarization: enabling diversity with identity. *Nat Rev Immunol,* 11**,** 750-61.

LE, W., CONNEELY, O. M., HE, Y., JANKOVIC, J. & APPEL, S. H. 1999. Reduced Nurr1 expression increases the vulnerability of mesencephalic dopamine neurons to MPTP-induced injury. *J Neurochem,* 73**,** 2218-21.

LE, W., ROWE, D., XIE, W., ORTIZ, I., HE, Y. & APPEL, S. H. 2001. Microglial activation and dopaminergic cell injury: an in vitro model relevant to Parkinson's disease. *J Neurosci,* 21**,** 8447-55.

LE, W. D., XU, P., JANKOVIC, J., JIANG, H., APPEL, S. H., SMITH, R. G. & VASSILATIS, D. K. 2003. Mutations in NR4A2 associated with familial Parkinson disease. *Nat Genet,* 33**,** 85-9.

LEE, H. S., BAE, E. J., YI, S. H., SHIM, J. W., JO, A. Y., KANG, J. S., YOON, E. H., RHEE, Y. H., PARK, C. H., KOH, H. C., KIM, H. J., CHOI, H. S., HAN, J. W., LEE, Y. S., KIM, J., LI, J. Y., BRUNDIN, P. & LEE, S. H. 2010. Foxa2 and Nurr1 synergistically yield A9 nigral dopamine neurons exhibiting improved differentiation, function, and cell survival. *Stem Cells,* 28**,** 501-12.

LEE, J. H. & LEE, M. J. 2012. Emerging roles of the ubiquitin-proteasome system in the steroid receptor signaling. *Arch Pharm Res,* 35**,** 397-407.

LEE, J. H., PARK, S. M., KIM, O. S., LEE, C. S., WOO, J. H., PARK, S. J., JOE, E. H. & JOU, I. 2009. Differential SUMOylation of LXRalpha and LXRbeta mediates transrepression of STAT1 inflammatory signaling in IFN-gamma-stimulated brain astrocytes. *Mol Cell,* 35**,** 806-17.

LEE, M. B., LEBEDEVA, L. A., SUZAWA, M., WADEKAR, S. A., DESCLOZEAUX, M. & INGRAHAM, H. A. 2005. The DEAD-box protein DP103 (Ddx20 or Gemin-3)

represses orphan nuclear receptor activity via SUMO modification. *Mol Cell Biol,* 25**,** 1879-90.

LEE, M. K., STIRLING, W., XU, Y., XU, X., QUI, D., MANDIR, A. S., DAWSON, T. M., COPELAND, N. G., JENKINS, N. A. & PRICE, D. L. 2002. Human alpha-synuclein-harboring familial Parkinson's disease-linked Ala-53 --> Thr mutation causes neurodegenerative disease with alpha-synuclein aggregation in transgenic mice. *Proc Natl Acad Sci U S A,* 99**,** 8968-73.

LEE, S. H., KWON, J. Y., KIM, S. Y., JUNG, K. & CHO, M. L. 2017. Interferon-gamma regulates inflammatory cell death by targeting necroptosis in experimental autoimmune arthritis. *Sci Rep,* 7**,** 10133.

LENZ, K. M. & NELSON, L. H. 2018. Microglia and Beyond: Innate Immune Cells As Regulators of Brain Development and Behavioral Function. *Front Immunol,* 9**,** 698.

LESSLICH, H. M., KLAPAL, L., WILKE, J., HAAK, A. & DIETZEL, I. D. 2022. Adjusting the neuron to astrocyte ratio with cytostatics in hippocampal cell cultures from postnatal rats: A comparison of cytarabino furanoside (AraC) and 5-fluoro-2'-deoxyuridine (FUdR). *PLoS One,* 17**,** e0265084.

LEYVA, F. J., ANZINGER, J. J., MCCOY, J. P., JR. & KRUTH, H. S. 2011. Evaluation of transduction efficiency in macrophage colony-stimulating factor differentiated human macrophages using HIV-1 based lentiviral vectors. *BMC Biotechnol,* 11**,** 13.

LI, T., YANG, Z., LI, S., CHENG, C., SHEN, B. & LE, W. 2018. Alterations of NURR1 and Cytokines in the Peripheral Blood Mononuclear Cells: Combined Biomarkers for Parkinson's Disease. *Front Aging Neurosci,* 10**,** 392.

LI, X., LUO, Y., YU, L., LIN, Y., LUO, D., ZHANG, H., HE, Y., KIM, Y. O., KIM, Y., TANG, S. & MIN, W. 2008. SENP1 mediates TNF-induced desumoylation and cytoplasmic translocation of HIPK1 to enhance ASK1-dependent apoptosis. *Cell Death Differ,* 15**,** 739-50.

LILLEY, C. M., ALARCON, A., NGO, M. H., ARAUJO, J. S., MARRERO, L. & MIX, K. S. 2022. Orphan Nuclear Receptor NR4A2 Is Constitutively Expressed in Cartilage and Upregulated in Inflamed Synovium From hTNF-Alpha Transgenic Mice. *Front Pharmacol,* 13**,** 835697.

LIN, S. J., ZHANG, Y., LIU, N. C., YANG, D. R., LI, G. & CHANG, C. 2014. Minireview: Pathophysiological roles of the TR4 nuclear receptor: lessons learned from mice lacking TR4. *Mol Endocrinol,* 28**,** 805-21.

LIN, X., PARISIADOU, L., SGOBIO, C., LIU, G., YU, J., SUN, L., SHIM, H., GU, X. L., LUO, J., LONG, C. X., DING, J., MATEO, Y., SULLIVAN, P. H., WU, L. G., GOLDSTEIN, D. S., LOVINGER, D. & CAI, H. 2012. Conditional expression of Parkinson's disease-related mutant α-synuclein in the midbrain dopaminergic neurons causes progressive neurodegeneration and degradation of transcription factor nuclear receptor related 1. *J Neurosci,* 32**,** 9248-64.

LIU, W., TASO, O., WANG, R., BAYRAM, S., GRAHAM, A. C., GARCIA-REITBOECK, P., MALLACH, A., ANDREWS, W. D., PIERS, T. M., BOTIA, J. A., POCOCK, J. M., CUMMINGS, D. M., HARDY, J., EDWARDS, F. A. & SALIH, D. A. 2020. Trem2 promotes anti-inflammatory responses in microglia and is suppressed under pro-inflammatory conditions. *Hum Mol Genet,* 29**,** 3224-3248.

LIU, W., ZENG, M. & FU, N. 2021. Functions of nuclear receptors SUMOylation. *Clin Chim Acta,* 516**,** 27-33.
LOIS, L. M. & LIMA, C. D. 2005. Structures of the SUMO E1 provide mechanistic insights into SUMO activation and E2 recruitment to E1. *EMBO J,* 24**,** 439-51.
LUISI, B. F., XU, W. X., OTWINOWSKI, Z., FREEDMAN, L. P., YAMAMOTO, K. R. & SIGLER, P. B. 1991. Crystallographic analysis of the interaction of the glucocorticoid receptor with DNA. *Nature,* 352**,** 497-505.
LYST, M. J. & STANCHEVA, I. 2007. A role for SUMO modification in transcriptional repression and activation. *Biochem Soc Trans,* 35**,** 1389-92.
MAHAJAN, R., DELPHIN, C., GUAN, T., GERACE, L. & MELCHIOR, F. 1997. A small ubiquitin-related polypeptide involved in targeting RanGAP1 to nuclear pore complex protein RanBP2. *Cell,* 88**,** 97-107.
MAHAJAN, S., SAINI, A., CHANDRA, V., NANDURI, R., KALRA, R., BHAGYARAJ, E., KHATRI, N. & GUPTA, P. 2015. Nuclear Receptor Nr4a2 Promotes Alternative Polarization of Macrophages and Confers Protection in Sepsis. *J Biol Chem,* 290**,** 18304-14.
MAIRA, M., MARTENS, C., PHILIPS, A. & DROUIN, J. 1999. Heterodimerization between members of the Nur subfamily of orphan nuclear receptors as a novel mechanism for gene activation. *Mol Cell Biol,* 19**,** 7549-57.
MANGELSDORF, D. J. & EVANS, R. M. 1995. The RXR heterodimers and orphan receptors. *Cell,* 83**,** 841-50.
MANGELSDORF, D. J., THUMMEL, C., BEATO, M., HERRLICH, P., SCHÜTZ, G., UMESONO, K., BLUMBERG, B., KASTNER, P., MARK, M., CHAMBON, P. & EVANS, R. M. 1995. The nuclear receptor superfamily: the second decade. *Cell,* 83**,** 835-9.
MARTIN, D. P., WALLACE, T. L. & JOHNSON, E. M., JR. 1990. Cytosine arabinoside kills postmitotic neurons in a fashion resembling trophic factor deprivation: evidence that a deoxycytidine-dependent process may be required for nerve growth factor signal transduction. *J Neurosci,* 10**,** 184-93.
MATSUMOTO, T., SAKARI, M., OKADA, M., YOKOYAMA, A., TAKAHASHI, S., KOUZMENKO, A. & KATO, S. 2013. The androgen receptor in health and disease. *Annu Rev Physiol,* 75**,** 201-24.
MAXWELL, M. A. & MUSCAT, G. E. 2006. The NR4A subgroup: immediate early response genes with pleiotropic physiological roles. *Nucl Recept Signal,* 4**,** e002.
MCEVOY, A. N., MURPHY, E. A., PONNIO, T., CONNEELY, O. M., BRESNIHAN, B., FITZGERALD, O. & MURPHY, E. P. 2002. Activation of nuclear orphan receptor NURR1 transcription by NF-kappa B and cyclic adenosine 5'-monophosphate response element-binding protein in rheumatoid arthritis synovial tissue. *J Immunol,* 168**,** 2979-87.
MCGEER, P. L., ITAGAKI, S., BOYES, B. E. & MCGEER, E. G. 1988. Reactive microglia are positive for HLA-DR in the substantia nigra of Parkinson's and Alzheimer's disease brains. *Neurology,* 38**,** 1285-91.
MCQUADE, A. & BLURTON-JONES, M. 2022. Human Induced Pluripotent Stem Cell-Derived Microglia (hiPSC-Microglia). *Methods Mol Biol,* 2454**,** 473-482.
MCQUADE, A., COBURN, M., TU, C. H., HASSELMANN, J., DAVTYAN, H. & BLURTON-JONES, M. 2018. Development and validation of a simplified method to

generate human microglia from pluripotent stem cells. *Mol Neurodegener,* 13**,** 67.

MELCHIOR, F. 2000. SUMO--nonclassical ubiquitin. *Annu Rev Cell Dev Biol,* 16**,** 591-626.

METIVIER, R., PENOT, G., FLOURIOT, G. & PAKDEL, F. 2001. Synergism between ERalpha transactivation function 1 (AF-1) and AF-2 mediated by steroid receptor coactivator protein-1: requirement for the AF-1 alpha-helical core and for a direct interaction between the N- and C-terminal domains. *Mol Endocrinol,* 15**,** 1953-70.

MEULMEESTER, E., KUNZE, M., HSIAO, H. H., URLAUB, H. & MELCHIOR, F. 2008. Mechanism and consequences for paralog-specific sumoylation of ubiquitin-specific protease 25. *Mol Cell,* 30**,** 610-9.

MIA, S., WARNECKE, A., ZHANG, X. M., MALMSTROM, V. & HARRIS, R. A. 2014. An optimized protocol for human M2 macrophages using M-CSF and IL-4/IL-10/TGF-beta yields a dominant immunosuppressive phenotype. *Scand J Immunol,* 79**,** 305-14.

MICHELHAUGH, S. K., VAITKEVICIUS, H., WANG, J., BOUHAMDAN, M., KRIEG, A. R., WALKER, J. L., MENDIRATTA, V. & BANNON, M. J. 2005. Dopamine neurons express multiple isoforms of the nuclear receptor nurr1 with diminished transcriptional activity. *J Neurochem,* 95**,** 1342-50.

MIZUNO, T., DOI, Y., MIZOGUCHI, H., JIN, S., NODA, M., SONOBE, Y., TAKEUCHI, H. & SUZUMURA, A. 2011. Interleukin-34 selectively enhances the neuroprotective effects of microglia to attenuate oligomeric amyloid-beta neurotoxicity. *Am J Pathol,* 179**,** 2016-27.

MO, Y. Y., YU, Y., THEODOSIOU, E., EE, P. L. & BECK, W. T. 2005. A role for Ubc9 in tumorigenesis. *Oncogene,* 24**,** 2677-83.

MOORE, D. J., ZHANG, L., DAWSON, T. M. & DAWSON, V. L. 2003. A missense mutation (L166P) in DJ-1, linked to familial Parkinson's disease, confers reduced protein stability and impairs homo-oligomerization. *J Neurochem,* 87**,** 1558-67.

MORAS, D. & GRONEMEYER, H. 1998. The nuclear receptor ligand-binding domain: structure and function. *Curr Opin Cell Biol,* 10**,** 384-91.

MOSLEY, R. L., HUTTER-SAUNDERS, J. A., STONE, D. K. & GENDELMAN, H. E. 2012. Inflammation and adaptive immunity in Parkinson's disease. *Cold Spring Harb Perspect Med,* 2**,** a009381.

MOUNT, M. P., LIRA, A., GRIMES, D., SMITH, P. D., FAUCHER, S., SLACK, R., ANISMAN, H., HAYLEY, S. & PARK, D. S. 2007. Involvement of interferon-gamma in microglial-mediated loss of dopaminergic neurons. *J Neurosci,* 27**,** 3328-37.

MUFFAT, J., LI, Y., YUAN, B., MITALIPOVA, M., OMER, A., CORCORAN, S., BAKIASI, G., TSAI, L. H., AUBOURG, P., RANSOHOFF, R. M. & JAENISCH, R. 2016. Efficient derivation of microglia-like cells from human pluripotent stem cells. *Nat Med,* 22**,** 1358-1367.

MUKHOPADHYAY, D. & DASSO, M. 2007. Modification in reverse: the SUMO proteases. *Trends Biochem Sci,* 32**,** 286-95.

MUNARRIZ, E., BARCAROLI, D., STEPHANOU, A., TOWNSEND, P. A., MAISSE, C., TERRINONI, A., NEALE, M. H., MARTIN, S. J., LATCHMAN, D. S., KNIGHT, R. A.,

MELINO, G. & DE LAURENZI, V. 2004. PIAS-1 is a checkpoint regulator which affects exit from G1 and G2 by sumoylation of p73. *Mol Cell Biol,* 24**,** 10593-610.
NAHRENDORF, M. & SWIRSKI, F. K. 2016. Abandoning M1/M2 for a Network Model of Macrophage Function. *Circ Res,* 119**,** 414-7.
NAMANJA, A. T., LI, Y. J., SU, Y., WONG, S., LU, J., COLSON, L. T., WU, C., LI, S. S. & CHEN, Y. 2012. Insights into high affinity small ubiquitin-like modifier (SUMO) recognition by SUMO-interacting motifs (SIMs) revealed by a combination of NMR and peptide array analysis. *J Biol Chem,* 287**,** 3231-40.
NG, Y. H., CHANDA, S., JANAS, J. A., YANG, N., KOKUBU, Y., SUDHOF, T. C. & WERNIG, M. 2021. Efficient generation of dopaminergic induced neuronal cells with midbrain characteristics. *Stem Cell Reports,* 16**,** 1763-1776.
NIELSEN, M. C., ANDERSEN, M. N. & MOLLER, H. J. 2020. Monocyte isolation techniques significantly impact the phenotype of both isolated monocytes and derived macrophages in vitro. *Immunology,* 159**,** 63-74.
OBERG, M., FABRIK, I., FABRIKOVA, D., ZEHETNER, N. & HARTLOVA, A. 2021. The role of innate immunity and inflammation in Parkinson s disease. *Scand J Immunol,* 93**,** e13022.
OH, M., KIM, S. Y., GIL, J. E., BYUN, J. S., CHA, D. W., KU, B., LEE, W., KIM, W. K., OH, K. J., LEE, E. W., BAE, K. H., LEE, S. C. & HAN, B. S. 2020. Nurr1 performs its anti-inflammatory function by regulating RasGRP1 expression in neuro-inflammation. *Sci Rep,* 10**,** 10755.
OH, M. S., HONG, S. J., HUH, Y. & KIM, K. S. 2009. Expression of transgenes in midbrain dopamine neurons using the tyrosine hydroxylase promoter. *Gene Ther,* 16**,** 437-40.
OH, Y., KIM, Y. M., MOURADIAN, M. M. & CHUNG, K. C. 2011. Human Polycomb protein 2 promotes α-synuclein aggregate formation through covalent SUMOylation. *Brain Res,* 1381**,** 78-89.
OHGIDANI, M., KATO, T. A., SETOYAMA, D., SAGATA, N., HASHIMOTO, R., SHIGENOBU, K., YOSHIDA, T., HAYAKAWA, K., SHIMOKAWA, N., MIURA, D., UTSUMI, H. & KANBA, S. 2014. Direct induction of ramified microglia-like cells from human monocytes: dynamic microglial dysfunction in Nasu-Hakola disease. *Sci Rep,* 4**,** 4957.
OHSAWA, K., IMAI, Y., KANAZAWA, H., SASAKI, Y. & KOHSAKA, S. 2000. Involvement of Iba1 in membrane ruffling and phagocytosis of macrophages/microglia. *J Cell Sci,* 113 (Pt 17)**,** 3073-84.
OHSHIMA, T., KOGA, H. & SHIMOTOHNO, K. 2004. Transcriptional activity of peroxisome proliferator-activated receptor gamma is modulated by SUMO-1 modification. *J Biol Chem,* 279**,** 29551-7.
OKABE, T., TAKAYANAGI, R., IMASAKI, K., HAJI, M., NAWATA, H. & WATANABE, T. 1995. cDNA cloning of a NGFI-B/nur77-related transcription factor from an apoptotic human T cell line. *J Immunol,* 154**,** 3871-9.
OLANOW, C. W., SAVOLAINEN, M., CHU, Y., HALLIDAY, G. M. & KORDOWER, J. H. 2019. Temporal evolution of microglia and alpha-synuclein accumulation following foetal grafting in Parkinson's disease. *Brain,* 142**,** 1690-1700.

OLIVIERO, F., LUKOWICZ, C., BOUSSADIA, B., FORNER-PIQUER, I., PASCUSSI, J. M., MARCHI, N. & MSELLI-LAKHAL, L. 2020. Constitutive Androstane Receptor: A Peripheral and a Neurovascular Stress or Environmental Sensor. *Cells,* 9.

ORDENTLICH, P., YAN, Y., ZHOU, S. & HEYMAN, R. A. 2003. Identification of the antineoplastic agent 6-mercaptopurine as an activator of the orphan nuclear hormone receptor Nurr1. *J Biol Chem,* 278**,** 24791-9.

OUYANG, J. & GILL, G. 2009. SUMO engages multiple corepressors to regulate chromatin structure and transcription. *Epigenetics,* 4**,** 440-4.

OUYANG, J., SHI, Y., VALIN, A., XUAN, Y. & GILL, G. 2009. Direct binding of CoREST1 to SUMO-2/3 contributes to gene-specific repression by the LSD1/CoREST1/HDAC complex. *Mol Cell,* 34**,** 145-54.

OWERBACH, D., MCKAY, E. M., YEH, E. T., GABBAY, K. H. & BOHREN, K. M. 2005. A proline-90 residue unique to SUMO-4 prevents maturation and sumoylation. *Biochem Biophys Res Commun,* 337**,** 517-20.

PAN, T., XIE, W., JANKOVIC, J. & LE, W. 2005. Biological effects of pramipexole on dopaminergic neuron-associated genes: relevance to neuroprotection. *Neurosci Lett,* 377**,** 106-9.

PARK, C. H., KANG, J. S., YOON, E. H., SHIM, J. W., SUH-KIM, H. & LEE, S. H. 2008. Proneural bHLH neurogenin 2 differentially regulates Nurr1-induced dopamine neuron differentiation in rat and mouse neural precursor cells in vitro. *FEBS Lett,* 582**,** 537-42.

PASCUAL, G., FONG, A. L., OGAWA, S., GAMLIEL, A., LI, A. C., PERISSI, V., ROSE, D. W., WILLSON, T. M., ROSENFELD, M. G. & GLASS, C. K. 2005. A SUMOylation-dependent pathway mediates transrepression of inflammatory response genes by PPAR-gamma. *Nature,* 437**,** 759-63.

PASCUAL, G. & GLASS, C. K. 2006. Nuclear receptors versus inflammation: mechanisms of transrepression. *Trends Endocrinol Metab,* 17**,** 321-7.

PAUL, S. N., WINGENFELD, K., OTTE, C. & MEIJER, O. C. 2022. Brain mineralocorticoid receptor in health and disease: From molecular signalling to cognitive and emotional function. *Br J Pharmacol,* 179**,** 3205-3219.

PEI, L., CASTRILLO, A., CHEN, M., HOFFMANN, A. & TONTONOZ, P. 2005. Induction of NR4A orphan nuclear receptor expression in macrophages in response to inflammatory stimuli. *J Biol Chem,* 280**,** 29256-62.

PENG, Y., SCHONEBERG, N., ESPOSITO, M. S., GEIGER, J. R. P., SHAROTT, A. & TOVOTE, P. 2022. Current approaches to characterize micro- and macroscale circuit mechanisms of Parkinson's disease in rodent models. *Exp Neurol,* 351**,** 114008.

PEREIRA, R. V., CABRAL, F. J., GOMES, M. S., BABA, E. H., JANNOTTI-PASSOS, L. K., CARVALHO, O., RODRIGUES, V., AFONSO, R. J., CASTRO-BORGES, W. & GUERRA-SÁ, R. 2011. Molecular characterization of SUMO E2 conjugation enzyme: differential expression profile in Schistosoma mansoni. *Parasitol Res,* 109**,** 1537-46.

PERLMANN, T. & JANSSON, L. 1995. A novel pathway for vitamin A signaling mediated by RXR heterodimerization with NGFI-B and NURR1. *Genes Dev,* 9**,** 769-82.

PICHLER, A., GAST, A., SEELER, J. S., DEJEAN, A. & MELCHIOR, F. 2002. The nucleoporin RanBP2 has SUMO1 E3 ligase activity. *Cell,* 108**,** 109-20.

PICHLER, A., KNIPSCHEER, P., SAITOH, H., SIXMA, T. K. & MELCHIOR, F. 2004. The RanBP2 SUMO E3 ligase is neither HECT- nor RING-type. *Nat Struct Mol Biol,* 11**,** 984-91.

POTASHKIN, J. A., BLUME, S. R. & RUNKLE, N. K. 2010. Limitations of animal models of Parkinson's disease. *Parkinsons Dis,* 2011**,** 658083.

POUKKA, H., KARVONEN, U., JANNE, O. A. & PALVIMO, J. J. 2000. Covalent modification of the androgen receptor by small ubiquitin-like modifier 1 (SUMO-1). *Proc Natl Acad Sci U S A,* 97**,** 14145-50.

POUNTNEY, D. L., HUANG, Y., BURNS, R. J., HAAN, E., THOMPSON, P. D., BLUMBERGS, P. C. & GAI, W. P. 2003. SUMO-1 marks the nuclear inclusions in familial neuronal intranuclear inclusion disease. *Exp Neurol,* 184**,** 436-46.

POURCET, B., STAELS, B. & GLINEUR, C. 2013. PPAR SUMOylation: some useful experimental tips. *Methods Mol Biol,* 952**,** 145-61.

POWELL, S. K., O'SHEA, C., TOWNSLEY, K., PRYTKOVA, I., DOBRINDT, K., ELAHI, R., ISKHAKOVA, M., LAMBERT, T., VALADA, A., LIAO, W., HO, S. M., SLESINGER, P. A., HUCKINS, L. M., AKBARIAN, S. & BRENNAND, K. J. 2021. Induction of dopaminergic neurons for neuronal subtype-specific modeling of psychiatric disease risk. *Mol Psychiatry*.

PSAKHYE, I. & JENTSCH, S. 2012. Protein group modification and synergy in the SUMO pathway as exemplified in DNA repair. *Cell,* 151**,** 807-820.

QIAN, Y., CHEN, X. X., WANG, W., LI, J. J., WANG, X. P., TANG, Z. W., XU, J. T., LIN, H., YANG, Z. Y., LI, L. Y., SONG, X. B., GUO, J. Z., BIAN, L. G., ZHOU, L., LU, D. & DENG, X. L. 2020. Transplantation of Nurr1-overexpressing neural stem cells and microglia for treating parkinsonian rats. *CNS Neurosci Ther,* 26**,** 55-65.

QIN, L., WU, X., BLOCK, M. L., LIU, Y., BREESE, G. R., HONG, J. S., KNAPP, D. J. & CREWS, F. T. 2007. Systemic LPS causes chronic neuroinflammation and progressive neurodegeneration. *Glia,* 55**,** 453-62.

RAI, M. A., HAMMONDS, J., PUJATO, M., MAYHEW, C., ROSKIN, K. & SPEARMAN, P. 2020. Comparative analysis of human microglial models for studies of HIV replication and pathogenesis. *Retrovirology,* 17**,** 35.

RAJAN, S., JANG, Y., KIM, C. H., KIM, W., TOH, H. T., JEON, J., SONG, B., SERRA, A., LESCAR, J., YOO, J. Y., BELDAR, S., YE, H., KANG, C., LIU, X. W., FEITOSA, M., KIM, Y., HWANG, D., GOH, G., LIM, K. L., PARK, H. M., LEE, C. H., OH, S. F., PETSKO, G. A., YOON, H. S. & KIM, K. S. 2020. PGE1 and PGA1 bind to Nurr1 and activate its transcriptional function. *Nat Chem Biol,* 16**,** 876-886.

RITE, I., MACHADO, A., CANO, J. & VENERO, J. L. 2007. Blood-brain barrier disruption induces in vivo degeneration of nigral dopaminergic neurons. *J Neurochem,* 101**,** 1567-82.

RODRIGUEZ, M. S., DARGEMONT, C. & HAY, R. T. 2001. SUMO-1 conjugation in vivo requires both a consensus modification motif and nuclear targeting. *J Biol Chem,* 276**,** 12654-9.

ROMANO, S., SAVVA, G. M., BEDARF, J. R., CHARLES, I. G., HILDEBRAND, F. & NARBAD, A. 2021. Meta-analysis of the Parkinson's disease gut microbiome suggests alterations linked to intestinal inflammation. *NPJ Parkinsons Dis,* 7**,** 27.

ROODVELDT, C., LABRADOR-GARRIDO, A., GONZALEZ-REY, E., LACHAUD, C. C., GUILLIAMS, T., FERNANDEZ-MONTESINOS, R., BENITEZ-RONDAN, A.,

ROBLEDO, G., HMADCHA, A., DELGADO, M., DOBSON, C. M. & POZO, D. 2013. Preconditioning of microglia by alpha-synuclein strongly affects the response induced by toll-like receptor (TLR) stimulation. *PLoS One,* 8**,** e79160.

RYTINKI, M. M., KAIKKONEN, S., PEHKONEN, P., JÄÄSKELÄINEN, T. & PALVIMO, J. J. 2009. PIAS proteins: pleiotropic interactors associated with SUMO. *Cell Mol Life Sci,* 66**,** 3029-41.

SABLIN, E. P., KRYLOVA, I. N., FLETTERICK, R. J. & INGRAHAM, H. A. 2003. Structural basis for ligand-independent activation of the orphan nuclear receptor LRH-1. *Mol Cell,* 11**,** 1575-85.

SAIJO, K., WINNER, B., CARSON, C. T., COLLIER, J. G., BOYER, L., ROSENFELD, M. G., GAGE, F. H. & GLASS, C. K. 2009. A Nurr1/CoREST pathway in microglia and astrocytes protects dopaminergic neurons from inflammation-induced death. *Cell,* 137**,** 47-59.

SAITOH, H. & HINCHEY, J. 2000. Functional heterogeneity of small ubiquitin-related protein modifiers SUMO-1 versus SUMO-2/3. *J Biol Chem,* 275**,** 6252-8.

SAKURADA, K., OHSHIMA-SAKURADA, M., PALMER, T. D. & GAGE, F. H. 1999. Nurr1, an orphan nuclear receptor, is a transcriptional activator of endogenous tyrosine hydroxylase in neural progenitor cells derived from the adult brain. *Development,* 126**,** 4017-26.

SAMPSON, D. A., WANG, M. & MATUNIS, M. J. 2001. The small ubiquitin-like modifier-1 (SUMO-1) consensus sequence mediates Ubc9 binding and is essential for SUMO-1 modification. *J Biol Chem,* 276**,** 21664-9.

SAMPSON, T. R., DEBELIUS, J. W., THRON, T., JANSSEN, S., SHASTRI, G. G., ILHAN, Z. E., CHALLIS, C., SCHRETTER, C. E., ROCHA, S., GRADINARU, V., CHESSELET, M. F., KESHAVARZIAN, A., SHANNON, K. M., KRAJMALNIK-BROWN, R., WITTUNG-STAFSHEDE, P., KNIGHT, R. & MAZMANIAN, S. K. 2016. Gut Microbiota Regulate Motor Deficits and Neuroinflammation in a Model of Parkinson's Disease. *Cell,* 167**,** 1469-1480 e12.

SATOH, J., KINO, Y., ASAHINA, N., TAKITANI, M., MIYOSHI, J., ISHIDA, T. & SAITO, Y. 2016. TMEM119 marks a subset of microglia in the human brain. *Neuropathology,* 36**,** 39-49.

SAUCEDO-CARDENAS, O. & CONNEELY, O. M. 1996. Comparative distribution of NURR1 and NUR77 nuclear receptors in the mouse central nervous system. *J Mol Neurosci,* 7**,** 51-63.

SAWADA, M., IMAMURA, K. & NAGATSU, T. 2006. Role of cytokines in inflammatory process in Parkinson's disease. *J Neural Transm Suppl***,** 373-81.

SAYAF, K., ZANOTTO, I., RUSSO, F. P., GABBIA, D. & DE MARTIN, S. 2021. The Nuclear Receptor PXR in Chronic Liver Disease. *Cells,* 11.

SCHMID, C. D., SAUTKULIS, L. N., DANIELSON, P. E., COOPER, J., HASEL, K. W., HILBUSH, B. S., SUTCLIFFE, J. G. & CARSON, M. J. 2002. Heterogeneous expression of the triggering receptor expressed on myeloid cells-2 on adult murine microglia. *J Neurochem,* 83**,** 1309-20.

SCHULZ, S., CHACHAMI, G., KOZACZKIEWICZ, L., WINTER, U., STANKOVIC-VALENTIN, N., HAAS, P., HOFMANN, K., URLAUB, H., OVAA, H., WITTBRODT, J., MEULMEESTER, E. & MELCHIOR, F. 2012. Ubiquitin-specific protease-like 1

(USPL1) is a SUMO isopeptidase with essential, non-catalytic functions. *EMBO Rep,* 13**,** 930-8.
SCHWABE, J. W., CHAPMAN, L., FINCH, J. T. & RHODES, D. 1993. The crystal structure of the estrogen receptor DNA-binding domain bound to DNA: how receptors discriminate between their response elements. *Cell,* 75**,** 567-78.
SEELER, J. S., BISCHOF, O., NACERDDINE, K. & DEJEAN, A. 2007. SUMO, the three Rs and cancer. *Curr Top Microbiol Immunol,* 313**,** 49-71.
SENTIS, S., LE ROMANCER, M., BIANCHIN, C., ROSTAN, M. C. & CORBO, L. 2005. Sumoylation of the estrogen receptor alpha hinge region regulates its transcriptional activity. *Mol Endocrinol,* 19**,** 2671-84.
SEVER, R. & GLASS, C. K. 2013. Signaling by nuclear receptors. *Cold Spring Harb Perspect Biol,* 5**,** a016709.
SHAO, Q. H., YAN, W. F., ZHANG, Z., MA, K. L., PENG, S. Y., CAO, Y. L., YUAN, Y. H. & CHEN, N. H. 2019. Nurr1: A vital participant in the TLR4-NF-κB signal pathway stimulated by α-synuclein in BV-2 cells. *Neuropharmacology,* 144**,** 388-399.
SHARMA, S., SHEN, T., CHITRANSHI, N., GUPTA, V., BASAVARAJAPPA, D., SARKAR, S., MIRZAEI, M., YOU, Y., KREZEL, W. & GRAHAM, S. L. 2022. Retinoid X Receptor: Cellular and Biochemical Roles of Nuclear Receptor with a Focus on Neuropathological Involvement. *Mol Neurobiol,* 59**,** 2027-2050.
SHAW, B. F. & VALENTINE, J. S. 2007. How do ALS-associated mutations in superoxide dismutase 1 promote aggregation of the protein? *Trends Biochem Sci,* 32**,** 78-85.
SHI, Y., INOUE, H., WU, J. C. & YAMANAKA, S. 2017. Induced pluripotent stem cell technology: a decade of progress. *Nat Rev Drug Discov,* 16**,** 115-130.
SHIN, E. J., SHIN, H. M., NAM, E., KIM, W. S., KIM, J. H., OH, B. H. & YUN, Y. 2012. DeSUMOylating isopeptidase: a second class of SUMO protease. *EMBO Rep,* 13**,** 339-46.
SHINBO, Y., NIKI, T., TAIRA, T., OOE, H., TAKAHASHI-NIKI, K., MAITA, C., SEINO, C., IGUCHI-ARIGA, S. M. & ARIGA, H. 2006. Proper SUMO-1 conjugation is essential to DJ-1 to exert its full activities. *Cell Death Differ,* 13**,** 96-108.
SIERRA, A., ABIEGA, O., SHAHRAZ, A. & NEUMANN, H. 2013. Janus-faced microglia: beneficial and detrimental consequences of microglial phagocytosis. *Front Cell Neurosci,* 7**,** 6.
SINGH, V. K., SAINI, A., KALSAN, M., KUMAR, N. & CHANDRA, R. 2016. Describing the Stem Cell Potency: The Various Methods of Functional Assessment and In silico Diagnostics. *Front Cell Dev Biol,* 4**,** 134.
SMITH, G. A., ROCHA, E. M., ROONEY, T., BARNEOUD, P., MCLEAN, J. R., BEAGAN, J., OSBORN, T., COIMBRA, M., LUO, Y., HALLETT, P. J. & ISACSON, O. 2015. A Nurr1 agonist causes neuroprotection in a Parkinson's disease lesion model primed with the toll-like receptor 3 dsRNA inflammatory stimulant poly(I:C). *PLoS One,* 10**,** e0121072.
SMITH, J. A., DAS, A., RAY, S. K. & BANIK, N. L. 2012. Role of pro-inflammatory cytokines released from microglia in neurodegenerative diseases. *Brain Res Bull,* 87**,** 10-20.

SMITS, S. M., PONNIO, T., CONNEELY, O. M., BURBACH, J. P. & SMIDT, M. P. 2003. Involvement of Nurr1 in specifying the neurotransmitter identity of ventral midbrain dopaminergic neurons. *Eur J Neurosci,* 18**,** 1731-8.

SOLBERG, Y., SILVERMAN, W. F. & POLLACK, Y. 1993. Prenatal ontogeny of tyrosine hydroxylase gene expression in the rat ventral mesencephalon. *Brain Res Dev Brain Res,* 73**,** 91-7.

SONG, J., DURRIN, L. K., WILKINSON, T. A., KRONTIRIS, T. G. & CHEN, Y. 2004. Identification of a SUMO-binding motif that recognizes SUMO-modified proteins. *Proc Natl Acad Sci U S A,* 101**,** 14373-8.

SPATHIS, A. D., ASVOS, X., ZIAVRA, D., KARAMPELAS, T., TOPOUZIS, S., COURNIA, Z., QING, X., ALEXAKOS, P., SMITS, L. M., DALLA, C., RIDEOUT, H. J., SCHWAMBORN, J. C., TAMVAKOPOULOS, C., FOKAS, D. & VASSILATIS, D. K. 2017. Nurr1:RXRα heterodimer activation as monotherapy for Parkinson's disease. *Proc Natl Acad Sci U S A,* 114**,** 3999-4004.

SU, X., MAGUIRE-ZEISS, K. A., GIULIANO, R., PRIFTI, L., VENKATESH, K. & FEDEROFF, H. J. 2008. Synuclein activates microglia in a model of Parkinson's disease. *Neurobiol Aging,* 29**,** 1690-701.

SUN, G., CUI, Q. & SHI, Y. 2017. Nuclear Receptor TLX in Development and Diseases. *Curr Top Dev Biol,* 125**,** 257-273.

SUN, J. & ZHANG, Y. G. 2022. Vitamin D Receptor Influences Intestinal Barriers in Health and Disease. *Cells,* 11.

SURMEIER, D. J. 2018. Determinants of dopaminergic neuron loss in Parkinson's disease. *FEBS J,* 285**,** 3657-3668.

SYMONS, A., BEINKE, S. & LEY, S. C. 2006. MAP kinase kinase kinases and innate immunity. *Trends Immunol,* 27**,** 40-8.

TAIRA, T., SAITO, Y., NIKI, T., IGUCHI-ARIGA, S. M., TAKAHASHI, K. & ARIGA, H. 2004. DJ-1 has a role in antioxidative stress to prevent cell death. *EMBO Rep,* 5**,** 213-8.

TAKAHASHI, H., HATAKEYAMA, S., SAITOH, H. & NAKAYAMA, K. I. 2005. Noncovalent SUMO-1 binding activity of thymine DNA glycosylase (TDG) is required for its SUMO-1 modification and colocalization with the promyelocytic leukemia protein. *J Biol Chem,* 280**,** 5611-21.

TAKAHASHI, K., ISHIDA, M., KOMANO, H. & TAKAHASHI, H. 2008. SUMO-1 immunoreactivity co-localizes with phospho-Tau in APP transgenic mice but not in mutant Tau transgenic mice. *Neurosci Lett,* 441**,** 90-3.

TAKAHASHI, K., TANABE, K., OHNUKI, M., NARITA, M., ICHISAKA, T., TOMODA, K. & YAMANAKA, S. 2007. Induction of pluripotent stem cells from adult human fibroblasts by defined factors. *Cell,* 131**,** 861-72.

TAKAHASHI, K. & YAMANAKA, S. 2006. Induction of pluripotent stem cells from mouse embryonic and adult fibroblast cultures by defined factors. *Cell,* 126**,** 663-76.

TAN, J. A., HALL, S. H., HAMIL, K. G., GROSSMAN, G., PETRUSZ, P. & FRENCH, F. S. 2002. Protein inhibitors of activated STAT resemble scaffold attachment factors and function as interacting nuclear receptor coregulators. *J Biol Chem,* 277**,** 16993-7001.

TANNER, T. M., DENAYER, S., GEVERTS, B., VAN TILBORGH, N., KERKHOFS, S., HELSEN, C., SPANS, L., DUBOIS, V., HOUTSMULLER, A. B., CLAESSENS, F. &

HAELENS, A. 2010. A 629RKLKK633 motif in the hinge region controls the androgen receptor at multiple levels. *Cell Mol Life Sci,* 67**,** 1919-27.
TATHAM, M. H., JAFFRAY, E., VAUGHAN, O. A., DESTERRO, J. M., BOTTING, C. H., NAISMITH, J. H. & HAY, R. T. 2001. Polymeric chains of SUMO-2 and SUMO-3 are conjugated to protein substrates by SAE1/SAE2 and Ubc9. *J Biol Chem,* 276**,** 35368-74.
TATHAM, M. H., RODRIGUEZ, M. S., XIRODIMAS, D. P. & HAY, R. T. 2009. Detection of protein SUMOylation in vivo. *Nat Protoc,* 4**,** 1363-71.
THEKA, I., CAIAZZO, M., DVORETSKOVA, E., LEO, D., UNGARO, F., CURRELI, S., MANAGÒ, F., DELL'ANNO, M. T., PEZZOLI, G., GAINETDINOV, R. R., DITYATEV, A. & BROCCOLI, V. 2013. Rapid generation of functional dopaminergic neurons from human induced pluripotent stem cells through a single-step procedure using cell lineage transcription factors. *Stem Cells Transl Med,* 2**,** 473-9.
TORII, T., KAWARAI, T., NAKAMURA, S. & KAWAKAMI, H. 1999. Organization of the human orphan nuclear receptor Nurr1 gene. *Gene,* 230**,** 225-32.
TREUTER, E. & VENTECLEF, N. 2011. Transcriptional control of metabolic and inflammatory pathways by nuclear receptor SUMOylation. *Biochim Biophys Acta,* 1812**,** 909-18.
TRUONG, K., LEE, T. D. & CHEN, Y. 2012. Small ubiquitin-like modifier (SUMO) modification of E1 Cys domain inhibits E1 Cys domain enzymatic activity. *J Biol Chem,* 287**,** 15154-63.
UM, J. W. & CHUNG, K. C. 2006. Functional modulation of parkin through physical interaction with SUMO-1. *J Neurosci Res,* 84**,** 1543-54.
UMESONO, K. & EVANS, R. M. 1989. Determinants of target gene specificity for steroid/thyroid hormone receptors. *Cell,* 57**,** 1139-46.
URIZ-HUARTE, A., DATE, A., ANG, H., ALI, S., BRADY, H. J. M. & FUCHTER, M. J. 2020. The transcriptional repressor REV-ERB as a novel target for disease. *Bioorg Med Chem Lett,* 30**,** 127395.
VENTECLEF, N., JAKOBSSON, T., EHRLUND, A., DAMDIMOPOULOS, A., MIKKONEN, L., ELLIS, E., NILSSON, L. M., PARINI, P., JÄNNE, O. A., GUSTAFSSON, J. A., STEFFENSEN, K. R. & TREUTER, E. 2010. GPS2-dependent corepressor/SUMO pathways govern anti-inflammatory actions of LRH-1 and LXRbeta in the hepatic acute phase response. *Genes Dev,* 24**,** 381-95.
WAGNER, N. & WAGNER, K. D. 2020. The Role of PPARs in Disease. *Cells,* 9.
WALTHER, R. F., ATLAS, E., CARRIGAN, A., ROULEAU, Y., EDGECOMBE, A., VISENTIN, L., LAMPRECHT, C., ADDICKS, G. C., HACHE, R. J. & LEFEBVRE, Y. A. 2005. A serine/threonine-rich motif is one of three nuclear localization signals that determine unidirectional transport of the mineralocorticoid receptor to the nucleus. *J Biol Chem,* 280**,** 17549-61.
WANG, J., HU, W., CAI, S., LEE, B., SONG, J. & CHEN, Y. 2007. The intrinsic affinity between E2 and the Cys domain of E1 in ubiquitin-like modifications. *Mol Cell,* 27**,** 228-237.
WANG, Z., BENOIT, G., LIU, J., PRASAD, S., AARNISALO, P., LIU, X., XU, H., WALKER, N. P. & PERLMANN, T. 2003. Structure and function of Nurr1 identifies a class of ligand-independent nuclear receptors. *Nature,* 423**,** 555-60.

WATANABE, K., UENO, M., KAMIYA, D., NISHIYAMA, A., MATSUMURA, M., WATAYA, T., TAKAHASHI, J. B., NISHIKAWA, S., NISHIKAWA, S., MUGURUMA, K. & SASAI, Y. 2007. A ROCK inhibitor permits survival of dissociated human embryonic stem cells. *Nat Biotechnol,* 25**,** 681-6.

WATSON, P. J., FAIRALL, L. & SCHWABE, J. W. 2012. Nuclear hormone receptor co-repressors: structure and function. *Mol Cell Endocrinol,* 348**,** 440-9.

WEGER, S., HAMMER, E. & HEILBRONN, R. 2005. Topors acts as a SUMO-1 E3 ligase for p53 in vitro and in vivo. *FEBS Lett,* 579**,** 5007-12.

WEI, W., YANG, P., PANG, J., ZHANG, S., WANG, Y., WANG, M. H., DONG, Z., SHE, J. X. & WANG, C. Y. 2008. A stress-dependent SUMO4 sumoylation of its substrate proteins. *Biochem Biophys Res Commun,* 375**,** 454-9.

WENDELN, A. C., DEGENHARDT, K., KAURANI, L., GERTIG, M., ULAS, T., JAIN, G., WAGNER, J., HASLER, L. M., WILD, K., SKODRAS, A., BLANK, T., STASZEWSKI, O., DATTA, M., CENTENO, T. P., CAPECE, V., ISLAM, M. R., KERIMOGLU, C., STAUFENBIEL, M., SCHULTZE, J. L., BEYER, M., PRINZ, M., JUCKER, M., FISCHER, A. & NEHER, J. J. 2018. Innate immune memory in the brain shapes neurological disease hallmarks. *Nature,* 556**,** 332-338.

WESTON, A. D., BLUMBERG, B. & UNDERHILL, T. M. 2003. Active repression by unliganded retinoid receptors in development: less is sometimes more. *J Cell Biol,* 161**,** 223-8.

WHITE, J. H., FERNANDES, I., MADER, S. & YANG, X. J. 2004. Corepressor recruitment by agonist-bound nuclear receptors. *Vitam Horm,* 68**,** 123-43.

WONG, M. L. & MEDRANO, J. F. 2005. Real-time PCR for mRNA quantitation. *Biotechniques,* 39**,** 75-85.

WU, Q., CHAMBLISS, K., UMETANI, M., MINEO, C. & SHAUL, P. W. 2011. Non-nuclear estrogen receptor signaling in the endothelium. *J Biol Chem,* 286**,** 14737-43.

WU, S. Y. & CHIANG, C. M. 2009. Crosstalk between sumoylation and acetylation regulates p53-dependent chromatin transcription and DNA binding. *EMBO J,* 28**,** 1246-59.

WYSS-CORAY, T. & MUCKE, L. 2002. Inflammation in neurodegenerative disease--a double-edged sword. *Neuron,* 35**,** 419-32.

XICOY, H., WIERINGA, B. & MARTENS, G. J. 2017. The SH-SY5Y cell line in Parkinson's disease research: a systematic review. *Mol Neurodegener,* 12**,** 10.

XU, P. Y., LIANG, R., JANKOVIC, J., HUNTER, C., ZENG, Y. X., ASHIZAWA, T., LAI, D. & LE, W. D. 2002. Association of homozygous 7048G7049 variant in the intron six of Nurr1 gene with Parkinson's disease. *Neurology,* 58**,** 881-4.

XU, X., VATSYAYAN, J., GAO, C., BAKKENIST, C. J. & HU, J. 2010. HDAC2 promotes eIF4E sumoylation and activates mRNA translation gene specifically. *J Biol Chem,* 285**,** 18139-43.

XU, Z. & AU, S. W. 2005. Mapping residues of SUMO precursors essential in differential maturation by SUMO-specific protease, SENP1. *Biochem J,* 386**,** 325-30.

YAMASHITA, D., YAMAGUCHI, T., SHIMIZU, M., NAKATA, N., HIROSE, F. & OSUMI, T. 2004. The transactivating function of peroxisome proliferator-activated receptor gamma is negatively regulated by SUMO conjugation in the amino-terminal domain. *Genes Cells,* 9**,** 1017-29.

YAN, A., ZHANG, Y., LIN, J., SONG, L., WANG, X. & LIU, Z. 2018. Partial Depletion of Peripheral M1 Macrophages Reverses Motor Deficits in MPTP-Treated Mouse by Suppressing Neuroinflammation and Dopaminergic Neurodegeneration. *Front Aging Neurosci,* 10**,** 160.

YAN, C. H., LEVESQUE, M., CLAXTON, S., JOHNSON, R. L. & ANG, S. L. 2011. Lmx1a and lmx1b function cooperatively to regulate proliferation, specification, and differentiation of midbrain dopaminergic progenitors. *J Neurosci,* 31**,** 12413-25.

YANG, X. J. & GREGOIRE, S. 2006. A recurrent phospho-sumoyl switch in transcriptional repression and beyond. *Mol Cell,* 23**,** 779-86.

YANG, Y., FU, W., CHEN, J., OLASHAW, N., ZHANG, X., NICOSIA, S. V., BHALLA, K. & BAI, W. 2007. SIRT1 sumoylation regulates its deacetylase activity and cellular response to genotoxic stress. *Nat Cell Biol,* 9**,** 1253-62.

YAO, L., LI, P., CHEN, Q., HU, A., WU, Y. & LI, B. 2022. Protective effects of endotoxin tolerance on peripheral lipopolysaccharide-induced neuroinflammation and dopaminergic neuronal injury. *Immunopharmacol Immunotoxicol,* 44**,** 326-337.

YEH, E. T., GONG, L. & KAMITANI, T. 2000. Ubiquitin-like proteins: new wines in new bottles. *Gene,* 248**,** 1-14.

YUN, S. M., CHO, S. J., SONG, J. C., SONG, S. Y., JO, S. A., JO, C., YOON, K., TANZI, R. E., CHOI, E. J. & KOH, Y. H. 2013. SUMO1 modulates Aβ generation via BACE1 accumulation. *Neurobiol Aging,* 34**,** 650-62.

YUNUS, A. A. & LIMA, C. D. 2006. Lysine activation and functional analysis of E2-mediated conjugation in the SUMO pathway. *Nat Struct Mol Biol,* 13**,** 491-9.

YUNUS, A. A. & LIMA, C. D. 2009. Structure of the Siz/PIAS SUMO E3 ligase Siz1 and determinants required for SUMO modification of PCNA. *Mol Cell,* 35**,** 669-82.

ZARRAGA-GRANADOS, G., MUCINO-HERNANDEZ, G., SANCHEZ-CARBENTE, M. R., VILLAMIZAR-GALVEZ, W., PENAS-RINCON, A., ARREDONDO, C., ANDRES, M. E., WOOD, C., COVARRUBIAS, L. & CASTRO-OBREGON, S. 2020. The nuclear receptor NR4A1 is regulated by SUMO modification to induce autophagic cell death. *PLoS One,* 15**,** e0222072.

ZETTERSTRÖM, R. H., SOLOMIN, L., JANSSON, L., HOFFER, B. J., OLSON, L. & PERLMANN, T. 1997. Dopamine neuron agenesis in Nurr1-deficient mice. *Science,* 276**,** 248-50.

ZETTERSTRÖM, R. H., WILLIAMS, R., PERLMANN, T. & OLSON, L. 1996. Cellular expression of the immediate early transcription factors Nurr1 and NGFI-B suggests a gene regulatory role in several brain regions including the nigrostriatal dopamine system. *Brain Res Mol Brain Res,* 41**,** 111-20.

ZHANG, Y. Q. & SARGE, K. D. 2008. Sumoylation of amyloid precursor protein negatively regulates Abeta aggregate levels. *Biochem Biophys Res Commun,* 374**,** 673-8.

ZHENG, T. & ZHANG, Z. 2021. Activated microglia facilitate the transmission of alpha-synuclein in Parkinson's disease. *Neurochem Int,* 148**,** 105094.

ZHU, C., KROS, J. M., VAN DER WEIDEN, M., ZHENG, P., CHENG, C. & MUSTAFA, D. A. 2017. Expression site of P2RY12 in residential microglial cells in astrocytomas correlates with M1 and M2 marker expression and tumor grade. *Acta Neuropathol Commun,* 5**,** 4.

ZWART, W., DE LEEUW, R., RONDAIJ, M., NEEFJES, J., MANCINI, M. A. & MICHALIDES, R. 2010. The hinge region of the human estrogen receptor determines functional synergy between AF-1 and AF-2 in the quantitative response to estradiol and tamoxifen. *J Cell Sci,* 123**,** 1253-61.

ZÁRRAGA-GRANADOS, G., MUCIÑO-HERNÁNDEZ, G., SÁNCHEZ-CARBENTE, M. R., VILLAMIZAR-GÁLVEZ, W., PEÑAS-RINCÓN, A., ARREDONDO, C., ANDRÉS, M. E., WOOD, C., COVARRUBIAS, L. & CASTRO-OBREGÓN, S. 2020. The nuclear receptor NR4A1 is regulated by SUMO modification to induce autophagic cell death. *PLoS One,* 15**,** e0222072.